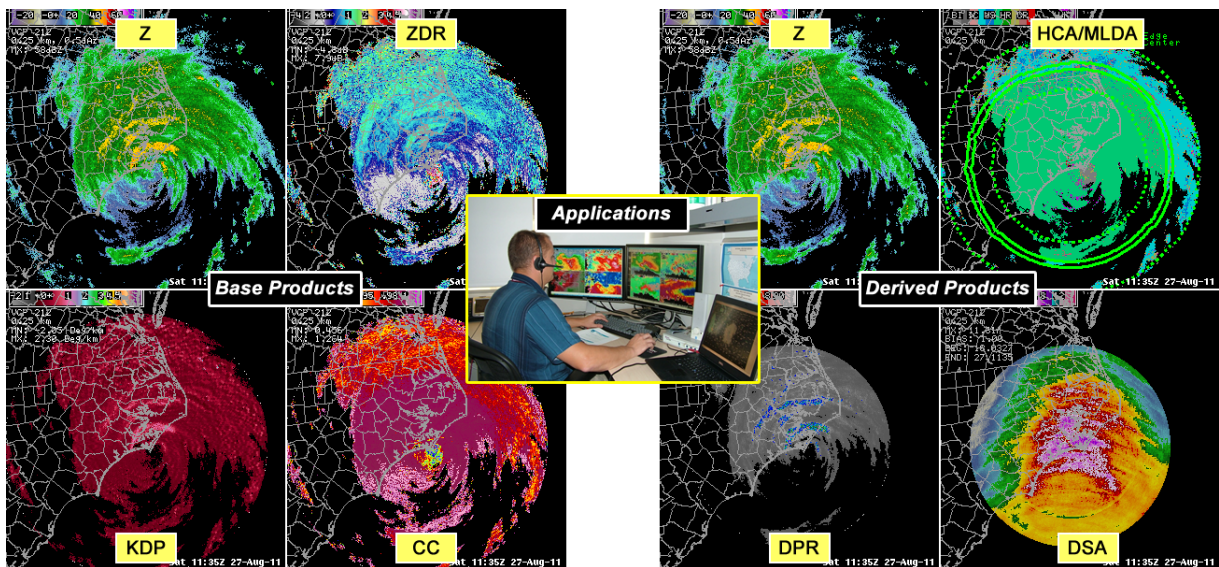


Dual-Polarization Radar Operations Course



Presented by the
Warning Decision Training Branch

TABLE OF CONTENTS

Correlation Coefficient (CC)	6
Correlation Coefficient (CC) Product Characteristics	6
D-2D CC Display	7
What is Correlation Coefficient?	8
Pulses Behaving Similarly:	
High Correlation Coefficient	9
Pulses Behaving Differently:	
Low Correlation Coefficient	11
Physical Interpretation	11
Correlation Coefficient Weaknesses (Limitations)	13
Degradation with Range	14
Mixture of hydrometeors	14
Beam Broadening and the Melting Layer	15
Non-uniform Beam Filling (NBF)	16
Range Folding in Batch Cuts	17
Correlation Coefficient (CC) Operational Applications (Strengths)	18
Meteorological and Non-meteorological Echoes	18
Melting Layer	19
Rain vs. Snow	20
Significant Severe Hail	21
Irregularly Shaped Hydrometeors	23
Tornadic Debris	23
Differential Reflectivity (ZDR)	26
Differential Reflectivity (ZDR) Characteristics	26
D-2D ZDR Display	27
What is Differential Reflectivity?	29
Physical Interpretation	30
Rain	31
Hail	33
Snow and Ice Crystals	33
Non-Meteorological Echoes	35
Differential Reflectivity Limitations	36
Bias Towards Larger Hydrometeors	36
Particle Density	37
Mie Scattering Effects	38
Low Signal to Noise Ratio/Correlation Coefficient	39
Depolarization	40
Batch Cuts & Range Folding	41
Differential Reflectivity Operational Applications (Strengths)	42
Hail Detection	43
Updraft (ZDR column)	43

Tornadic Debris Signature (TDS)	44
Melting Layer.....	44
Rain/Snow Transition Area.....	45
Frozen Precipitation Types.....	46
Non-Meteorological Echoes (Birds/Insects)	47
Specific Differential Phase (KDP)	48
Specific Differential Phase (KDP) Characteristics.....	48
D-2D KDP Display	49
Physical Interpretation	51
Characteristic of FDP in Rain.....	52
Characteristic of FDP in Hail.....	53
Characteristic of FDP in Snow and Ice Crystals	54
Characteristic of FDP in Non-Meteorological Echoes	54
What is KDP?	55
Specific Differential Phase (KDP) Limitations (Weaknesses)	59
KDP Not Shown for CC<0.90.....	60
Noise in Low SNR.....	61
Non-Uniform Beam Filling (NBF)	62
Range Folding in the Batch Cuts	63
Specific Differential Phase (KDP) Operational Applications (Strengths)	63
Heavy Rain Only	64
Rain, Hail, or Rain Mixed with Hail.....	65
Cold vs. Warm Rain Processes.....	67
Hydrometeor Classification (HC).....	68
Hydrometeor Classification (HC) Characteristics.....	68
D-2D Display	69
AWIPS Cursor Readout	70
Hydrometeor Classification (HC) Operational Applications (Strengths)	75
Safety Net for Base Data Analysis	75
Input for Precipitation Algorithm	76
Provides Quick Look at Regions of Interest.....	76
Hydrometeor Classification (HC) Limitations (Weaknesses)	77
Overlapping Polarimetric Characteristics Between Classes	78
Subjective and Empirical Fuzzy-logic Membership Functions and Weights	79
Uncertainty Not Portrayed.....	80
It's an Algorithm	80
Ground Truth.....	81
Range Folding in Batch Cuts	81
Melting Layer (ML)	84
Melting Layer (ML) Characteristics	84

Melting Layer (ML) Operational Application (Strengths)	89
Updates Every Volume Scan	89
Aids in Interpreting Base Data	89
Melting Layer (ML) Limitations (Weaknesses)	90
Situations with Unlikely ML Detection	91
Two Melting Levels.....	93
Unrealistic Discontinuities	94
Performance in Mountainous Regions.....	95
Recommendations	96

Dual-Pol Quantitative Precipitation Estimation (QPE)98

New Quantitative Precipitation Estimation (QPE) Products with Dual-Pol	100
Hybrid Hydroclass (HHC).....	101
Digital Precipitation Rate (DPR).....	102
Digital Accumulation Array (DAA)	103
One Hour Accumulation (OHA).....	104
Storm-Total Accumulation Products (DSA and STA).....	105
Digital One-Hour Difference (DOD) and Digital Storm-Total Difference (DSD)	109
Digital User-Selectable Accumulation (DUA)	111
Dual-Pol Quantitative Precipitation Estimation (QPE) Operational Applications (Strengths)	114
Dual-Pol Quantitative Precipitation Estimation (QPE) Limitations	115
Dependency on HCA Output.....	115
No Biases Applied.....	117
Small Sample to Derive Z Relations in Frozen Precipitation.....	117
Standard Radar Limitations	117

Winter Weather Nowcasting. 118

Winter Weather Nowcasting Methodology	119
Characteristics of the Melting Layer in Dual-Pol Base Data Products	119
Steps to Detecting Melting Layer Using PCR All-Tilts	121
Dual-Pol Products and the Wet Bulb Zero Height.....	123
Characteristics of a Well-Defined Melting Layer	125
Melting Layer Exists	126
Sleet Potential	126
No Melting Layer Detected	129
Drizzle	133
Snow	134
Limitations of Dual-Pol Winter Weather Signatures	140
Below Beam Effects	140
Melting Layer Not Always Well-Defined	140
Diagnostic Tool Only	140

Hail Detection 142

Physical Characteristics of Hail	142
Characteristics of Hail in Dual-Pol Base Products	142
Detecting Hail with PCR All-Tilts	143
FSI Characteristics of a Hail Shaft	146
Three-Body Scatter Spike (TBSS)	148
TBSS Cross Section	149
Special Case: Giant Hail Detection	150
Melting or Mostly Melted Hail Signature.....	150
Strengths of Dual-Pol Hail Detection	156
Limitations of Dual-Pol Hail Detection	157

Tornado Debris Detection 158

Tornadic Debris Signature (TDS)	158
Physical Characteristics of Tornadic Debris	158
Dual-Pol Characteristics of Tornadic Debris	159
When to Check for Tornadic Debris Signature	160
How to Check for Tornadic Debris Signatures	161
Strengths of Dual-Pol Tornadic Debris Detection	163
Limitations of Dual-Pol Tornadic Debris Detection	164
No Lead Time.....	164
Tornado Must Be at Close Range	164
Tornado Must Hit Something to Produce a Signature.....	164
Debris Signature Might Be Upstream of the Strongest Couplet.....	165

ZDR Columns 168

Definition of a ZDR Column	168
How to Find ZDR Columns	170
Detecting ZDR Columns in Panel Combo/Rotate	170
Identifying ZDR Columns Using CAPPI in FSI.....	173
ZDR Column Applications	173
Relative Updraft Strength	174
Storm Splitting	176
ZDR Column Limitations	178

Heavy Rain Detection 180

Heavy Rain Detection in a Tropical Environment	181
Heavy Rain Detection in a Continental Environment	183
Heavy Rain Mixed with Hail	185
KDP and Rainfall Rate	186
Methodology to Detect Heavy Rain Using Panel/Combo Rotate	187
Using Dual-Pol Products During Flash Flood Warning Operations.....	188
Strengths of Using Dual-Pol to Detect Heavy Rain	188
Limitations of Dual-Pol Heavy Rain Detection	189

Non-Precipitation Echoes	190
Dual-Pol Advantage: Distinguishing Non-meteorological Echo	190
Ground Clutter and Anomalous Propagation	190
Dual-Pol Characteristics of Ground Clutter and AP	191
Biological Scatterers	192
Migrating Birds	193
Local Birds Dispersing	195
Insects	197
Wind Turbines	199
Smoke Plumes	202
Chaff	203
Conclusion	205

Lesson 1: Correlation Coefficient (CC)

Correlation Coefficient is abbreviated “CC” across the NWS, but you’ll see it listed in research papers as ρ_{HV} (RHO in GR Analyst). CC is arguably the most important dual-pol base product because it allows forecasters the ability to determine if radar echoes are dominated by a homogeneous precipitation type, a mixture of precipitation types, or non-precipitation.

Correlation Coefficient is available in 4-bit and 8-bit data levels, each with a unique product resolution.

Correlation Coefficient (CC) Product Characteristics

8-bit Correlation Coefficient

- Resolution: 0.13 nm (0.25 km, 250 m) x 1.0 degree for all elevation angles and VCPs
- Data Levels: 256
 - Min. = 0.2, Max. = 1.05
 - Precision: to the nearest 0.00333
- Range: 162 nm
- RPG Product Code: DCC

4-bit Correlation Coefficient

- Resolution: 0.54 nm (1 km, 1000 m) x 1.0 degree for all elevation angles and VCPs
- Data Levels: 16
 - Min. = 0.2, Max = 1.05
 - Precision: to the nearest 0.01 to 0.25
- Range: 124 nm
- RPG Product Code: CC

Correlation Coefficient Product Description

- RPG ID: kxxx (where xxx = 3-letter radar ID)

- Elevation angle: x.x in degrees
- Product name: CC 8-bit or CC 4-bit
- Date: Day of week, time in UTC and date
- Units: unitless

Correlation Coefficient Product Annotations:

- VCP: 11, 12, 21, 121, 211, 212, 221, 31, or 32
- Range Resolution: 0.25 km (8-bit), 1 km (4-bit)

All overlays are displayable on this product.

D-2D CC Display The CC product will appear on your D-2D screen as seen on the right in Figure 1-1. A reflectivity image has been provided on the left for reference.

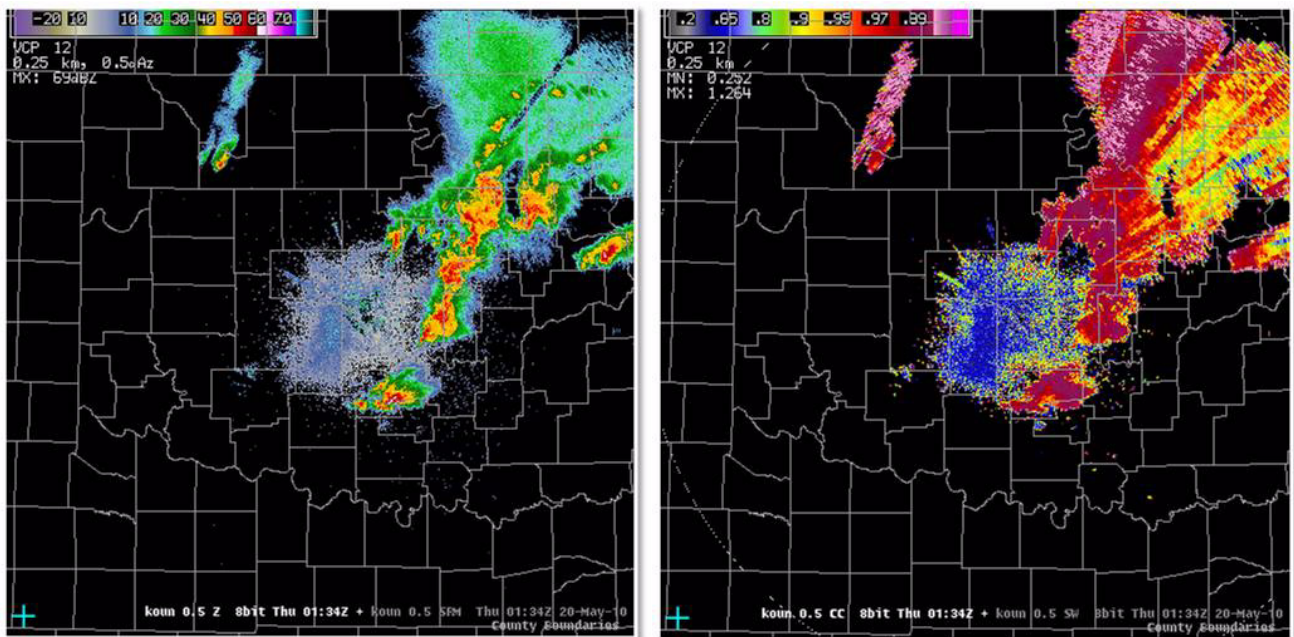


Figure 1-1. D2D Reflectivity (Z, left) and Correlation Coefficient (CC, right) product display

Individual CC products can be found for each elevation angle inside your dedicated radar's drop-down menu. Also, the CC product can be found in conjunction with other data. These are illustrated in Figure 1-2.

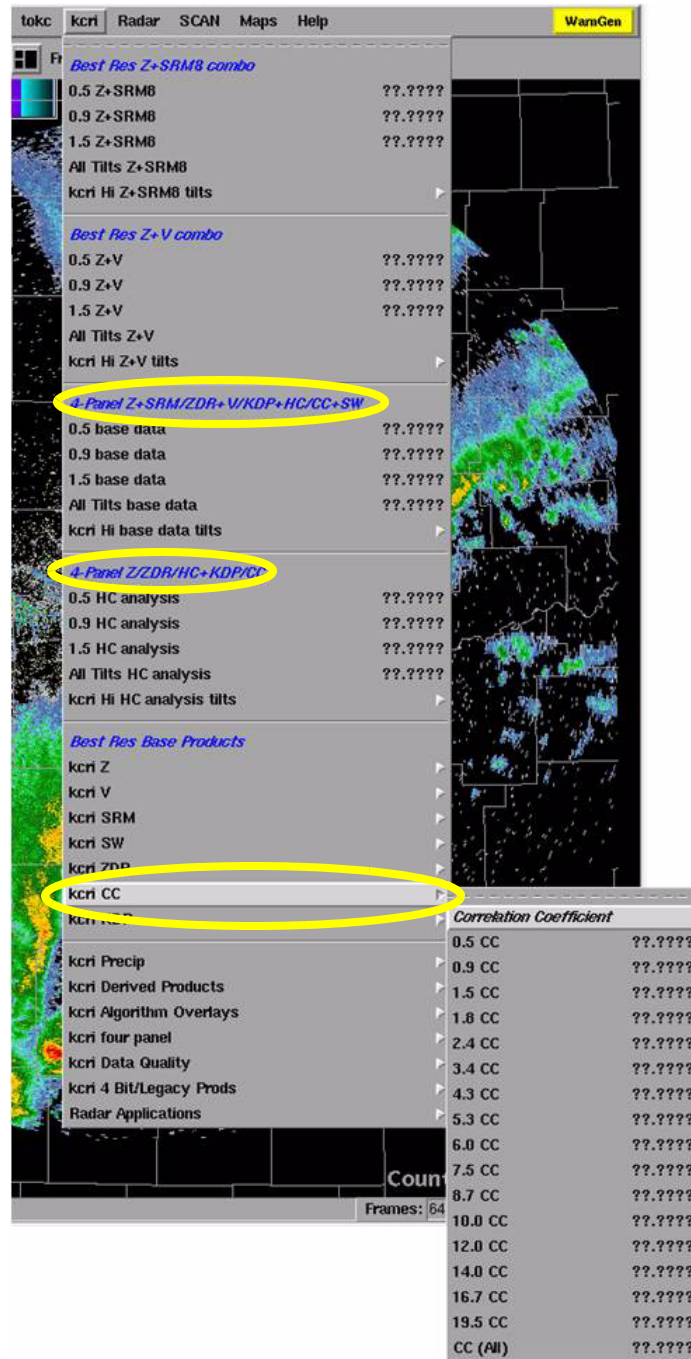


Figure 1-2. D-2D drop down menu for dedicated radar. Yellow ovals indicate where CC products can be found in the menu.

The correlation coefficient is a measure of how similarly the horizontally and vertically polarized pulses are behaving within a pulse volume. Its values can range from 0.2 to 1.05 and are unitless. In

What is Correlation Coefficient?

AWIPS and the RPG, this variable is referred to as CC, but in the literature it will be referred to as ρ_{HV} (see Fig. 1-3).

Definition	Possible Range of Values	Units	Abbreviated Name
Measure of how similarly the horizontally and vertically polarized pulses are behaving within a pulse volume	0.2 to 1.05	None	CC (AWIPS) ρ_{HV} (Literature)

Figure 1-3. Summary of definition and characteristics of correlation coefficient

So, what does it mean, exactly, for the pulses to behave similarly within a pulse volume? We'll look at two cases:

- When the pulses behave very similarly resulting in high CC
- When the pulses behave very differently resulting in low CC

The best way to describe this behavior is to look at phasor notation for the pulses. Recall that velocity uses phasor notation to determine the Doppler frequency shift which gives the radial velocity in the pulse volume.

Pulses Behaving Similarly: High Correlation Coefficient

Looking at pulse 1 in Figure 1-4, note the phasor representations for the horizontal and vertical power returns. Moving on to pulse 2, we see that the magnitudes of the horizontal and vertical pulses have remained the same as pulse 1, but the angles, or phases, of have changed. Note that the changes in the phases of the horizontal and vertical pulses are the same. Looking at pulse 3, we see that the phases of the horizontal and vertical pulses have not changed, but the magnitudes

have changed. However, just like the phases from pulse 1 to pulse 2, the magnitudes of the horizontal and vertical pulses from pulse numbers 2 to 3 have changed by the same amount.

High Correlation Coefficient

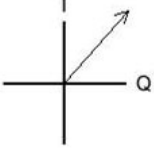
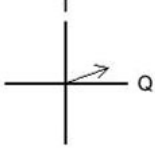
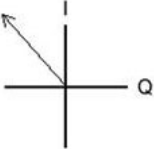
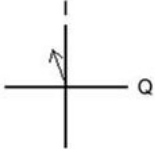
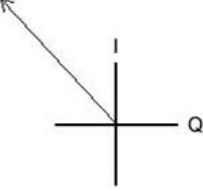
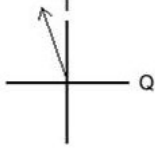
Pulse #	Horizontal	Vertical
1		
2		
3		

Figure 1-4. Examples of pulse-to-pulse changes in phasor magnitude and phase for a scenario yielding high CC.

As long as the magnitude, phases or both the magnitudes and phases of the horizontal and vertical pulses change in a similar manner from pulse to pulse in a resolution volume, the CC will be high (i.e. near 1).

Pulses Behaving Differently: Low Correlation Coefficient

In Figure 1-5, pulse 1 remains the same as in Figure 4. Looking at pulse 2, we see that the magnitudes of the horizontal and vertical pulses have not changed, but the phases have changed. However, here the angles have changed differently for the horizontal and vertical pulses. Going from pulse 2 to pulse 3, we see that the phases have not changed, but the magnitudes have changed. Unlike the previous example, the magnitudes for the horizontal and vertical pulses have not changed in a similar manner. In other words, if the magnitude, phases or both the magnitude and phases change differently between the horizontal and vertical pulses from pulse-to-pulse, then there is little correlation between the horizontal and vertical pulses and the result is low CC ($\sim < 0.70$).

Pulse #	Horizontal	Vertical
1		
2		
3		

Figure 1-5. Examples of pulse-to-pulse changes in phasor magnitude and phase for a scenario yielding low CC.

Physical Interpretation

Non-meteorological echoes, such as birds and insects, have complex shapes that are highly variable, often returning CC below 0.8 (Fig. 1-6, left). Meteorological echoes that have complex shapes,

mixed phases, etc., result in lower CC values as the horizontal and vertical pulses tend to behave differently (Fig. 1-6, middle). Finally, for meteorological echoes that are fairly uniform in shape, type, and size, such as rain or snow, the horizontal and vertical pulses behave very similarly resulting in CC greater than 0.97 (Fig. 1-6, right).

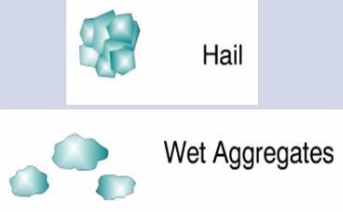
<u>Non-Meteorological</u> (birds, insects, etc.)	<u>Metr (Non-Uniform)</u> (hail, melting snow, etc.)	<u>Metr (Uniform)</u> (rain, snow, etc.)
		
<p>Complex scattering from pulse-to-pulse. Horizontal and vertical pulses change in different manners from pulse-to-pulse</p>	<p>Somewhat complex scattering from pulse-to-pulse. Moderate differences from pulse-to-pulse for the horizontal and vertical pulses</p>	<p>Well-behaved scattering from pulse-to-pulse. Little differences from pulse-to-pulse for the horizontal and vertical pulses</p>
<p>Low CC (< 0.7)</p>	<p>Moderate CC (0.80 to 0.97)</p>	<p>High CC (> 0.97)</p>

Figure 1-6. Physical interpretation of non-meteorological, non-uniform meteorological and uniform meteorological scatterers in the Correlation Coefficient product output.

Applying a general physical interpretation and using results backed up by research, a chart of typical values of CC was developed (see Fig. 1-7). Most meteorological echoes tend to have CC values greater than 0.9. Exceptions include giant hail and melting snow flakes, which can dip to as low as 0.70. For non-meteorological echoes, the correlation coefficient is rarely greater than 0.90 except for certain types of static ground clutter which can get as high as 0.99 in some cases.

Typical Values for CC

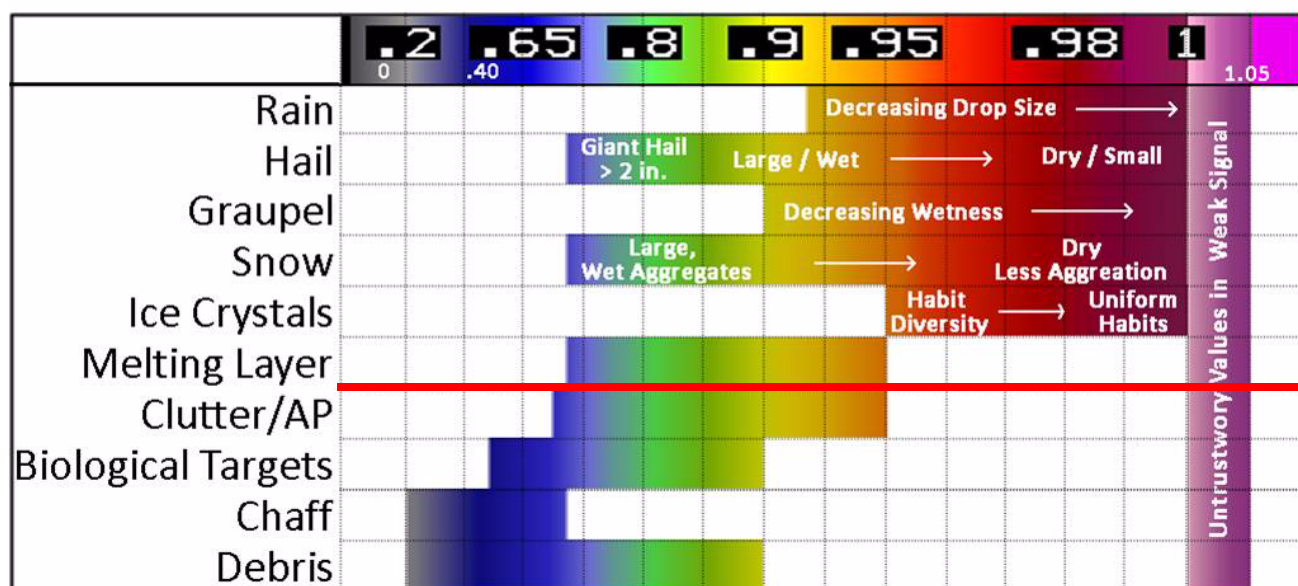


Figure 1-7. Typical values for correlation coefficient (CC) for the various echoes. Meteorological echoes are listed above the red line, and non-meteorological echoes below.

Correlation Coefficient Weaknesses (Limitations)

Dual-Polarization products, like other Doppler radar products, have limitations that forecasters need to be aware of before applying them operationally. Here we will consider the following as factors affecting CC:

- Degradation with range
- Mixture of hydrometeors
- Beam broadening and the melting layer

- Non-uniform beam filling (NBF)
- Range folding in batch cuts

The estimation of CC degrades with range due to decreasing signal to noise ratio (SNR). Another area where low SNR will degrade CC is along the fringes of precipitation. In Figure 1-8 note regions of degraded CC with values greater than 1.0, or light pink values in AWIPS. Note the occurrence of noisy CC values within the region of weak (< 20dBZ) reflectivity to the northwest of the radar (large, white oval). Since reflectivity here is fairly weak, SNR is rather low. The same thing is occurring along the fringes of the precipitation to the east, noted within the slim, white oval. Forecasters should expect to see noisy and/or pink CC (values greater than 1.0) in every CC product, regardless of climate, wherever SNR becomes low enough.

Degradation with Range

Virtually without exception, scatterers within the beam are not perfectly uniform. Thus, particle

Mixture of hydrometeors

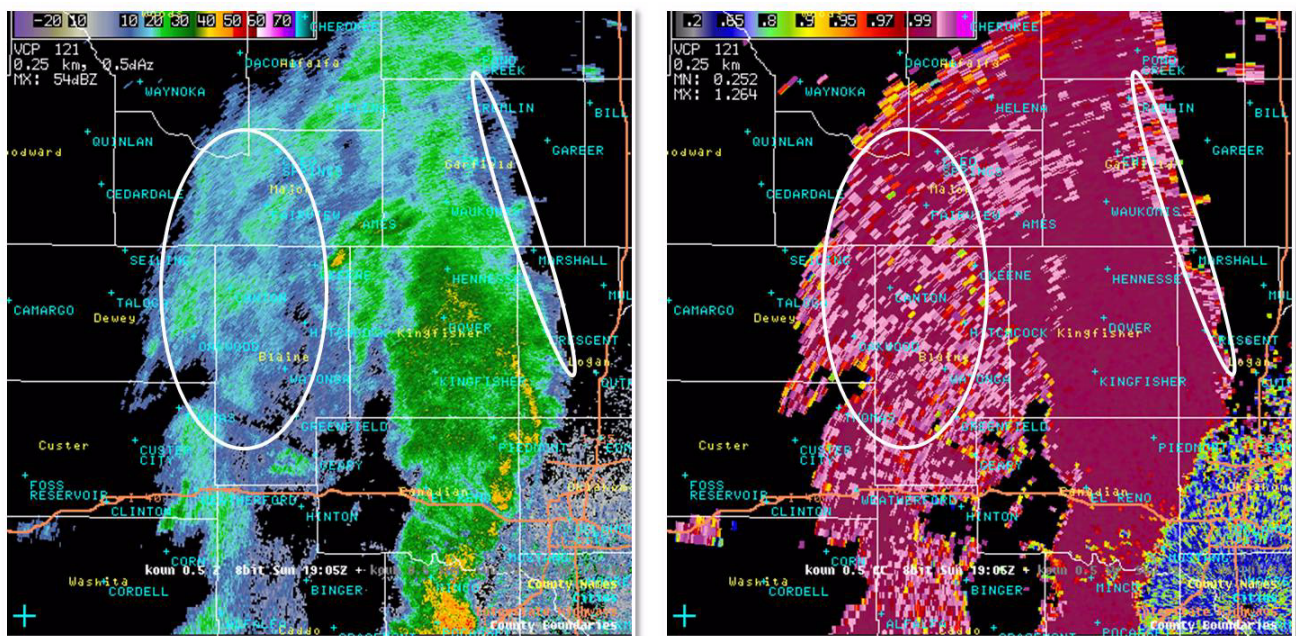


Figure 1-8. Reflectivity (left) and CC (right) for a precipitation event showing degradation of CC with range (large white oval northwest of the radar) and low signal to noise ratio (narrow white oval north of the radar).

diversity within the pulse volume results in a non-uniform distribution of hydrometeor type and/or characteristics. Lower CC can be caused by high diversity in:

- Hydrometeor shapes
- Hydrometeor size
- Backscatter differential phase shift
- Hydrometeor orientation

A diversity of echo types within a pulse volume leads to a decrease in correlation coefficient. The amount of decrease in the correlation coefficient is dependent upon the relative contributions of each hydrometeor type/characteristic present to the overall signal. The lowest correlation coefficient will occur when relatively equal contributions of each hydrometeor type/characteristic to the signal are similar. For example, if snow and rain contribute relatively equally to the signal, the correlation coefficient will be lower than if the rain contributed more than the snow to the signal and vice versa.

Beam Broadening and the Melting Layer

Typically, the melting layer is not more than a few hundred meters thick and, as you will learn in the winter weather applications module, the dual-pol products (particularly CC) are excellent at identifying the melting layer. In the melting layer CC values range roughly from 0.85-0.95. Recall, though, that at far ranges the radar beam broadens. For example, at just 60 km (32 nm), the radar beam is already 1 km wide in the vertical! This broadening means that at farther distances the beam center can be farther above or below the melting layer and still sample it. This ultimately leads to a smearing of the melting layer signature and the appearance that it is deeper than it actually is. Looking at Fig. 1-9 on page 1-16, the image on the

right is a CC image where you can see the broadening of the melting layer signature in CC at farther ranges. The top and bottom of the melting layer signature are denoted with white lines. Note that the melting layer signature (i.e. lower CC) has become deeper with range. This is solely a result of beam broadening. A reflectivity image is on the left for reference.

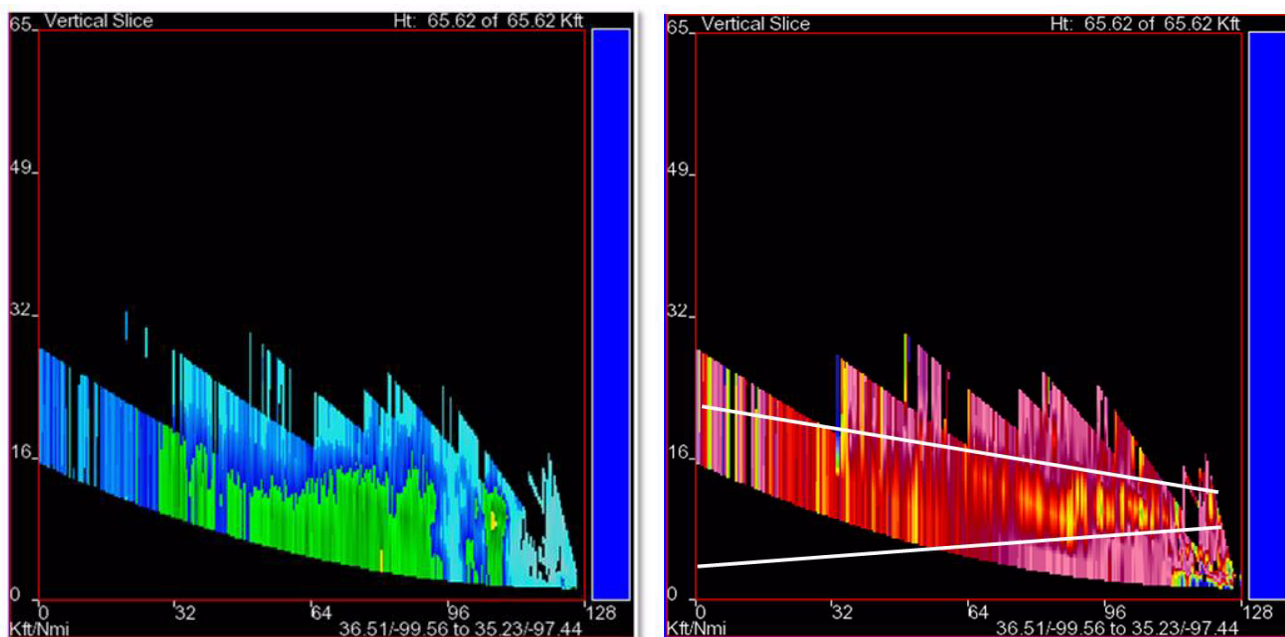


Figure 1-9. Reflectivity (left) and CC (right) cross sections. Notice the broadening of the melting layer in the CC image.

Non-uniform beam filling (NBF) was discussed in a previous section, and it affects CC most noticeably when significant gradients of differential phase (to be discussed in the lesson on KDP) occur within a pulse volume. These gradients can either be in the horizontal or vertical, causing decreased CC down-radial. NBF is most likely to occur in a supercell with a strong hail core or in a line of storms oriented along a radial. An example of this CC artifact is illustrated in the radially-aligned line of storms shown in Fig. 1-10, page 1-17 on the right. As seen in this example, the reduction in CC is often radially-oriented and extends pretty much all

Non-uniform Beam Filling (NBF)

the way down-radial to the edge of the domain. A reflectivity image is provided on the left for your reference.

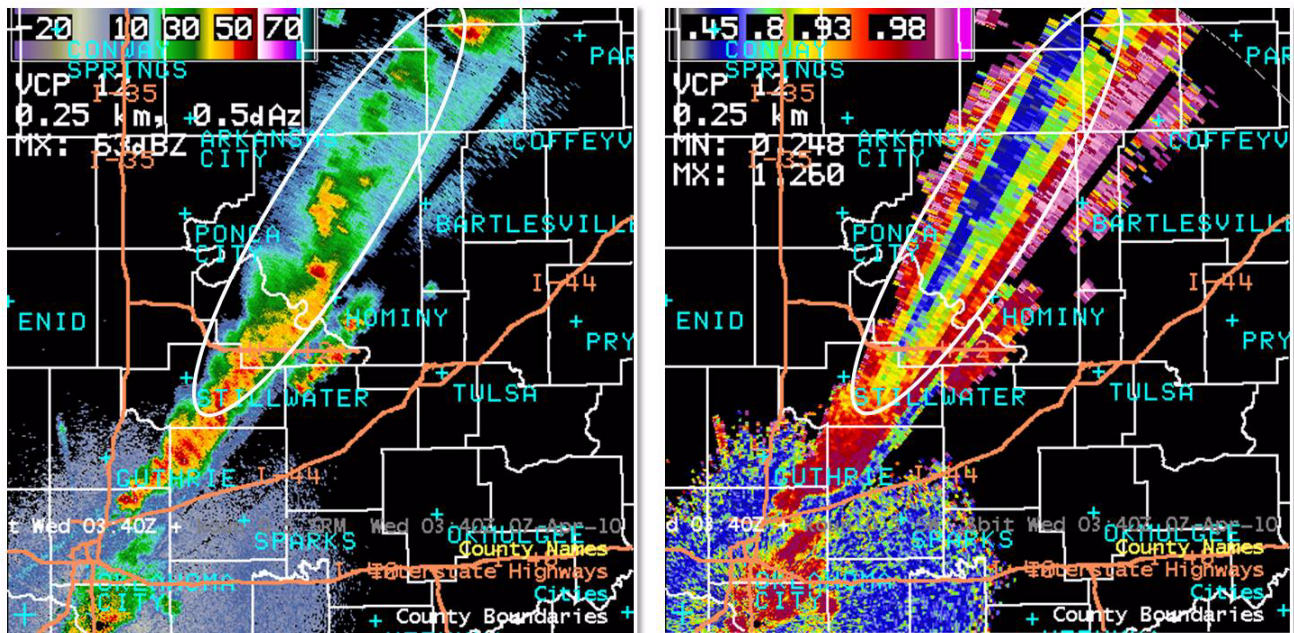


Figure 1-10. Reflectivity (left) and CC (right) images of a line of storms. Notice how the alignment of storms along a radial reduce CC in the same region due to non-uniform beam filling.

Range Folding in Batch Cuts

Sometimes in the batch cuts, range folding may obscure some of the CC data. As a refresher, the batch cuts for the WSR-88D network are elevation angles between 1.65 degrees and 6.5 degrees. In these cuts each radial uses a series of alternating low and high PRF pulses. The dual-pol variables are only computed using the high PRF pulses which are subject to range folding. Figure 1-11 shows an example from the 2.4 degree elevation scan. Note that where there is range folding in the velocity, there is also range folding in CC.

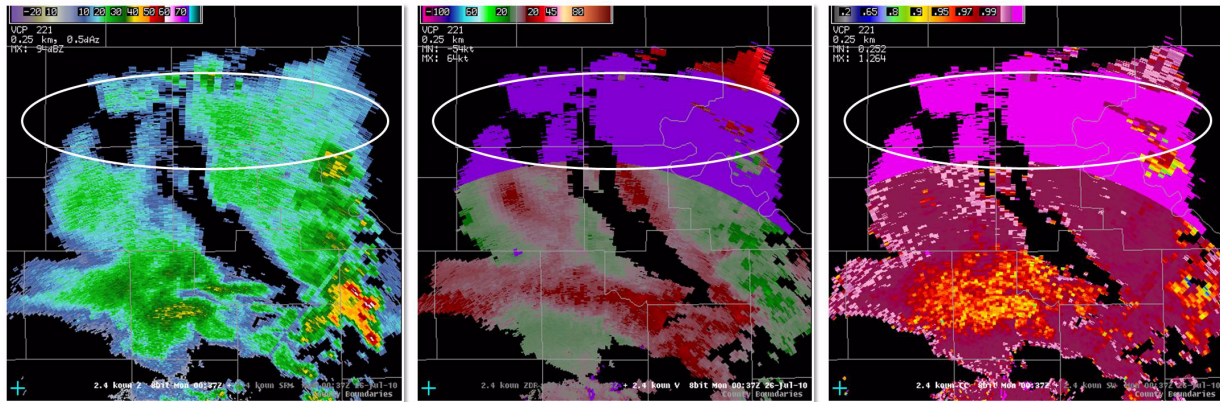


Figure 1-11. Reflectivity (left), Velocity (middle) and Correlation Coefficient (right) showing range folding in the batch cut elevations.

CC products can be used to aid in identifying the following:

- Meteorological vs. Non-meteorological
- Melting layer
- Rain vs. snow
- Large hail
- Irregularly shaped hydrometeors
- Tornadic debris

Correlation Coefficient (CC) Operational Applications (Strengths)

The biggest advantage of correlation coefficient is its ability to discriminate between meteorological and non-meteorological echoes. In the reflectivity image in Figure 1-12, we see a line of storms oriented SW to NE just south of the radar (largest oval). Just behind the line indicated with an arrow are some high reflectivity echoes, but something does not look right about them. If the reflectivity product were looped or the velocity product was consulted, it would become evident that it is AP. However, this AP extends right into the line of precipitation (medium and small ovals) and it is more difficult to tell that it is AP anymore. In addition, non-zero velocities are starting to show up (not shown). Looking at the CC image (right) in Figure

Meteorological and Non-meteorological Echoes

1-12, the AP can be identified in regions of low CC, whether it is by itself or embedded in precipitation (white oval). When trying to distinguish precipitation from AP, look for smooth fields of CC greater than 0.9. Figure 1-12. Areas of noisy CC less than 0.85 most likely indicate non-precipitation echoes. Be sure to compare CC with Z, V and ZDR for a more effective analysis. More information on identifying meteorological versus non-meteorological echoes will be covered in the “Non-Precipitation Echoes” application module.

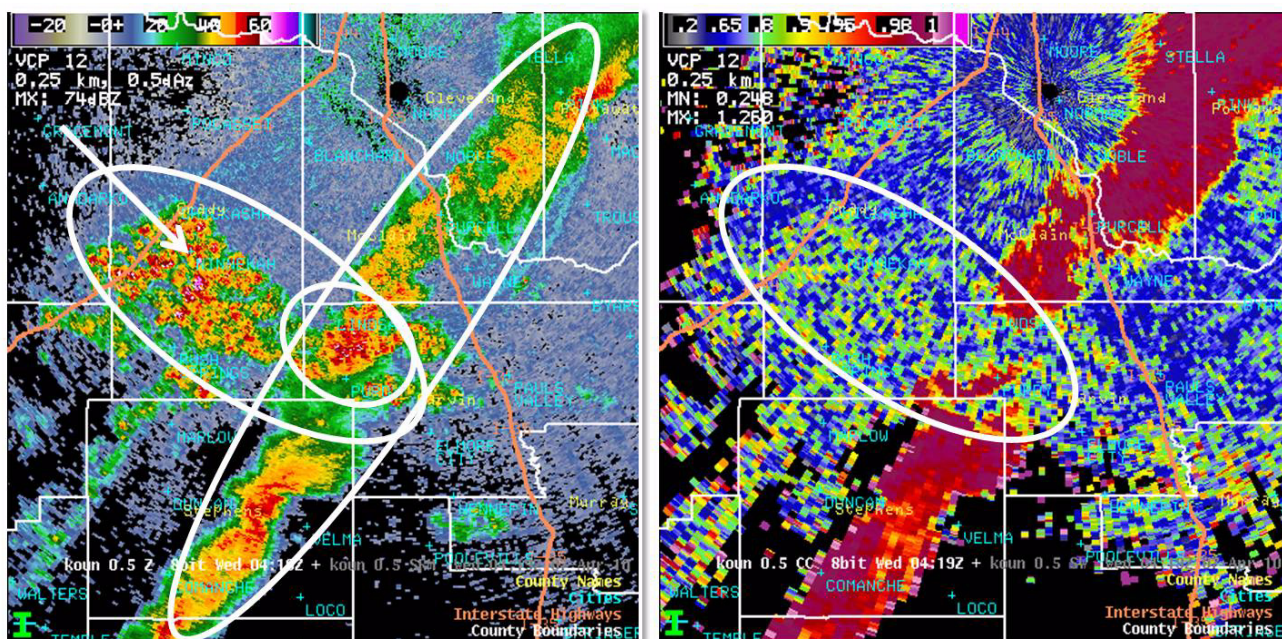


Figure 1-12. Reflectivity (left) and CC (right) showing that non-meteorological echoes (in this case AP) can be distinguished from meteorological echoes by their low (<0.85), noisy CC.

Melting Layer

Another significant advantage of correlation coefficient is identification of the melting layer. In reflectivity the melting layer is often identifiable as a bright band, but not always. With correlation coefficient the melting layer is usually identified by a ring of low correlation coefficient (~0.85) surrounded by higher correlation coefficient (~0.98) as seen in Figure 1-13. This signature is due to the presence of mixed-phase hydrometeors. The outer edge of the ring marks the height where dry snow begins

to melt and transitions to wet snow. The inner edge of the ring marks the height where the wet snow becomes a water droplet with some ice at its core.

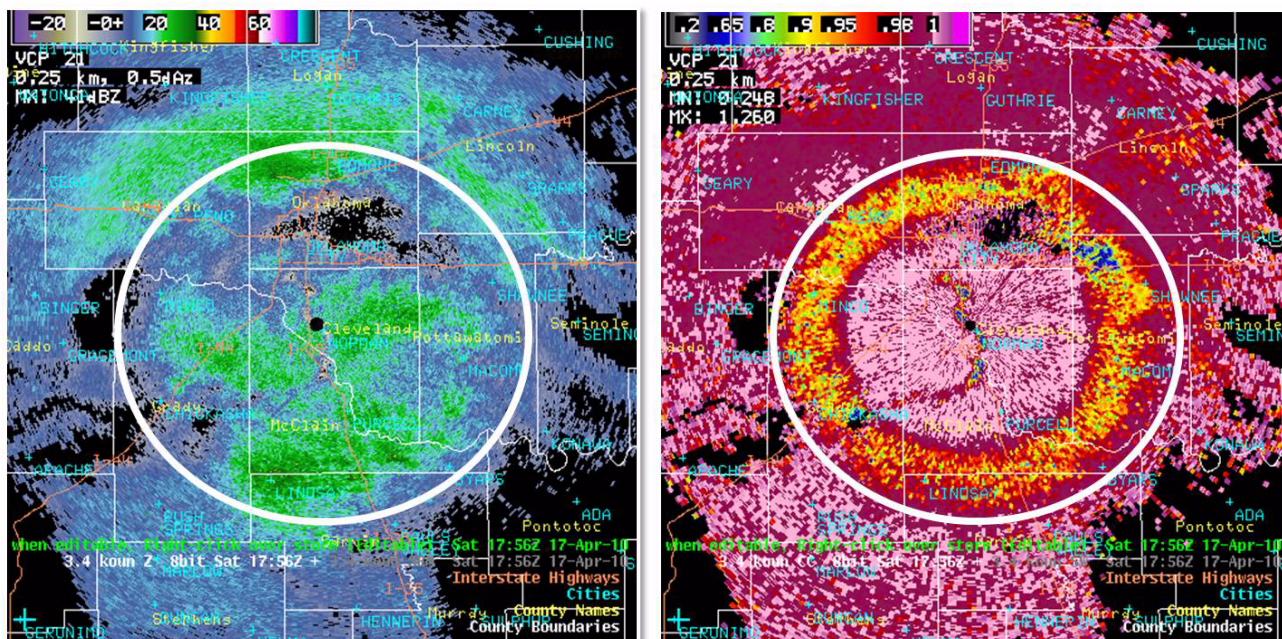


Figure 1-13. Reflectivity (left) and CC (right) show the distinct signature of CC in the melting layer illustrated in this example. Notice the bright band isn't visible in Z.

During the transition period of rain to snow at the ground, CC can help a forecaster better geographically locate the transition from rain to snow. It is simply the manifestation of the melting layer signature near the ground. Therefore, look for a drop in CC associated with the melting of snow to rain near the surface. As always, be sure to compare radar data with other observations (i.e., surface observations, etc.). Thus, overlay surface observations (if available) when trying to identify this feature and add other polarimetric variables (i.e. differential reflectivity) to help in delineating rain vs. snow at the ground.

Rain vs. Snow

In Figure 1-14, east of the radar there are some strong returns and surface temperatures that are near 0°C. However, reflectivity alone is not enough

to indicate what type of precipitation is occurring at the ground. When CC is added to the analysis, it becomes readily apparent where the transition from rain to snow is occurring. East of the white line in Figure 1-14, CC values are between 0.9 and 0.95. Surface temperatures are just above freezing and METAR data in these areas indicated rain. The reduced CC values in this area suggest a mixture of hydrometeors and are a good indication of melting going on at the height of the beam. To the west of the white line, CC remains very high (~0.99) and there is no indication of a comparable melting layer on the north or west side of the domain. In this area, surface temperatures remain below freezing and snow is being reported. Therefore, this transition from fairly uniform high CC to reduced CC east of the radar is a good indicator of the location of the rain/snow transition.

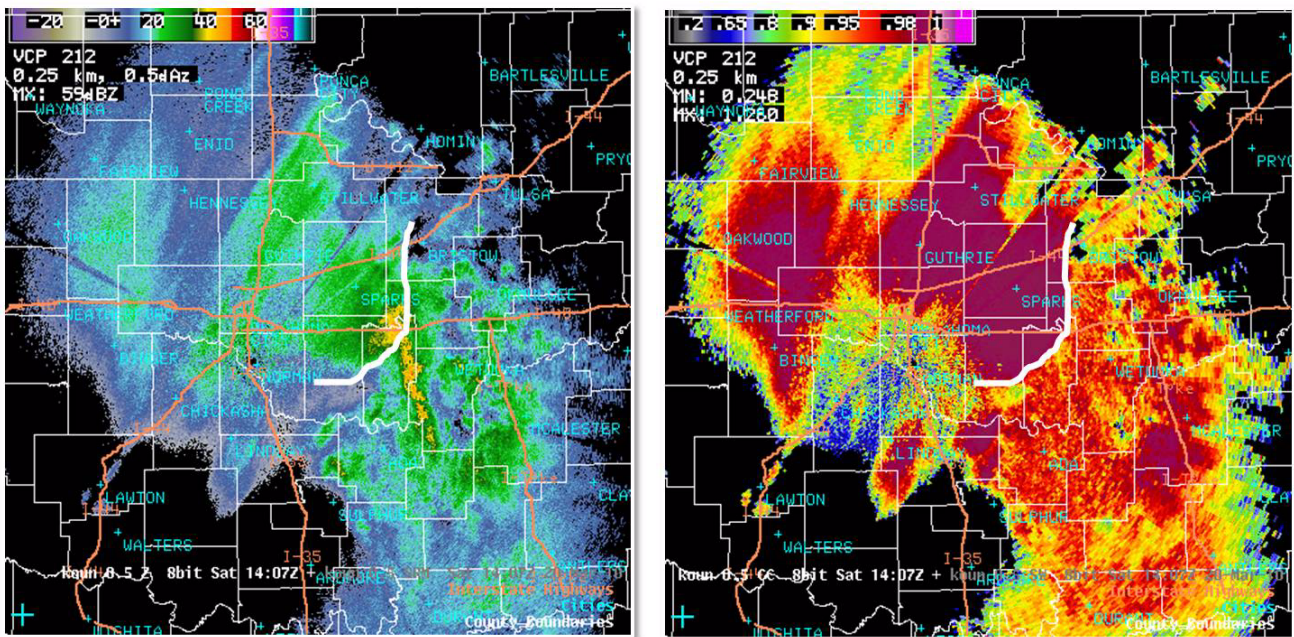


Figure 1-14. Reflectivity (left) and CC (right) show rain-snow transition marked by a white line separating areas of high and low CC

Significant Severe Hail

Large hail, which is defined here as greater than one inch in diameter, will have significantly reduced correlation coefficient. Typical values will

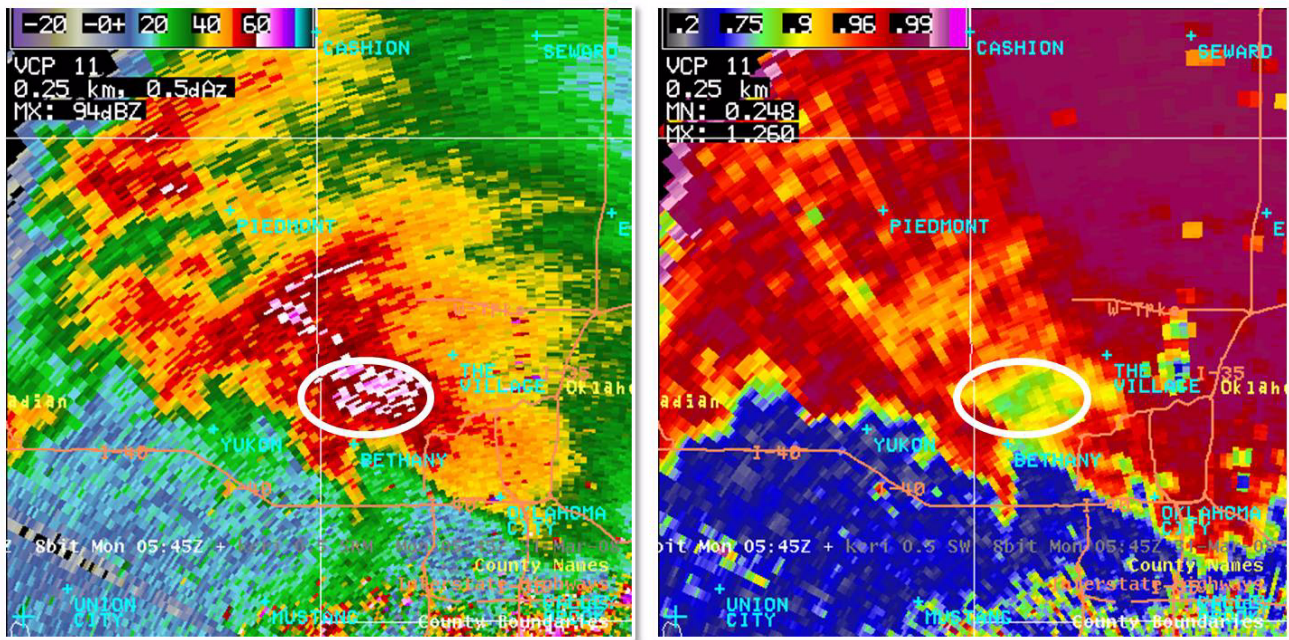


Figure 1-15. Reflectivity (left) and CC (right) from a supercell storm. Large hail was occurring inside the oval. Note the reduced CC.

start out around 0.93 and decrease to as low as 0.8 as the hail becomes significantly large. There have not been research yet on the ability to discriminate between sub-severe and hail up to roughly golfball in diameter. However, a significant drop in correlation coefficient to roughly 0.80 is associated with increased Mie scattering effects and thus potential for hail larger than golfballs at the ground.

Giant hail, which is defined historically as greater than 2 inches in diameter, is an example of this more pronounced reduction in correlation coefficient due to Mie scattering effects. Typical values will decrease to as low as 0.8 as the hail becomes significantly large (> 3.5 inches in diameter). Some cases have had CC as low as 0.7, though this is rare! Figure 1-15 shows reflectivity and correlation coefficient for of a supercell in NW Oklahoma City. 2.5 inch hail was reported at the ground inside the white oval. Note the high reflectivity and low CC.

Irregularly Shaped Hydrometeors

As is often the case, if giant hail has a complex shape (i.e. many protuberances), the correlation coefficient will decrease even further due to the complex scattering nature of the hail. Figure 1-16 shows a 7-inch hailstone with many protuberances. If measured by dual-pol radar, this hailstone most likely would have had very low CC (probably below 0.8).



Figure 1-16. One of the Aurora, NE hailstones of 22 June 2003.

Tornadic Debris

When a tornado is located near a radar (within ~75 km) and is causing considerable damage to structures, this lofted debris has been noted to produce a distinct radar reflectivity signature (i.e. debris ball). In correlation coefficient, the debris field is noted by a significant drop due to complex scattering by the debris. It is important to remember that this signature will only appear if a tornado is already occurring and producing damage. It is not a precursor signature!

A significant drop in correlation coefficient will occur only in areas where considerable surface “tracers” are lofted high enough to be seen by the

Lesson 2: Differential Reflectivity (ZDR)

Differential Reflectivity (ZDR) provides information about the median shape of the radar echo, and because of this, provides a good estimate on the median size of rain drops and for the detection of hail. ZDR is available in 4-bit and 8-bit data levels, each with a unique product resolution.

Differential Reflectivity (ZDR) Characteristics

8-bit Differential Reflectivity Resolution, Range, and Data Levels

- Resolution: 0.13 nm (0.25 km, 250 m) x 1.0 degree for all elevation angles and VCPs
- Data levels: 256
 - Min. = - 7.9 dB, Max. = + 7.9 dB
 - Precision: to the nearest 0.0625 dB
- Range: 162 nm
- RPG Product Code: DZD

4-bit Differential Reflectivity Resolution, Range, and Data Levels

- Resolution: 0.54nm (1 km, 1000 m) x 1.0 degree for all elevation angles and VCPs
- Data levels: 16
 - Min. = - 4 dB, Max. = + 6 dB
 - Precision: variable from 0.25 to 3 dB
- Range: 124 nm
- RPG Product Code: ZDR

Differential Reflectivity Product Description

- RPG ID: kxxx (where xxx = 3-letter radar ID)
- Elevation Angle: x.x in degrees
- Product Name: 8-bit ZDR, 4-bit ZDR
- Date: Day of week, time in UTC and date

- Units: decibels (dB)

Differential Reflectivity Product Annotations:

- VCP: 11, 12, 21, 121, 211, 212, 221, 31, or 32
- Range resolution: 0.25 km (8-bit), 1 km (4-bit)

All overlays are displayable on this product.

D-2D ZDR Display ZDR as seen in D-2D is shown in Figure 2-1. A reflectivity image has been provided on the left for reference.

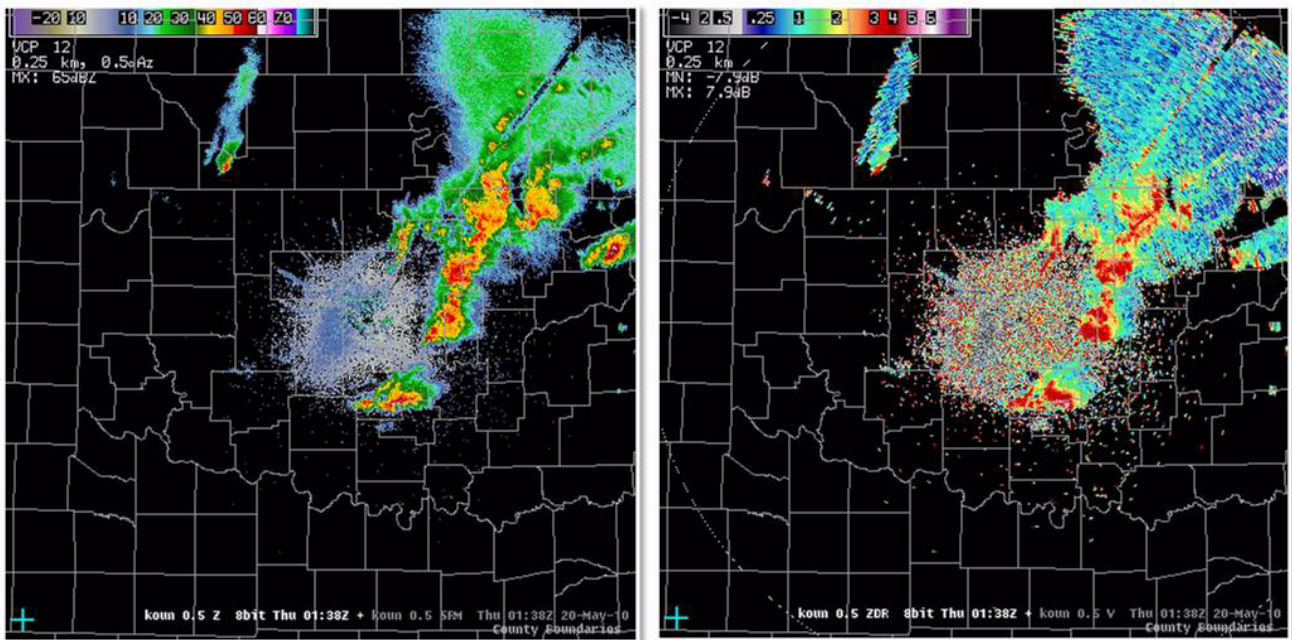


Figure 2-1. The image on the right is what the ZDR product looks like in D2D. A reflectivity image is shown on the left for reference

Individual ZDR products for each elevation angle can be found inside your dedicated radar's drop-down menu. ZDR can also be found in the 4-panel layouts combined with other data (see Fig. 2-2).

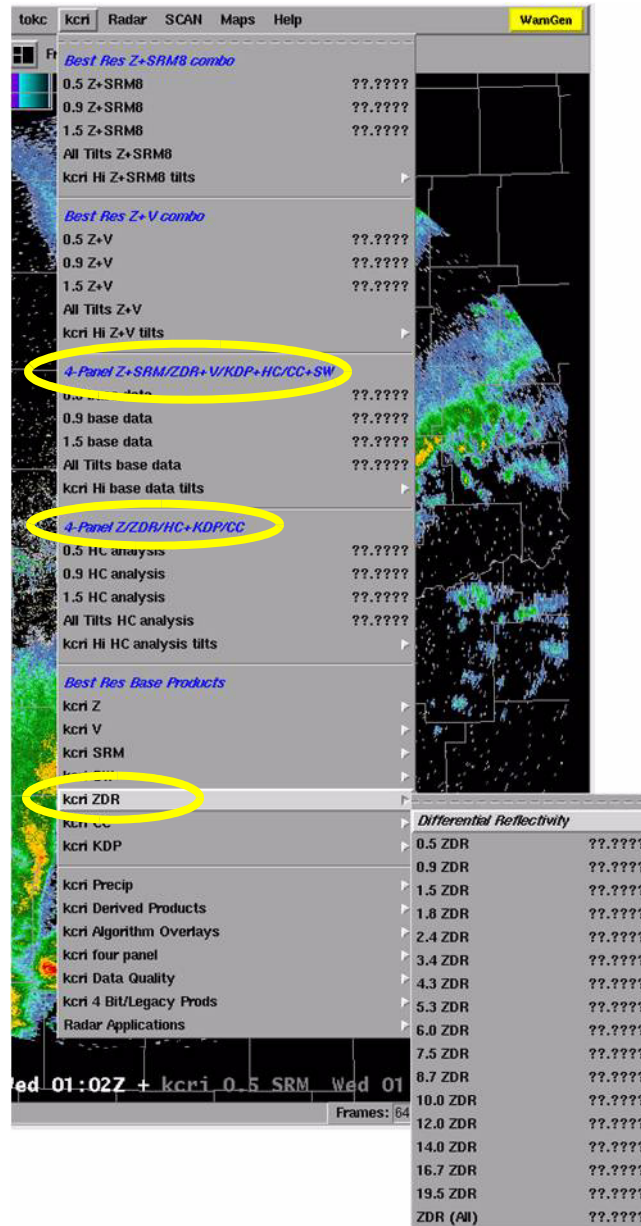


Figure 2-2. Menus for ZDR selection in AWIPS. ZDR products can be found in the sections indicated by yellow ovals.

Definition	Possible Range of Values	Units	Abbreviated Name
Difference between the horizontal and vertical reflectivity factors	-7.9 to +7.9	Decibels (dB)	ZDR

$$ZDR = Z_H - Z_V$$

Figure 2-3. Differential Reflectivity definition, characteristics and equation.

What is Differential Reflectivity?

Differential reflectivity is a measure of the log of the ratio of the horizontal to vertical power returns in a pulse volume. In dBZ units, it is the difference between horizontal and vertical reflectivities (see Fig. 2-3). Its values range from -7.9 to 7.9 decibels (dB). In AWIPS and the literature, differential reflectivity is abbreviated as ZDR.

The ZDR product in AWIPs D-2D displays values from -7.9 to +7.9 dB. However, when values dip below -3.956 dB, cursor readout will not show the actual product value, it will show a ~-3.956, as

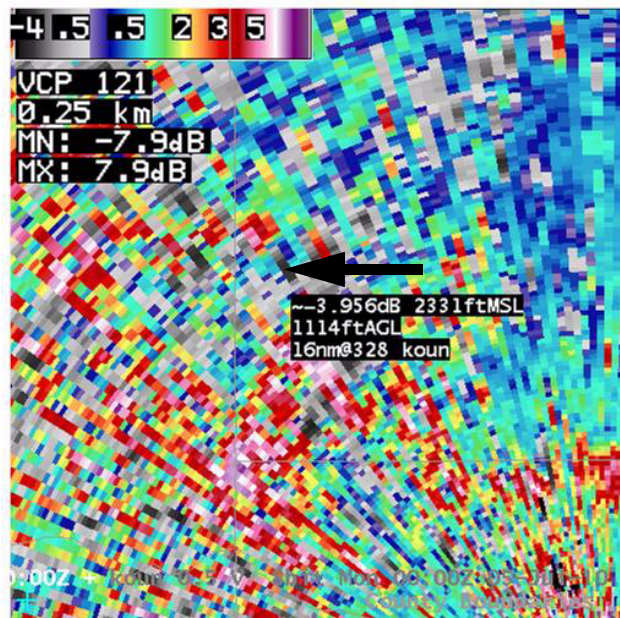


Figure 2-4. The arrow points to pixel with actual ZDR less than -3.956dB. However, cursor readout does not go below this value, so ~-3.956dB is displayed.

seen in Figure 2-4. This should not inhibit physical interpretation as most meteorological scatterers will produce values greater than -2dB.

The chart in Figure 2-5 summarizes the general physical interpretation of differential reflectivity. For spherical hydrometeors such as drizzle, the reflectivity values for both the horizontal and vertical dimensions of the hydrometeors are approximately equal. This leads to a difference of horizontal to vertical reflectivity of approximately 0, which means ZDR is approximately 0 dB. The same logic can be applied for the horizontally and vertically oriented columns. Horizontally oriented hydrometeors such as rain drops will have a positive ZDR, while vertically oriented hydrometeors such as ver-

Physical Interpretation

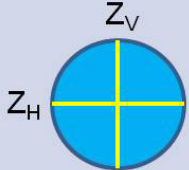
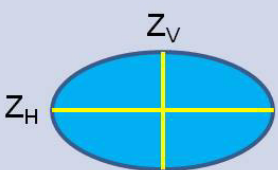
<u>Spherical</u> (drizzle, small hail, etc.)	<u>Horizontally Oriented</u> (rain, melting hail, etc.)	<u>Vertically Oriented</u> (i.e. vertically oriented ice crystals)
		
$Z_H \sim Z_V$	$Z_H > Z_V$	$Z_H < Z_V$
$Z_H - Z_V \sim 0$	$Z_H - Z_V > 0$	$Z_H - Z_V < 0$
ZDR ~ 0 dB	ZDR > 0 dB	ZDR < 0 dB

Figure 2-5. Differential reflectivity (ZDR) is a good indicator of the mean drop shape of the dominant hydrometeor within the resolution volume.

Typical Values for ZDR (dB)

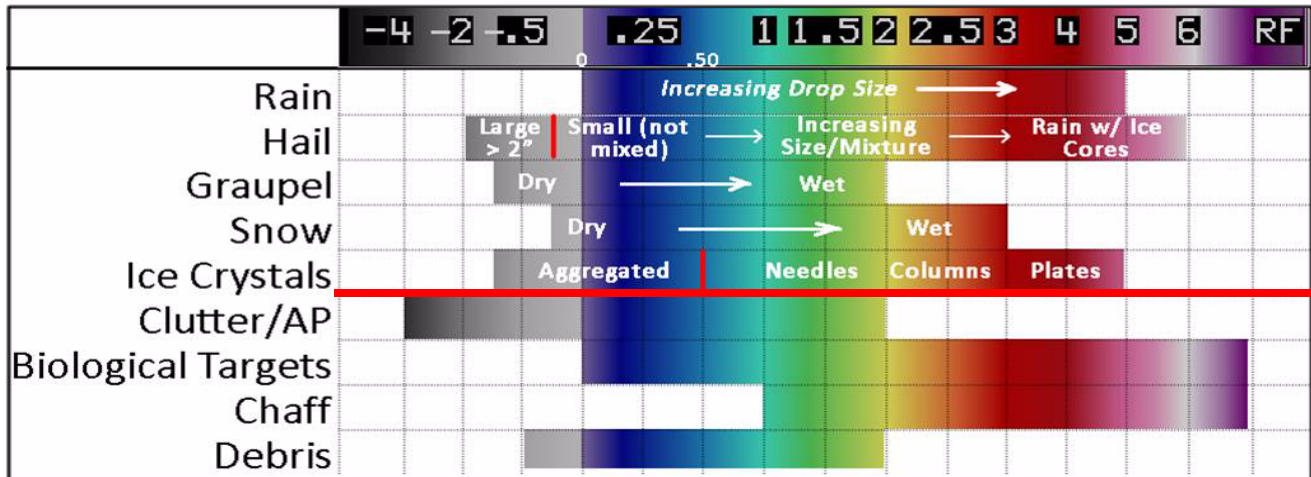


Figure 2-6. Typical values for differential reflectivity for the echo types listed on the left side.

tically oriented ice crystals will have negative a ZDR.

Let's consider typical values of ZDR by taking a moment to review Figure 2-6. Notice how there is not as clear of a break between meteorological and non-meteorological echoes (indicated in the figure with a horizontal red line) as with the Correlation Coefficient.

That being the case, it is important to delve a little deeper into different hydrometeor and non-hydrometeor types and examine their typical ZDR values. The types we will examine are:

- Rain
- Hail
- Snow and ice crystals
- Non-meteorological echoes

Rain The nice thing about rain is that there is a pretty strong relationship between raindrop diameter and shape. Smaller rain drops tend to be spherical, but as the raindrops become larger, they become

more oblate. This relationship between raindrop diameter and shape leads to a very nice relationship between major axis diameter (the large dimension of the rain drop) and the ZDR value. This concept is summarized in the chart in Figure 2-7. For example, when the major axis of a rain drop has a diameter of 1.75 mm, the ZDR is approximately 1.9 dB. However, when the diameter of a rain drop has a diameter of 4.00 mm, the ZDR is approximately 4.5 dB.

Major Axis Diameter (mm)	Image	ZDR (dB)
< 0.3 mm		~ 0.0 dB
1.35 mm		~ 1.3 dB
1.75 mm		~1.9 dB
2.65 mm		~2.8 dB
2.90 mm		~3.3 dB
3.68 mm		~4.1 dB
4.00 mm		~4.5 dB

Figure 2-7. Theoretical relationship between major axis diameter and corresponding ZDR value for rain.

Hail Unlike rain, hail does not have a definite relationship between size and shape because the shape of hail varies for any given size. Also, hail tends to tumble as it falls. The effective spherical appearance biases ZDR toward 0 dB when hail is present within the sample volume (see Fig. 2-8). A classic hail signature in dual-pol occurs when high Z is associated with low ZDR. There is an exception when small hail (typically 1 inch or less) becomes completely water-coated due to melting processes. A small, water-coated hailstone tends to stabilize, causing the hailstone to appear as a giant raindrop to the radar. This leads to very high ZDR values on the order of 5 to 6 dB in some cases.

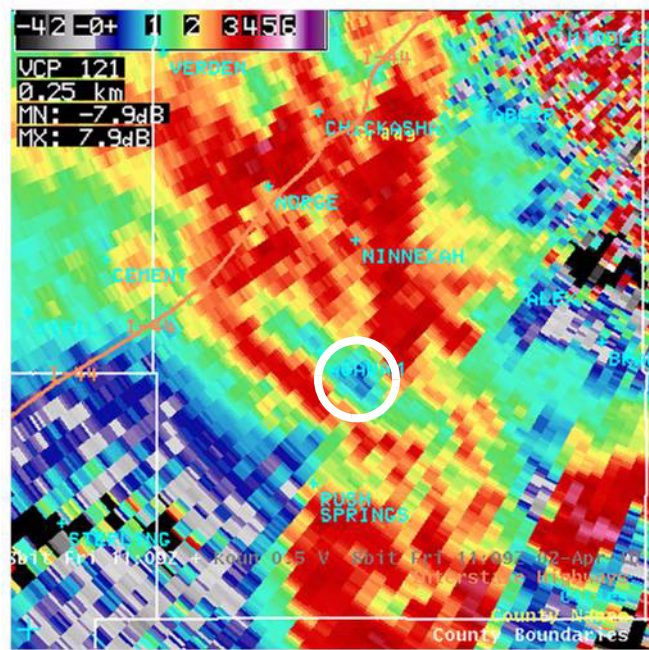


Figure 2-8. Case where hail is falling at the area indicated by the white circle. Note the small ZDR values relative to its surroundings.

Snow and Ice Crystals Snow and ice crystals probably make up the most widely varying areas of ZDR physical interpretation and are also among the less understood/researched areas. Snow and ice crystals

can take on different sizes and shapes along with varying degrees of particle density. With snow, it's helpful to know if it is wet snow or dry aggregated snow. With ice crystals, knowing whether they are low-density or high density is useful. Is it a needle, plate or column? Are they preferentially aligned? Theory has tried to explain what ZDR values to expect in snow and ice, and some research has been conducted to understand it better with observations, but lack of verification has made it difficult.

Some recurring themes have emerged that look promising. First, aggregated dry snow (dry means no trace of melting, aggregated means clusters or two or more crystals stuck together) tends to have very low ZDR (~0.2 to 0.3 dB) and very high CC (0.98 or 0.99). Wet snow tends to have higher ZDR (~2-3 dB) because it is starting to acquire a water coating and appears as giant raindrops, and much lower CC (< 0.97). Ice crystals have much more variability due to their various shapes and sizes, potential to be high-density or low-density, and variability of alignment. Typically ice crystals will fall with no preferred orientation and will be low density leading to weakly positive ZDR (< 1 dB). However, there are times when they can become preferentially aligned which can lead to very high positive or slightly negative ZDR, depending on the nature of the orientation. The chart in Figure 2-9 gives expected ranges of ZDR for different types of snow and ice.

Snow	ZDR
Dry / Aggregated	0.2 to 0.3 dB
Wet / Melting	2 to 3 dB
Ice	ZDR
Low-density / Random orientation	< 1 dB
High-density / Preferred Orientation (Horizontal)	As high as 4 to 5 dB
High-density / Preferred Orientation (Vertical)	- 2 to 0 dB

Figure 2-9. This chart shows expected values of ZDR for different types of snow and ice crystals.

Non-Meteorological Echoes

Non-meteorological echoes have even more variability in shapes and sizes than do meteorological echoes thus increasing the variability of ZDR values for these echo types. The types of non-meteorological echoes forecasters using dual-pol radar will be able to distinguish are ground clutter, normal or anomalous propagation (AP), biological scatterers and chaff. For ground clutter ZDR will typically appear very noisy and have both high and low values. Birds and insects, however, have a little more stability in ZDR values and can give you a clue into their orientation and flight direction. There will be more information on this at the end of the lesson in the section for ZDR applications.

The major limitations of ZDR involve:

- Bias towards larger hydrometeors
- Particle density
- Mie scattering
- Low signal to noise ratio (SNR)
- Depolarization
- Range folding in the batch cuts

Differential Reflectivity Limitations

Recall that radar reflectivity is strongly dependent on particle diameter. Since ZDR is the difference between the horizontal and vertical reflectivity, and reflectivity is biased towards larger particles, ZDR likewise will be biased towards larger particles. Even though there may be a mixture of hydrometeor types and sizes within the pulse volume, the ZDR value displayed will be weighted toward the larger hydrometeors' intrinsic values.

Bias Towards Larger Hydrometeors

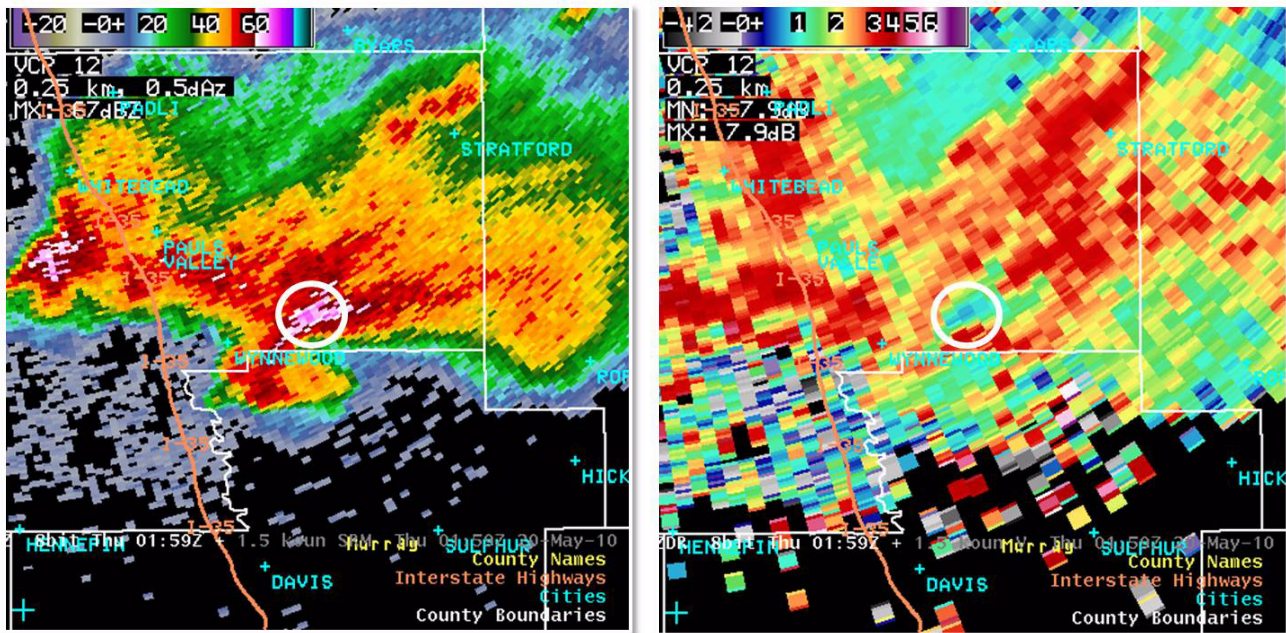


Figure 2-10. Reflectivity (Z, left) and Differential Reflectivity (ZDR, right) of an intense convective storm. Note that in the high Z core (white circle), ZDR is very low. This is from hail.

Looking at Z in Figure 2-10, there are values upward of 65 to 70 dBZ, indicating hail is present.

Upon inspection of ZDR, we see values of approximately or slightly less than 1 dB. Recall that with pure hail the expected value of ZDR would be near 0 dB ZDR, and with pure rain it would be 2 or 4 dB for higher Z. Therefore, the hydrometeors in Figure 2-10 most likely represent a mixture of hail and rain. ZDR is biased towards the lower values by the presence of the hail in the volume.

Particle Density Lower particle density will yield lower ZDR values. Figure 2-11 shows ice with a density of 0.92 g/mL compared to raindrops of the same size and concentration, but a density of 1 g/mL. Because the ice is less dense, it will yield lower ZDR values than the rain drop. In operations this will be noted by a general decrease in ZDR when the targets are ice (i.e. snow) rather than liquid (rain). NOTE: High density ice particles (needles) that are horizontally oriented can have significantly positive ZDR.

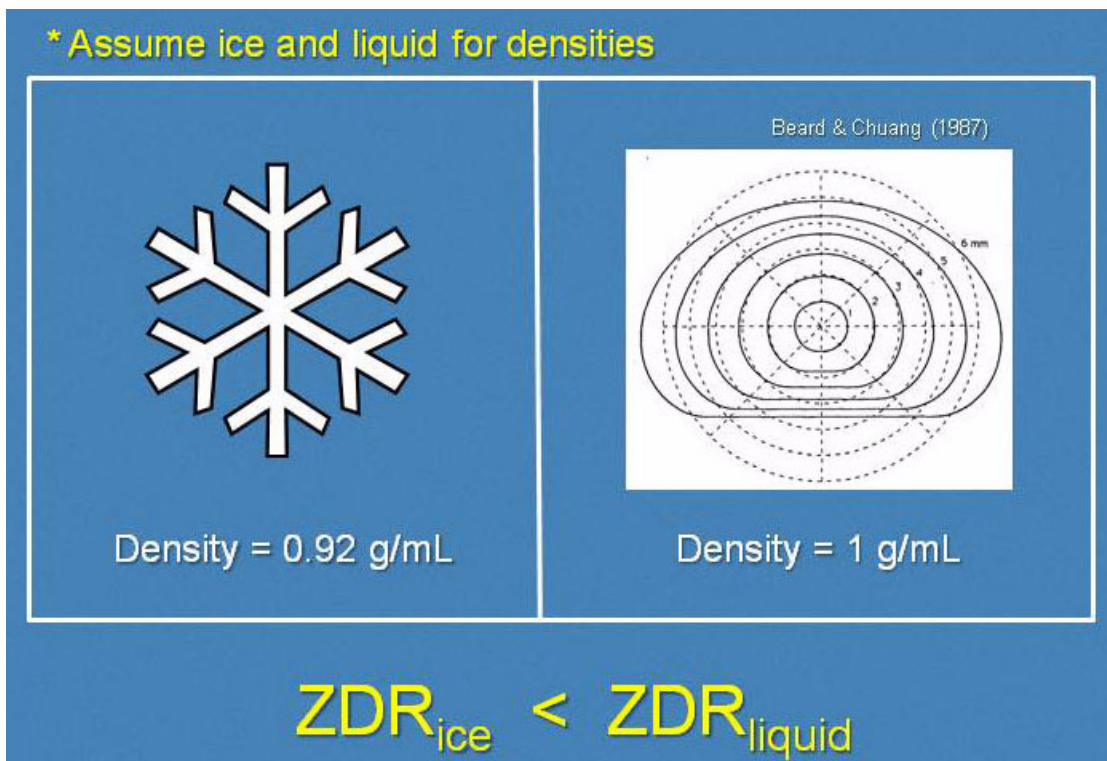


Figure 2-11. Precipitation particles can vary greatly in density leading to differences in ZDR despite having similar shapes and sizes.

Mie Scattering Effects

As a particle's diameter approaches 2 inches, ZDR can switch signs due to Mie scattering effects (see Fig. 2-12). For example, a horizontally oriented hail stone will typically have a positive ZDR. However, if the hailstone diameter is larger than 2 inches, it may have a negative ZDR due to Mie scattering effects. Keep in mind when viewing hail producing storms that a strong reflectivity core with negative ZDR may indicate very large horizontally oriented hail. Similarly, large, vertically-oriented particles may produce positive ZDR. To tell if a particular bin is experiencing Mie scattering effects, look at CC. CC for non-Mie, or Rayleigh, scattering should be higher (> 0.93), whereas for Mie scattering the CC should be lower (< 0.9).

Also note that the largest hail in supercell storms will often fall in the high reflectivity gradient adjacent to, but outside, the Z core. Thus, the effect of Mie scattering may not be confined to that high

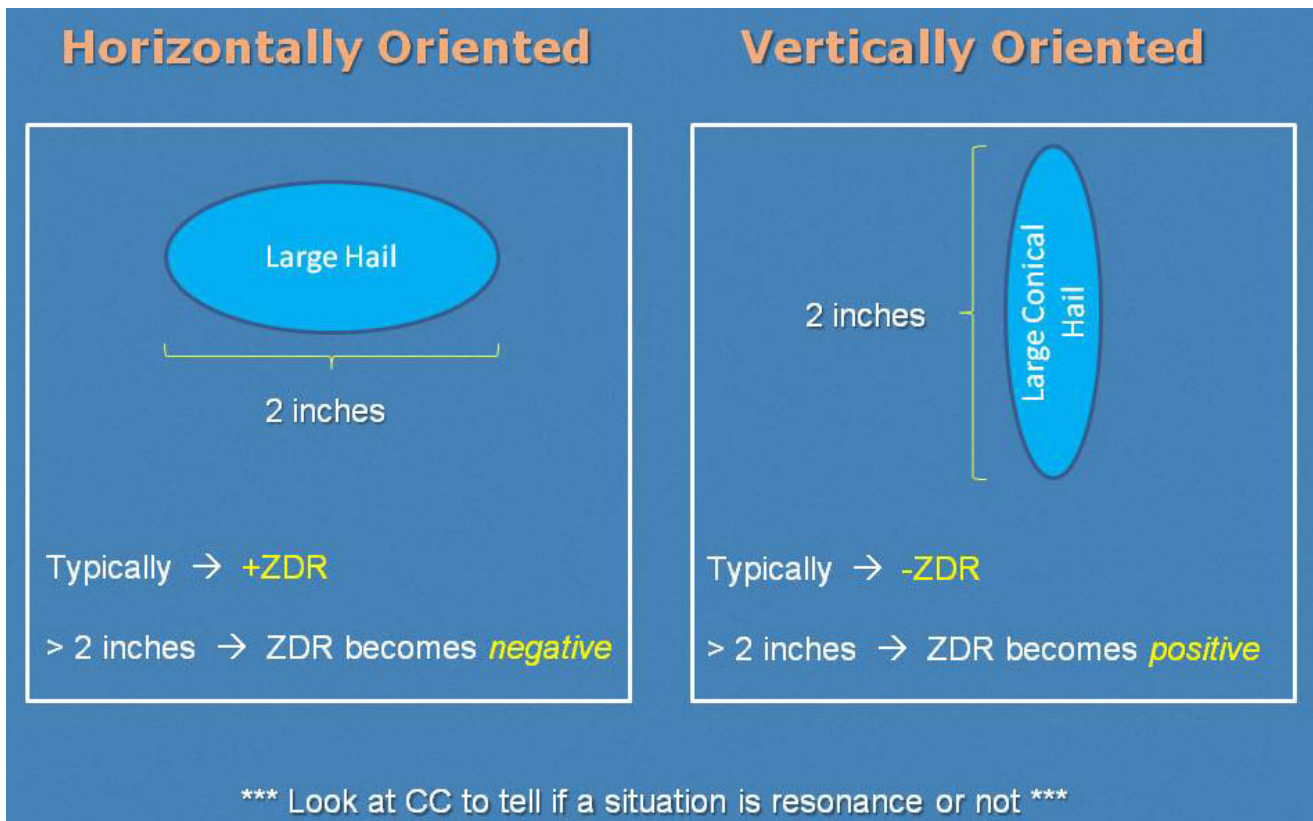


Figure 2-12. Mie scattering effects as a function of hydrometeor orientation and size. Note the switch in sign of ZDR at $D > 2$ inches.

reflectivity core. When the TBSS is present, there is a very strong likelihood of Mie scattering effects.

Low Signal to Noise Ratio/Correlation Coefficient

In regions of low signal-to-noise ration (SNR) and low correlation coefficient (CC), the differential reflectivity will be subject to significant error rates. Therefore, these regions may contain noisier ZDR data. Thus, be more skeptical of ZDR values in areas with CC is less than 0.9. Figure 2-13 shows data affected by low CC and low SNR. In the upper left portion of ZDR and CC, near the radar, CC is low and ZDR appears noisy (white oval). This is most likely due to non-meteorological echoes lowering CC and increasing the error in ZDR. On the southern side of the storm, the low CC appears to be due to the low SNR, which sub-

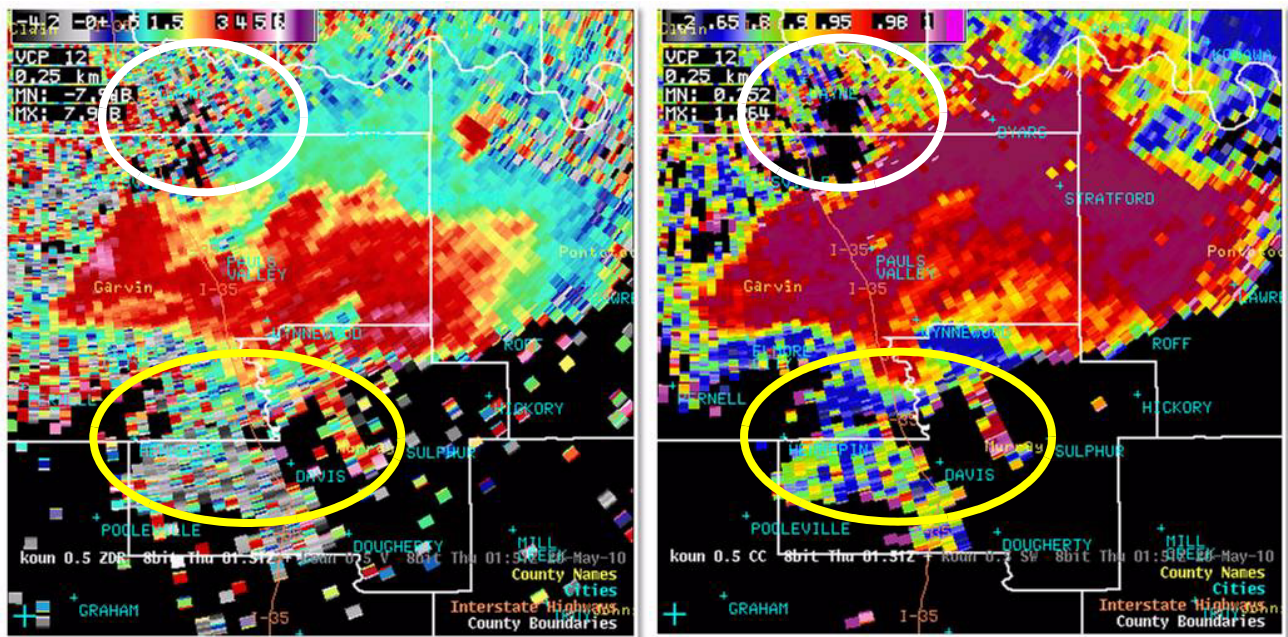


Figure 2-13. Example of how low SNR and low CC (right) can make ZDR (left) appear noisy. sequentially has increased the error in ZDR making it look noisy (yellow oval).

Sometimes a portion of a pulse will be scattered back towards the radar in the opposite polarization of the transmitted pulse. For example, a portion of the horizontally transmitted pulse may be reflected back to the radar oriented in the vertical. This switch in polarization of the returned power is referred to as depolarization. Depolarization happens only when the mean canting angle of the hydrometeors in a pulse volume is something other than 0° or 90° . In other words, the hydrometeors are not aligned in the plane of the transmitted pulses. This usually only occurs in ice crystals that are aligned by an electric field inside a thunderstorm, and is best seen at higher elevation angles. Depolarization only affects ZDR and shows up as radial spikes of high and/or low ZDR

Depolarization

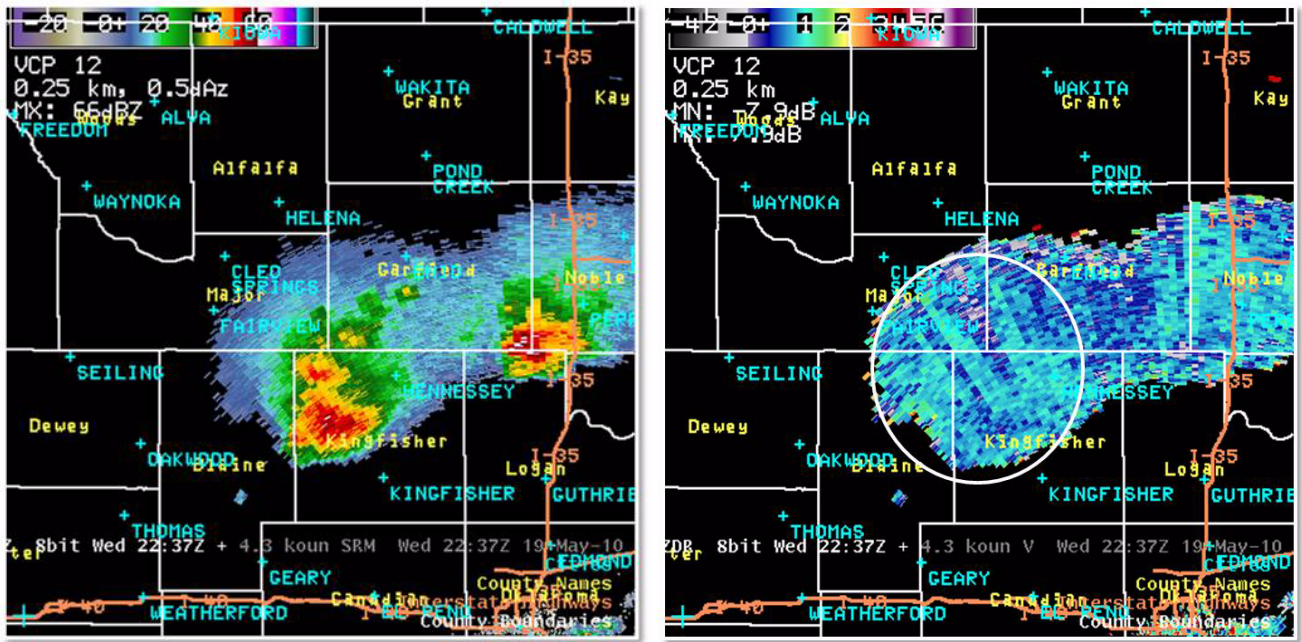


Figure 2-14. “Z (left) and ZDR (right) illustrating depolarization in supercell thunderstorms. Note the alternating radials of positive and negative ZDR (white circle).

based on the type of depolarization occurring in the region illuminated (see Fig. 2-14).

Batch Cuts & Range Folding

The last limitation of ZDR is that some signatures in ZDR may be obscured by range folding in the

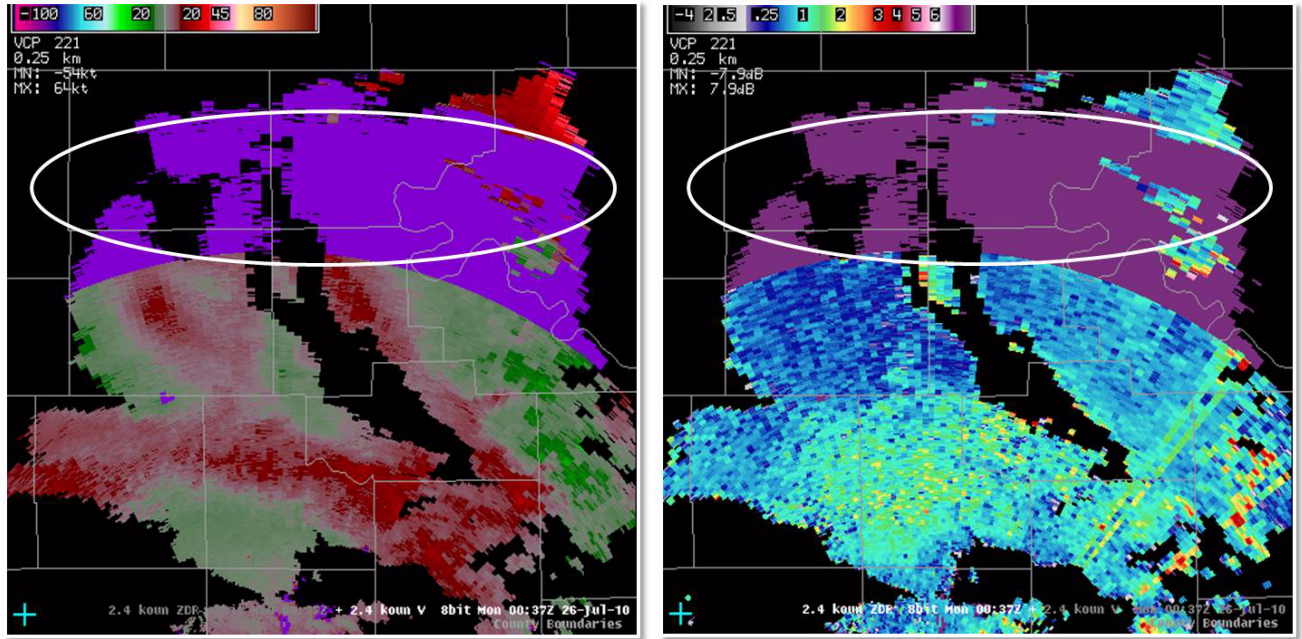


Figure 2-15. A storm that occurred 26 July 2010 at 0037 UTC from the 2.4 degree elevation scan. Note that where there is range folding in the velocity (left, white oval), there is also range folding in ZDR (right white oval).

batch cuts. Note that range folding in the ZDR product is expected to be in the same locations as in the velocity products (see Fig. 2-15). Recall, batch cut elevations are 1.65° through 6.5°.

Operational applications of ZDR include, but are not limited to, the identification of the following:

- Hail detection
- Updraft (ZDR Column)
- Tornadic debris identification
- Melting layer
- Rain/snow transition area
- Frozen precipitation types
- Non-meteorological echo (Birds/Insects)

Differential Reflectivity Operational Applications (Strengths)

More about these operational applications can be found in the Dual-Pol Applications section of the course and this training guide.

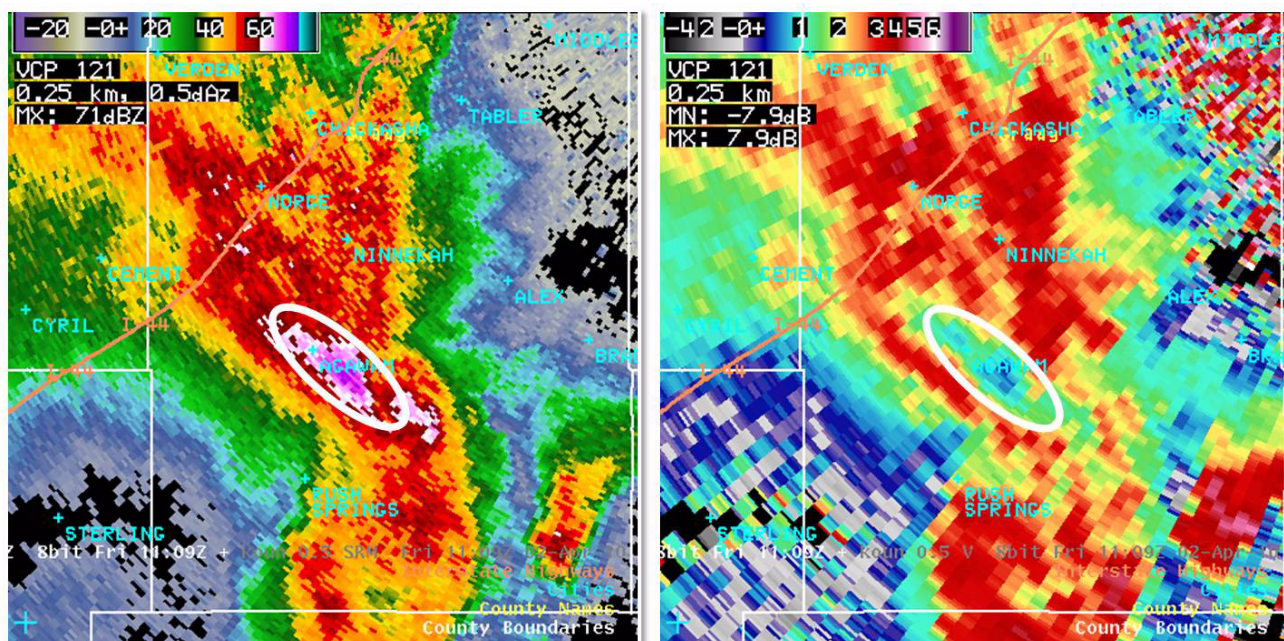


Figure 2-16. Reflectivity (left) and differential reflectivity (right) images showing a classic example of a hail signature. Note the high Z with low ZDR.

Hail Detection Figure 2-16 illustrates a common hail signature in ZDR. Here the storm has a high reflectivity core of around 70 dBZ, hinting that hail is a definite possibility. Associated with these high reflectivity values are low ZDR values (< 1.0 dB). High Z with low ZDR is an excellent signature for hail.

Updraft (ZDR column) When intense updrafts develop and enough liquid water is present within them, this liquid water will be lofted well above the environmental 0°C level. The result is an area of positive ZDR above the environmental 0°C level. Figure 2-17 shows an example of a ZDR column. The melting layer height was roughly 10,500 feet and we are looking at 15,700 feet. Note from the reflectivity image on the left, we see a supercell with an inflow notch and hook echo denoted by the white circle. The location of the inflow notch should be roughly the location of the low-level updraft. In the ZDR image in Figure 2-17, there is a localized area of enhanced ZDR (> 2 dB) in the same region. Thus, it is likely this is where a portion of the updraft is

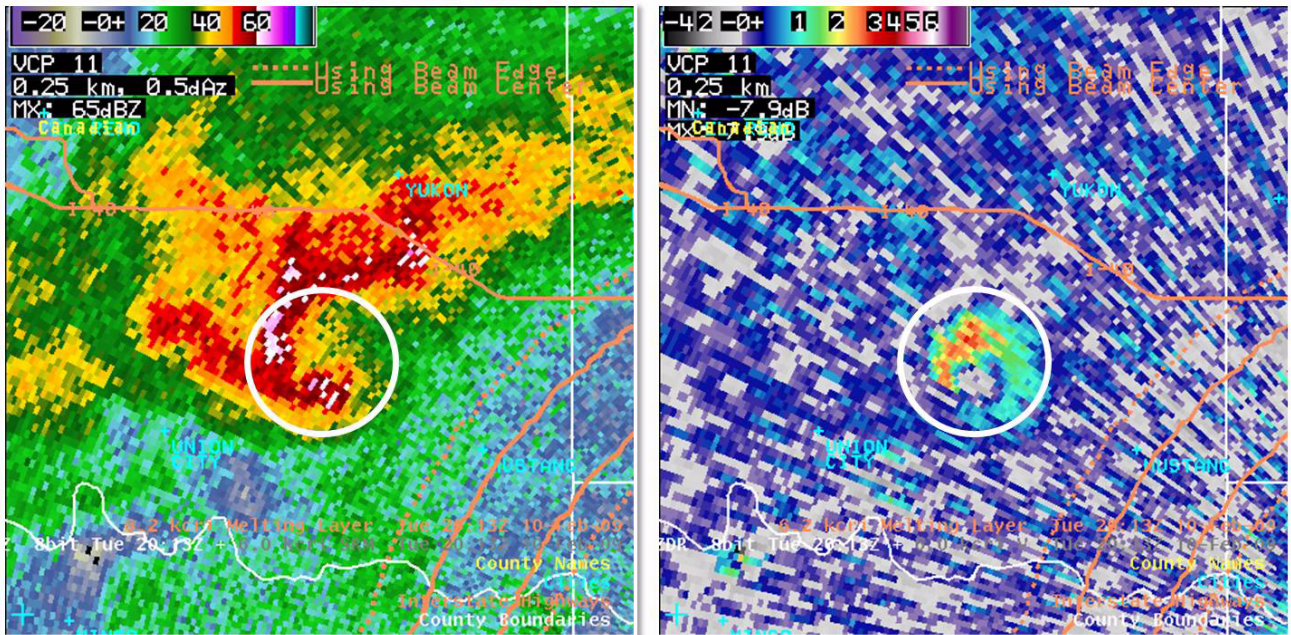


Figure 2-17. Reflectivity (left) and differential reflectivity(right) showing the relationship of a ZDR column (white circle) to the updraft region of a supercell.

located within this storm. Hail production is a certainty given the presence of liquid several thousands of feet above the 0°C level, but this doesn't necessarily mean severe-sized hail will reach the surface.

Figure 2-18 shows an example of how ZDR can be used to detect debris lofted by a tornado. On the left is a classic hook echo along with the associated velocity (middle) indicating gate-to-gate shear. In ZDR (right), we see a localized area of depressed ZDR values near the tip of the hook echo and co-located with the Doppler velocity couplet. These depressed ZDR values are caused by debris lofted by a tornado. The random orientation of the debris causes a local minimum in ZDR values. CC is typically the best indicator of lofted debris.

Tornadic Debris Signature (TDS)

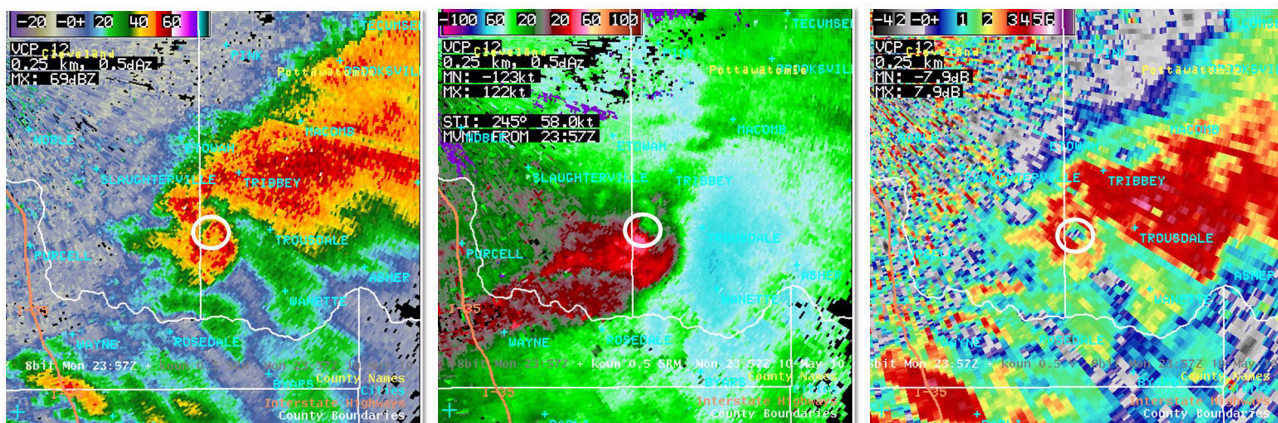


Figure 2-18. Reflectivity (left), velocity (middle) and differential reflectivity (right) for a tornadic storm. Note the encircled region in the hook echo on the reflectivity image and the matching ZDR image highlights a tornado.

When precipitation develops aloft in the form of snow, it may melt as it descends. These melting flakes are often detected as a “bright band” or layer of higher reflectivity. ZDR will also increase in the melting layer due to increased oblateness of the melting snow. Likewise, decreased CC within the melting layer will cause noisier ZDR. An exam-

Melting Layer

ple can be seen in Fig. 2-19 on page 1-45. Note that in this case there is not a pronounced ring of high reflectivity or bright band. However, in the ZDR image there is a ring of higher (and noisier) ZDR. This correlates well with the ring of low CC seen in the melting layer.

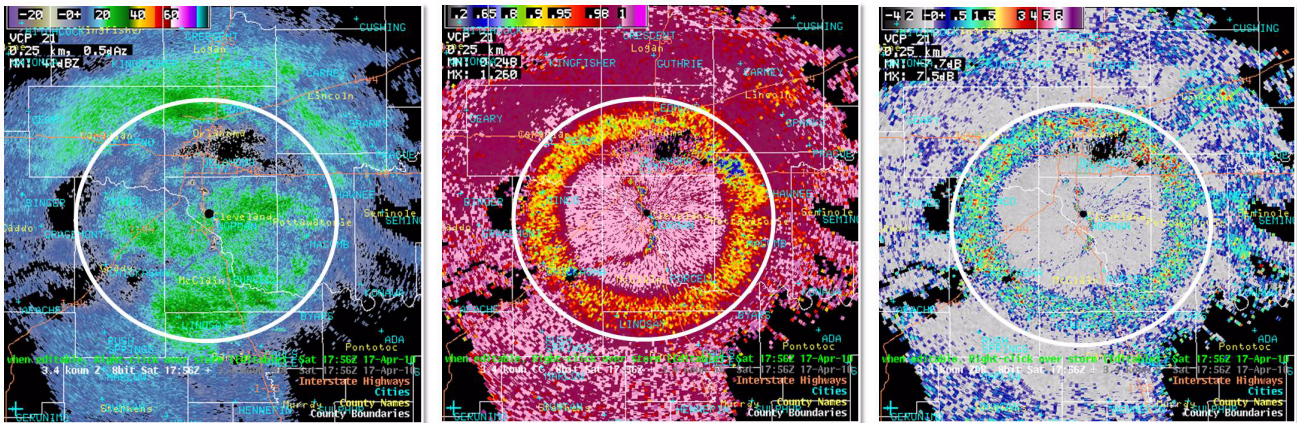


Figure 2-19. Reflectivity (left), correlation coefficient (middle) and differential reflectivity (right) of a melting layer at the 3.4 degree tilt during a stratiform rain event. Note that there is not a pronounced ring of high reflectivity typically associated with the bright band (melting layer), but there is a ring of higher (and noisier) differential reflectivity.

Rain/Snow Transition Area

ZDR in rain is typically greater than 1 dB, where ZDR in snow is typically less than 0.5 dB (exceptions being melting/wet snow and individual ice crystals). This fact often leads to a demarcation line between regions of rain and snow. In Figure 2-20 we see an example of the transition from rain to snow. At the surface, rain was occurring east of the white line and snow was occurring to the west. The reflectivity field shows some subtle differences which might indicate a change from rain to snow, but it is more obvious in the ZDR field. ZDR in rain was around 2 dB while in snow it was around 0.5 dB. It is important to remember to compare dual-pol data with surface observations for confirmation of precipitation type at the surface.

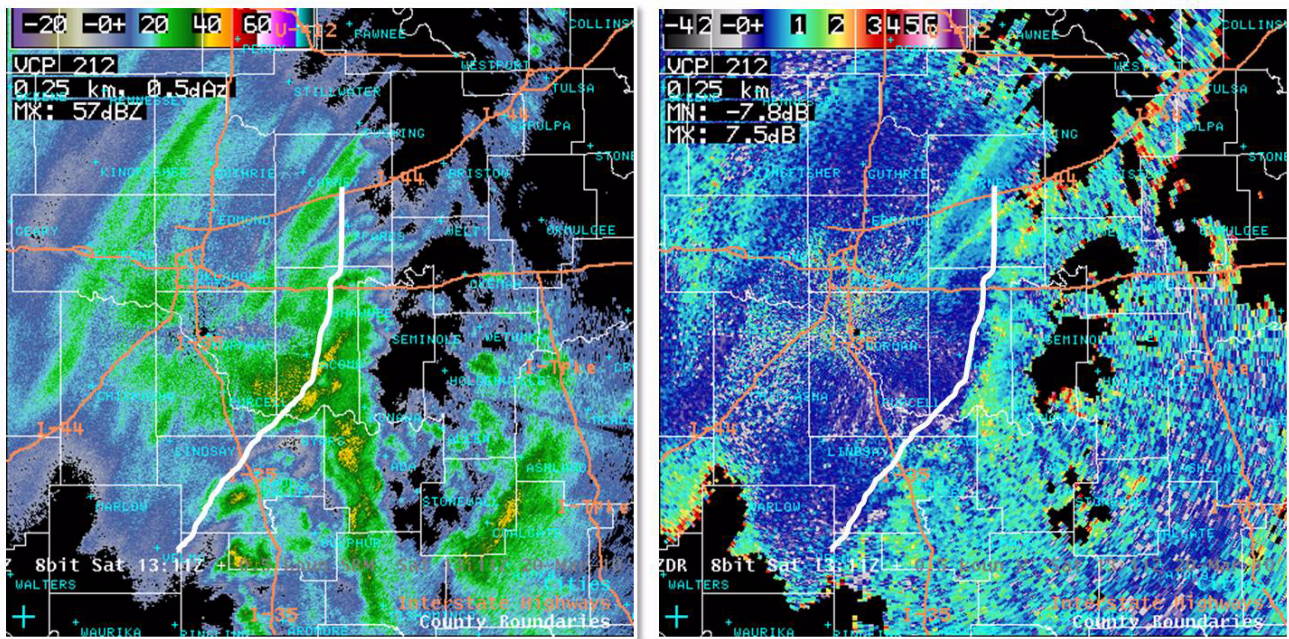


Figure 2-20. Reflectivity (left) and differential reflectivity (right) showing a rain-snow transition line (white line). Note that in the reflectivity image there is a subtle change in reflectivity “texture” when going from rain to snow but this is much more obvious in the ZDR image.

Typically ice particles will have low ZDR (< 1 dB) due to their low density nature. However, when high-density ice particles form and become oriented either horizontally or vertically, the ZDR will change. Horizontally-oriented, high-density particles will exhibit high ZDR (> 2 dB) and vertically-oriented, high-density particles will exhibit negative ZDR values. Therefore, ZDR in frozen precipitation might help determine the type of ice crystals that are falling. More research is needed on determining ice crystal type and if whether or not it provides any benefit.

Frozen Precipitation Types

As an example, in Figure 2-21, a NNE to SSW band of frozen precipitation is over SW Oklahoma, and ZDR values are in the 0.2 to 0.3 dB range along the southern end of the band. However to the north, ZDR values are approaching 1 dB. The reflectivity values in both regions are fairly similar. Most likely there are differences in the type of ice particles falling in these two regions, and it could be affecting the amount of snow fall at the ground.

Though it's understood that the type of snow is different (aggregated vs. not) in these two ovals, much more research is needed to determine how that affects snow accumulation.

Non-Meteorological Echoes (Birds/Insects)

Birds and insects will have distinct ZDR signatures. According to previous studies, birds will have ZDR values that are slightly less than insects. Values for birds can be anywhere from slightly negative (-2 to -3 dB) to substantially positive (+6 or +7 dB) mostly depending on the viewing angle and Mie scattering effects. For insects, ZDR values typically are positive and will range from +1 to greater than +7.9 dB. ZDR values also depend on viewing angle when it comes to insects, but not as much on Mie scattering because they are smaller than birds. Finally, birds are most prominent at night whereas insects are most prominent during the day, though both do co-exist quite often. Knowing your local bird/insect population and habits will help in interpretation.

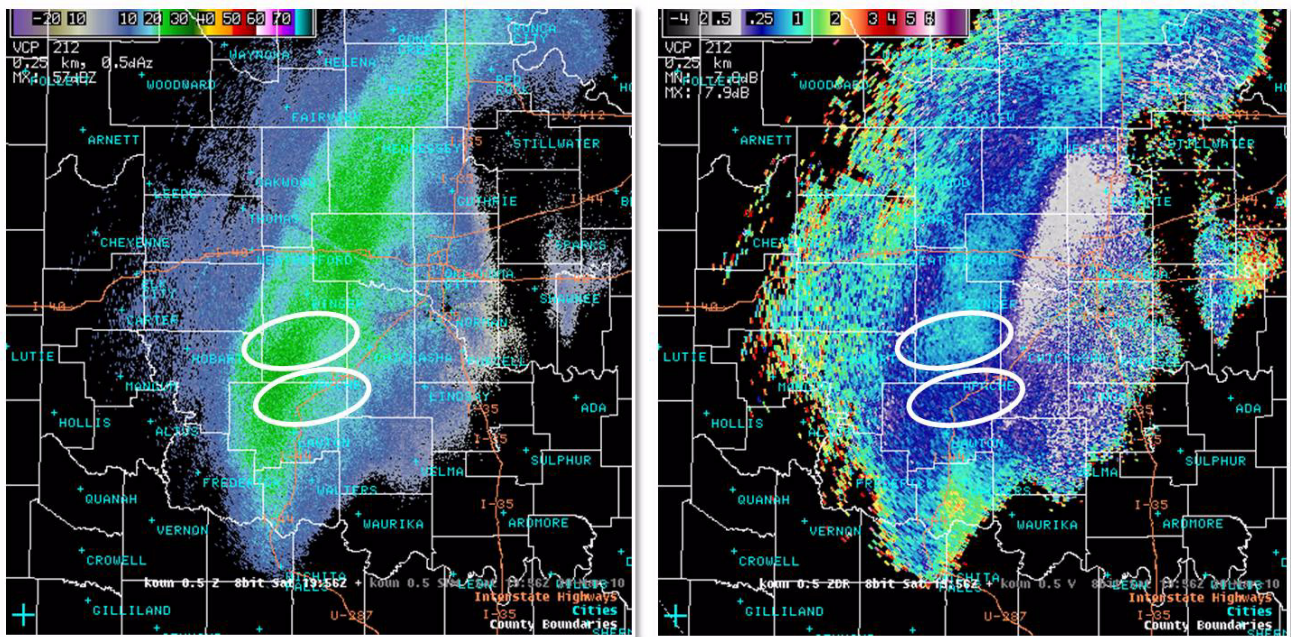


Figure 2-21. Reflectivity (left) and ZDR (right) of a band of frozen precipitation. Note the change in ZDR in the northern oval as compared to that in the south oval, indicating the presence of two different ice crystal types.

Lesson 3: Specific Differential Phase (KDP)

Specific Differential Phase provides information about liquid water content. Specific Differential Phase (KDP) is available in 4-bit and 8-bit data levels, each with a unique product resolution.

Specific Differential Phase (KDP) Characteristics

8-bit Specific Differential Phase

- Resolution: 0.13 nm (0.25 km, 250 m) x 1.0 degree for all elevation angles and VCPs
- Data levels: 256
 - Min. = -2, Max. = +10 deg/km
 - Precision: to the nearest 0.05 deg/km
- Range: 162 nm
- RPG Product Code: DKD

4-bit Specific Differential Phase

- Resolution: 1 km (0.54 nm) x 1.0 degree for all elevation angles and VCPs
- Data levels: 16
 - Min. = -2, Max. = +7 deg/km
 - Precision: to the nearest 0.25 to 3 deg/km
- Range: 124 nm
- RPG Product Code: KDP

Specific Differential Phase Product Description

- RPG ID: kxxx
- Elevation Angle: x.x in degrees
- Product name: KDP 8-bit or KDP 4-bit
- Date: Day of week, time in UTC, and date
- Units: deg/km

Specific Differential Phase Product Annotations:

- VCP: 11, 12, 21, 121, 211, 212, 221, 31, or 32
- Range resolution: 0.25 km (8-bit), 1 km (4-bit)

All overlays are displayable on this product.

D-2D KDP Display The KDP product will appear on your D-2D screen as seen on the right in Figure 3-1. A reflectivity image has been provided on the left for reference.

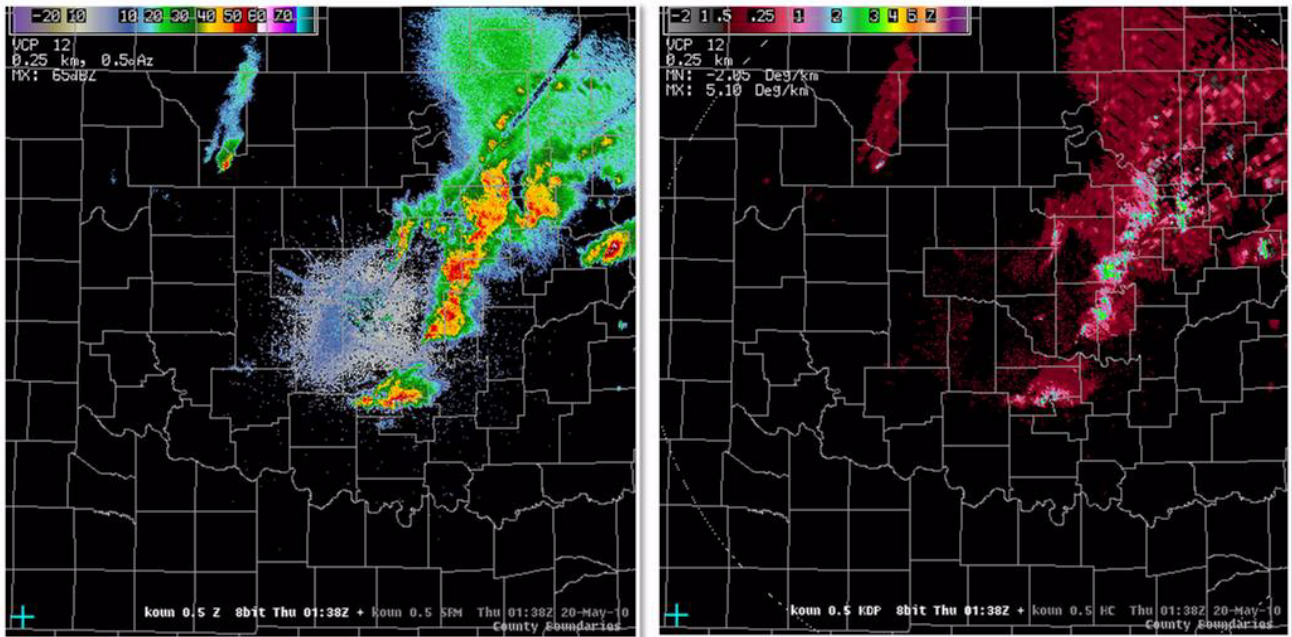


Figure 3-1. Sample D-2D display with reflectivity on the left and KDP on the right

Individual KDP products can be found for each elevation angle inside your dedicated radar's drop-down menu. Also, the KDP product can be found in conjunction with other data. These are indicated by yellow ovals in Figure 3-2.

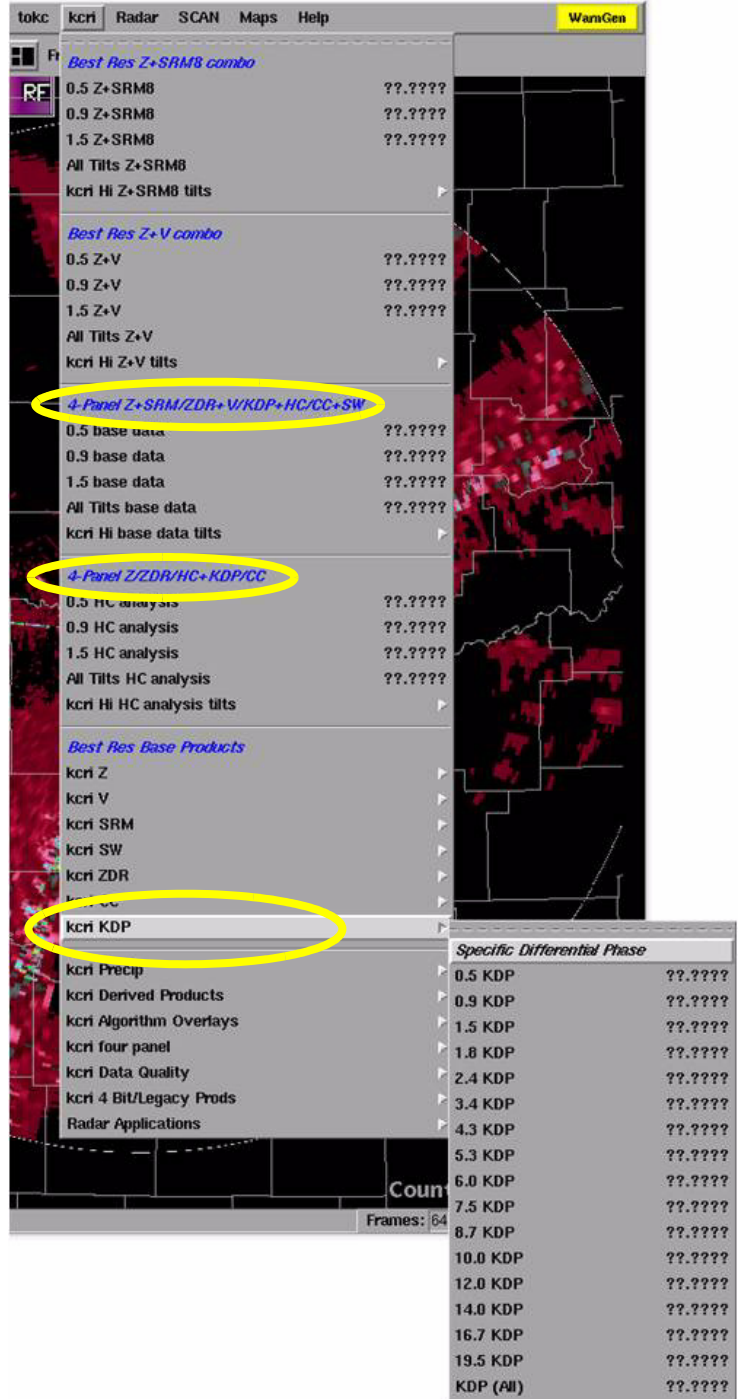


Figure 3-2. D-2D menu showing location of KDP product.

Physical Interpretation

As the horizontally and vertically polarized pulses propagate through a medium (i.e. rain, hail, etc.), the two pulses attenuate (or slow down) causing each of their phases to change (or shift) as shown in Figure 3-3. Most targets do not cause equal phase shifting in the horizontal and vertical due to target shape and concentration, which leads to a difference in horizontal and vertical phase shifts.

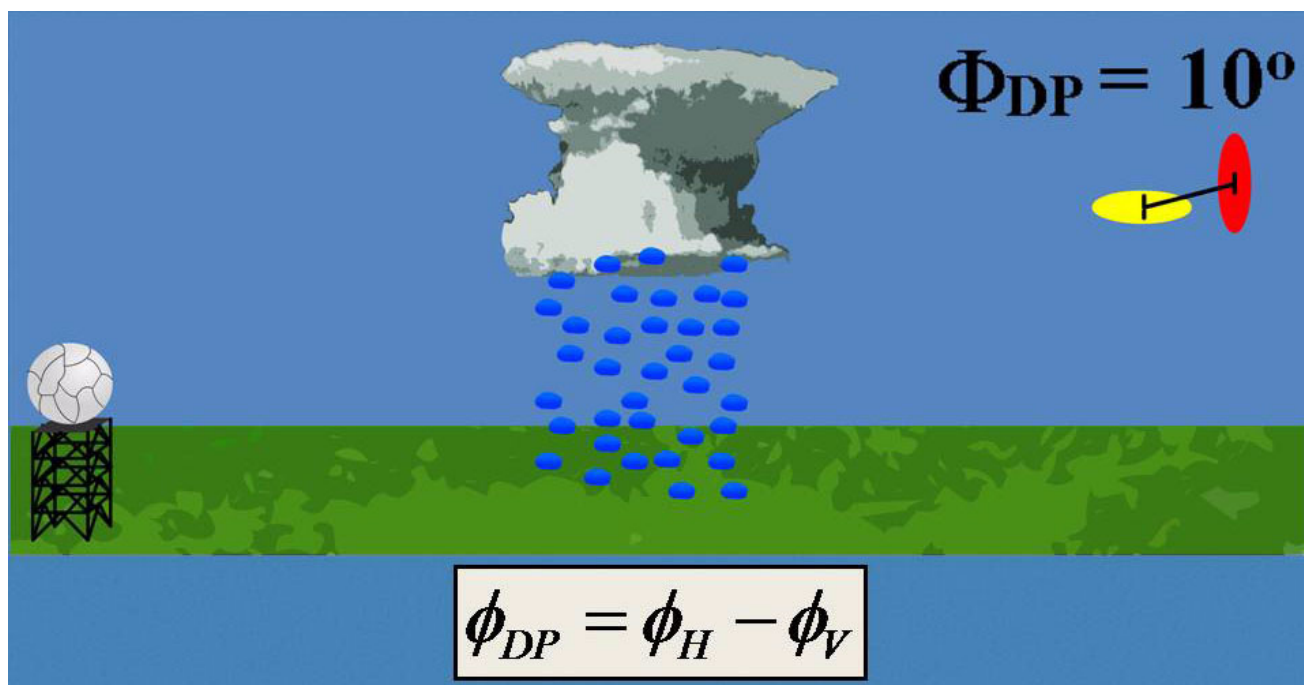


Figure 3-3. The change or shift in phases of the horizontal (yellow) and vertical (red) pulses. The difference between horizontal and vertical phases results in differential phase shift (see equation).

The difference between the horizontal and vertical phase shifts is called differential phase shift (see equation in Fig. 3-3). Mercifully, the equation is just a simple subtraction, such that positive differential phase shift occurs when horizontal phase shift is greater than vertical. Much like differential reflectivity (ZDR), the shape of the target affects the differential phase shift (see Fig. 3-4):

- Horizontally oriented targets will produce an increasing, positive differential phase shift with increasing range.

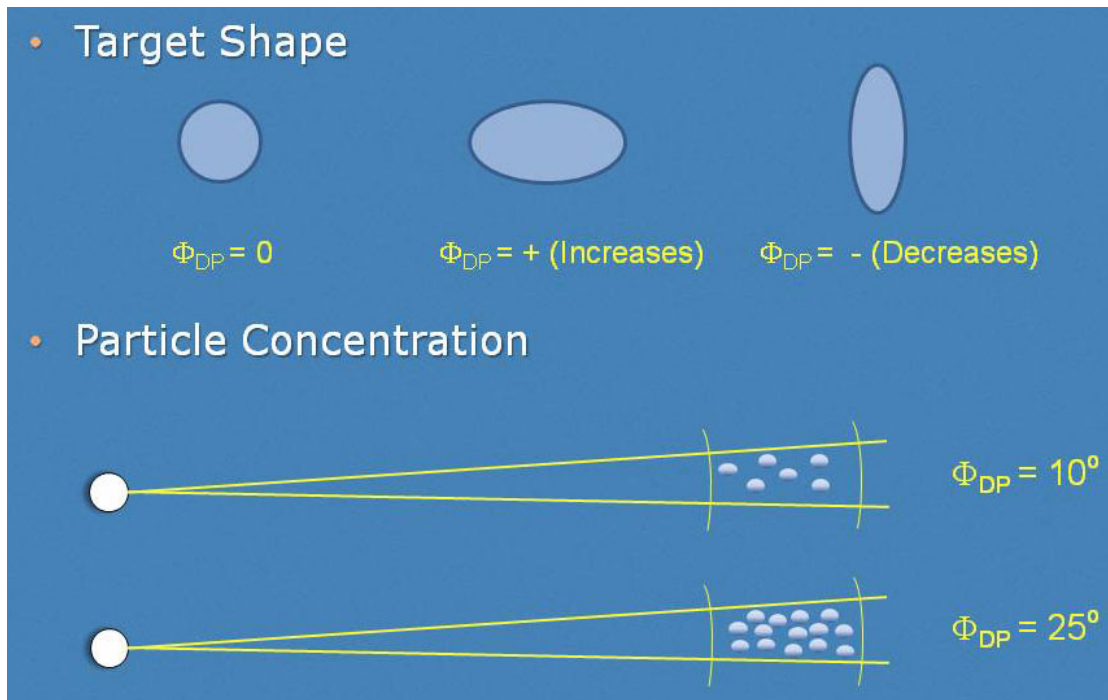


Figure 3-4. General physical interpretation of Φ_{DP} .

- Vertically oriented targets will produce a decreasing, negative differential phase shift with increasing range.
- Spherical targets will produce near zero differential phase shifts with increasing range.

Additionally, unlike ZDR, differential phase shift is dependent on particle concentration. Increasing the number of particles will result in an increase in differential phase shift. For example, the more horizontally oriented targets there are within a pulse volume, the higher the positive differential phase shifting.

Recall that larger raindrops are more oblate (larger in the horizontal direction) than smaller raindrops. It is expected that extremely small raindrops, such as drizzle, will have near zero differential phase shift and larger raindrops will have larger, positive differential phase shift. In Figure 3-5, one pulse volume has a moderate amount of medium-sized

Characteristic of Φ_{DP} in Rain

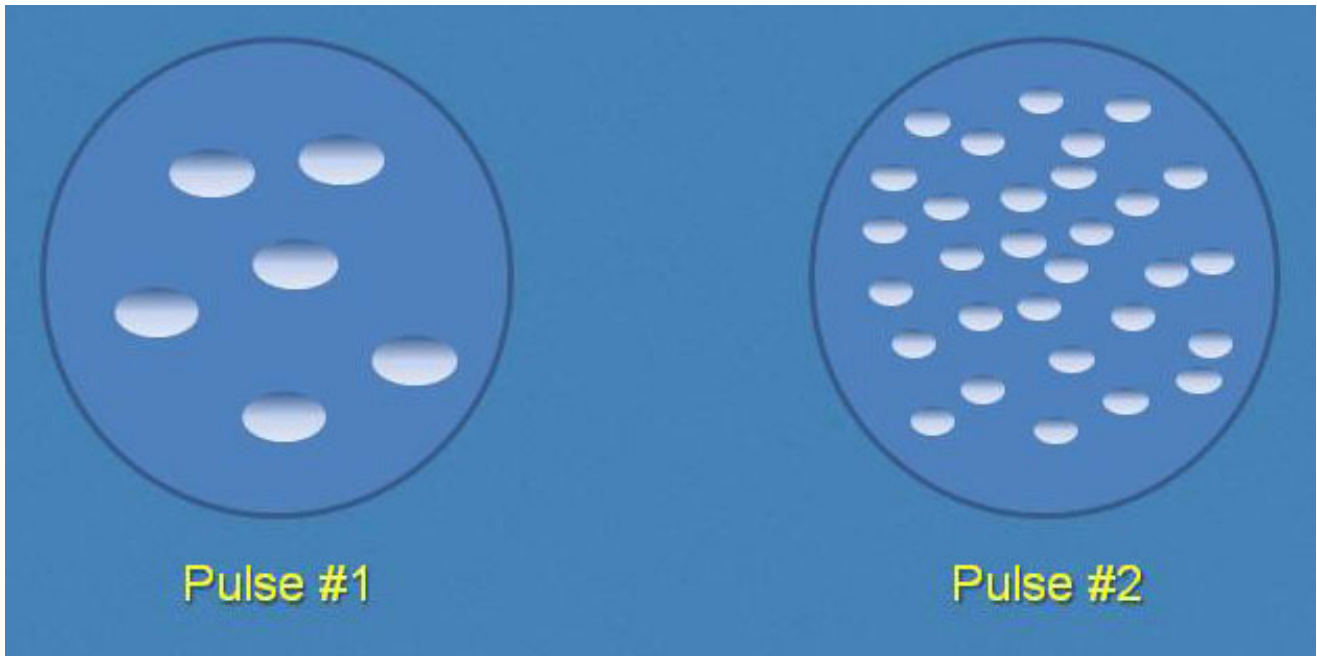


Figure 3-5. Larger raindrop size will yield a more positive Φ_{DP} , however so do higher concentrations of smaller raindrops.

raindrops and a second pulse volume has a large amount of smaller raindrops. Even though the medium-sized raindrop should have higher differential phase shift than a single, smaller raindrop, the higher concentration of smaller drops could actually make the differential phase shift in the second pulse volume higher than in the first pulse volume.

Characteristic of Φ_{DP} in Hail

Since hail tends to tumble as it falls, it appears on radar to be spherical. This means hail will typically have near 0 degrees of differential phase shifting. One caveat is that nearly-melted, small, sub-severe hail appears on radar as large raindrops. This can cause very high differential phase shifts. For the most part, differential phase shifting is unaffected by the presence of hail. Figure 3-6 shows 2 pulse volumes, each with the same amount and type of rain. Pulse #2 contains hail but

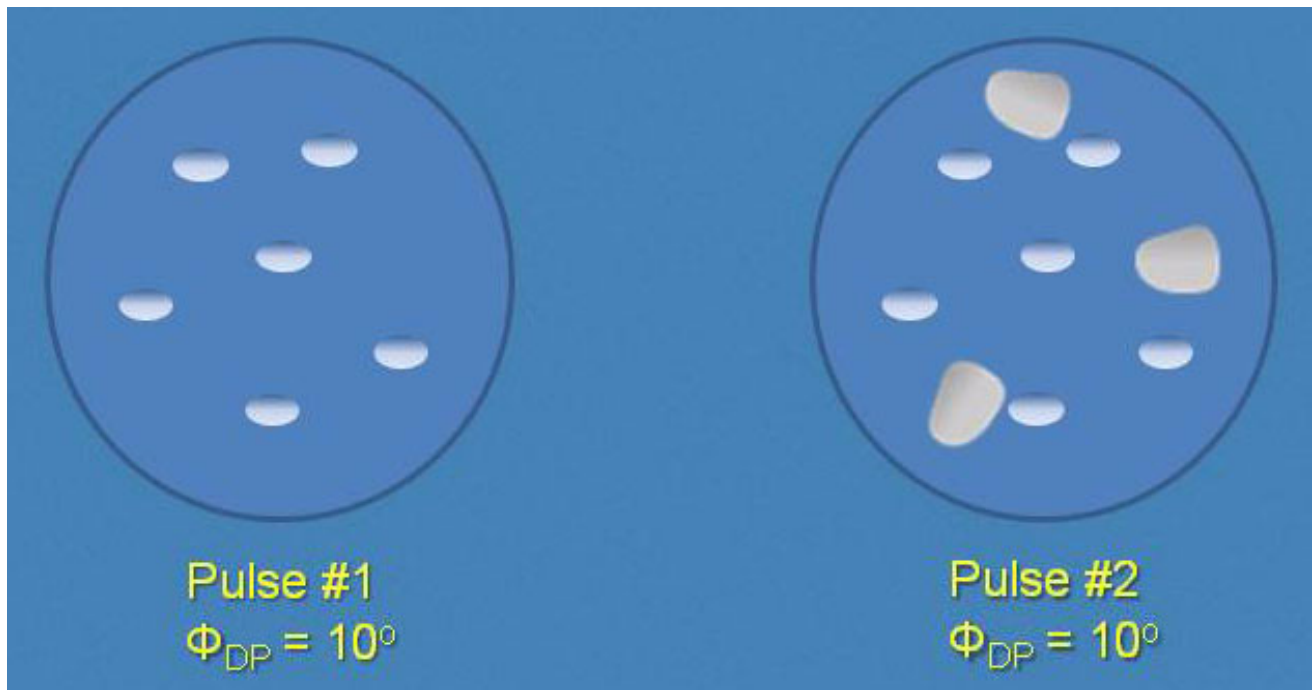


Figure 3-6. Two pulses with the same size and number of rain drops. Pulse #1 has no hail and Pulse #2 has a few hail stones. Both pulse volumes result in the same Φ_{DP} .

Pulse #1 does not. In this case, the differential phases for the two pulses are identical.

Since most ice and snow crystals do not fall with a preferred orientation, differential phase shifts in snow and ice crystal regions are typically near 0°C . The one exception to this rule is when ice crystals become aligned due to some outside force, such as a strong electric field inside a thunderstorm. This crystal alignment can cause significant non-zero differential phase shifting. Depending on the orientation of the alignment, the differential phase shifting can be positive or negative. It is positive when the alignment is in the horizontal, and negative when the alignment is in the vertical.

In non-meteorological echoes, differential phase shift is very noisy. This is primarily due to the effects of backscatter differential phase shifting. To this point, we have only looked at what is called

Characteristic of Φ_{DP} in Snow and Ice Crystals

Characteristic of Φ_{DP} in Non-Meteorological Echoes

propagation differential phase shift. Backscatter differential phase shift is the amount of differential phase shift that occurs once the pulse scatters off of an object. In short, meteorological echoes typically experience no backscatter differential phase shift, whereas non-meteorological echoes such as birds and ground clutter experience significant backscatter differential phase shift. The amount of backscatter differential phase shift is highly variable depending on the object shape and size. For these reasons, specific differential phase (discussed next and viewable in AWIPS) is not computed in ground clutter or biological scatterers that cause CC to drop below 0.90.

What is KDP? How do we get from differential phase to specific differential phase, the product you see in AWIPS? Specific differential phase is defined as the range derivative of the differential phase shift between the horizontal and vertical pulse phases (see Fig. 3-7). The factor of 2 in the denominator accounts for the trip out and back by the pulses. Possible values range from -2 to 10 in units of degrees per kilometer. In AWIPS and in research

Definition	Possible Range of Values	Units	Abbreviated Name
The range derivative of the differential phase shift between the horizontal and vertical pulse phases	-2 to 10	Degrees per Kilometer (deg/km)	KDP

$$KDP = \frac{\phi_{DP}(r_2) - \phi_{DP}(r_1)}{2(r_2 - r_1)}$$

Figure 3-7. Specific differential phase general characteristics and equation.

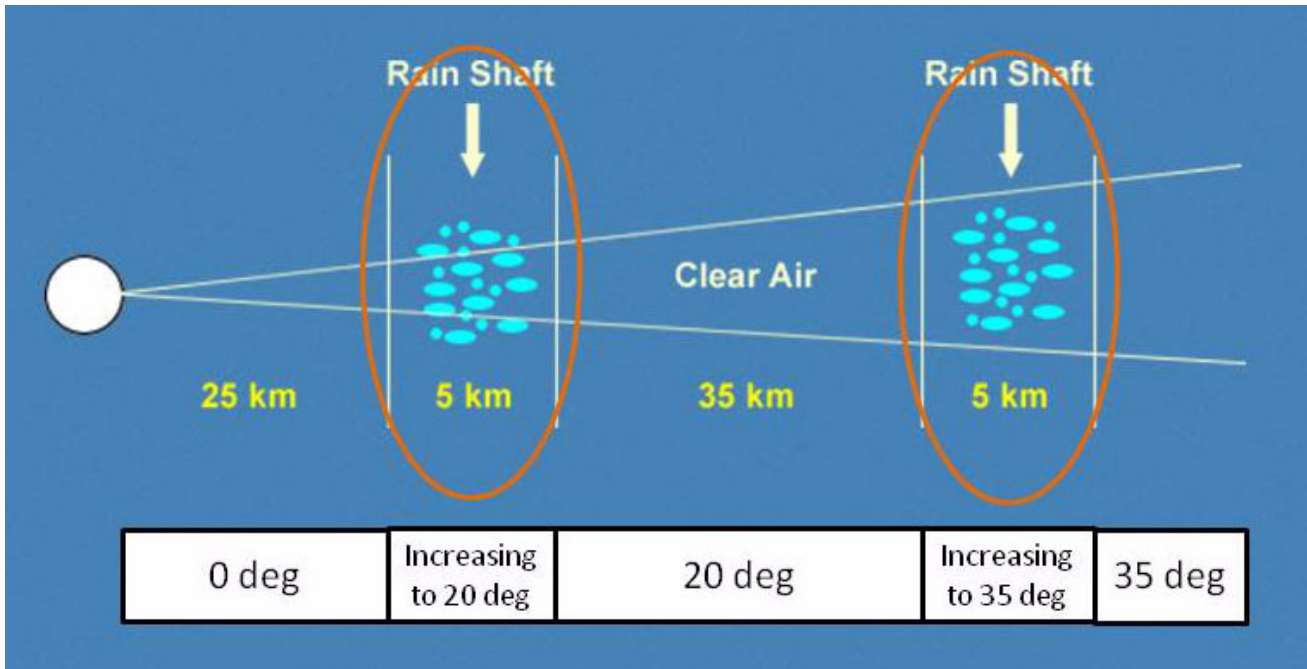


Figure 3-8. Two rain-shafts 30 km and 70 km from the radar illustrating how Φ_{DP} is cumulative.

papers you will see specific differential phase abbreviated as KDP.

What is the reason for KDP? Let's look at the example of Φ_{DP} for the two rain shafts illustrated in Figure 3-8. As the horizontal and vertical pulses propagate toward the first rain shaft through clear air, they experience zero differential phase shifting, so Φ_{DP} is zero. As the pulses go through the first rain shaft, the horizontal pulse slows down more than the vertical pulse resulting in a positive differential phase shift of 20 degrees. After exiting the rain shaft, the pulses enter clear air and experience zero additional differential phase shift. However, those bins in the clear air will show a differential phase shift of 20 degrees, as any differential phase shift values are carried down radial. In the second rain shaft, the differential phase shift will increase again, this time by 15 degrees. In those bins and any bin further down-range, the differential phase shift will be 35 degrees. As you can see, the differential phase shift is cumulative and

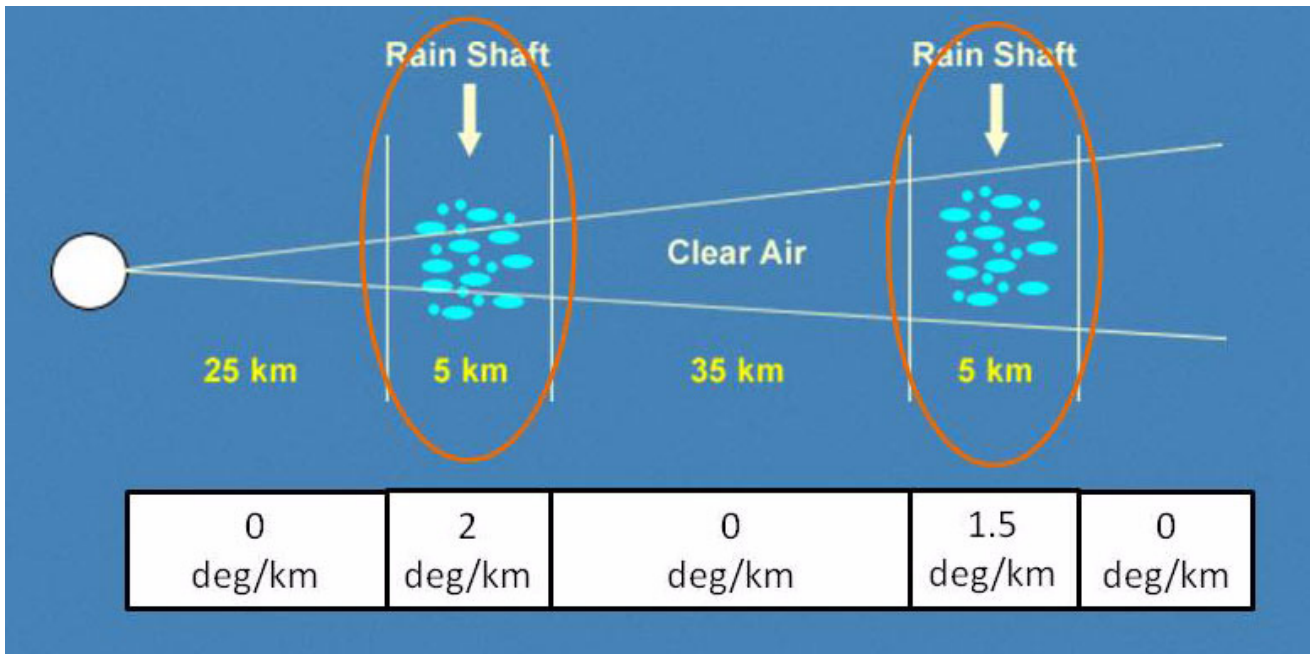


Figure 3-9. Illustration of KDP for the same scenario as Fig. 3-8.

the absolute value tells you nothing about what is going on in that particular range bin, but rather all that has happened along the radial up to that point.

Now we'll look at the same example except using KDP, or the range derivative of Φ_{DP} (see Fig. 3-9). Up until the rain shaft, no differential phase shifting occurs, so 0 degrees divided over any distance will give 0 degrees/distance. Therefore, any gate within 25 km of the radar has a KDP of 0 deg/km. Inside the rain shaft, there is a differential phase shift of 20 degrees. Dividing this by twice the distance over which it occurred (10 km) results in a KDP of 2 deg/km. In the clear air past the first rain shaft, the differential phase shift remains 20 degrees but does not change over this distance. KDP will return to 0 deg/km in this region because the difference between any two differential phase shifts over any distance in this region will be zero.

In the second rain shaft, the differential phase shift increases from 20 degrees to 35 degrees, so it

increases by 15 degrees. Dividing this value by twice the distance over which it occurred (10 km) gives a KDP of 1.5 deg/km. Past the second rain shaft, the KDP returns to 0 deg/km for the same reasons it did in the clear air in between the two rain shafts. KDP is much better at revealing what is happening at a particular bin than is Φ_{DP} .

Knowing the characteristics of Φ_{DP} in certain meteorological situations, we can easily develop a good sense of the characteristics of KDP. In pure hail not mixed with rain, since the Φ_{DP} is very near zero because of hail's tumbling nature, it only makes sense that KDP will also be near zero. This same logic can be applied to snow/ice crystals that have no preferential orientation. The near-zero Φ_{DP} results in near-zero KDP. Rain is basically the only meteorological echo to have a range of non-zero KDP values. Since rain is oblate and can vary in concentration, KDP is positive in rain and can get as high as 8 or 9 deg/km. Another situation which results in significant, positive or negative KDP would be preferentially oriented ice crystals in electrified regions of thundestorms. Lastly for non-meteorological echoes, the noisy nature of Φ_{DP} results in noisy KDP.

Typical Values for KDP (deg/km)

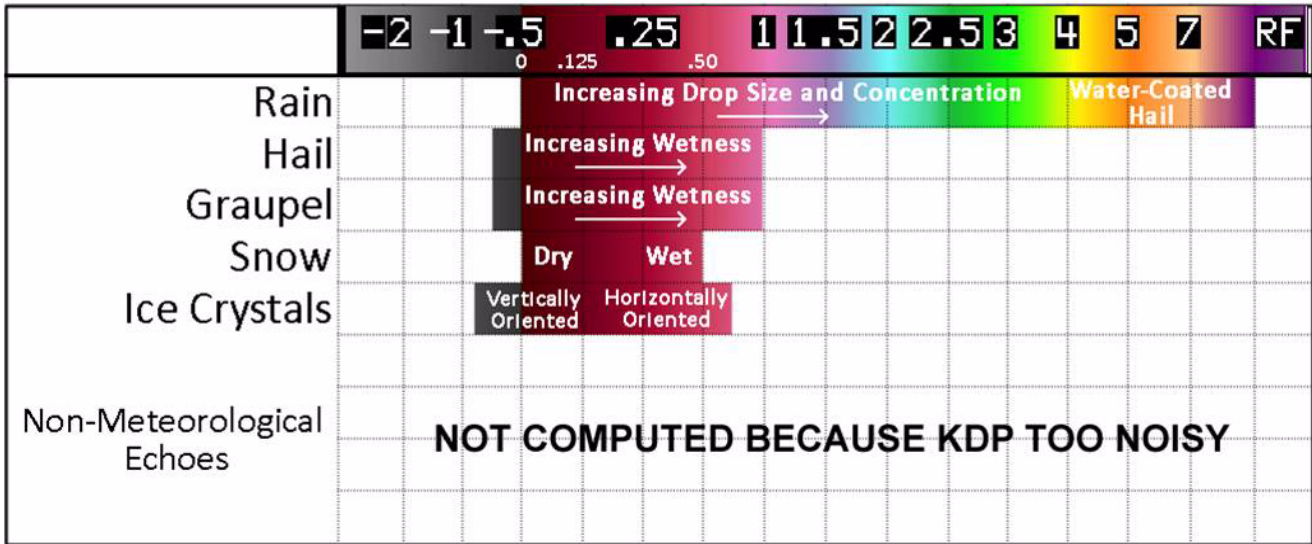


Figure 3-10. Typical values expected for selected meteorological echoes. KDP is too noisy to be reliable with regards to non-meteorological echoes

Figure 3-10 summarizes what kinds of KDP to expect for selected meteorological and non-meteorological echoes. Note that non-meteorological echoes do not have values shown here because KDP is too noisy to be reliable for these types of echoes and is not computed in these areas, as discussed in the limitations section next.

Specific Differential Phase (KDP) Limitations (Weaknesses)

When looking at KDP, remember that KDP is:

- Not computed in bins with $CC < 0.90$ (black holes in the data)
- Noisy in low SNR
- Affected by Non-Uniform Beam Filling (NBF)
- Affected by range folding in the batch cuts

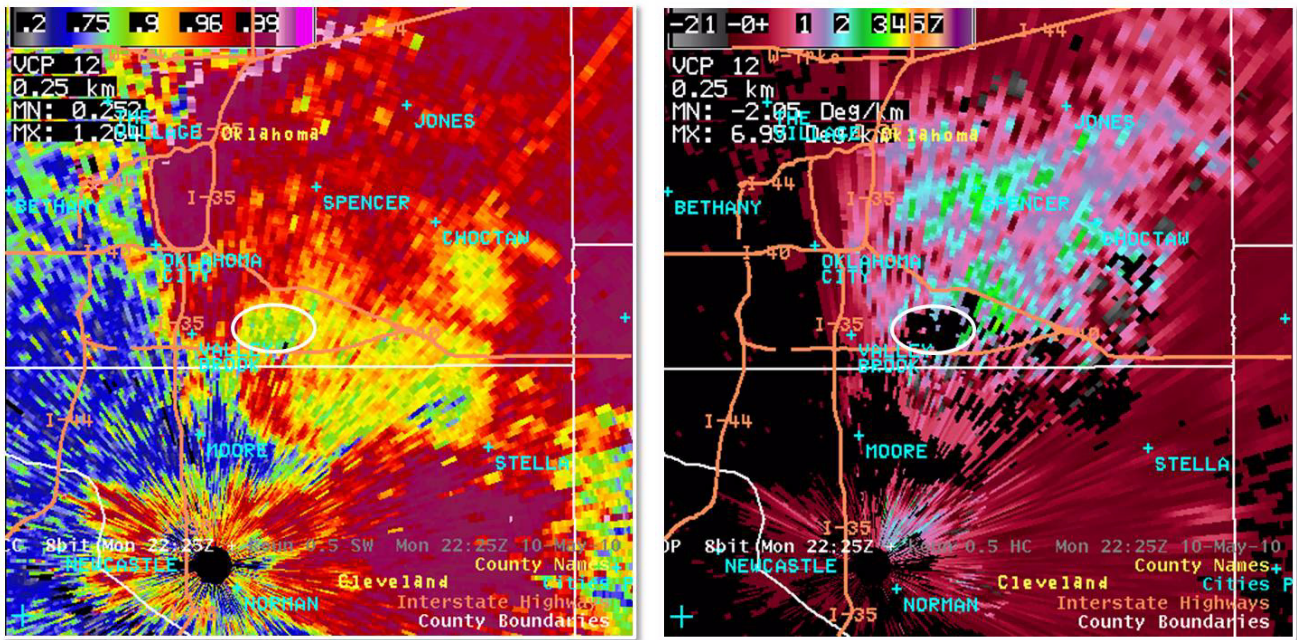


Figure 3-11. Correlation coefficient (CC, left) and specific differential phase (KDP, right) from a supercell that produced softball-sized hail and an EF-4 tornado. Notice the hail core (inside oval) containing CC below 0.90 and the corresponding black hole in the KDP data.

When the CC is below 0.9, Φ_{DP} accumulates significant errors making it appear very noisy. This noisy Φ_{DP} makes it useless to compute KDP. Therefore, in bins with CC less than 0.9, KDP will not be plotted, so it will appear as black holes in the data. Figure 3-11 shows an example of this phenomenon.

KDP Not Shown for CC < 0.90

Noise in Low SNR In areas of low SNR, KDP will become noisy. SNR is often low when reflectivity is low at far ranges and along the very edges of storms. The white oval in Figure 3-12 shows noisy KDP in an area of low SNR. KDP may be seen alternating between high and low values as you look down-radial.

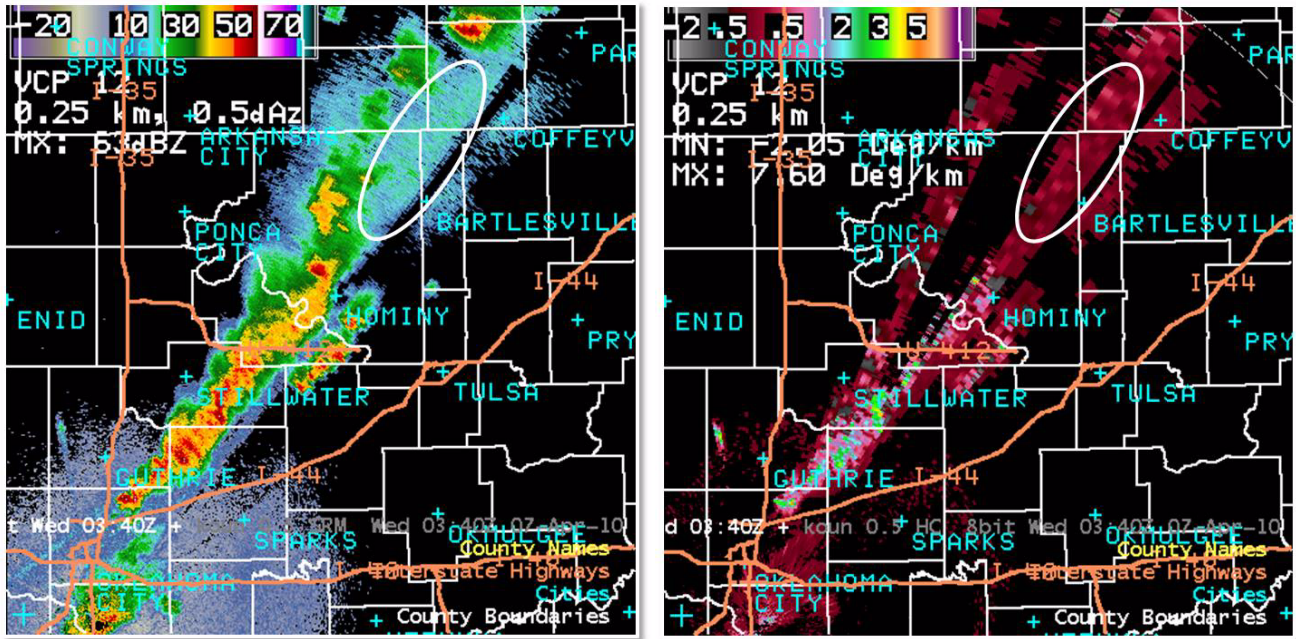


Figure 3-12. Reflectivity (Z, left) and specific differential phase (KDP, right). The echoes highlighted are at far range from the radar and have low returns (< 25 dBZ). Therefore, the SNR is very low. Looking at KDP, we see that it looks very speckled (or noisy).

Like CC, KDP is adversely affected by non-uniform beam filling (NBF). Recall that NBF occurs when significant gradients of reflectivity and/or the polarimetric variables occur within a pulse volume. This gradient can either be in the horizontal or vertical. The same applies for KDP primarily because if CC becomes affected by NBF and drops below 0.9, KDP becomes unreliable, and is not computed. Therefore, KDP will be unreliable/unavailable in areas where lines of storms align along a radial (see Fig. 3-13), down-radial of significant hail cores, and at long ranges.

Non-Uniform Beam Filling (NBF)

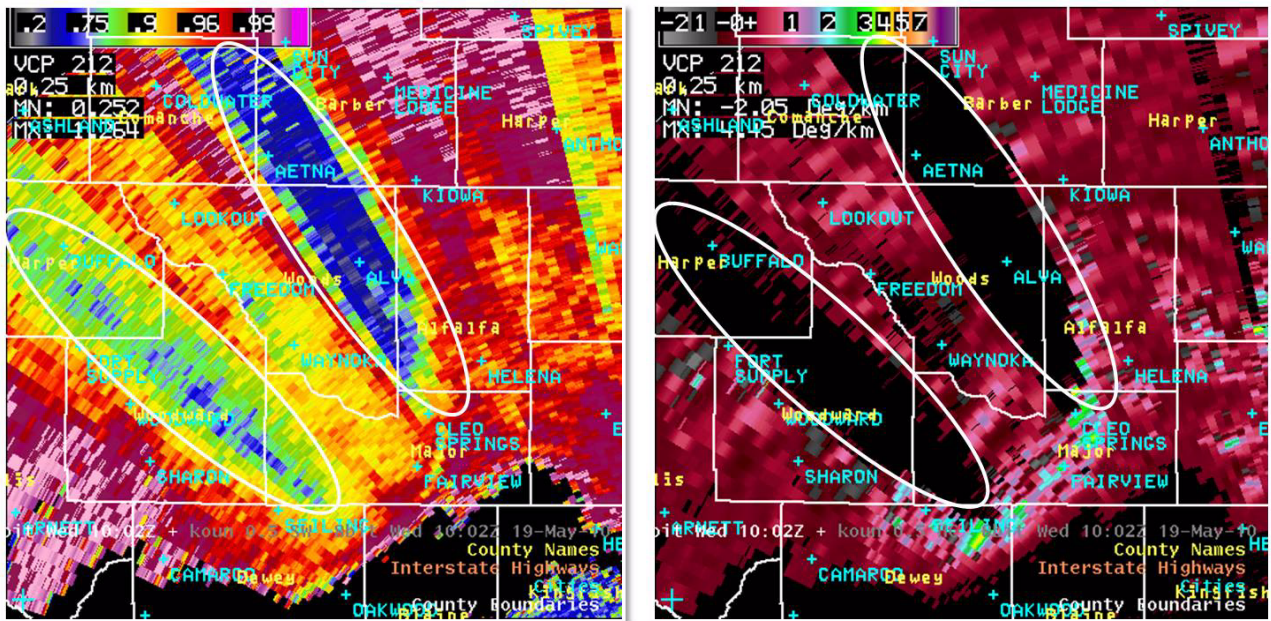


Figure 3-13. Example where non-uniform beam filling (NBF) has caused CC (left) to drop below 0.9 resulting in KDP (right) not being displayed.

Range Folding in the Batch Cuts

In the batch cuts, range folding may obscure some signatures in KDP. As a refresher, the batch cuts for the WSR-88D network are elevation angles between 1.65 degrees and 6.5 degrees. In these cuts each radial uses a series of alternating low and high PRF pulses, but the dual-pol variables are only computed using the high PRF pulses which are subject to range folding. Figure 3-14 shows range folding in the KDP display at the same locations where there is range folding in the velocity display.

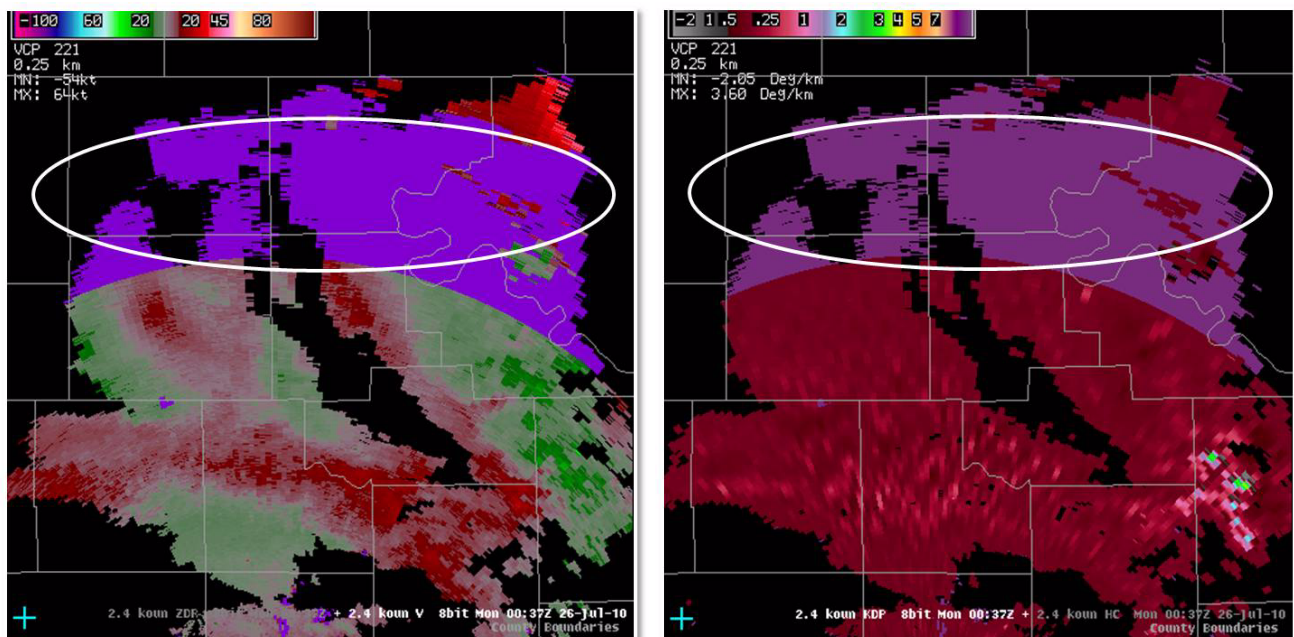


Figure 3-14. Velocity (left) and KDP (right) from 26 July 2010 at 0037 UTC from the 2.4 degree elevation scan. Note that where there is range folding in the velocity, there is also range folding in KDP (see white ovals).

Specific Differential Phase (KDP) Operational Applications (Strengths)

Operational applications of KDP include detecting areas of heavy rain, specifically:

- Heavy rain only
- Heavy rain mixed with hail
- Cold vs. warm rain processes

The primary advantage of KDP is its ability to detect heavy rain situations. In Figure 3-15 the two white ovals encircle two areas of >40 dBZ echoes that are fairly uniform in intensity. Looking at KDP, we see higher KDP values in the northernmost oval, and lower KDP values in the southernmost oval despite reflectivity values being almost identical. This indicates that heavier rainfall is taking place in the northernmost oval than in the southernmost oval.

Heavy Rain Only

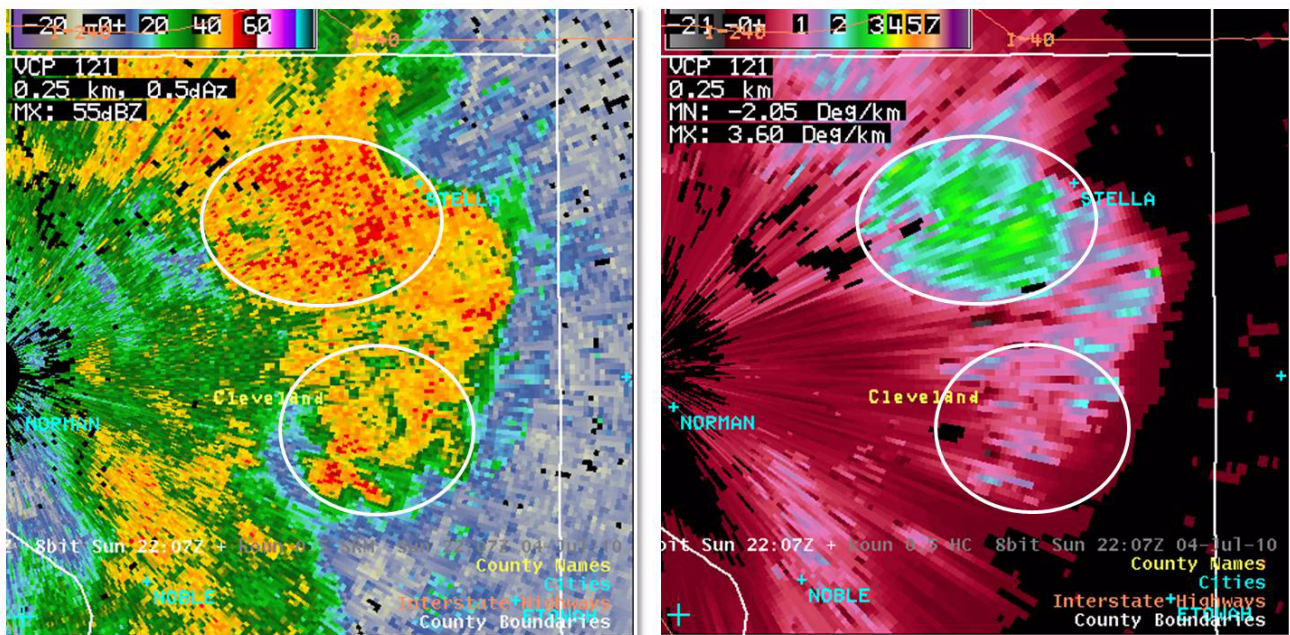


Figure 3-15. Reflectivity (left) and KDP (right) during a heavy rain event. Notice higher values of KDP in the northernmost oval indicating heavy rain in that area, compared to southernmost oval, which has lower KDP, despite similar reflectivity values.

good-sized, very oblate hydrometeors falling in this region. Looking at KDP, the values are near 1 to 1.5 deg/km. There is most likely no hail in this region and the drops that are falling are most likely large and low in concentration. Moving a bit closer to the core, take a look at the central oval in Figure 3-16. Reflectivities are once again near 50 dBZ. However, ZDR values in the region are near 0.5 dB and KDP values are near 0 deg/km. This tells us that there is mostly hail in this region with little or no liquid water falling to the surface. The last area we'll look at is the white oval just to the northwest. Reflectivities are near 60 dBZ and ZDR values are around 3 to 4 dB. However, now KDP is on the order of 5 deg/km. This is possibly due to melting/mostly melted hail (given the 60 dBZ) and a substantial amount of liquid water falling with the hail in this region. Either way, there is more liquid water in this region than the other two.

Cold vs. Warm Rain Processes

Recall from earlier that KDP could be used to discern two different rain rates even when reflectivity was the same (see Fig. 3-15). In Figure 3-17, ZDR in the northern area has values between 1.5 and 2.5 dB. To the south, the ZDR values are approaching 3 dB. Remember from the ZDR lesson, this means that the drops to the south are larger in size than the drops to the north. However, the higher KDP values are to the north. This is because KDP is dependent not only on the shape of the particle, but on particle concentration. The drops to the north may have a smaller mean diameter than the drops to the south, but the higher KDP indicates a higher concentration of drops in the northern region than the southern. The reason for this difference is the type of process by which the drops formed. The drops to the north most likely formed via a warm rain process whereas the drops to the south formed via a cold rain process.

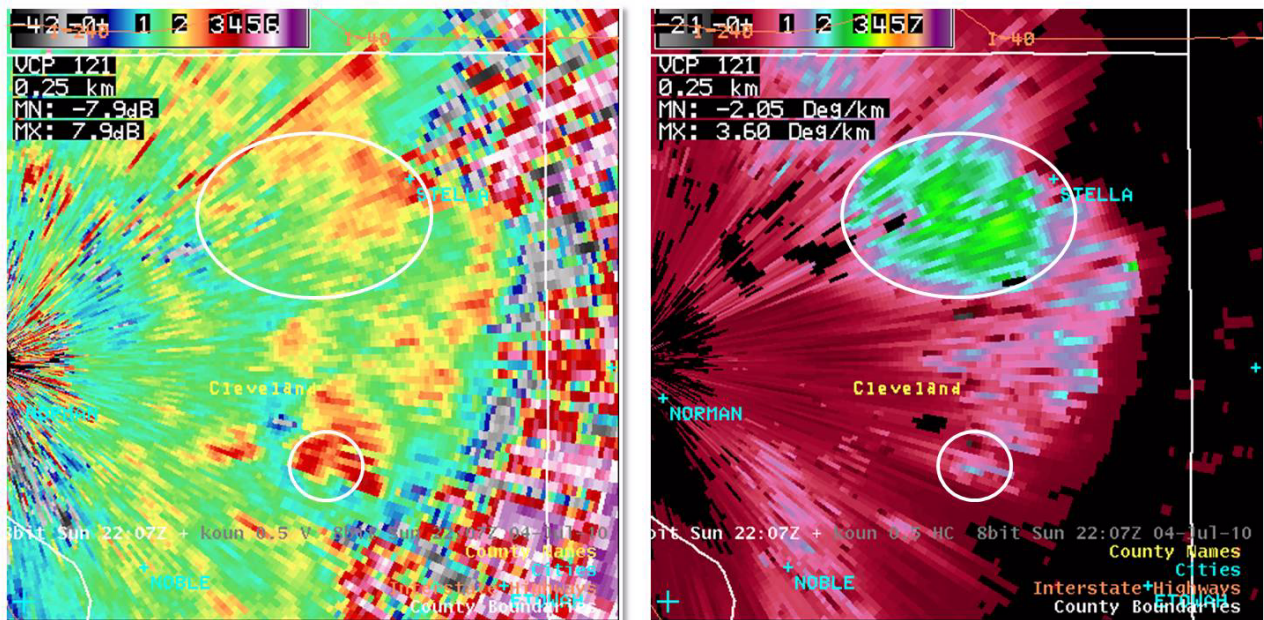


Figure 3-17. ZDR (left) and KDP (right) output from the same scan shown in Figure 3-15. The higher KDP values in the northern circle tells us that they likely formed via a warm rain process, whereas drops to the south formed via a cold rain process.

Lesson 4: Hydrometeor Classification (HC)

The purpose of the hydrometeor classification (HC) algorithm is to determine the most likely echo type for each radar bin from a list of pre-defined echo types. The algorithm determines the most likely echo type using Z, V, ZDR, CC and KDP values and the quality and reliability of those base products. The output is called the hydrometeor classification (HC) product and will be discussed in this lesson.

8-bit Hydrometeor Classification Resolution and Range

- Resolution: 0.13 nm (0.25 km, 250 m) x 1.0 degree for all elevation angles and VCPs
- Range: 162 nm
- RPG Product Code: DHC

4-bit Hydrometeor Classification Resolution and Range

- 0.54 nm (1 km, 1000 m) x 1.0 degree resolution available for all elevation angles and VCPs
- Range: 124 nm
- RPG Product Code: HC

Hydrometeor Classification Product Description

- RPG ID: kxxx
- Elevation Angle: x.x in degrees
- Product Name: HC 8-bit or HC 4-bit
- Units: unitless
- Date: Day of week, time in UTC, and date

Hydrometeor Classification Product Annotations:

Hydrometeor Classification (HC) Characteristics

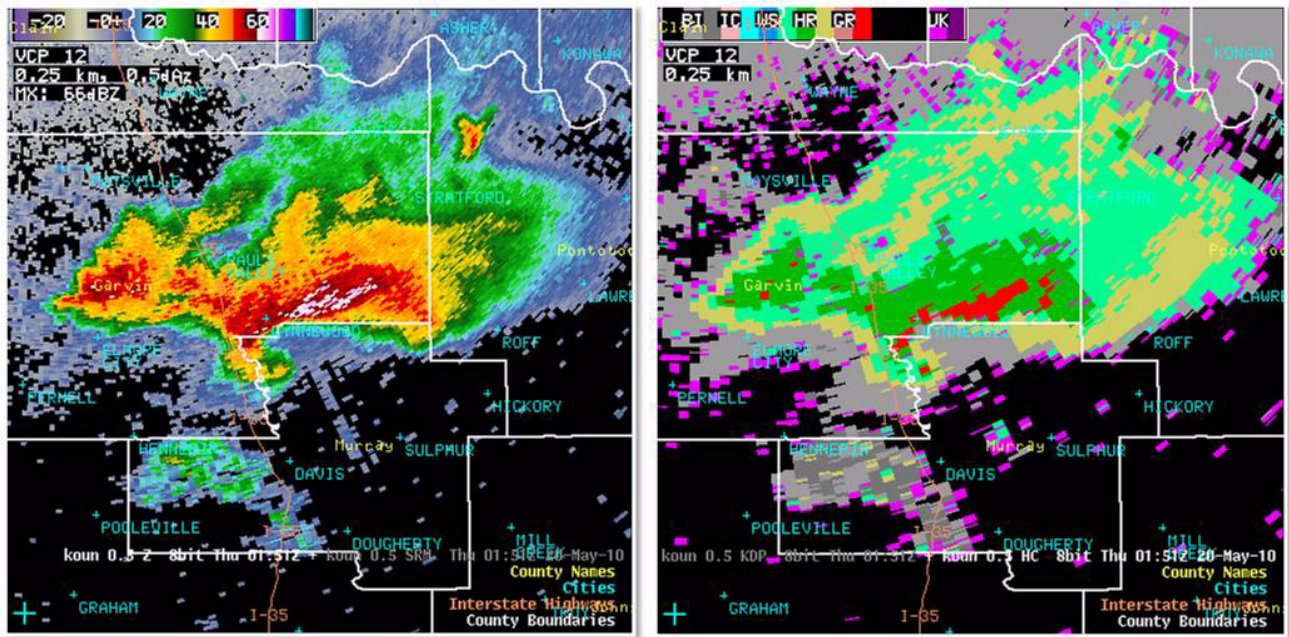


Figure 4-1. Reflectivity (Z, left) and corresponding Hydrometeor Classification (HC, right) product output for a supercell thunderstorm.

- VCP: 11, 12, 21, 121, 211, 212, 221, 31, or 32
- 0.25 km (8-bit), 1 km (4-bit): range resolution

All overlays are displayable on this product.

D-2D Display

The HC product will appear on your D-2D screen as seen on the right in Figure 4-1. A reflectivity image has been provided on the left for reference. The pre-defined list of possible echo classifications consists of 10 different classes of echoes. Figure 4-2 shows the color bar you will see in AWIPS. The 10 classes as shown in the AWIPS color bar are: biological scatterers (BI), ground clutter / anomalous propagation (GC), ice crystals (IC), dry snow (DS), wet snow (WS), light/moderate rain (RA), heavy rain (HR), big drops (BD), graupel (GR) and hail possibly mixed with rain (HA). The no data (ND) classification occurs when a bin's signal-to-noise ratio (SNR) is less than 5 dB and the unknown (UK) classification will be discussed later in the lesson. RF stands for range folding and this will most likely never affect the HC

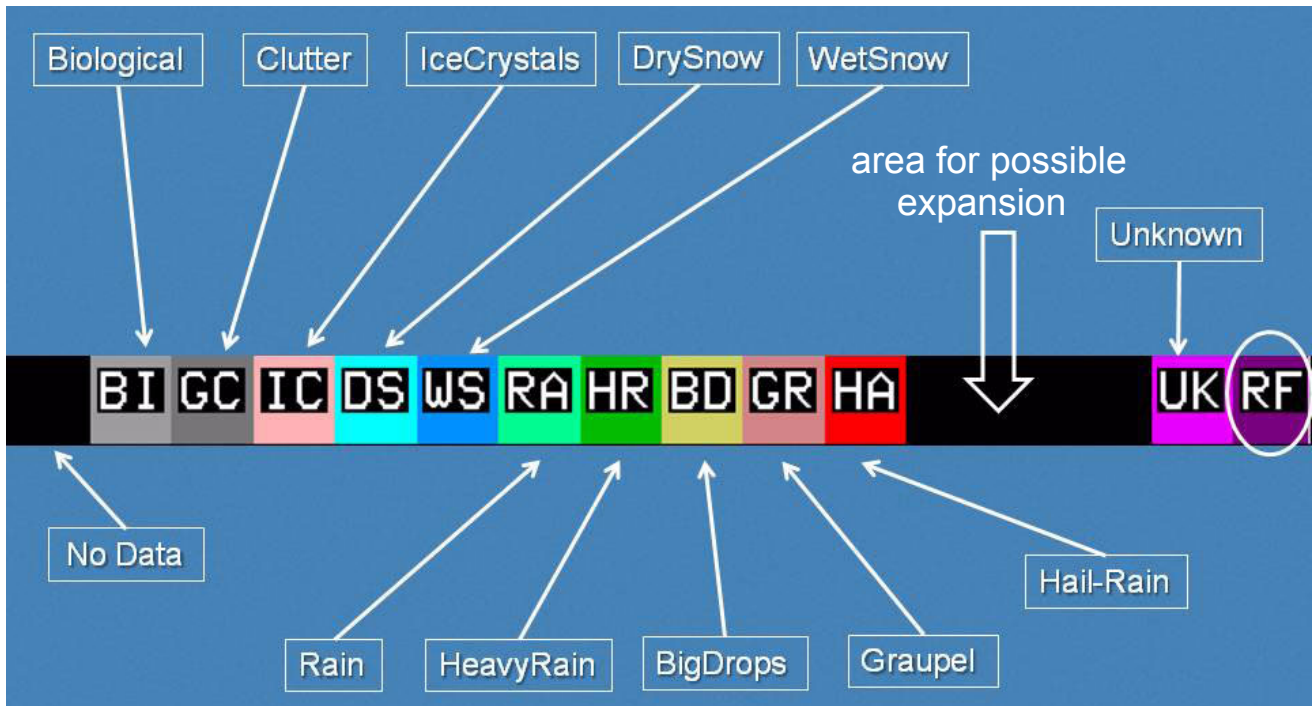


Figure 4-2. Pre-defined list of possible echo classifications for the Hydrometeor Classification (HC) product as they appear in the color bar in AWIPS.

product. The blank spots annotated by the large white arrow are for possible future expansion of the product as understanding of the dual-pol characteristics of precipitation and non-precipitation echoes improves.

The output of the HC product will appear in cursor readout as shown by the list in Figure 4-3. The image on the right shows an example of the HC cursor readout. In this case, the readout is indicating biological scatterers.

AWIPS Cursor Readout

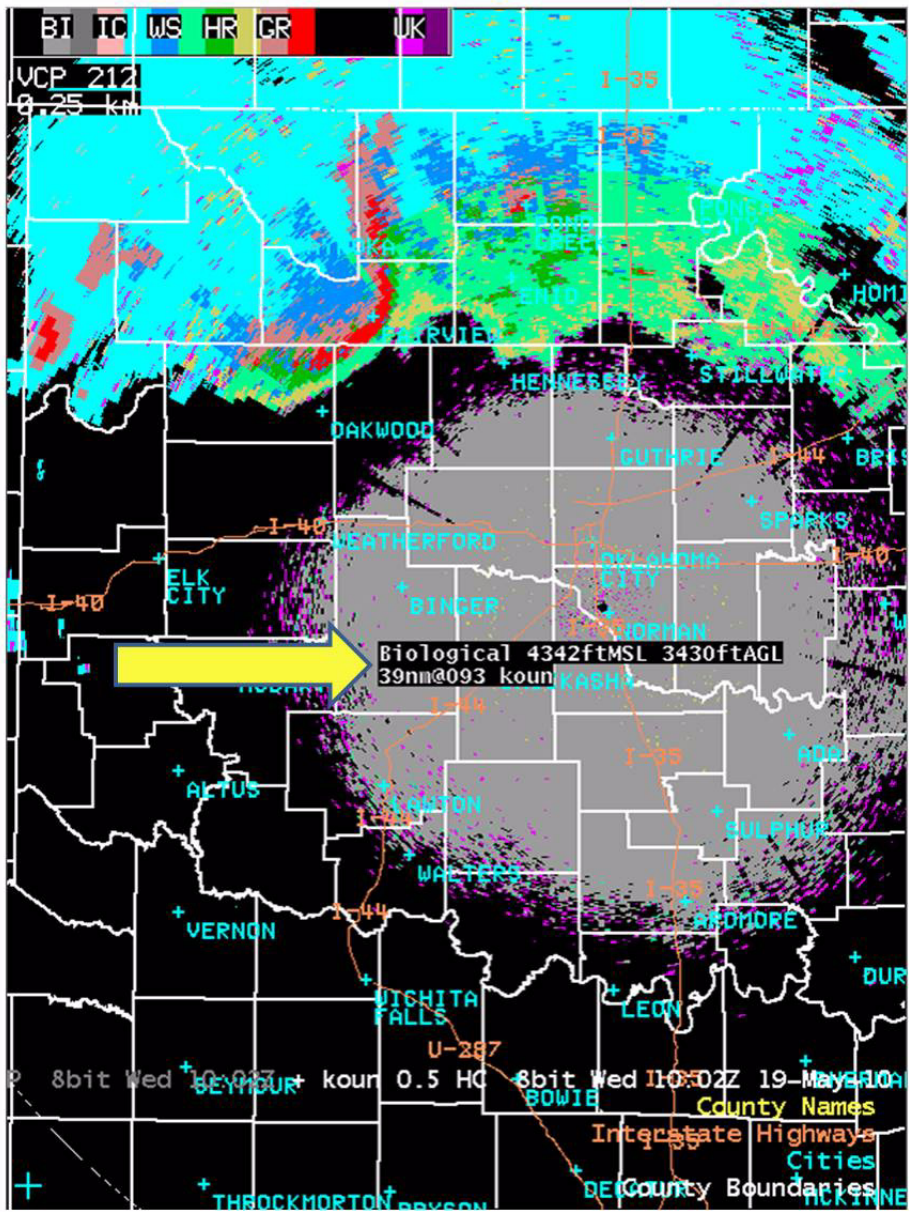


Figure 4-3. Example of cursor readout in the HCA product (yellow arrow).

The HC product includes the following categories:

- (BI) Biological scatters include things such as birds and/or insects.
- (GC) Ground clutter includes buildings, trees, cars, etc. that appear normally or as anomalous propagation (AP).
- (IC) Ice crystals are defined here as ice in the form of columns, needles, plates, etc.
- (DS) Dry snow includes snow flakes that are low-density.
- (WS) Wet snow includes snow flakes that have undergone some melting.
- (RA) Light to moderate rain can be thought of as rain rates less than 1 inch per hour.
- (HR) Heavy rain can be thought of as rain rates greater than 1 inch per hour.
- (BD) “Big Drops” is a special designation that has been created for large rain drops (at least 3-4 mm in diameter) that appear in low concentration and mainly appear along the leading edge of convective precipitation.
- (GR) Graupel includes precipitation in the form of soft ice/snow pellets.
- (HA) Hail-rain includes pure hail or hail possibly mixed with rain.
- (UK) Unknown includes bins where the algorithm could not decisively say what category that bin could fit into, either because the confidence value was too low or two categories were too close to decide.

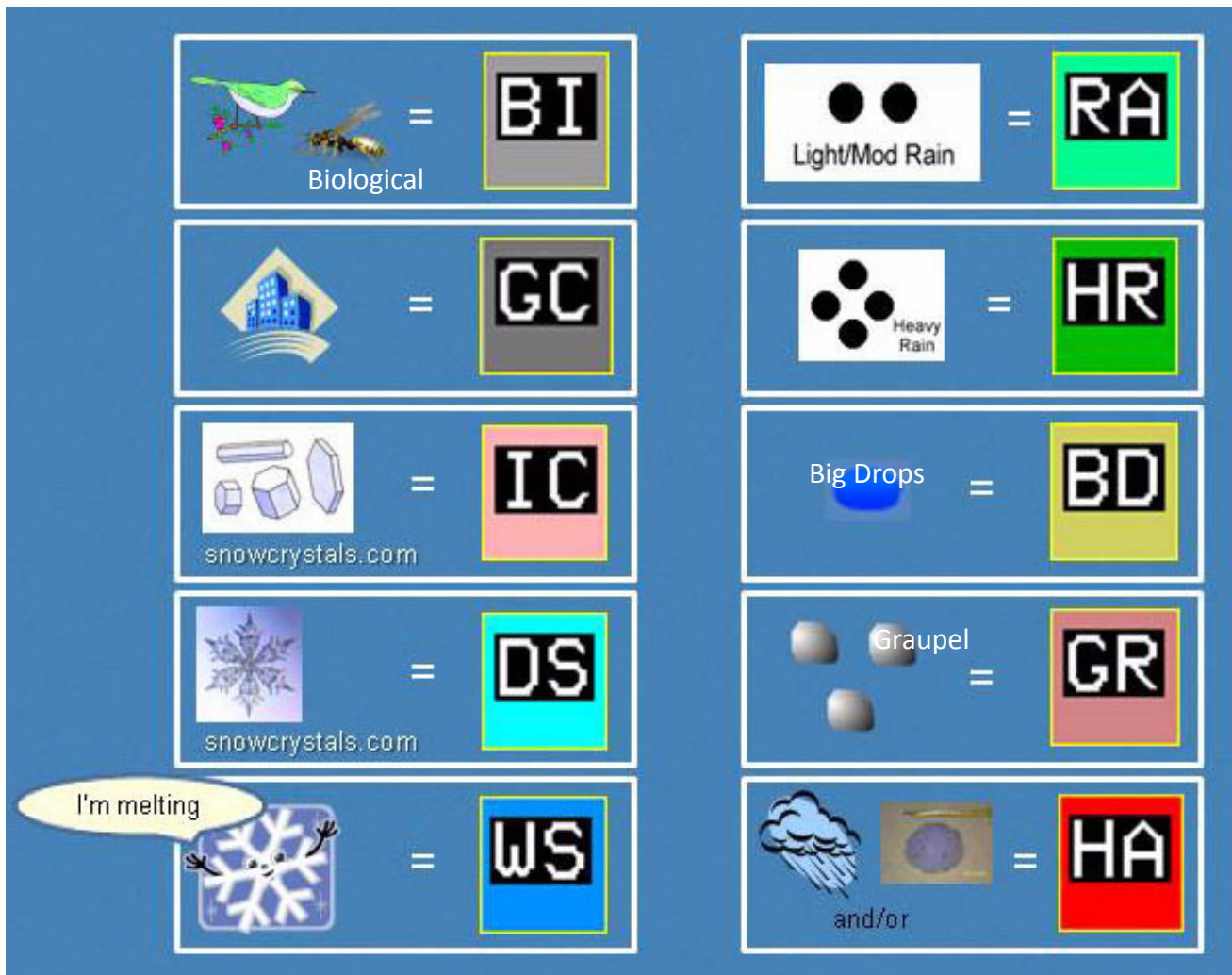


Figure 4-4. Illustration of the Hydrometeor Classification (HC) types

HC products can be loaded from your dedicated radar's drop-down menu from the menu bar in the D-2D window (see Fig. 4-5). The first two choices are 4-panel combinations of base data and the HC product. The third option is where you can find the individual HC products for each elevation angle.



Figure 4-5. D-2D menu display showing the location of the HC product.

Hydrometeor Classification (HC) Operational Applications (Strengths)

Applications of the HC include the following:

- Safety net for base data analysis
- Input for precipitation algorithms
- Quick look at possible areas of concern

Safety Net for Base Data Analysis

In an operational setting, the HC product will be most useful for supplementing base data analysis. Much like the Tornado Vortex Signature (TVS) algorithm can alert a forecaster to something possibly missed in base data analysis, the HC algorithm can do the same thing. However, just like the TVS algorithm may misclassify a signature, so might the HC. Therefore, it is recommended that the HC product be used in conjunction with the polarimetric base data, and not as a stand-alone product. In Fig. 4-6 on page 76, we see a reflectivity core of nearly 70 dBZ indicating that hail is likely. Looking at the HC product on the right, this echo has been classified as hail, which correlates well with the associated Z values. However, looking at some other areas in the HC product, there are some less suspicious echoes tagged as hail. More than likely, there is not hail occurring in these bins, but it might be a good idea to look closer at these areas and delve a little deeper into the other base data (ZDR, CC, etc.).

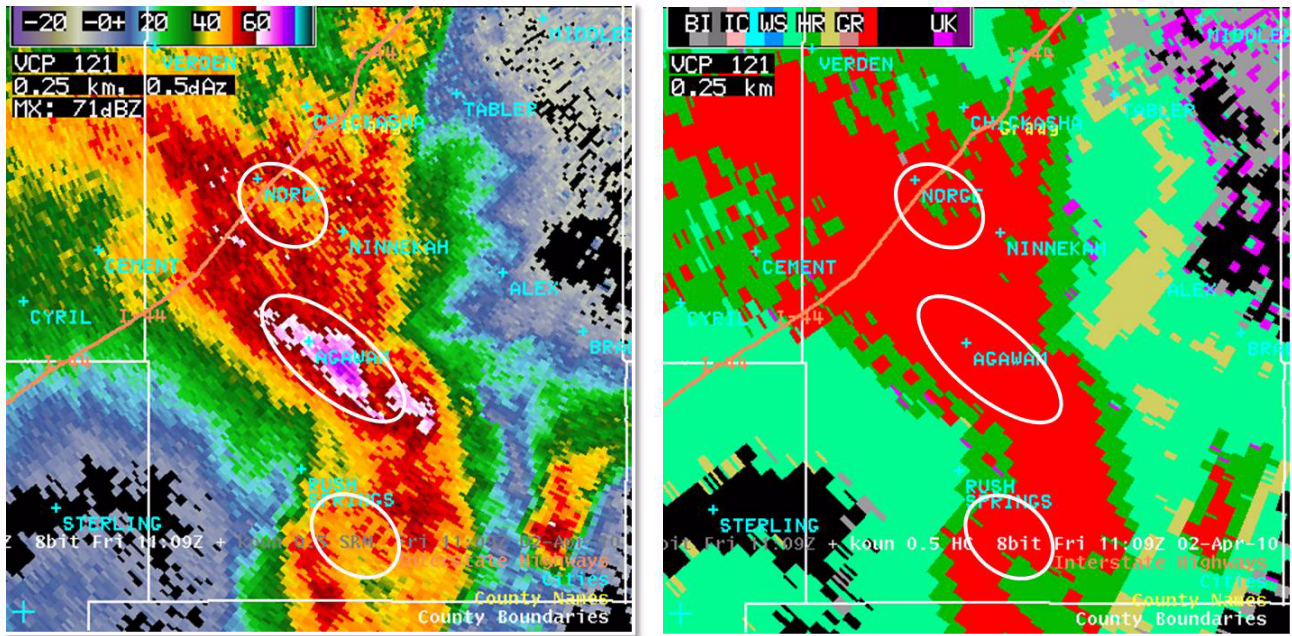


Figure 4-6. Reflectivity (left) and corresponding hydrometeor classification (HC) product (right). The HC product confirms hail where we would expect it, but also tags hail in areas where we would not expect it.

The dual-polarization quantitative precipitation estimation (QPE) algorithm uses the output of the HC algorithm to determine which precipitation relationship to use for each bin. This process has the potential to improve QPE in regions such as clutter and hail.

Input for Precipitation Algorithm

The HC product can help a forecaster more quickly hone in on an area of interest. Three examples come to mind where a quick look at regions of interest might be helpful. First, the base data may be providing subtle hints that might get overlooked by a forecaster. The second example would be during intense operations where multiple severe storms are occurring and a storm might be overlooked simply due to workload. The last example would be for aviation interests concerned about hail. This product could be used to find areas of possible hail to help focus interrogation.

Provides Quick Look at Regions of Interest

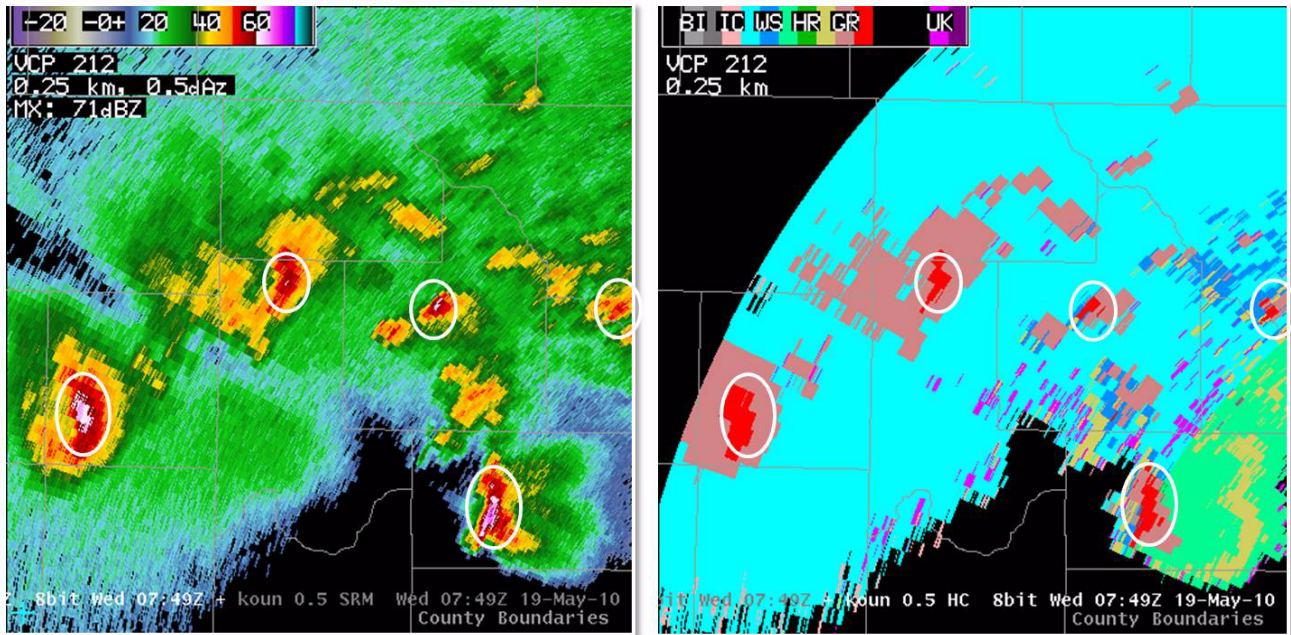


Figure 4-7. Reflectivity (left) and hydrometeor classification (HC) product output (right). Notice the HC product is indicating hail within the white ovals, alerting the forecaster to these areas.

Figure 4-7 shows an example where HC helps focus attention on a particular area of interest. In Z, the storms in the white circles have high reflectivity, so hail is a possibility. The HC algorithm has classified the same areas as hail-rain, which agrees with the initial analysis. In the middle storm, there are a few pixels of high Z and in the HC output they are tagged as hail. Where the forecaster might not be focusing attention is the storm farthest to the east (right edge of reflectivity image in Figure 4-7). Reflectivities are high, but areal coverage is small, and the absolute magnitude of the reflectivity is marginal. However, the HC is suggesting hail, so this might prompt a forecaster to look at the base data a little closer.

Hydrometeor Classification (HC) Limitations (Weaknesses)

Some limitations of HC include:

- Overlapping polarimetric characteristics between classes

- Subjective and empirical fuzzy-logic membership functions and weights
- Uncertainty not portrayed
- It is an Algorithm
- Ground truth
- Range folding in batch cuts

Some hydrometeor classes have very similar polarimetric characteristics. Checks have been put in place to help mitigate this problem, but the algorithm is not fool proof. Therefore, keep a critical eye open when viewing the HC output.

Overlapping Polarimetric Characteristics Between Classes

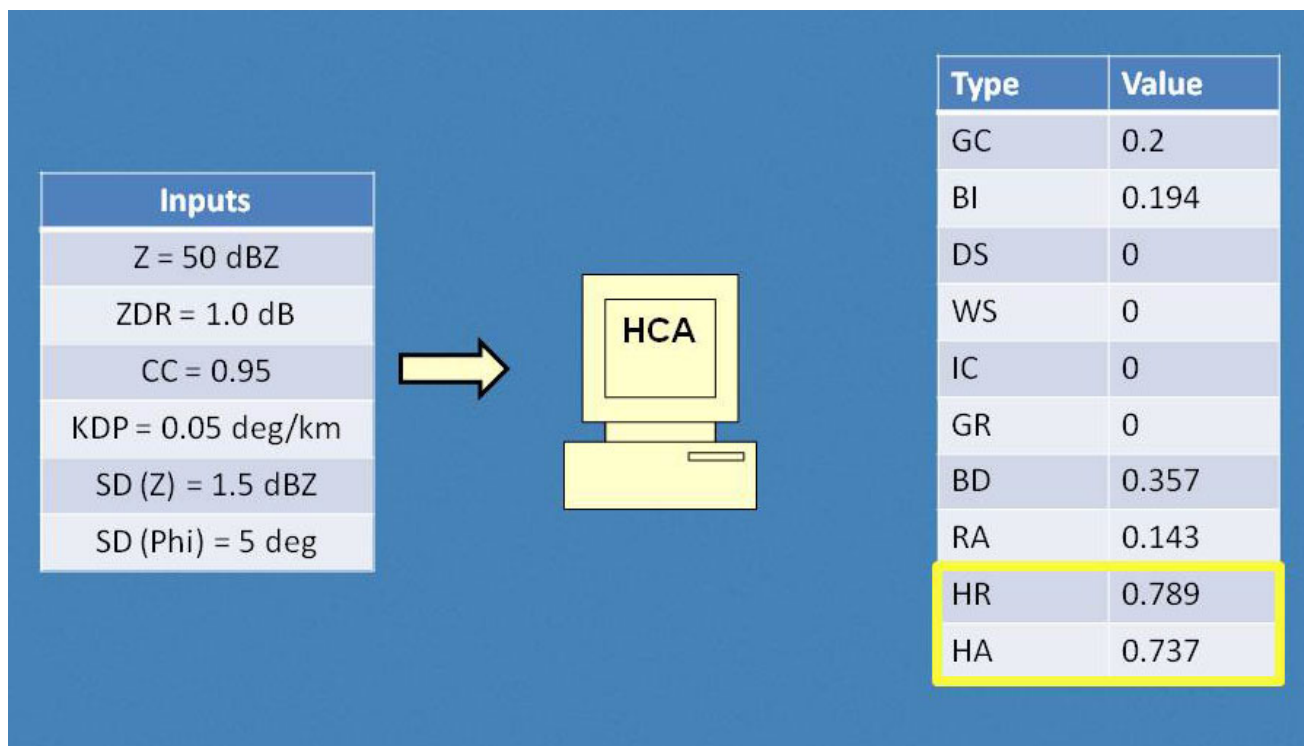


Figure 4-8. Unique set of inputs (left) yields high likelihood values (right) of both heavy rain and hail.

Figure 4-8 shows a radar bin’s polarimetric values. The SD(Z) and SD(Phi) are texture parameters for Z and Φ_{DP} that are good discriminators between non-meteorological and meteorological echoes. Running these through the algorithm, we see that heavy rain (HR) and hail-rain (HA) with rain have

likelihood values much higher than any of the other classes. Heavy rain has a likelihood value of 0.789 while hail-rain has a likelihood value of 0.737. The reason for the close likelihood values is because of the overlap of the polarimetric characteristics of heavy rain and hail possibly mixed with rain.

Subjective and Empirical Fuzzy-logic Membership Functions and Weights

Recall from the RDA/RPG training on the HC, that each classification has a fuzzy-logic membership function that defines a range of values where that classification is possible.

	X1	X2	X3	X4	Weight
Z	5	10	35	40	1.0
ZDR	-0.3	0.0	1.3	1.6	0.8
CC	0.95	0.98	1.0	1.01	0.6
KDP	0.001	0.003	10	100	1.0
SD(Z)	0	0.5	3.0	6.0	0.2
SD(Phi)	0	1	15	30	0.2

Figure 4-9. Table showing the membership function values and weights for dry snow in the Hydrometeor Classification Algorithm (HC)

The second through fifth columns in the chart in Figure 4-9 are the ranges of values for each input that defines the inputs' fuzzy logic membership functions for dry snow. The far right column represents the weighting each input gets in determining the overall likelihood value for that classification. The weighting factor is a number from 0 to 1 that determines how good each input variable is at discriminating the classification. The numbers in this chart are not important at this point. What is important is that these values were not objectively deter-

mined, rather they were subjectively or empirically determined based on many research studies. Since they were subjectively or empirically based, they may not be representative of all regions and might need tweaking in future upgrades to the algorithm.

Some classifications have heavily overlapping polarimetric characteristics, which can cause the likelihood values to be close. However, the algorithm is forced to only display the most likely output, and does not tell the forecaster anything about the likelihood value of other possible classifications. Therefore, it is imperative that a forecaster view the HC product with a critical eye. If you were expecting one output, and the HC gave another, it could well be that your expected output was “next in line”. In the example shown in Figure 4-9, the forecaster would only see HR displayed in the HC product and never know that HA was in close second.

Uncertainty Not Portrayed

As with any algorithm, the human is still the better interpreter. If reason and experience tell you, for example, that hail is occurring in a 75 dBZ core, but the HC is saying it is heavy rain, believe in reason and experience. As the old adage goes for algorithms, “Garbage in equals garbage out.”

It’s an Algorithm

Ground Truth Even if the classification is based on good data and looks “right”, it may not represent the type of precipitation reaching the ground. This scenario is more likely the farther the echo is away from the radar where below beam effects are a concern. Figure 4-10 shows a situation where the HC is tagging hail, but below the beam the hail completely melts and is rain at the ground.



Figure 4-10. Precipitation detected by the radar may not be the same as what reaches the ground, due to below beam effects

Range Folding in Batch Cuts Recall that the Dual-Pol variables are not computed in range folding in the batch cut elevations. Batch cut elevations are those elevations that are from 1.65 to 6.5 degrees. They are called batch because each radial uses alternating high/low PRF pulses to construct the base moments. However, for the dual-pol variables, it uses only the high PRF pulses which are subject to range folding. The HC product is still generated because Z and the height of the 0°C are provided. Therefore, be cautious when interpreting the HC product in areas where the dual-pol variables are experiencing range folding.

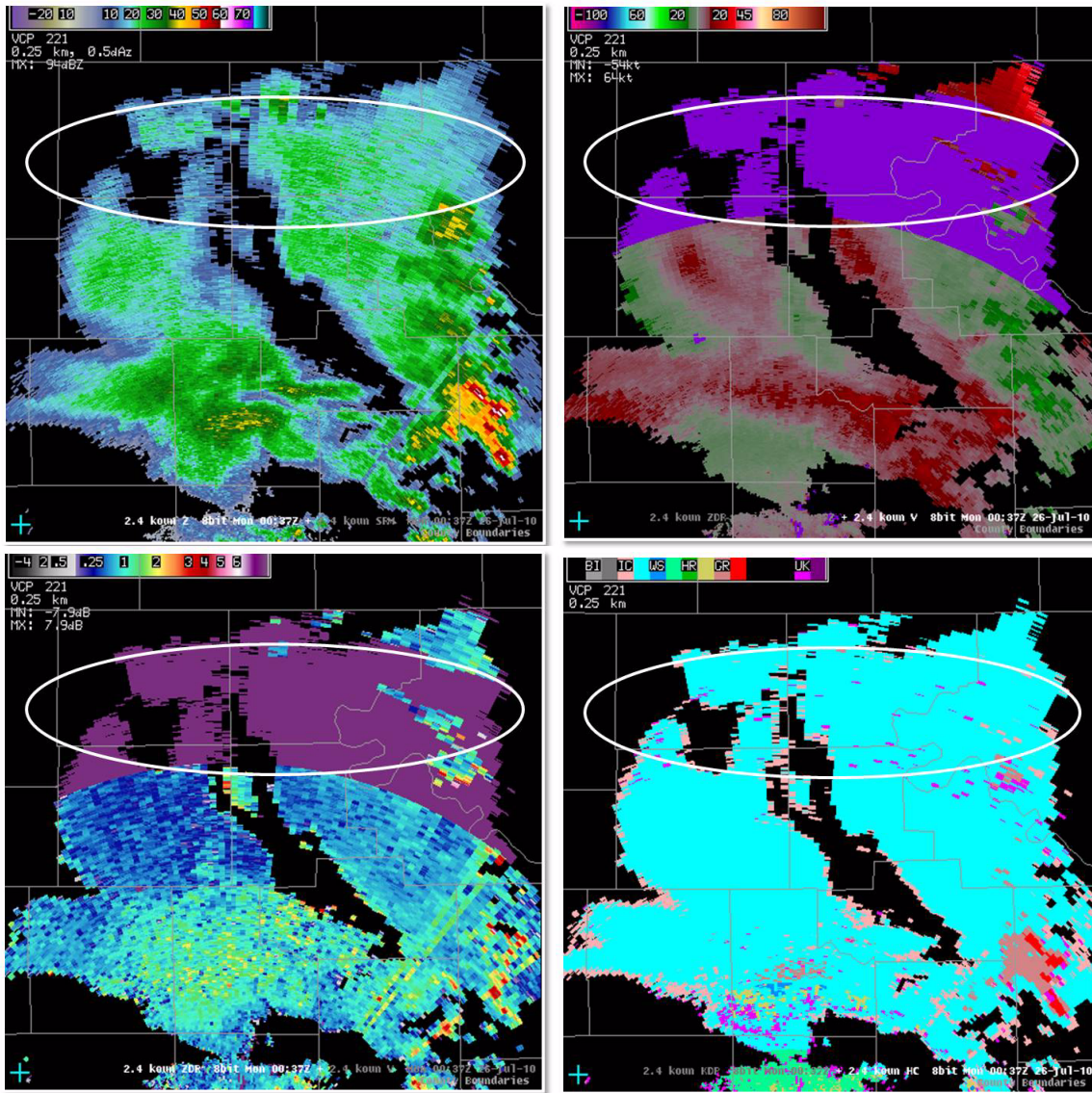


Figure 4-11. Reflectivity (top left), velocity (top right), differential reflectivity (bottom left) and hydrometeor classification (HC) for a 2.4 degree elevation scan. Notice the range folding ('purple haze') in the white oval in both velocity and ZDR, but not in HC.

Note in the velocity image in Figure 4-11 the large area of range folding to the north. Looking in ZDR, there is extensive range folding in this region. Now, look at the HC product. Where there is range folding, the algorithm is producing a classification in most of the bins. These classifications are based solely on Z and the height of the 0°C, so be

careful when interpreting the HC at any elevation with range folding.

Lesson 5: Melting Layer (ML)

As mentioned in previous lessons, the melting layer has distinct signatures in ZDR and CC. This characteristic is used by the melting layer detection algorithm (MLDA) to automatically detect a melting layer from the radar data and then display it as a graphic overlay in AWIPS. The green solid and dotted lines in Figure 5-1 represent the melting layer (ML) product and will be discussed in this lesson. This graphic is available every volume scan at every elevation angle. A more detailed look at the algorithm is discussed in the RPG lessons.

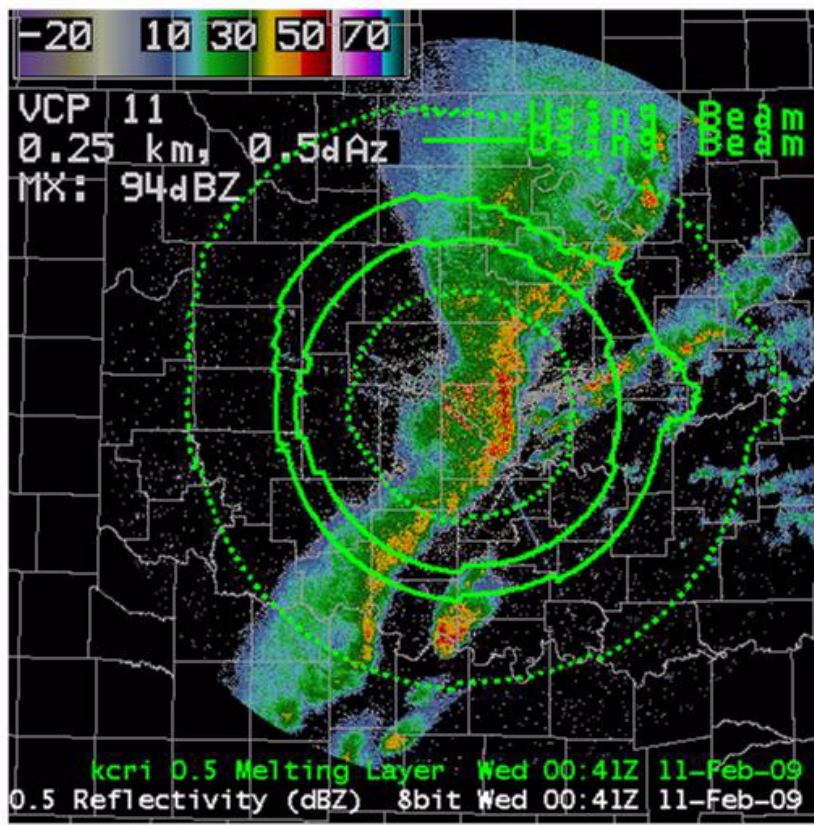


Figure 5-1. Melting Layer (ML) product overlaid on top of 0.5 degree reflectivity (Z)

Melting Layer Availability and Range

- Available on all elevation angles and VCPs

Melting Layer (ML) Characteristics

- Range: 124 nm

Melting Layer Product Description

- RPG ID: kxxx
- Elevation Angle: x.x in degrees
- RPG Product Code: ML
- Product Name: Melting Layer
- Units: n/a
- Date: Day of week and time in UTC

The heights of the top and bottom of the melting layer as determined by the Melting Layer Detection Algorithm (MLDA) are used to construct the graphic shown in Fig. 5-2 on page 1-86. The inner dotted green line indicates where the top of the beam intersects the height of the bottom of the melting layer. The inner solid green line indicates where the center of the beam intersects the height of the bottom of the melting layer. The outer solid green line indicates where the center of the beam intersects the height of the top of the melting layer. The outer dotted green line indicates where the bottom of the beam intersects the height of the top of the melting layer. So, the majority of the melting layer is within the solid lines, while any effect of the melting layer, no matter how small, falls in between the dashed lines. The “wiggles” in the rings will be explained in the limitations section.

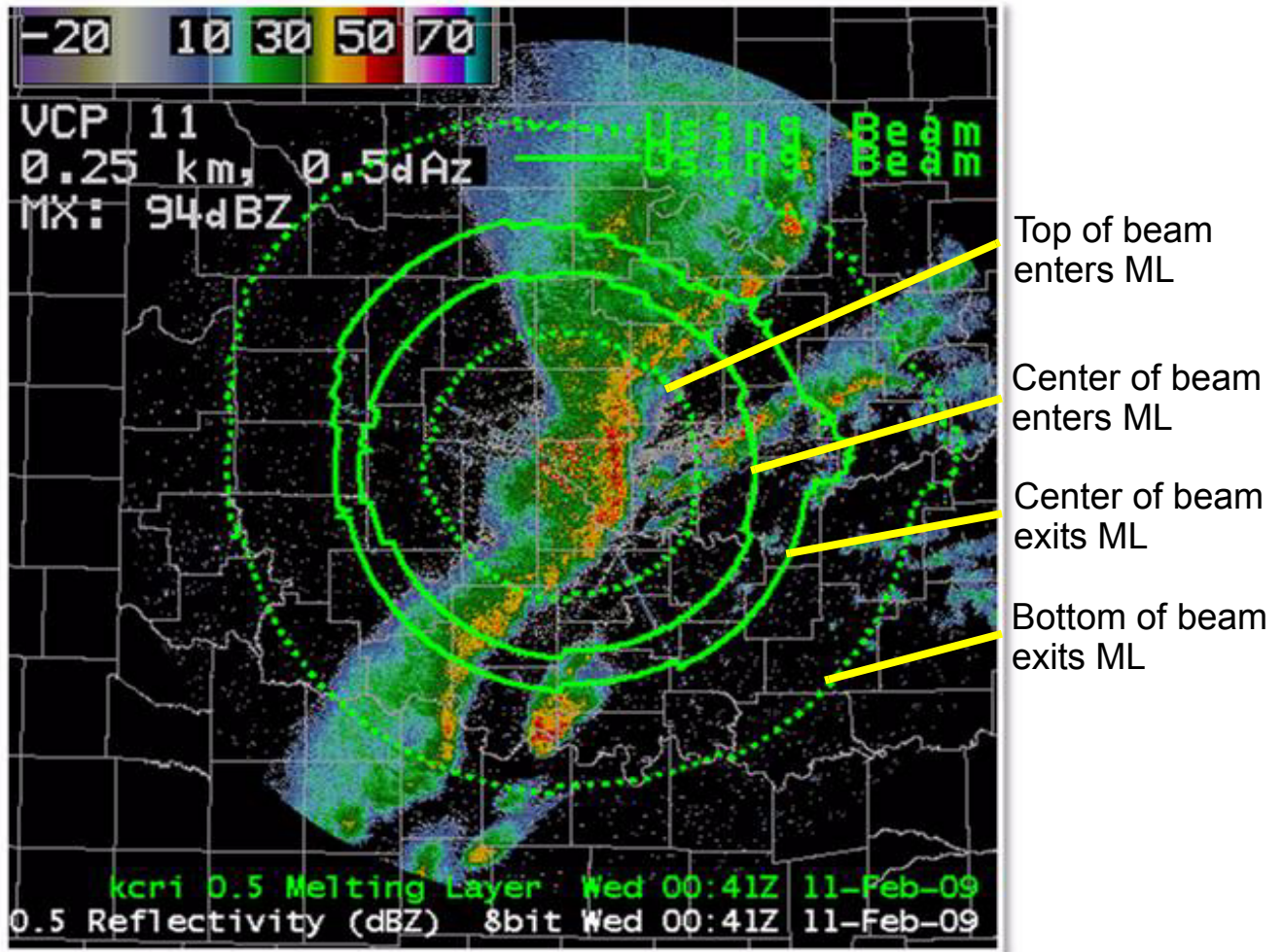


Figure 5-2. 0.5 degree melting layer (ML) product overlaid in 0.5 degree reflectivity. Dotted and solid green lines indicate melting layer heights as calculated by the melting layer detection algorithm (MLDA)

Figure 5-3 helps to better conceptualize the ML graphic as displayed in AWIPS. In this graphic the radar beam is a thick black line representing the center of the beam. The thin black lines on either side represent the beam edges. The two yellow lines represent the melting layer top and bottom as labeled. The dotted and solid vertical green lines represent the corresponding lines as displayed in AWIPS.

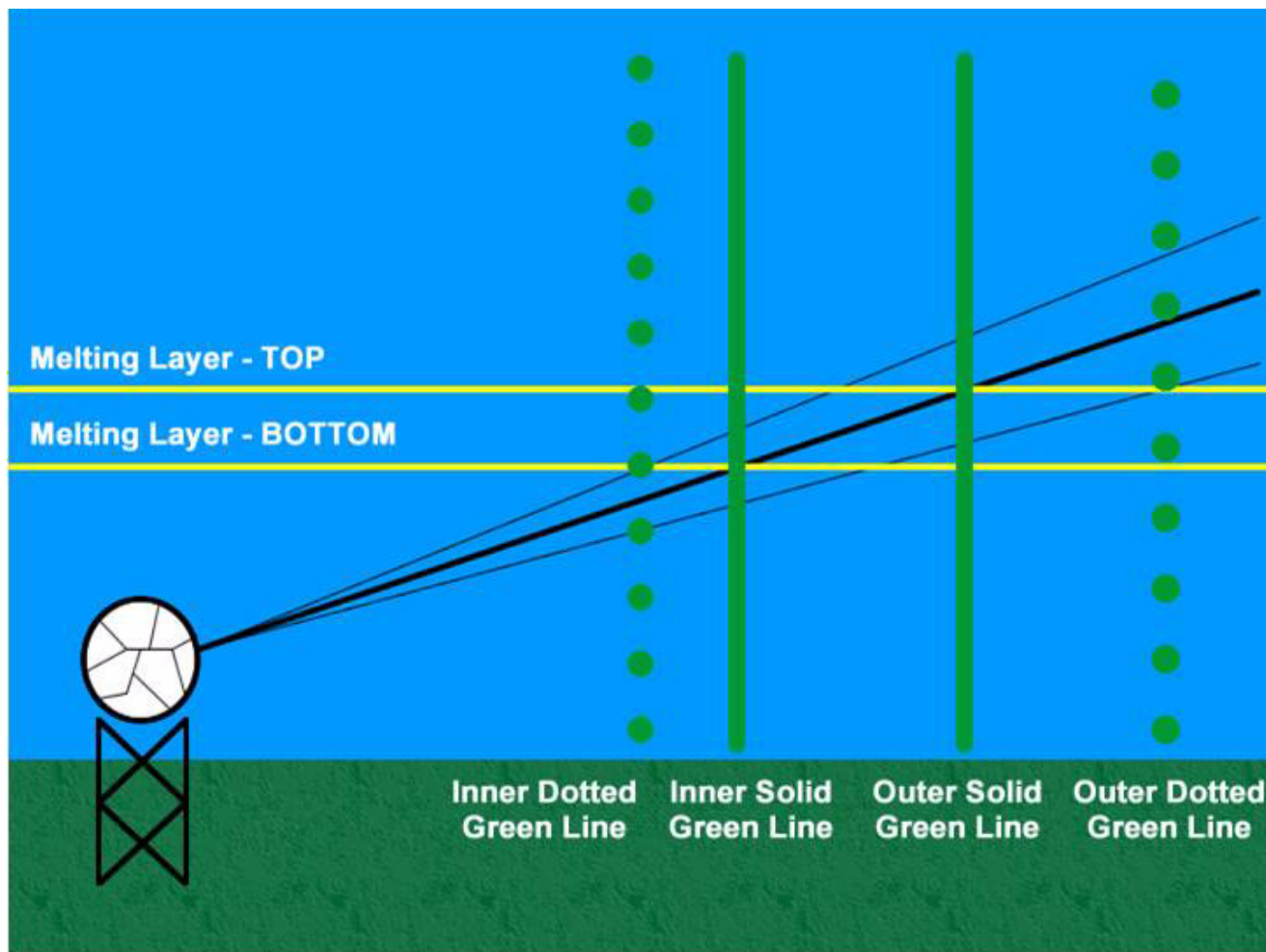


Figure 5-3. A graphical explanation of the melting layer (ML) product in AWIPS.

The ML product graphic can be found in two places in the dedicated radar's drop-down menu (See Fig. 5-4 on page 1-88.). It can be found in conjunction with the polarimetric variables and the HC product in a four panel layout (top oval). Or, it

can be loaded for each individual elevation angle in the dedicated radar's Algorithm Overlays menu (bottom oval). It is recommended that this product only be used on elevation based radar products, and that the elevation angles match between the ML product and the radar product.

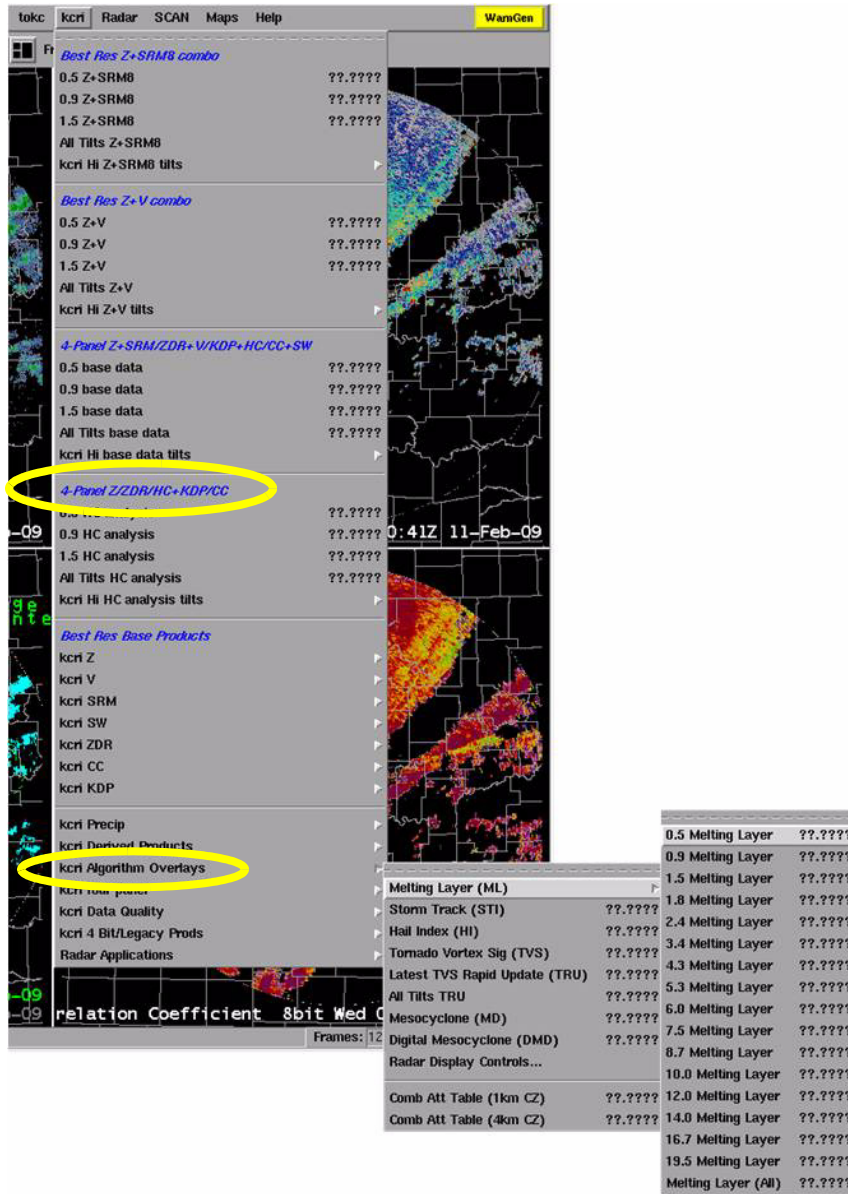


Figure 5-4. D-2D dedicated radar menu with locations of ML products circled.

**Melting Layer (ML)
Operational
Application
(Strengths)**

Strengths of the Melting Layer (ML) product include, but are not limited to:

- Updates every volume scan
- Aids in interpreting base data

**Updates Every Volume
Scan**

With the ML product, you will have updated ML heights every volume scan. Even if the number of wet snow detections needed to compute the melting layer via the dual-pol data is not met, the algorithm ingests a default 0°C height from the RPG adaptation data or the latest RUC model run.

**Aids in Interpreting Base
Data**

Another advantage is that the ML product can help in base data interpretation. Overlaying the ML product can help quickly identify the type of precipitation in the area of interest. This is most useful when the melting level is not uniform or the nearest sounding isn't representative of the area of interest. Fig. 5-5 on page 1-90 shows the 0.5 degree Z with the ML product overlay (left). With this product, one can more quickly tell where the echoes are relative to the melting layer without having to consult a sounding (like the one shown to the right) and then use cursor readout to see where that height is located in range. Remember not to ignore the skew-T data and use it for confirmation if things don't look right. In this example, the ML looks fairly accurate because the ML product has the 0°C height around 15,500 ft MSL while in the skew-T it is around 16,200 ft MSL.

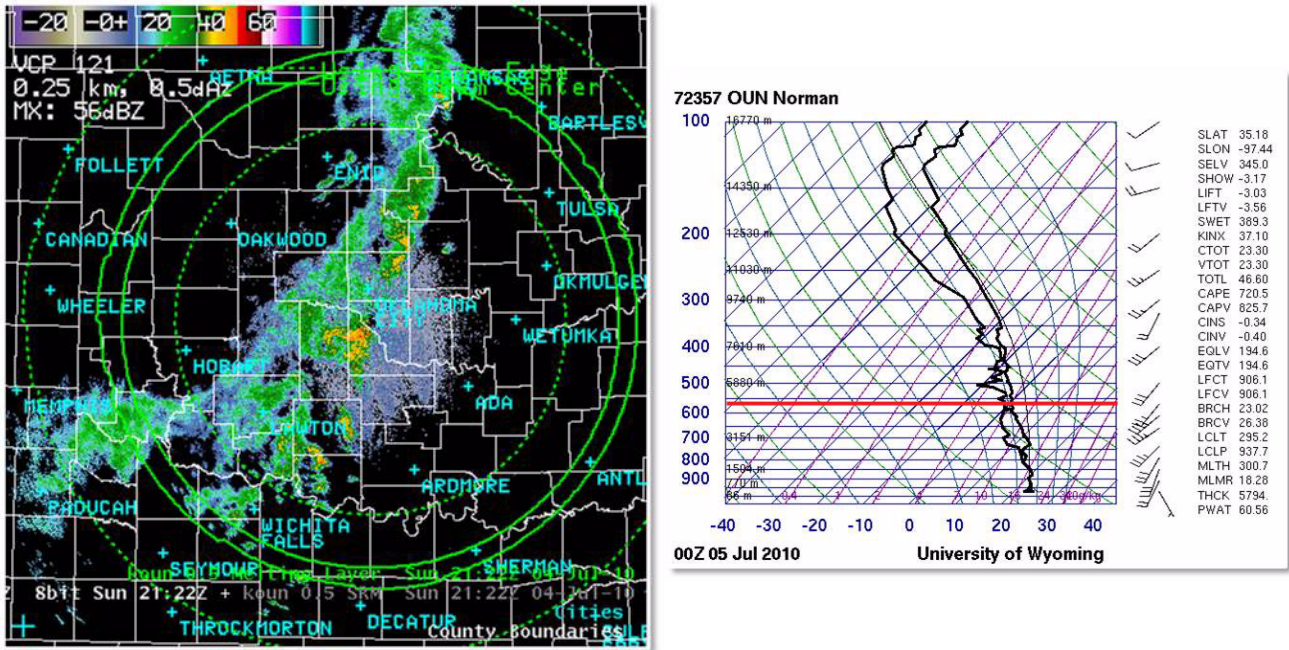


Figure 5-5. Although the melting layer product (left, overlaid on 0.5 degree Z data) is easier to use, verifying with a nearby sounding (right) ensures reliability. The 0°C height is highlighted on the sounding by a red line.

Limitations of the ML product include the following:

Melting Layer (ML) Limitations (Weaknesses)

- Polarimetric ML detection unlikely with:
 - Fast-moving cold fronts
 - Events with small areas of stratiform rain
 - Majority of domain is below freezing
 - Isolated storms at moderate to far range from radar
- Does not perform well when two melting levels are present
- Unrealistic discontinuities and false detections
- Performance in mountainous locations

**Situations with Unlikely
ML Detection**

Since the algorithm requires a sufficient amount of wet snow detections over either a 3 or 6 volume scan period, there are some situations where the algorithm will not detect a melting layer via polarimetric data.

Fast-Moving Cold Fronts: It does not perform well near fast moving cold fronts because the number of volume scan periods requirement to accumulate wet snow points makes it difficult for the algorithm to compute an accurate ML height.

Small Areas of Stratiform Rain: Events with small stratiform rain areas will not have enough wet snow points to compute a melting layer from the polarimetric data.

Majority of Area Below Freezing: If the majority of the area is below freezing, the MLDA will use the default 0°C height in the environmental data at the RPG.

Isolated Storms: As with small areas of stratiform rain, if there are just isolated storms around, there probably won't be enough wet snow points for the algorithm to function properly. Figure 5-6 exemplifies the case of isolated storms. With little areal coverage by isolated storms, the algorithm will not have enough wet snow points to determine a melting layer.

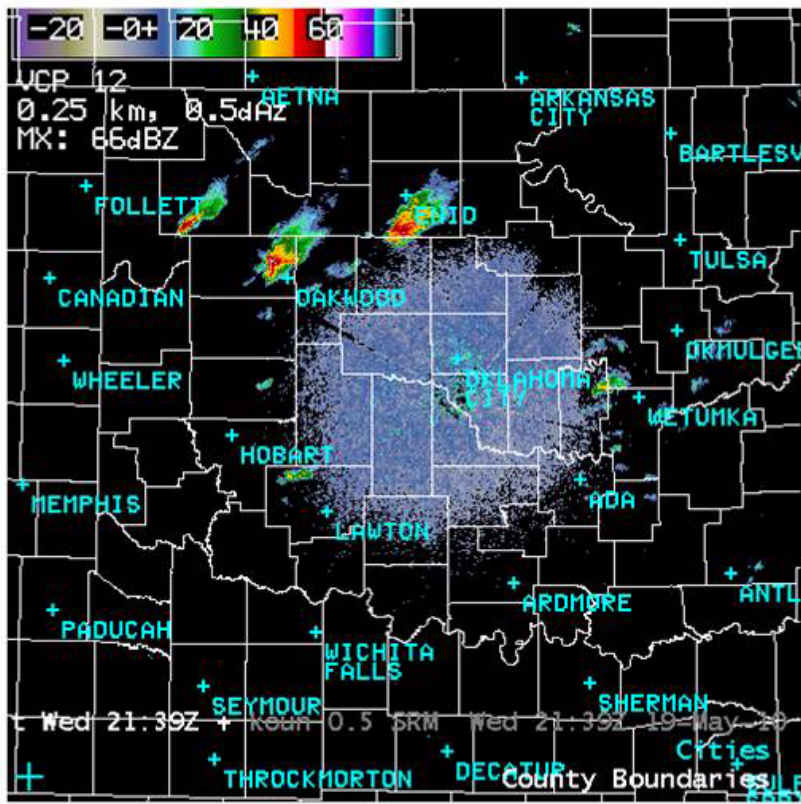


Figure 5-6. Isolated storms in northern Oklahoma exemplifying a situation where the MLDA would not use polarimetric data to determine a melting layer top and bottom because of too few data points.

Two Melting Levels

In the event there are two melting levels, the algorithm will only detect one of them. These types of situations often include sleeting events. It might be possible to see both in the data itself but only if the two melting levels are far enough apart for it to be resolved by the radar. In Figure 5-7, the image on the right is the 00Z sounding from OUN and on the left is the reflectivity with ML overlaid at 0100Z. In the sounding note there are two melting layers, but in the ML product, only one is shown. Implications of this are that the HC product will not show frozen precipitation at the ground (most likely will be rain). Therefore, having surface and sounding data available during these types of events is recommended.

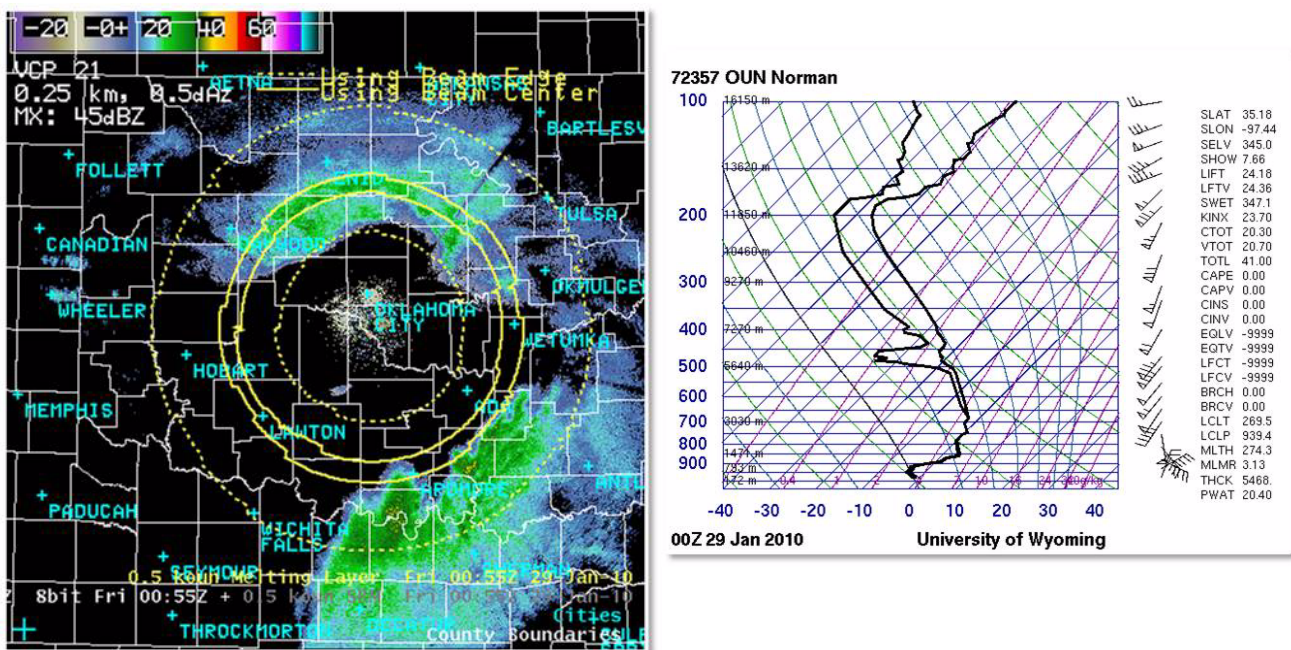


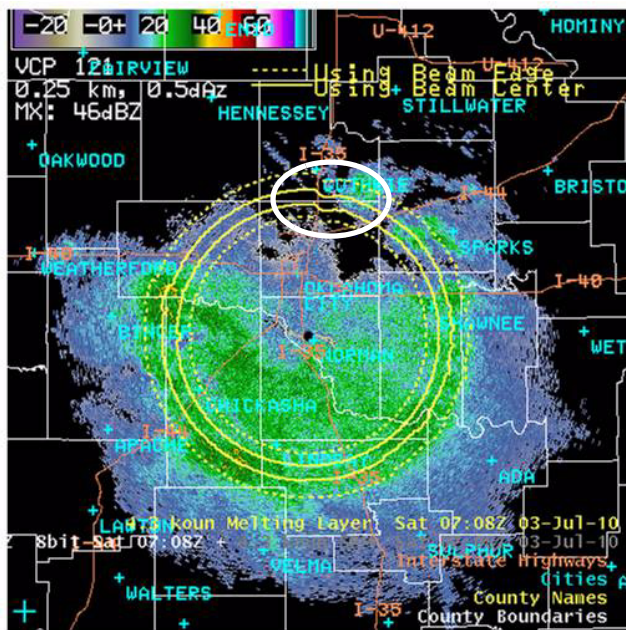
Figure 5-7. Reflectivity (Z) with melting layer (ML) product output (left) and corresponding nearest 00Z sounding (right). Notice the two melting levels on the sounding with only one displayed by the ML product.

Two situations to look out for when viewing the ML product are unrealistic discontinuities due to antenna wobble and algorithm error. **Antenna wobble** occurs after the radar dish has changed elevation angles and the radar dish does not get to exactly the defined elevation angles. This causes the beam to over- and undershoot the defined elevation angle for a few azimuths until it settles. The white oval in the image on the left of Figure 5-8 shows an example of antenna wobble as displayed in the ML output.

Unrealistic Discontinuities

Discontinuities caused by **algorithm error** will appear spiky and show up on every elevation angle at the same azimuth. The discontinuities caused by antenna wobble will be much smoother and will only appear on elevation angles where the antenna wobble occurs. The example on the right shows algorithm error to the east (white oval).

Antenna Wobble



Algorithm Error

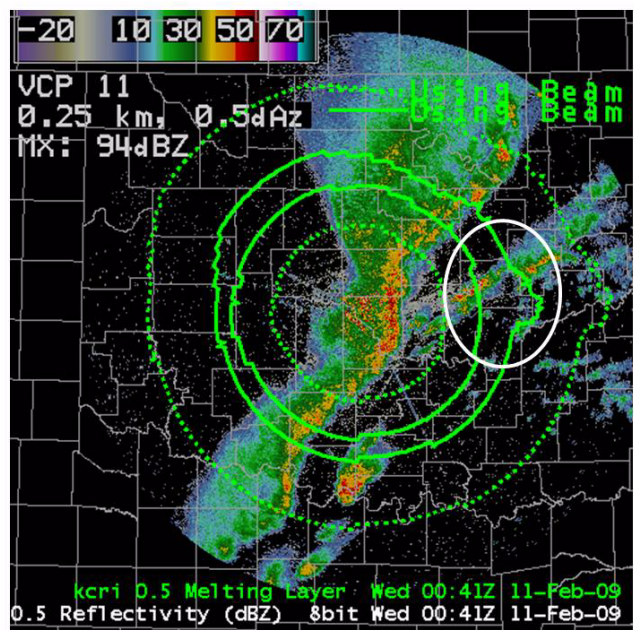


Figure 5-8. Examples of antenna wobble (left) and algorithm error (right) for melting layer product.

Performance in Mountainous Regions

Recall that the MLDA computes the ML product using data from the 4.0 through 10.0 degree elevation angles. In mountainous regions, the beam at these elevation angles might hit the melting layer very near the radar and be completely above the melting layer within the precipitation. The graph in Figure 5-9 illustrates this problem.

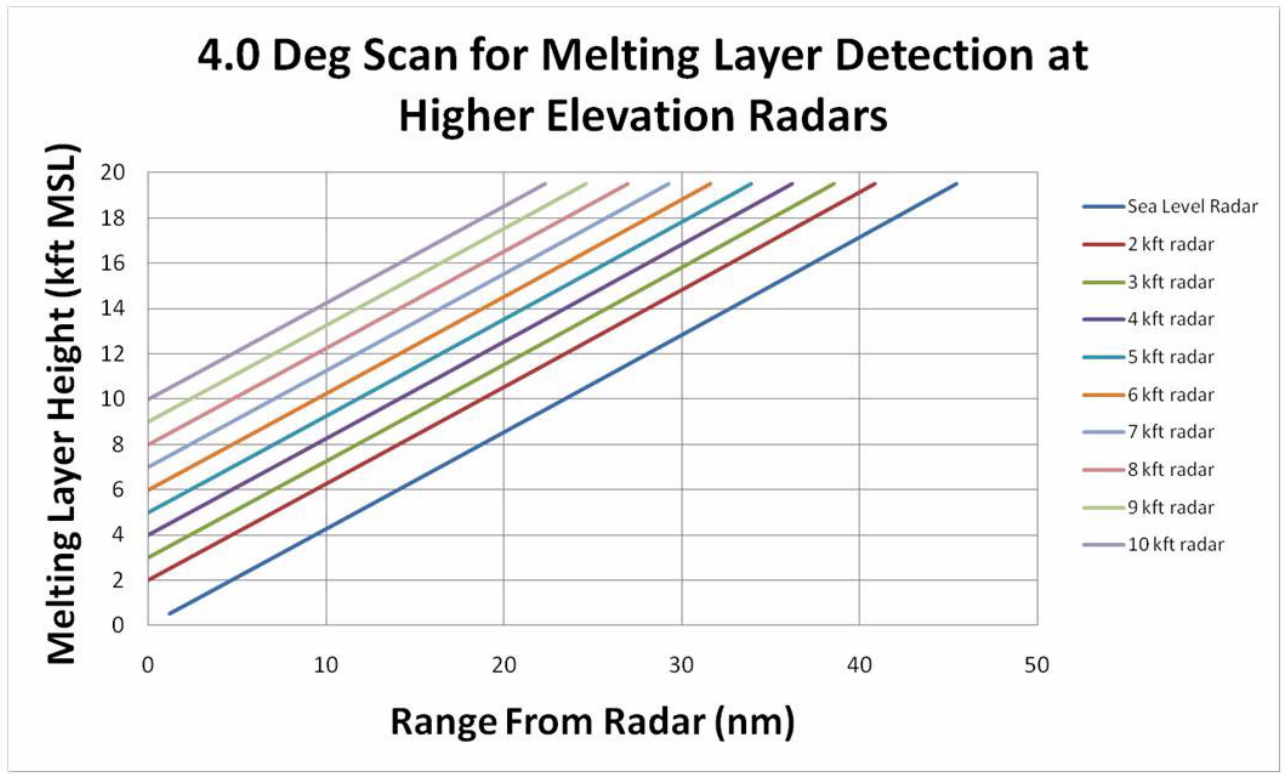


Figure 5-9. Graph of Melting Layer Height vs. Range From Radar based on a 4.0 degree scan. Notice that radars at higher elevations may pass through the melting layer very near the radar and be above it in the precipitation farther from the radar.

As an example, suppose your radar is at 10,000ft MSL, and the height of the melting layer is at 12,000 ft MSL. The top line on the graph represents the height of the 4.0 degree elevation scan from 0 to 50 nm from the radar. For our example then, the 4.0 degree elevation angle will cross the melting layer only 6 nm from the radar. If most of the precipitation is out past 6 nm, then the algorithm will not be able to detect the melting layer because the radar beam is overshooting the melt-

Lesson 6: Dual-Pol Quantitative Precipitation Estimation (QPE)

Recall that the legacy precipitation estimation algorithm uses the Hybrid Scan Reflectivity as input for a single $R(Z)$ relationship. For dual-pol quantitative precipitation estimation (QPE), the Hybrid Scan Hydroclass (HHC) product is used as input for a variety of rainfall rate relationships based on Z , ZDR , and KDP . This means that the rainfall rate relationship used for a particular location is specific to the dominant hydrometeor type at that location, potentially improving the estimation of rain rate compared to estimations based solely on reflectivity. Figure 6-1 illustrates the analogy between legacy and dual-pol precipitation estimation. This lesson will describe new dual-pol QPE products and the strengths and weaknesses of dual-pol QPE as a system.

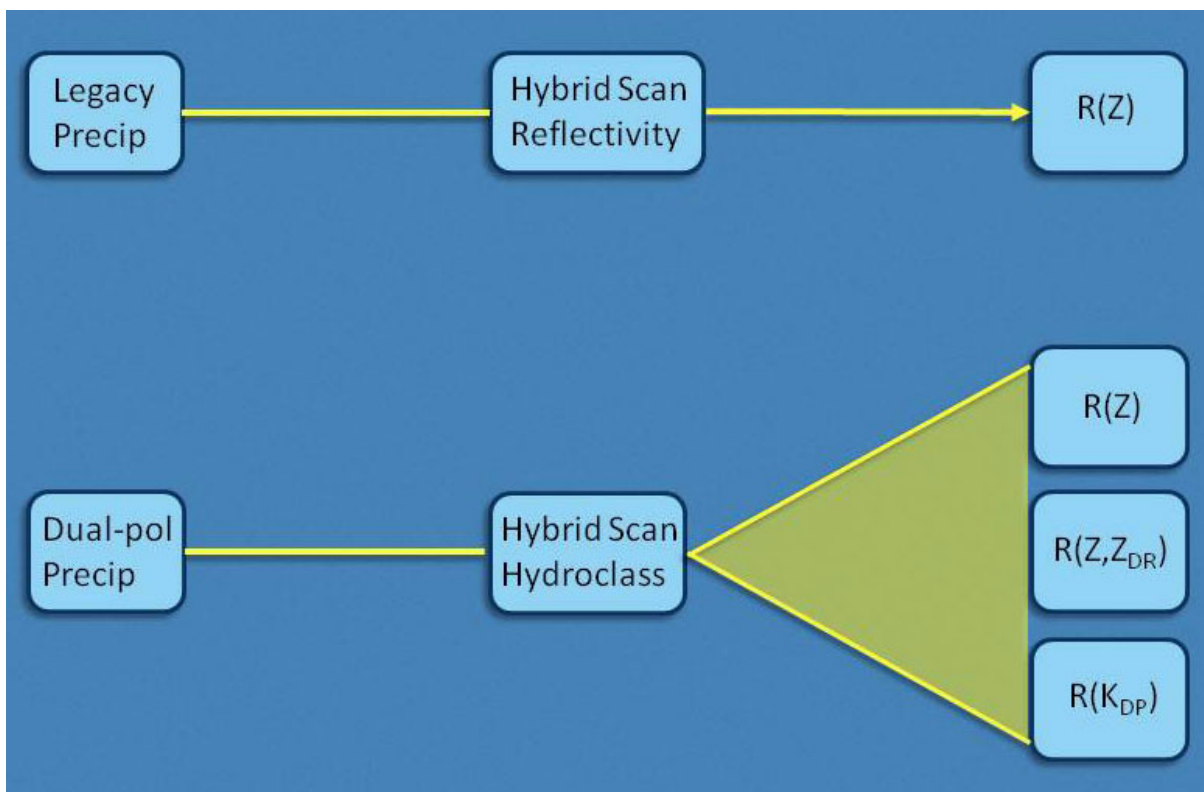


Figure 6-1. Legacy precipitation estimation (top) and dual-pol precipitation estimation processes (bottom).

Dual-pol QPE products can be loaded from any radar menu (see Fig. 6-2). Click on the menu of the desired dedicated radar, then select “kxxx Precip” to access the Dual Pol Precip submenu. Dual-pol products are located under the “Dual Pol Precip” section of the menu as shown by the yellow box on the right in Figure 6-2.

<i>Best Res Z+V combo</i>		<i>Legacy Precip Accum</i>	
0.5 Z+V	--,----	Storm Total Precip (STP)	--,----
0.9 Z+V	--,----	One Hour Precip (OHP)	--,----
1.5 Z+V	--,----	Three Hour Precip (THP)	--,----
All Tilts Z+V		User Selectable Precip (USP)	--,----
koun Hi Z+V tilts	▶	<i>Dual Pol Precip</i>	
<i>4-Panel Z+SRM/ZDR+V/KDP+HC/CC+SW</i>		Precip Analysis (4panel)	--,----
0.5 base data	--,----	Storm Total Accum (STA)	--,----
0.9 base data	--,----	One Hour Accum (OHA)	--,----
1.5 base data	--,----	One Hour Unbiased Accum (DAA)	--,----
All Tilts base data	--,----	Inst Precip Rate (DPR)	--,----
koun Hi base data tilts	▶	Hybrid Hydro Class (HHC)	--,----
<i>4-Panel Z/ZDR/HC+KDP/CC</i>		User Sel Accum (DUA)	--,----
0.5 HC analysis	--,----	User 1hr Accum	--,----
0.9 HC analysis	--,----	User 2hr Accum	--,----
1.5 HC analysis	--,----	User 3hr Accum	--,----
All Tilts HC analysis	--,----	User 6hr Accum	--,----
koun Hi HC analysis tilts	▶	User 12hr Accum	--,----
<i>Best Res Base Products</i>		User 24hr Accum	--,----
koun Z	▶	<i>Unbiased Dual Pol minus Legacy Accum</i>	
koun V	▶	Storm Total Accum (DSD)	--,----
koun SRM	▶	One Hour Accum (DOD)	--,----
koun SW	▶	<i>Snow</i>	
koun ZDR	▶	One Hour Snow Water Eq (OSW)	--,----
koun CC	▶	One Hour Snow Depth (OSD)	--,----
koun KDP	▶	Storm Total Snow Water (SSW)	--,----
koun Precip	▶	Storm Total Snow Depth (SSD)	--,----
koun Derived Products	▶	User Sel Snow Water Eq (USW)	--,----
koun Algorithm Overlays	▶	User Sel Snow Depth (USD)	--,----
koun four panel	▶	<i>Legacy Hybrid Scan</i>	
koun Data Quality	▶	8bit Hybrid Scan Z (DHR)	--,----
koun 4 Bit/Legacy Prods	▶	4bit Hybrid Scan Z (HSR)	--,----
Radar Applications	▶		

Figure 6-2. Menu as displayed in D-2D showing the location of the dual-pol QPE products.

There are nine new QPE products with dual-pol. Fig. 6-3 shows a table summarizing the key attributes of these new products. Many of the products are analogous to legacy precipitation products.

New Quantitative Precipitation Estimation (QPE) Products with Dual-Pol

Product Type	Product Name	Abbreviation	Resolution	Data Levels
Instantaneous	1. Hybrid Hydroclass	HHC	0.25 km X 1 deg.	256 (8-bit)
	2. Digital Precipitation Rate	DPR	0.25 km X 1 deg	65536 (16-bit)
Accumulation	3. Digital Accumulation Array	DAA	0.25 km X 1 deg	256 (8-bit)
	4. One Hour Accumulation	OHA	2 km X 1 deg	16 (4-bit)
	5. Digital Storm Total Accumulation	DSA	0.25 km X 1 deg	256 (8-bit)
	6. Storm Total Accumulation	STA	2 km X 1 deg	16 (4-bit)
Difference	7. Digital One Hour Difference	DOD	0.25 km X 1 deg	256 (8-bit)
	8. Digital Storm-Total Difference	DSD	0.25 km X 1 deg	256 (8-bit)
User-selectable	9. Digital User-Selectable Accumulation	DUA	0.25 km X 1 deg	256 (8-bit)

Figure 6-3. Table summarizing some of the attributes of the nine new dual-pol QPE products.

Hybrid Hydroclass (HHC) Hybrid Hydroclass (HHC) shows the hydrometeor classification that is used as input for the dual-pol precipitation algorithm. The HHC is constructed in a similar manner as the legacy DHR and has similar applications and limitations. The HHC product represents the radar’s best guess of echo type to be used in the dual-pol QPE algorithm. The product legend (“Filter Size: 9”) indicates that the data have been filtered to remove speckling (see Fig. 6-4). The filter is not adaptable, so the filter size in the upper left of the product will always be 9.

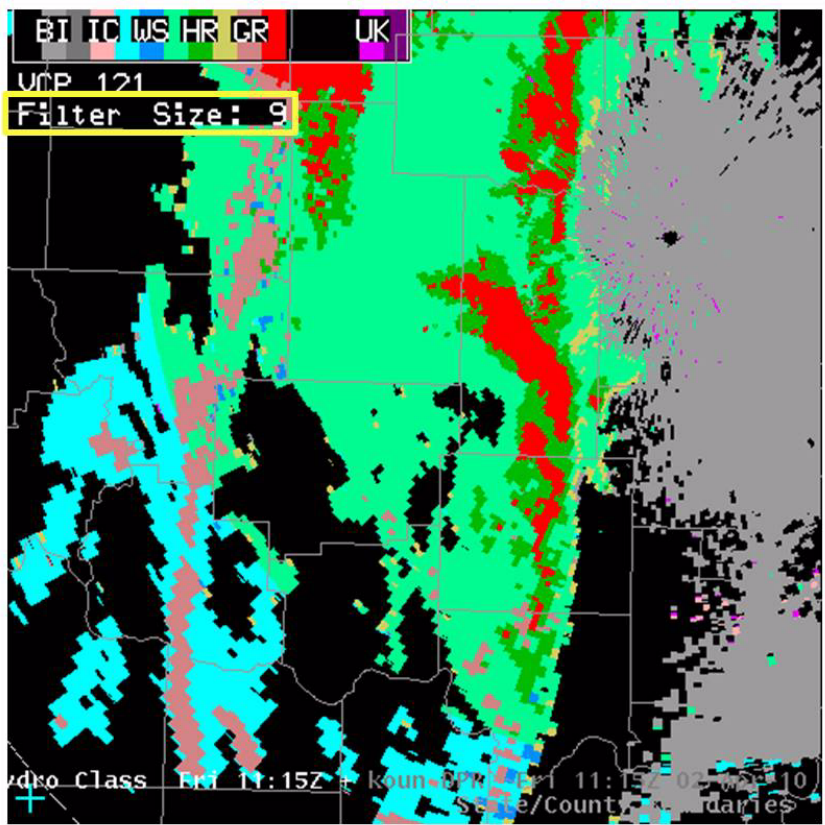


Figure 6-4. Example of Hybrid Hydroclass (HHC) product as seen in D-2D.

New with dual-pol is the ability to view the instantaneous precipitation rate using the Digital Precipitation Rate (DPR, see Fig. 6-5). One advantage of this product is that it can give you a good idea of where the heaviest rain is occurring in real-time, even when reflectivity might be ambiguous. The legend in the upper left lists the maximum precipitation rate anywhere in the product. One caution about DPR: because of file size, low bandwidth connections to some radars may not be able handle it.

Digital Precipitation Rate (DPR)

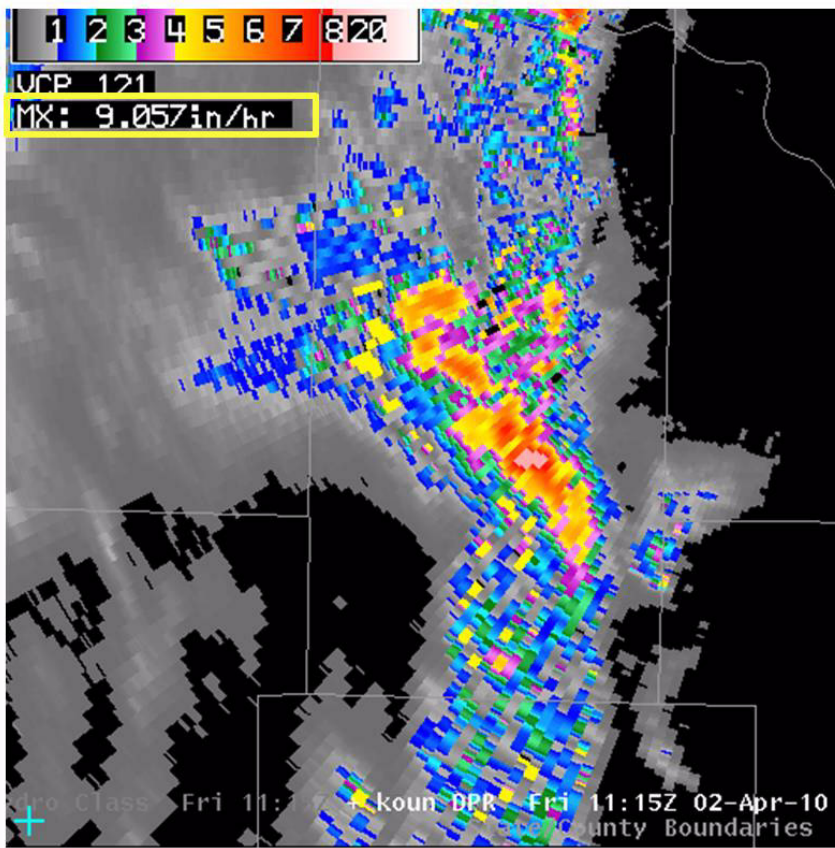


Figure 6-5. Example of the Digital Precipitation Rate (DPR) product as seen in D-2D.

Digital Accumulation Array (DAA)

The Digital Accumulation Array (DAA) is a 1-hour accumulation with no bias applied (see Fig. 6-6). This product was developed for users who want raw, unbiased 1 hour accumulation data and is similar to the legacy Digital Precipitation Array (DPA). It updated every volume scan. The legend in the corner lists the maximum accumulation in inches, the bias (which, of course, is 1.00 since there is never a bias applied to this product), and the product end time. The first two digits of the end time represent the day of the month and the last four digits are the time in UTC.

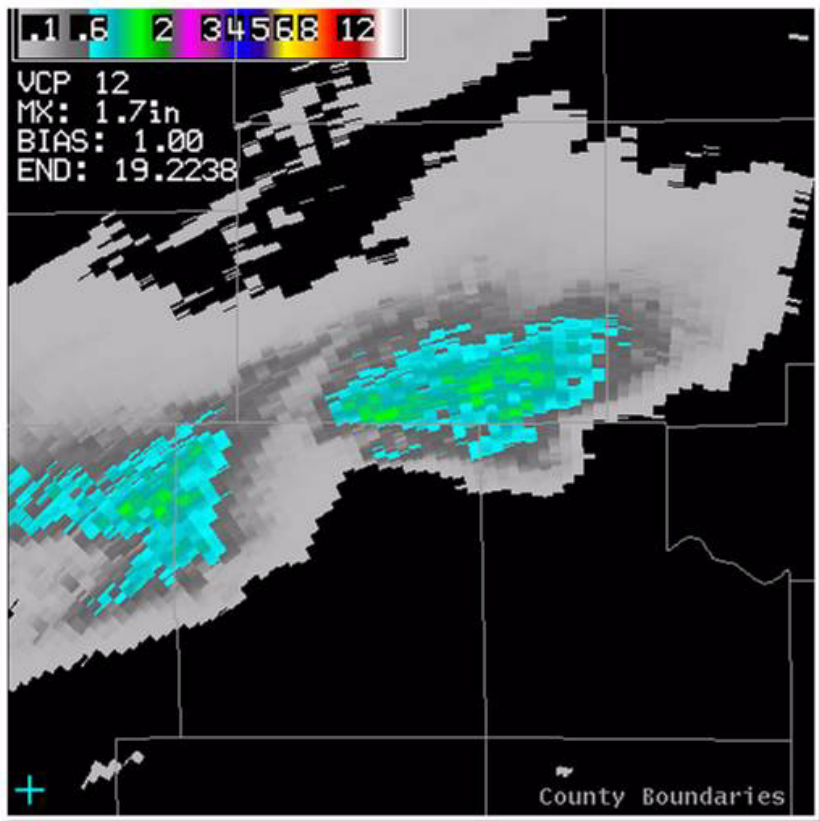


Figure 6-6. Example of the Digital Accumulation Array (DAA) product as seen in D-2D.

One Hour Accumulation, or OHA, is analogous to the legacy One Hour Precipitation (OHP) product (see Fig. 6-7). Like DAA, the legend in the upper left lists the maximum accumulation, the bias, and the product end time. It updates every volume scan.

One Hour Accumulation (OHA)

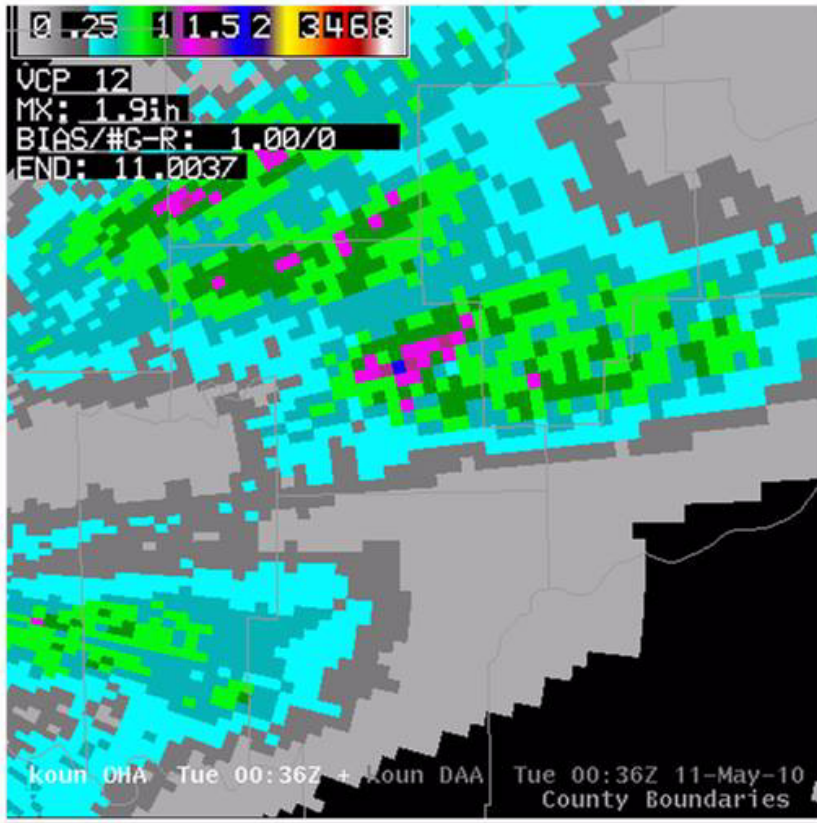


Figure 6-7. Example of One Hour Accumulation (OHA) product as seen in D-2D.

Storm-Total Accumulation Products (DSA and STA)

Digital Storm-Total Accumulation (DSA), like legacy Digital Storm-Total Precipitation (DSP), shows total accumulated rainfall since the beginning of an event (see Fig. 6-8). In the legend you will find the value of the maximum accumulation (anywhere in the product), the bias, and the beginning and ending times in the same format as in DAA. As with the legacy storm total products, one disadvantage is DSA may need to be reset manually at times. DSA may also include data gaps.

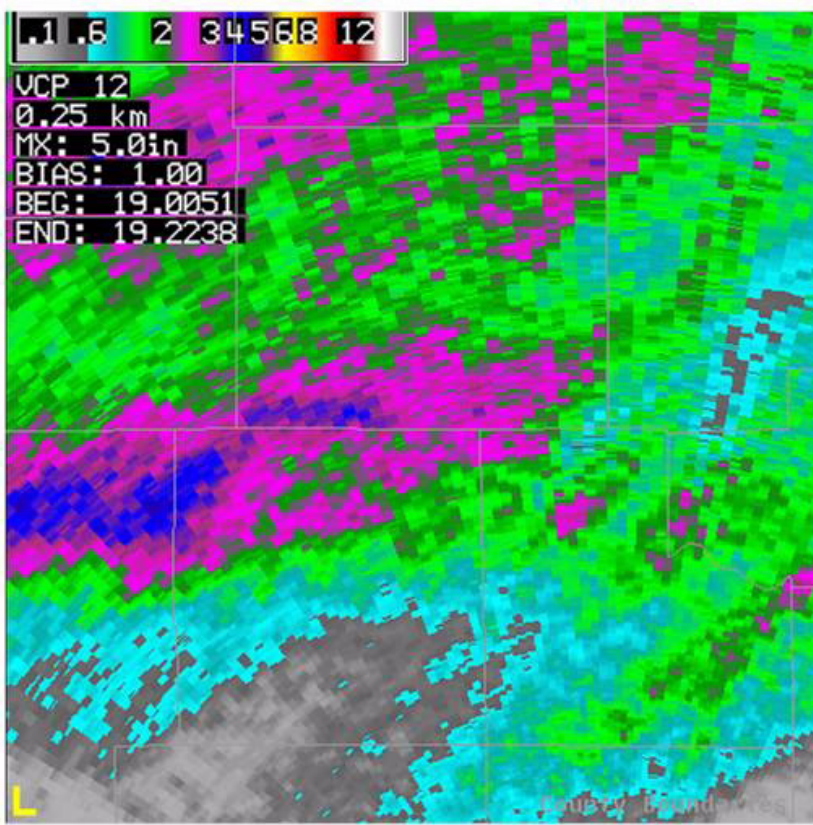


Figure 6-8. Example of Digital Storm-total Accumulation (DSA) product as seen in D-2D.

There is also a 2 km resolution, 4-bit version of this product, Storm Total Accumulation (STA, not shown), that matches the resolution and data levels of the legacy Storm Total Precipitation (STP) product.

Unfortunately, DSA is not labeled as such in the Precip menu in AWIPS. To load DSA, go to the Precip submenu and select “Storm Total Accum (STA)”, as seen in the yellow box in Figure 6-9.

All Tilts base data	??.????		
kcri Hi base data tilts		▶	<i>Legacy Precip Accum</i>
			Storm Total Precip (STP) ??.????
			One Hour Precip (OHP) ??.????
<i>4-Panel Z/ZDR/HC+KDP/CC</i>			Three Hour Precip (THP) ??.????
0.5 HC analysis	??.????		User Selectable Precip (USP) ??.????
0.9 HC analysis	??.????		
1.5 HC analysis	??.????		<i>Dual Pol Precip</i>
All Tilts HC analysis	??.????		Precip Analysis (4panel) ??.????
kcri Hi HC analysis tilts		▶	Storm Total Accum (STA) ??.????
			One Hour Accum (OHA) ??.????
<i>Best Res Base Products</i>			One Hour Unbiased Accum (DAA) ??.????
kcri Z		▶	Inst Precip Rate (DPR) ??.????
kcri V		▶	Hybrid Hydro Class (HHC) ??.????
kcri SRM		▶	User Sel Accum (DUA) ??.????
kcri SW		▶	User 1hr Accum ??.????
kcri ZDR		▶	User 2hr Accum ??.????
kcri CC		▶	User 3hr Accum ??.????
kcri KDP		▶	User 6hr Accum ??.????
			User 12hr Accum ??.????
kcri Precip		▶	User 24hr Accum ??.????
kcri Derived Products		▶	
kcri Algorithm Overlays		▶	<i>Unbiased Dual Pol minus Legacy Accum</i>
kcri four panel		▶	Storm Total Accum (DSD) ??.????
kcri Data Quality		▶	One Hour Accum (DOD) ??.????
kcri 4 Bit/Legacy Prods		▶	
Radar Applications		▶	

Figure 6-9. D-2D menu used to load Digital Storm-total Accumulation (DSA)

Similarly, to add DSA to the RPS list, go to the Dual Pol Precip submenu in the Add Product GUI and select “Storm Total Accum (STA)” (see Fig. 6-10). Be sure that 256 is selected in the “Data levels” drop down menu and 0.25 is selected in the “Resolution” drop down menu (see Fig. 6-11 on page 1-108).

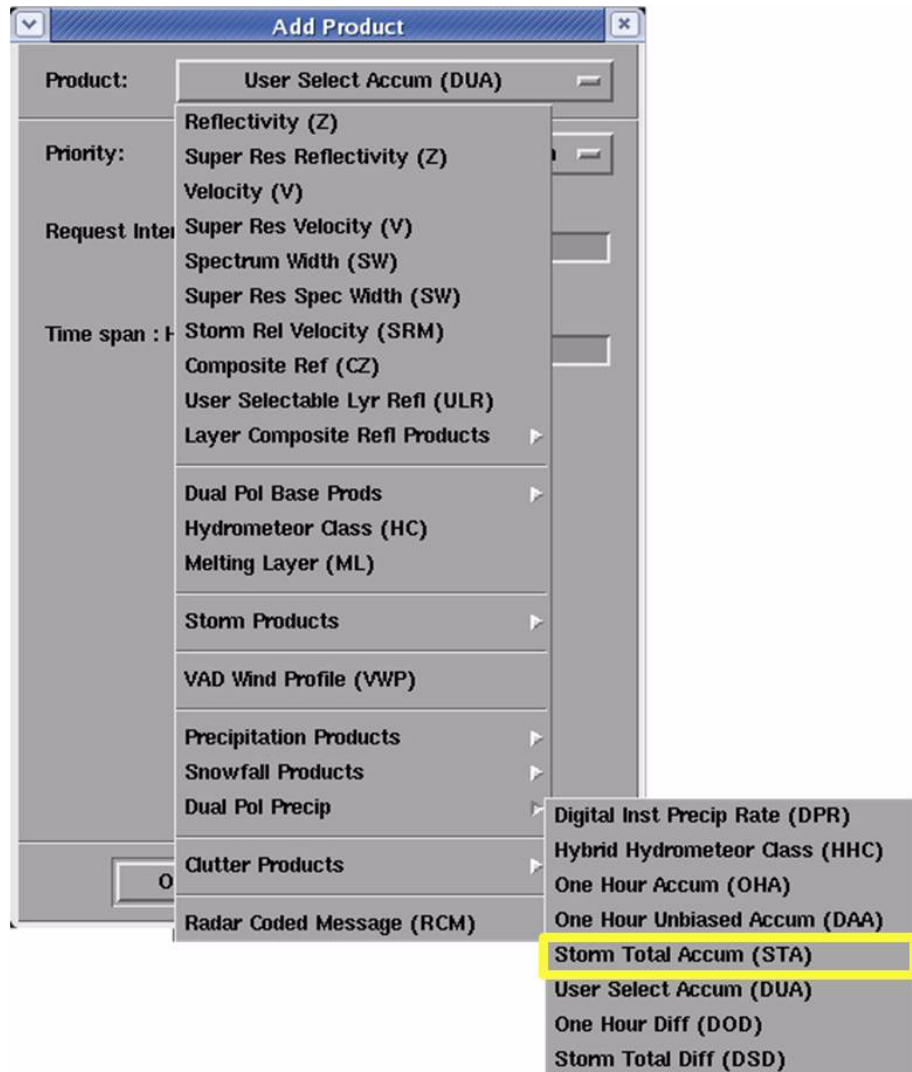


Figure 6-10. Add Digital Storm-Total Accumulation (DSA) to the RPS list through the “Add Product” GUI.

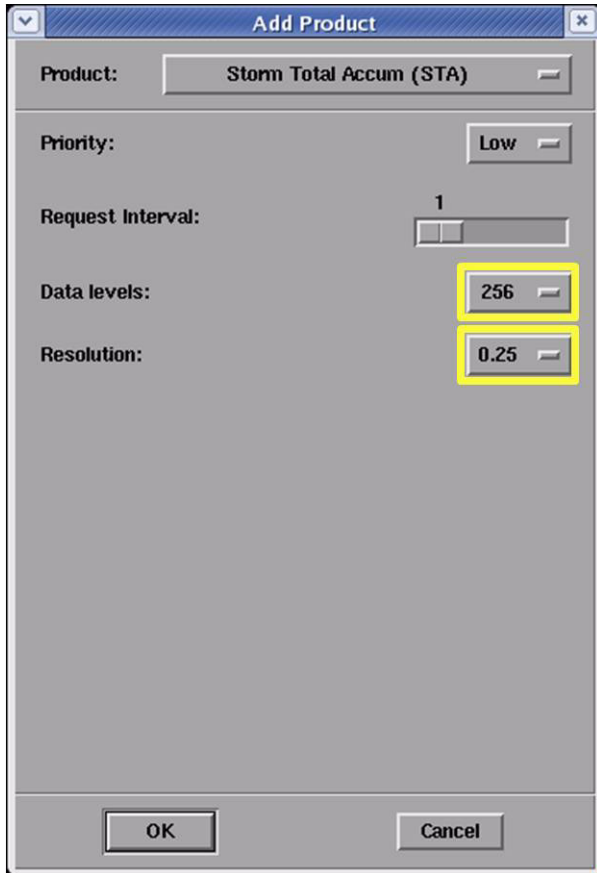


Figure 6-11. Select 256 data levels and 0.25 resolution (yellow boxes) to get DSA for RPS list.

If you really do want the 4-bit Storm Total Accumulation on the RPS list, select 16 under Data levels and 2 under Resolution. Any other combination of numbers in these two boxes will produce an error.

Digital One-Hour Difference (DOD) and Digital Storm-Total Difference (DSD)

There are two difference products to help compare legacy precipitation products to dual-pol products: Digital One-Hour Difference (DOD) and Digital Storm-Total Difference (DSD). DOD is the difference between dual-pol and legacy one hour accumulations while DSD is the difference between dual-pol and legacy storm total accumulations. Both difference products represent the dual-pol minus the legacy accumulations, updated each volume scan. These differences are taken with no bias applied.

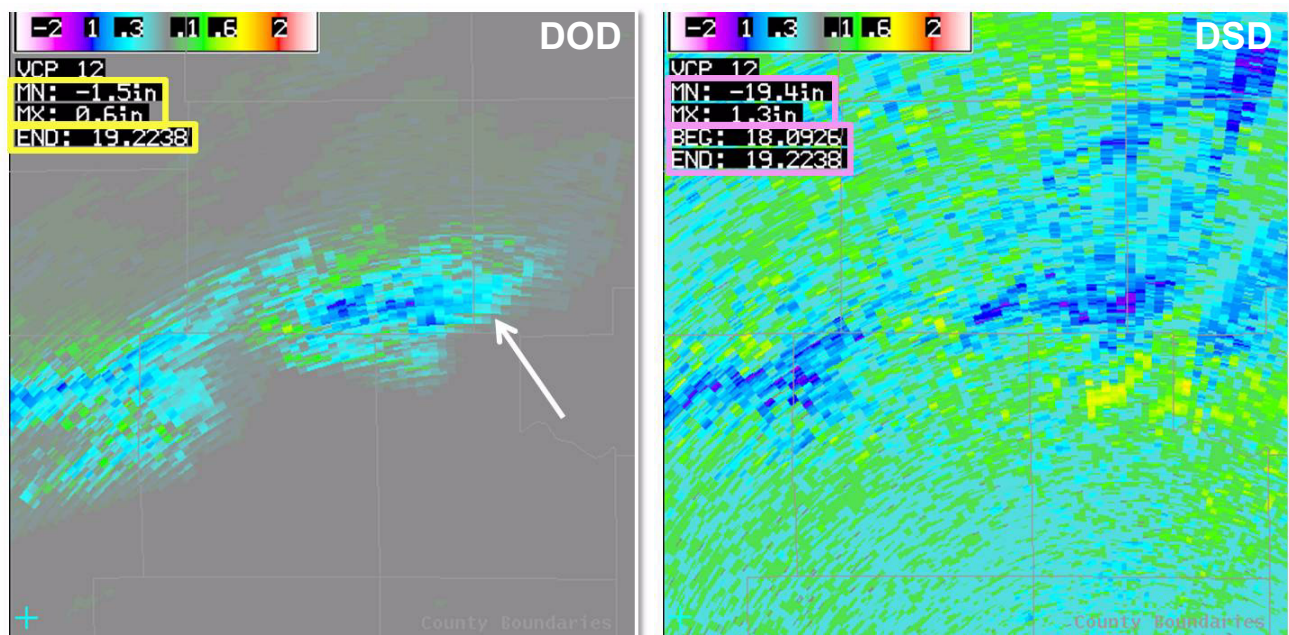


Figure 6-12. Examples of Digital One-hour Difference (DOD, left) and Digital Storm-total Difference (DSD, right) as seen in D-2D.

Figure 6-12 shows how the difference products look when displayed in AWIPS. Warmer colors, like the yellows and reds, indicate positive values, meaning the dual-pol precipitation estimate exceeds the legacy estimate. Cooler colors, like blues and greens, indicate negative values, meaning the dual-pol precipitation estimation is lower than the legacy precipitation estimation. In both DOD and DSD, maximum and minimum differences are listed in the legend in the upper left.

DOD also lists the product end time, while DSD lists both the beginning and ending times.

It is worth noting that while these products provide a way to see how the dual-pol and legacy precipitation estimates compare at a glance, they say nothing about which estimate is “right” or “wrong”. Also, as with STA, DSD may need to be reset manually at times and may include missing data. Finally, both of these products will often have a “stair stepped” appearance, as seen near the arrow in Figure 6-12. This structure is due to differences in range resolution between legacy and dual-pol.

Digital User-Selectable Accumulation (DUA)

Digital User-selectable Accumulation (DUA) is accumulated precipitation over a time period chosen by the user. This time period, or duration, can be as short as 15 minutes or up to 24 hours. One advantage of this is that a precipitation product that most suits the situation can be requested. Figure 6-13 shows the DUA product as seen in D-2D. The product legend in the upper left displays the maximum accumulation anywhere in the product, the bias, the product end time, and the duration. As with other accumulation products, caution is advised because DUA may contain missing data.

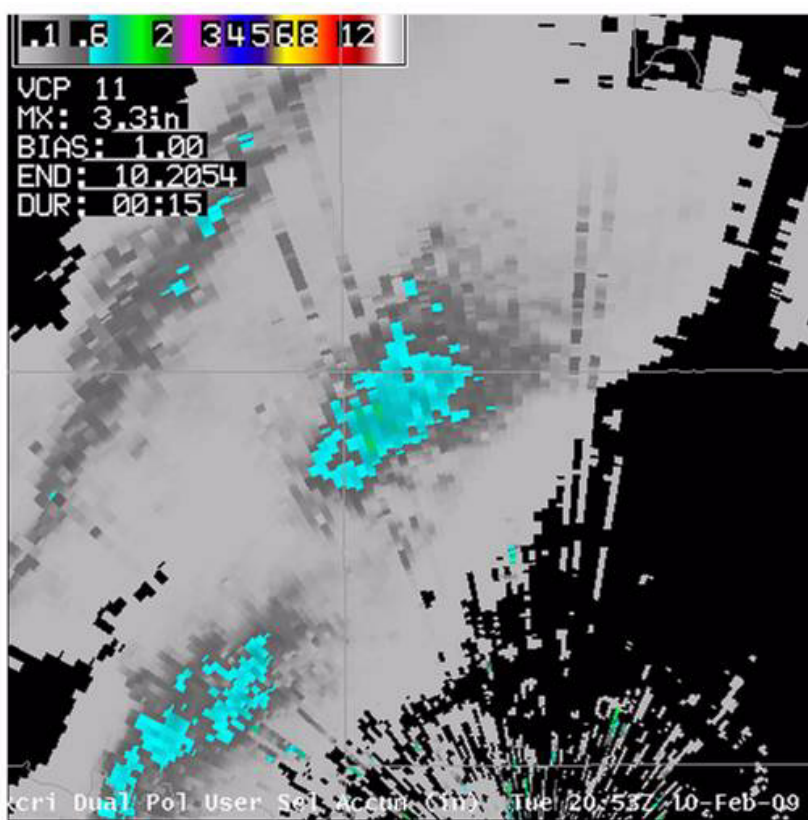


Figure 6-13. Digital User-Selectable Accumulation (DUA) product out as seen in D-2D.

Adding DUA to the RPS List

Once the radar has been upgraded to dual-pol, a one-hour DUA will be automatically generated every volume scan since it will be added to the national RPS list. A 24-hour DUA will also be automatically generated every day at 12Z. In addition,

DUA for other durations can be requested by adding them to the RPS list. Open the RPS list editor and choose “User Select Accum (DUA)” from the product drop down menu (see Fig. 6-14). Use the two slider bars to choose the desired duration of the product in hours and minutes. Up to 10 additional DUA products can be on the RPS list at once.

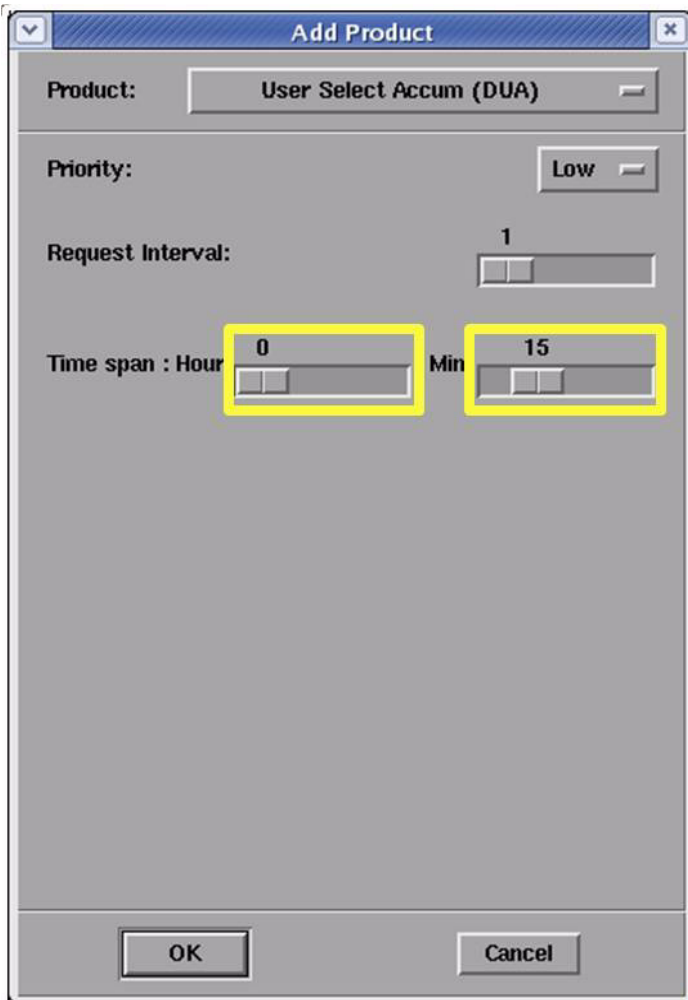


Figure 6-14. Specify DUA time periods through the “Add Product” GUI.

Loading in AWIPS You will notice on the precipitation submenu that there are a number of entries for DUA. The 6 entries, seen inside the larger yellow box in Figure 6-15, will load any DUA product exactly matching the duration given in the menu, if that product is on the RPS list. Any off-hour products will be under the “User Sel Accum (DUA)” menu entry, shown in the smaller yellow box in Figure 6-15.

All Tilts base data	??.????		
kcri Hi base data tilts		▶	<i>Legacy Precip Accum</i>
			Storm Total Precip (STP) ??.????
			One Hour Precip (OHP) ??.????
			Three Hour Precip (THP) ??.????
			User Selectable Precip (USP) ??.????
<i>4-Panel Z/ZDR/HC+KDP/CC</i>			
0.5 HC analysis	??.????		
0.9 HC analysis	??.????		
1.5 HC analysis	??.????		
All Tilts HC analysis	??.????		<i>Dual Pol Precip</i>
kcri Hi HC analysis tilts		▶	Precip Analysis (4panel) ??.????
			Storm Total Accum (STA) ??.????
			One Hour Accum (OHA) ??.????
			One Hour Unbiased Accum (DAA) ??.????
			Inst Precip Rate (DPR) ??.????
			Hybrid Hydro Class (HHC) ??.????
			User Sel Accum (DUA) ??.????
			User 1hr Accum ??.????
			User 2hr Accum ??.????
			User 3hr Accum ??.????
			User 6hr Accum ??.????
			User 12hr Accum ??.????
			User 24hr Accum ??.????
<i>Best Res Base Products</i>			
kcri Z		▶	
kcri V		▶	
kcri SRM		▶	
kcri SW		▶	
kcri ZDR		▶	
kcri CC		▶	
kcri KDP		▶	
kcri Precip		▶	
kcri Derived Products		▶	
kcri Algorithm Overlays		▶	
kcri four panel		▶	<i>Unbiased Dual Pol minus Legacy Accum</i>
kcri Data Quality		▶	Storm Total Accum (DSD) ??.????
kcri 4 Bit/Legacy Prods		▶	One Hour Accum (DOD) ??.????
Radar Applications		▶	

Figure 6-15. D-2D menu used to load Digital User-Selected Accumulation (DUA).

A word of caution: if more than 1 off-hour product is requested, for example, a 30 minute accumulation and a 90 minute accumulation, both products will be loaded from the same menu entry. To view both of these products, use the arrow keys to step

through them. It is recommended that only products with a duration matching a menu entry be requested for accumulations longer than 1 to 2 hours. This makes loading and viewing the products in AWIPS straightforward.

Here are a couple of best practices for using DUA. First, a 15 minute accumulation product can be used for CWAs prone to flash flooding that results from very intense, short-lived rain events. A 20 or 30 minute product would work well for this purpose, so having at least one short-term accumulation product on the RPS list is recommended. However, it is not recommended that you add more than one of these products, or any additional DUA products that do not have an explicit menu entry in AWIPS, since they will all load from the same menu entry in AWIPS. This will greatly reduce the ability to loop these products through time to watch for trends or motion of the greatest accumulations. Finally, the 2-hour DUA product is fairly convenient since it is on a time scale for potential flash flooding and has a menu entry in AWIPS.

DUA Best Practices

The advantages of using dual-pol QPE include:

- Should be more accurate than legacy precipitation estimation
 - Rain rate relationships specific to hydrometeor type
 - Lower sensitivity to hail or bright banding
 - Non-meteorological scatterers don't contribute to accumulation
- Potential for future improvements to product accuracy

Dual-Pol Quantitative Precipitation Estimation (QPE) Operational Applications (Strengths)

While research has shown improvement of the dual-pol QPE algorithm over the legacy PPS, the QPE algorithm is a work in progress. There is potential for future improvement to the accuracy of the dual-pol QPE products. Local research comparing dual-pol QPE to gages will need to be done to verify the degree to which improvements to rainfall estimation occur with dual-pol across all climate regimes.

Dual-Pol Quantitative Precipitation Estimation (QPE) Limitations

Limitations affecting dual-pol QPE include:

- Dependency on HCA output
- No biases applied
- Small sample to derive Z relations in frozen precipitation
- Standard radar limitations

Dependency on HCA Output

For dual-pol QPE, remember that there is an added level of complexity in the dependency of rain rate on HCA output. In some situations, hydrometeors may be misclassified as biological scatterers and no rain rate applied. Also, because the HCA depending on an accurate melting layer detection, when the MLDA is in significant error, HCA will place the transition zone between frozen and liquid precipitation in the wrong place. This can lead to inaccurately applied rainrates in those areas.

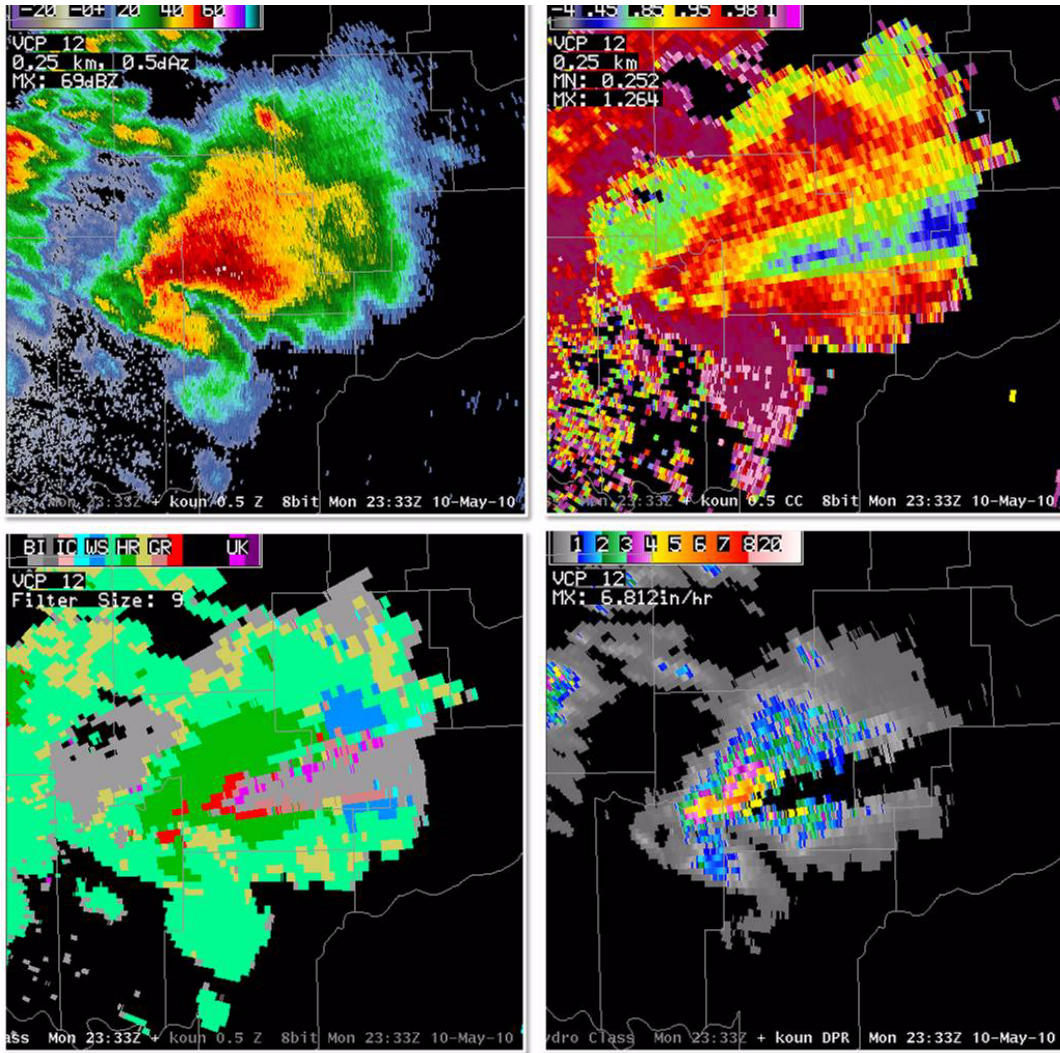


Figure 6-16. 0.5 degree Reflectivity (top left), coefficient correlation (top right), Hybrid Hydrometeor Classification (bottom left), and Digital Precipitation Rate (bottom right)

In the reflectivity image shown in Figure 6-16 (top left) there is a supercell east of the radar, with the radar location just off the image on the left side. Taking a look at CC (top right), there is a sharp reduction in CC in the hail core, but also a reduction in CC down-radial due to nonuniform beam filling (NBF). With CC this low, much of this echo is classified as biological, as seen in the Hybrid Hydroclass (HHC) product (lower left). A rain rate of zero is applied everywhere where there is bio-

logical scatter in the HHC. Taking a look at precipitation rate (lower right), there is a wedge of “no data” down-range from the hail core due to the incorrect classification of biological scatterers. In this case, storm motion was approximately parallel to the radials, exacerbating the problem.

No Biases Applied With RPG build 12.2, no biases applied to any of the dual-pol precipitation products. The plan is for biases to be applied at some point in the future.

Small Sample to Derive Z Relations in Frozen Precipitation The $R(Z)$ relations for frozen precipitation are derived empirically from central Oklahoma events. It is unknown whether these types of relationships apply everywhere.

Standard Radar Limitations When interpreting dual-pol QPE products keep in mind that all the standard radar limitations, such as below beam effects and beam broadening with range, still apply.

Lesson 7: Winter Weather Nowcasting

Dual-pol radar is a tool to help diagnose precipitation types at the surface, but it is meaningless without the context of temperature profiles and other mesoscale ingredients. This is because dual-pol radar gives users the ability to identify melting layers, as well as the ability to detect the presence of pure rain and pure snow. However, it's still a radar so detection of winter weather signatures is only valid at the height of the radar beam sampling the weather. All typical radar sampling limitations apply to dual-pol radar products. Given that so much can change in the lowest few thousand feet with winter weather, the issue of p-type at the ground becomes complex in a hurry. This is why it is necessary that you have a good handle on the expected temperature profiles, and incorporate cursor readout of temperature and perhaps the pop-up skew-T as you examine the radar data. A few degrees in the lowest thousand feet of the atmosphere can mean the difference between rain, snow, sleet, or freezing rain, and most of the radar coverage does not sample the lowest 1000 feet.

Winter Weather Nowcasting Methodology

Figure 1-17 shows the methodology for determining precipitation type for a winter weather event. This section will break down the tree into smaller parts that are easier to understand.

The first step to the methodology for winter weather nowcasting is to look for a melting layer in the dual-pol data, assuming that there is at least a chance of there being a melting layer. If the entire sounding is far below 0°C and expected to stay that way, you can skip this step. Using the radar is pretty easy if no melting layer exists as the only precipitation types the radar can sense at that point are snow or drizzle.

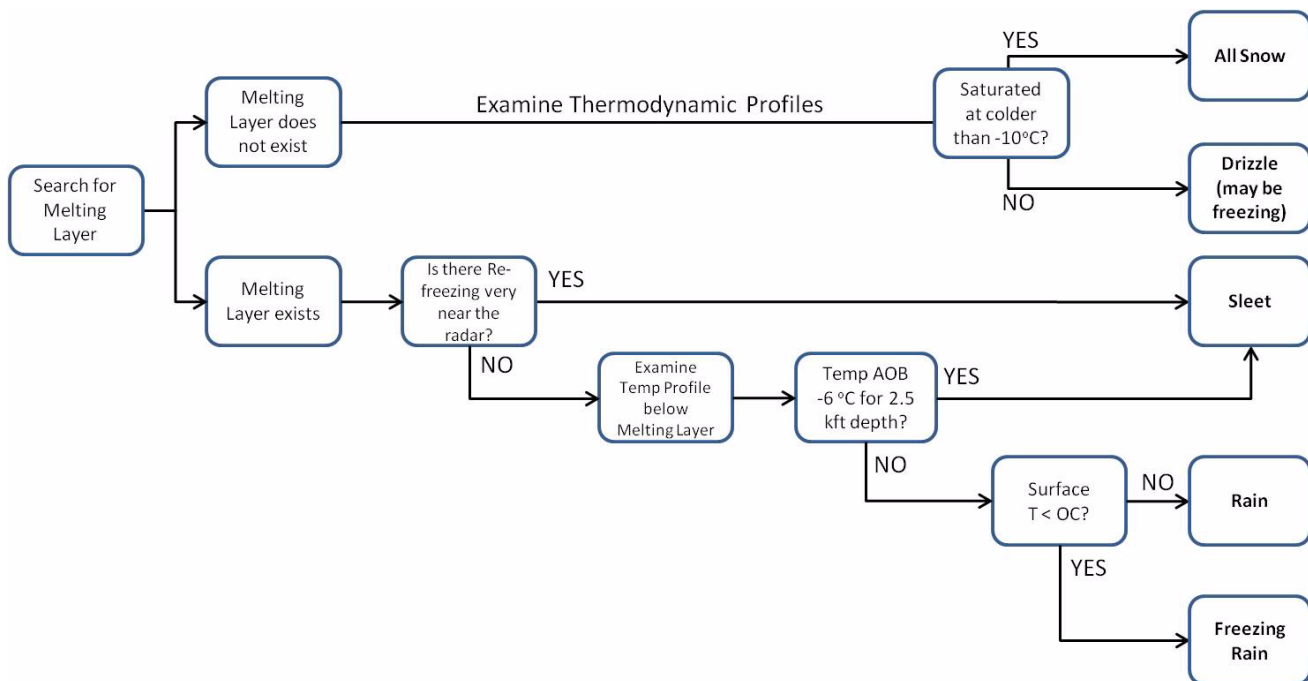


Figure 1-17. Winter weather decision tree incorporating dual-pol radar analysis

Characteristics of the Melting Layer in Dual-Pol Base Data Products

One of the strongest benefits of using dual-pol products in winter weather is the ability to quickly and easily detect a melting layer, even when reflectivity data are ambiguous. In the dual-pol products, the melting layer will stand out as an area of enhanced reflectivity, as indicated by the arrow in Figure 1-18 on page 1-120. In ZDR, the melting layer will be marked by noisy, positive values due to the presence of flattened rain drops

and/or partially melted, water-coated hydrometeors. Notice the abrupt drop off to values near 0 dB above the melting layer. Below the melting layer, where liquid hydrometeors prevail, ZDR is positive, but with lower values than in the melting layer.

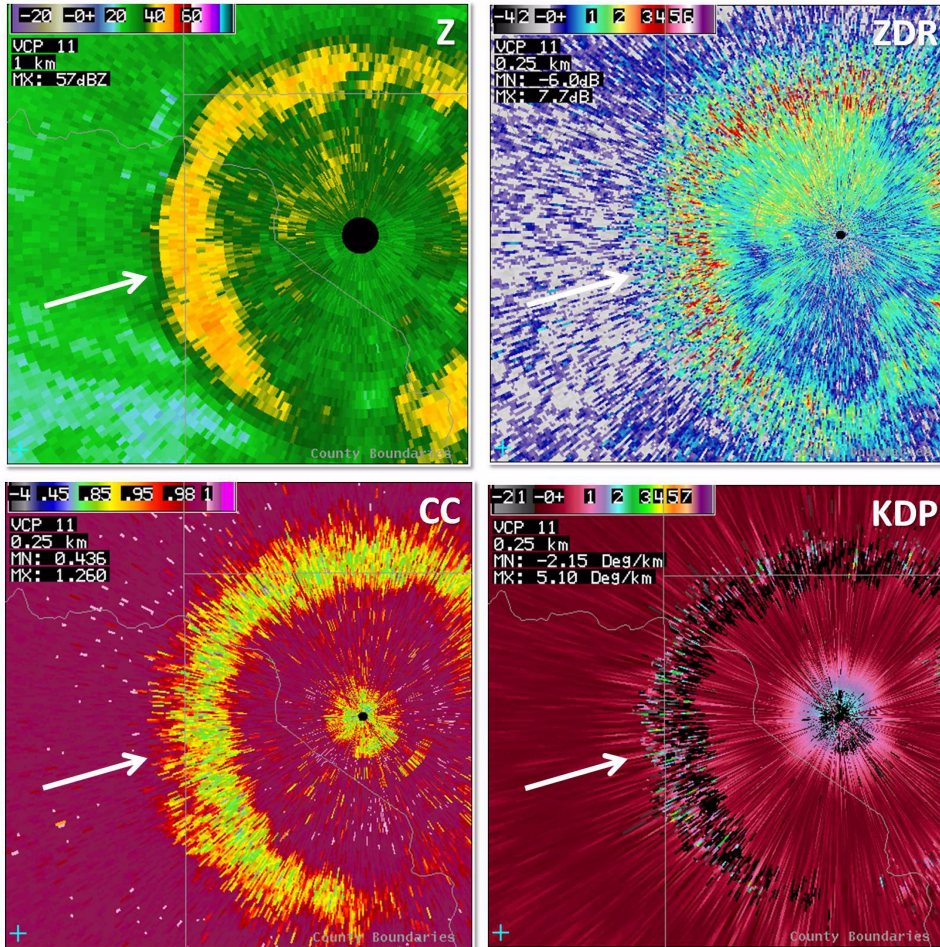


Figure 1-18. Melting layer as seen in reflectivity (top left), differential reflectivity (top right), correlation coefficient (bottom left), and specific differential phase (bottom right).

The melting layer probably stands out best in CC with a sharp reduction in values caused by the mixed-phase hydrometeors. In well-behaved, constant-height melting layers with lots of precipitation surrounding the radar, the melting layer will form a very distinct band of reduced CC at a consistent range. KDP is generally noisy and slightly enhanced within the melting layer. Because the melting layer is so easily detected with CC and Z,

they may be enough for an accurate melting layer analysis.

Steps to Detecting Melting Layer Using PCR All-Tilts

Using All-Tilts to detect the melting layer can be very effective. The following steps are recommended:

1. Toggle Reflectivity and Correlation Coefficient
2. Examine all elevation angles
3. Examine ZDR to confirm ML band

The example in Figure 1-19 shows a “well behaved” melting layer in which there is plenty of precipitation around the radar and the melting layer is constant across the radar umbrella. Keep in mind this is from April and no winter precipitation was expected.

Toggle Z + CC Toggle between reflectivity and correlation coefficient. This helps you determine where there is precipitation, and where there are non-precipitation echoes. Avoid areas of really low reflectivity as correlation coefficient tends to be inaccurate (and often > 1.0). Look for areas of reduced correlation coefficient that are at a constant range from the radar. In Figure 1-19 CC forms a perfect ring. Even at 0.5 deg, there is a band of reduced CC at a constant range. This is the melting layer, and everything inside the ring is liquid/completely melted.

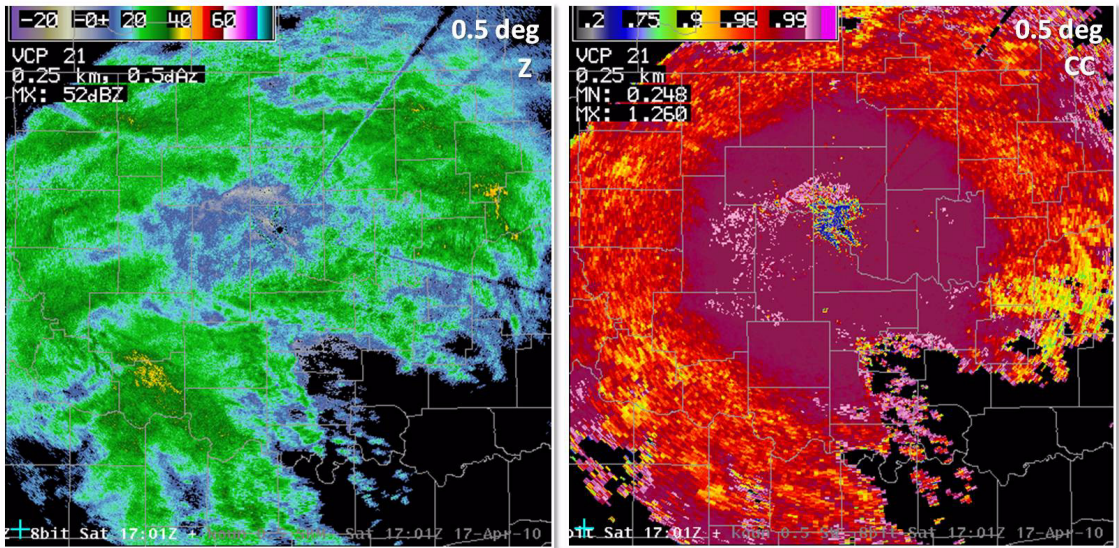


Figure 1-19. 0.5 degree reflectivity (left) and correlation coefficient (right) showing a well-defined melting layer signature at constant range.

Since there is a melting layer at 0.5 deg, it's a good idea to look aloft to gain a better handle on the melting layer top and bottom (see Fig. 1-20). Again, toggle Z and CC aloft. The higher the elevation angle, the narrower the band in CC should get but there also needs to be precipitation very near the radar to see it.

Examine All Elevation Angles

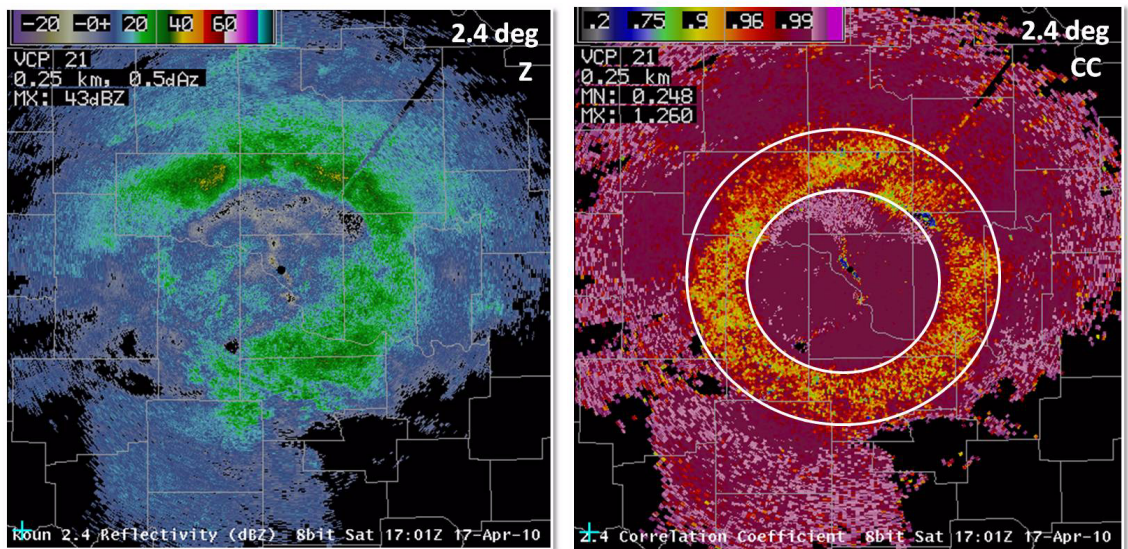


Figure 1-20. 2.4 degree of reflectivity (left) and correlation coefficient (right) showing the melting layer aloft.

Examine ZDR to Confirm
ML Band

Finally, toggle to ZDR to confirm the presence of the melting layer (see Fig. 5). There should be a significant increase in ZDR within the band of lower CC, and it's also very noisy.

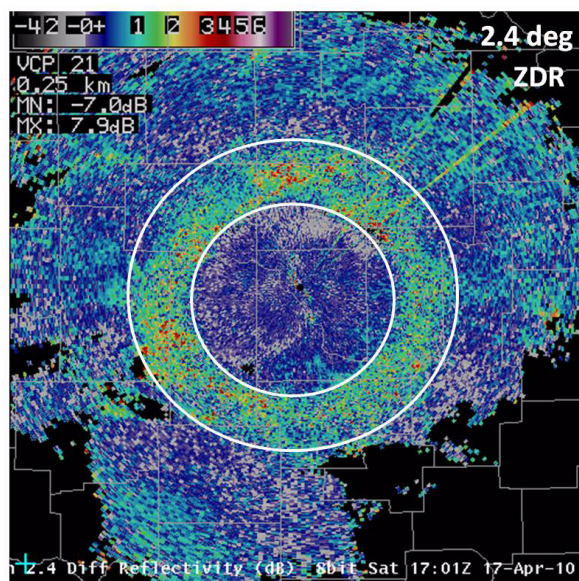
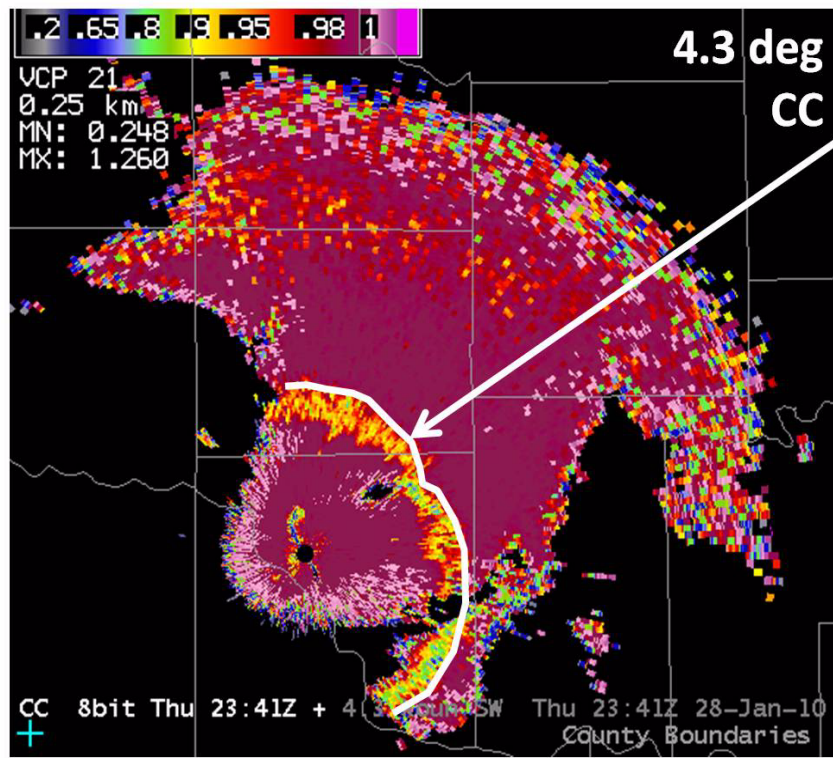


Figure 1-21. 2.4 degree differential reflectivity (ZDR) showing a well-defined melting layer at constant range.

Dual-Pol Products and the Wet Bulb Zero Height

An advantage of using dual-pol radar products to identify the melting layer is that they provide an accurate, up to the minute value for the wet bulb zero height *within* precipitation (see Fig. 1-22). Even high resolution local models can't give an accurate web-bulb zero height every 5 minutes within the precipitation core, where it matters the most. This can be used in the winter weather forecast process to compare to model output and diagnose where the models might have errors in the vertical profile of temperature. In some areas, 500 vertical feet can make all the difference between an inch of rain or 10 inches of snow. This is a nice thing to be able to evaluate and re-evaluate during an event.



Top of the melting layer = Wet Bulb Zero

Figure 1-22. Dual-pol radar products provide an accurate wet bulb zero height approximately every five minutes.

Characteristics of a Well-Defined Melting Layer

Within the melting layer ring, you should see the characteristics of pure rain immediately below the bottom of the melting layer, with very high CC and positive ZDR and KDP (see Fig. 1-23). For the most part, it's left up to the forecaster to determine whether or not the rain will refreeze into sleet, or perhaps reach the surface as freezing rain. This of course hinges on your ability to accurately assess the temperature profile in the lowest few thousand feet. Indeed, the need for human forecasters is significant in these events, even with dual-pol radar.

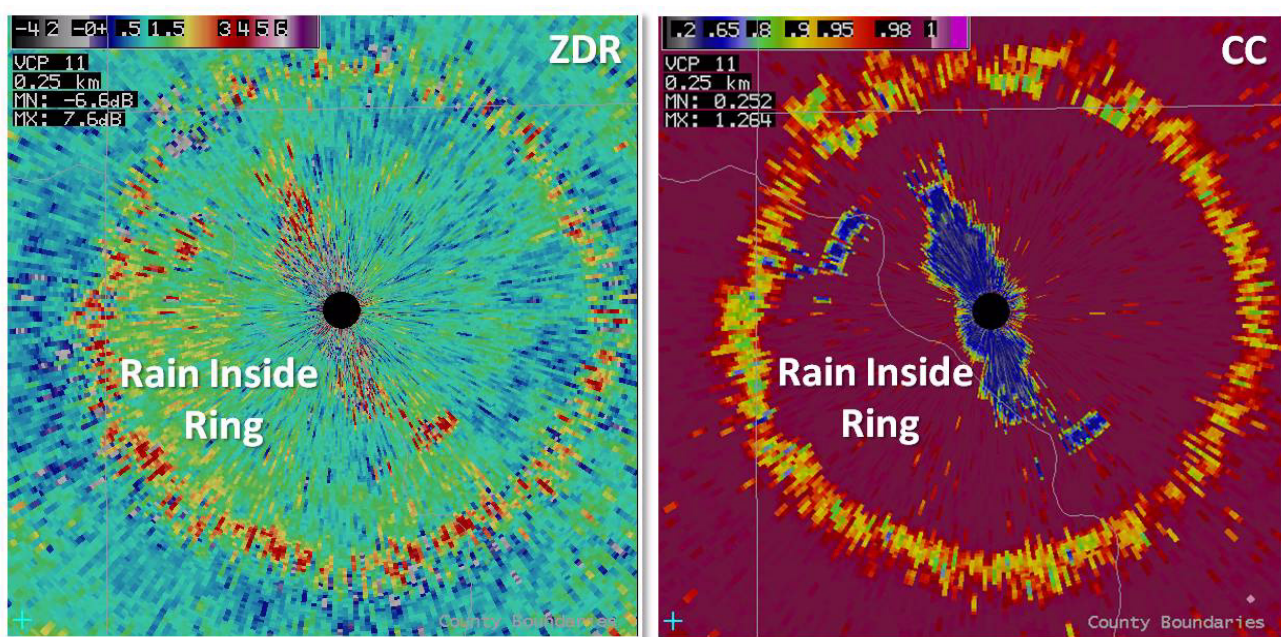


Figure 1-23. Example of a well-defined melting layer as seen in differential reflectivity (left) and correlation coefficient (right).

Following the outline of the decision tree shown in Figure 1-24, the next few sections will cover tips for events where there is a well-defined melting layer.

Melting Layer Exists

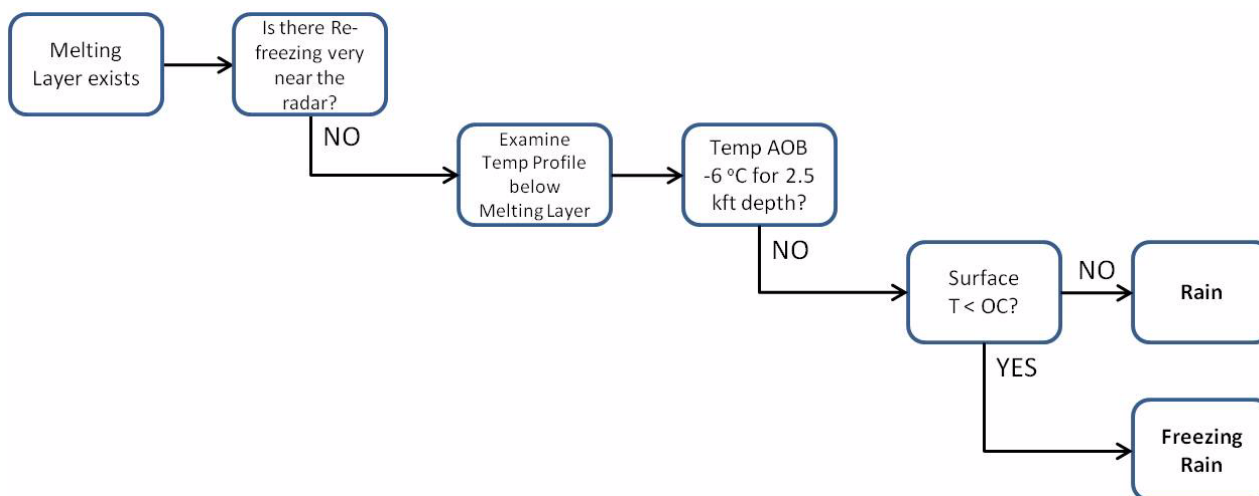
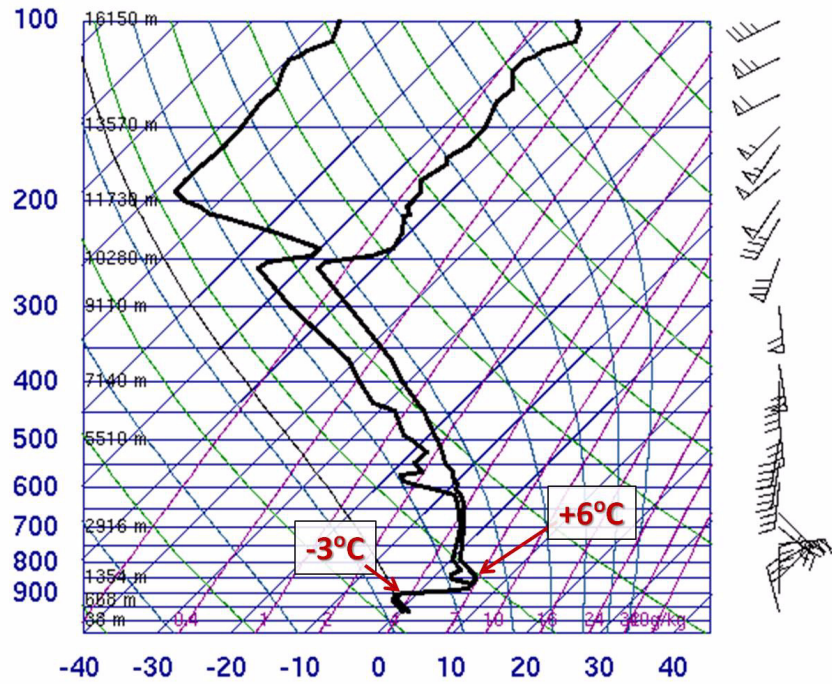


Figure 1-24. Decisions to be made once the existence of a melting layer has been confirmed.

Because of the importance of the environmental context for the determination of sleet, start with a sounding (see Fig. 1-25). It's pretty clear that the sounding shown in Figure 1-25 would result in a melting layer on radar, since the warm nose is +6°C, and the coldest air near the surface is -3°C. Sleet is possible right now but given how shallow the below freezing air is, it's not very likely. Surface temperatures are also just above freezing. However, much colder and deeper air advected from the north is expected in the near future.

Sleet Potential

72357 OUN Norman



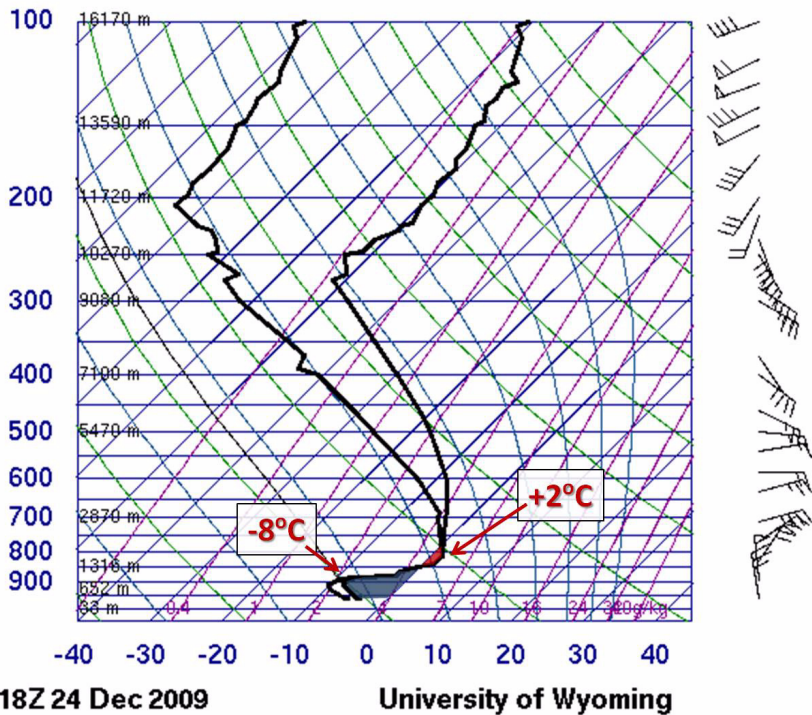
12Z 24 Dec 2009

University of Wyoming

Figure 1-25. 12Z sounding showing potential for sleet.

Looking at the 18Z sounding in Figure 1-26, temperatures have significantly cooled at all levels. The warm nose is just +2°C, and the coldest air near the surface is now -8°C.

72357 OUN Norman



18Z 24 Dec 2009

University of Wyoming

Figure 1-26. Six hours after the 12Z sounding in (see Fig. 1-25), temperatures have cooled at all levels.

Regardless of what the warm nose looks like on this or any sounding, a radar analysis provides much greater confidence in identifying if melting is occurring. In these kinds of events, always focus on the near-surface cold air below the warm nose since the radar is limited there. In this event, sleet looks very likely given the freezing layer is over 3000 feet thick and is as cold as -8°C .

Pure sleet is very rare to see in radar data because it has to be completely frozen to be properly identified as such, and this usually occurs very close to the ground. The radar beam would have a hard time sampling the re-freezing layer that close to the surface. The images in Figure 1-27 do not show pure sleet directly, but this is an example of the rare case where there are pockets of re-freezing. Notice the reduction in CC inside the oval to

the east of the radar. The melting layer is clearly outside of this range, shown to the northeast of this oval with CC in yellow. Closer to the radar another pocket of lower CC shows up and is most likely caused by the rain re-freezing into sleet.

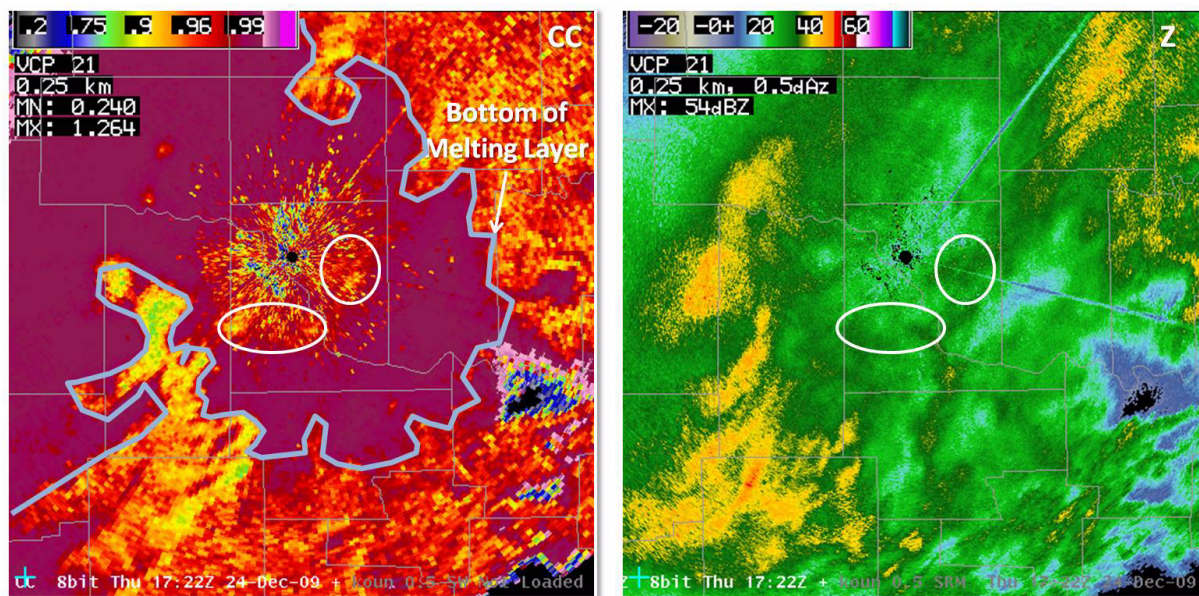


Figure 1-27. Correlation coefficient (left) and reflectivity (right) showing re-freezing near the radar.

In summary, in very rare cases there may be a re-freezing signature, implying the presence of sleet. However, there are problems with detecting a re-freezing layer:

1. Normally a complete re-freezing into sleet occurs in the lowest 1000 feet AGL. Thus, precipitation needs to be refreezing very close to the radar to even detect it in the first place.
2. Being so close to the radar, often times various forms of clutter will affect detection of the re-freezing layer. CC and ZDR are particularly affected by residual clutter.

No Melting Layer Detected

Back to the decision tree (see Fig. 1-28): If there's no re-freezing layer, which will often be the case,

it's solely up to the forecaster to determine if sleet is likely.

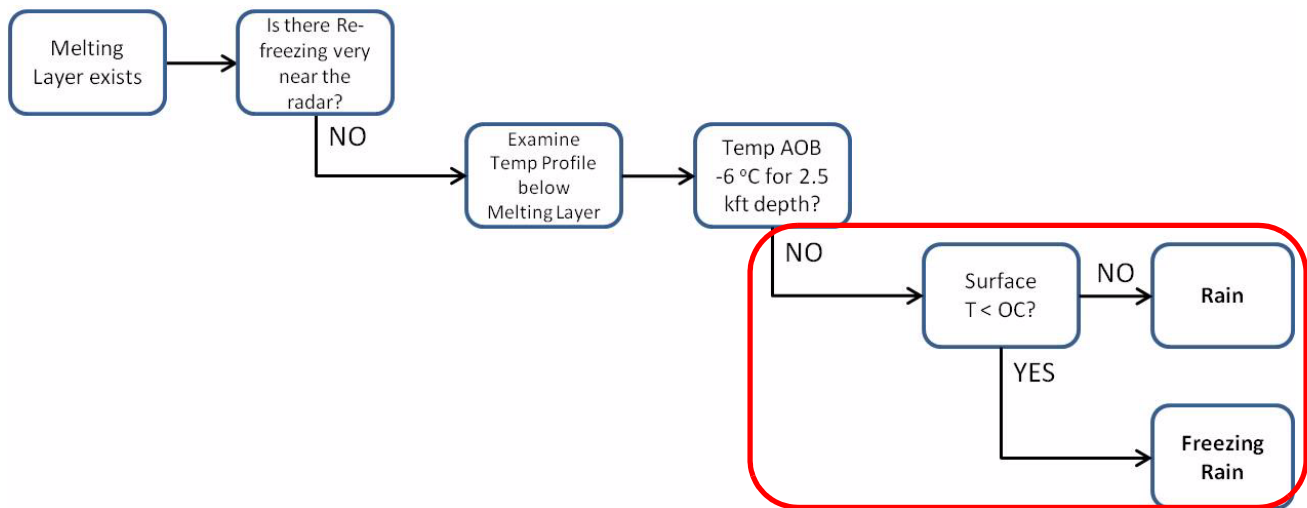


Figure 1-28. Decisions to be made if no re-freezing is seen near the radar.

Before examining the case where no melting layer is detected, or equally as important, no melting layer was expected in the first place, let's look at a caveat. What happens when melting is expected, but a well-defined melting layer is not found? This will be common in many winter events. Here, as with other examples, well-defined implies a nice, loosely-symmetric ring of lower correlation coefficient values around the radar at a nearly constant range. If a well-defined layer doesn't exist, there are things you can do but it must be done on a precipitation core by precipitation core basis.

In the case shown in Figure 1-29, notice the area of low CC southwest of the radar inside this white polygon. It contains much higher ZDR and higher reflectivity than surrounding areas, indicating that there is melting taking place. North of the radar, reflectivity is lower, CC is all 0.98 or higher, and ZDR is right around 0.2 dB, an excellent indicator of aggregated dry snow. Though not shown in this image, there is no melting layer on higher elevations north of the radar, confirming that the radar is detecting all snow in this area. The precipitation to the southwest is more convective in nature, forming along the nose of low-level warm advection. This is just one example. With winter weather events, uncertainty and local effects come into play that will need to be addressed.

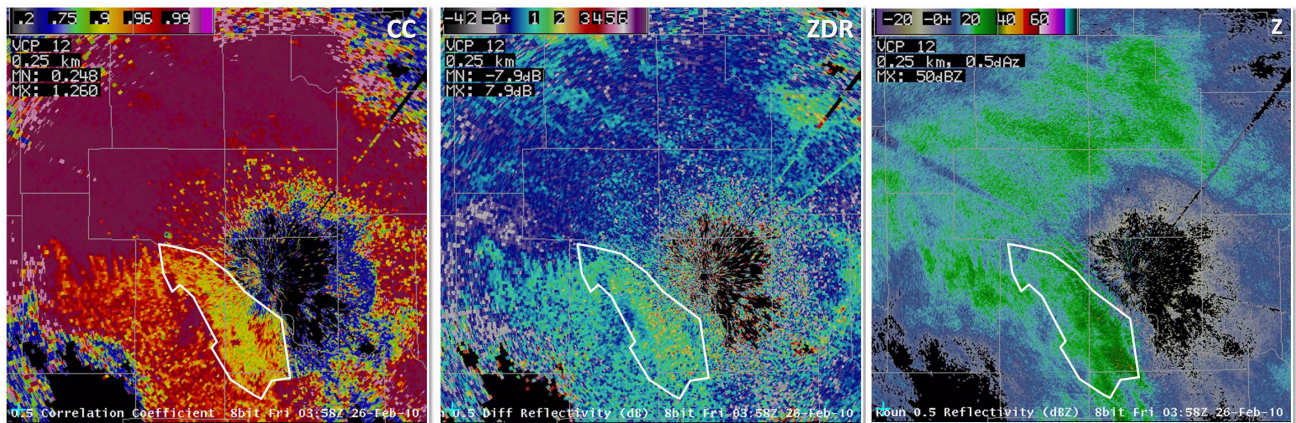


Figure 1-29. Correlation Coefficient (left), differential reflectivity (middle) and reflectivity (right) showing no well-defined melting layer, but notice melting southwest of the radar (white polygon).

Now examine the case where a melting layer does not exist (Fig.1-30). .

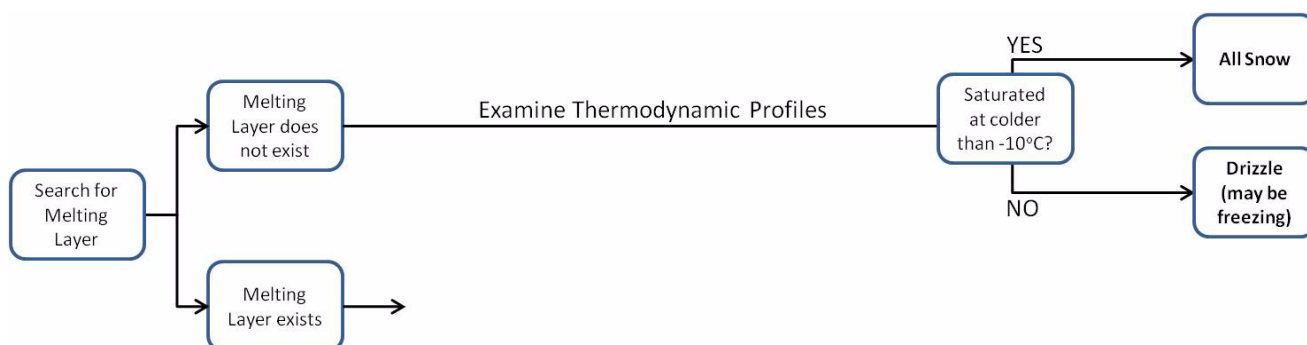


Figure 1-30. Decisions to be made if no melting layer is detected.

In the absence of a melting layer, there are two potential precipitation types that the radar is seeing: all snow or drizzle (possibly freezing). Below beam effects are the biggest factor in final precipitation type at the surface. Snow at the radar beam height can easily melt before reaching the surface if precipitation is far enough away from the radar that the radar doesn't sample the melting layer. Keep in mind where the radar beam is sampling the precipitation in terms of height above the ground. As a forecaster you'll have to diagnose what may be happening below the beam, so you'll need to have a good handle on thermodynamic profiles. The next two sections will examine the dual-pol characteristics of snow and drizzle.

Drizzle Drizzle is made up of tiny liquid drops, with diameters less than 0.5 mm by definition. With such small diameters, the drops are spherical, fall very slowly, and are associated with low reflectivity, generally 20 dBZ or less. Thus, always be mindful of the potential for poor quality dual-pol products in weak signal associated with drizzle, especially as you increase range from radar.

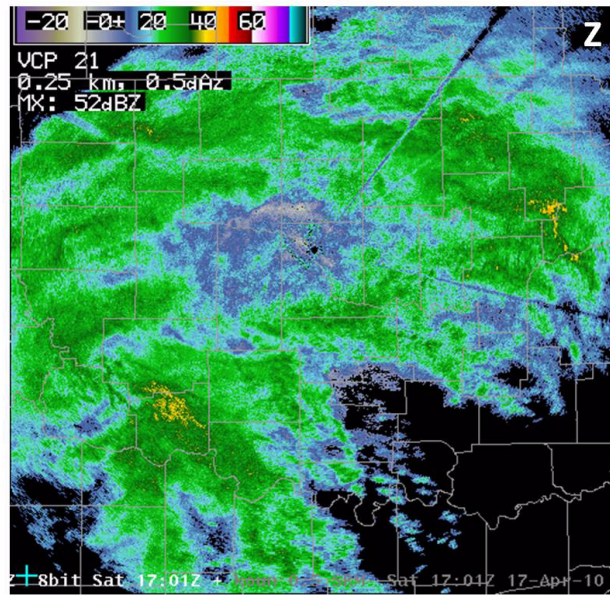


Figure 1-31. Reflectivity image of widespread drizzle.

To verify the presence of drizzle and the strength of the signal, use CC. If the signal is strong enough, you will always see CC close to 0.99 but less than 1.0 in drizzle (Fig. 1-32, left). Toggling over to ZDR (Fig. 1-32, right), drizzle has values very near 0 dB. In this event, there was drizzle occurring inside the white oval, roughly within the yellow polygon, verified by numerous surface observations. The areas of higher ZDR shown with lighter blue and greens inside the oval but not within the yellow polygon are areas of light rain, comprised of very small drops but technically not drizzle. The area north of the yellow polygon (red circle) probably contains drizzle as well. However, given that CC is above 1 in spots, our confidence

in the quality of the dual-pol products is not as strong.

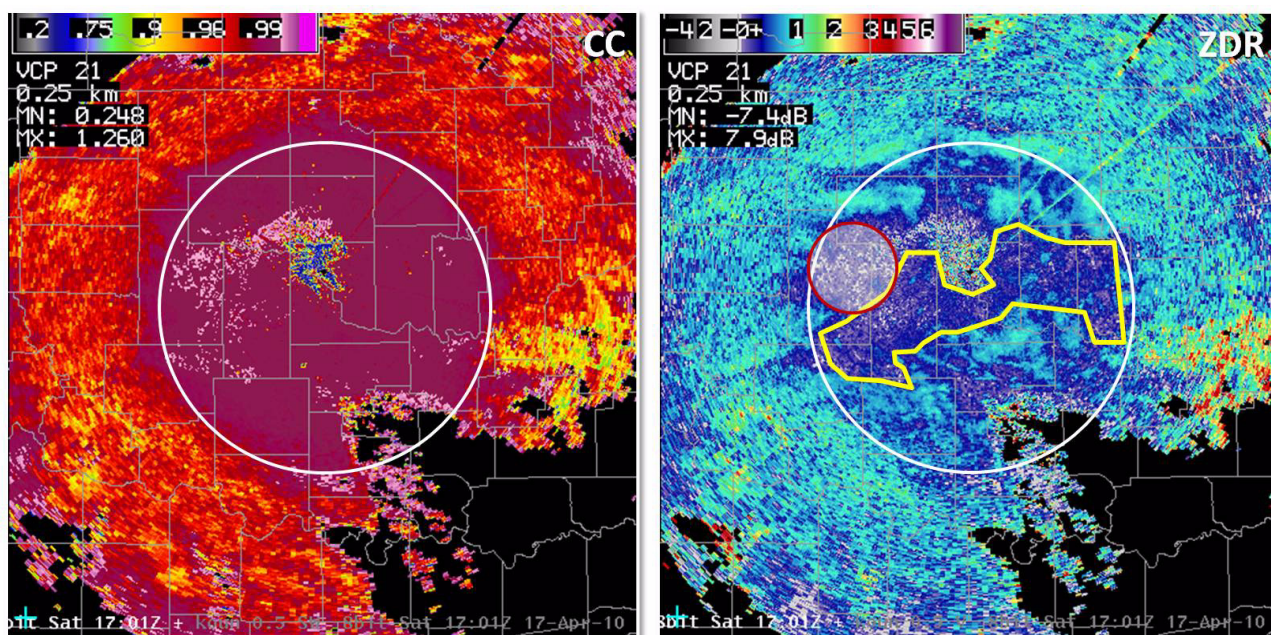


Figure 1-32. Correlation coefficient (left) and differential reflectivity (left) of the same drizzle event shown in Figure 1-31. Notice very high CC and low, but positive, ZDR near the radar.

Let's consider snow that is not melting, known as dry snow. To identify dry snow using dual-pol radar products, we must assume it is aggregated. Individual, pristine crystals are not considered dry snow in this context. Dry snow is several ice crystals, such as dendrites, plates, columns, or needles stuck together to form snowflakes that have very low density.

Snow

For dry aggregated snow reflectivity is fairly low, normally less than 40 dBZ. CC will be very high in dry snow, above 0.97. ZDR is fairly low, but still slightly positive, roughly 0.1 – 0.3 dB. In fact, a smooth appearance to ZDR in the 0.1 to 0.3dB range is one of the sure-fire things in dual-pol: given your knowledge that it's all frozen, this will nearly always indicate dry, aggregated snow.

Figure 1-33 shows a snow band southwest of the radar. Notice CC is high everywhere there is strong enough reflectivity, indicating that all the precipitation is the same type, shape, and size. ZDR inside the polygon is right around 0.2 dB, indicating dry, aggregated snow.

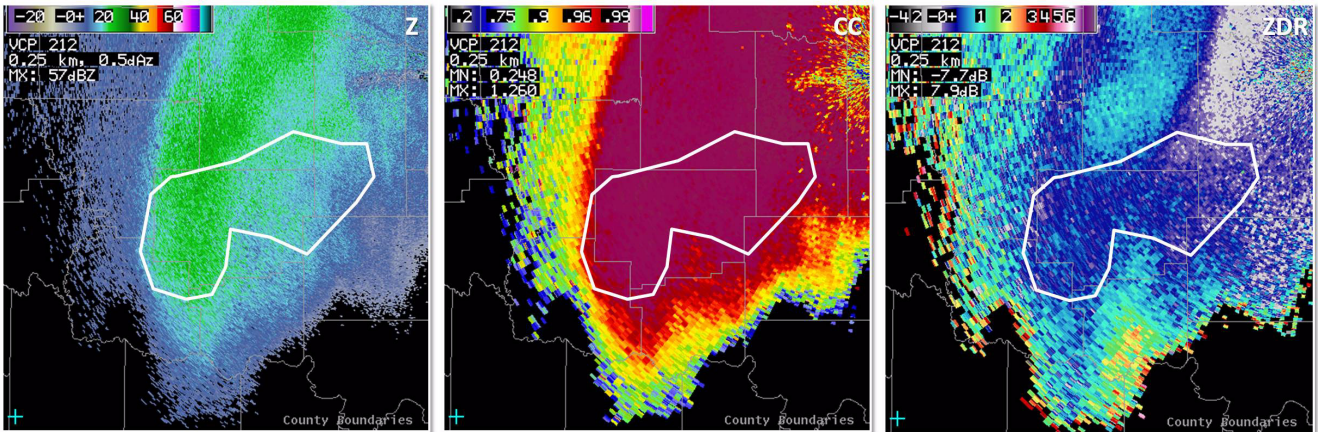


Figure 1-33. Reflectivity (left), correlation coefficient (middle) and differential reflectivity (right) of a snow band southwest of the radar.

Notice that north of the oval ZDR increases to about 1 dB (Fig.1-34). In this area there's a good chance the snow particles are higher density and pristine (i.e., dendrites). Recall from the ZDR lesson that an increase in particle density, such as going from aggregates to pristine dendrites or columns, will also increase ZDR values. Melting can also be ruled out as the cause for higher ZDR values since CC is still 0.99 and reflectivity doesn't increase in that region.

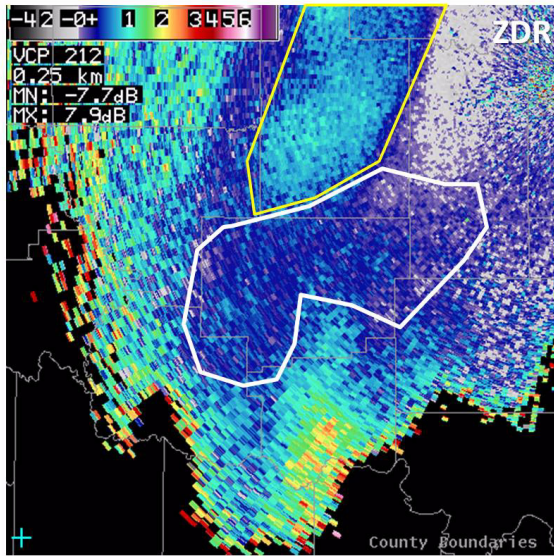


Figure 1-34. Same ZDR image as Figure 17. Notice the area of ~1dB differential reflectivity north of the previously identified dry snow

What about other types of snow? If the crystals are dry, all will have very high CC. Reflectivity can be as high as 50 dBZ in extremely heavy dendritic growth zones. However, reflectivity normally will be fairly low, especially in less than extreme snow-fall rates. Dendrites, plates, columns, and needles will all have higher ZDR than that associated with aggregated dry snow for two reasons: 1) they have a higher particle density than dry aggregated snow and 2) they often fall with their major axes in the horizontal. For pristine crystals, look for anything roughly higher than 0.5 dB.

Figure 1-35 is a graphic of crystal type growth based on temperature and supersaturation. It's useful because if the temperature of the layer is known with a pretty high degree of accuracy, the crystal type can be inferred.

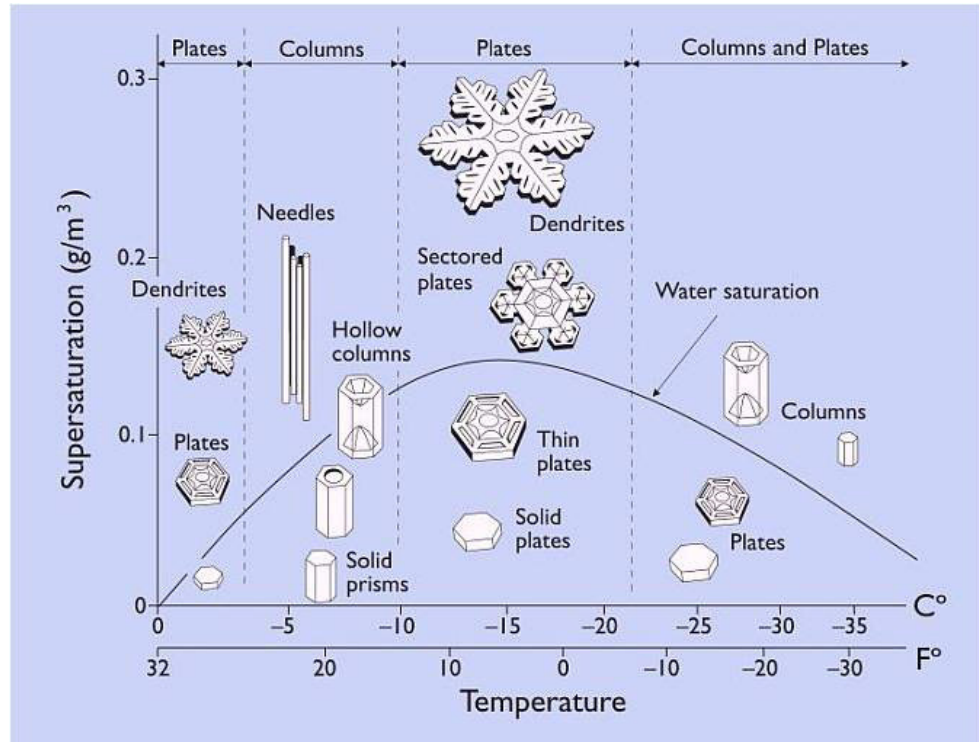


Figure 1-35. Crystal formation at varying cloud temperatures and supersaturation.

Dendrite Formation Though it's new and needs to be applied in other parts of the U.S., there is great promise that the dual-pol base products can detect the dendritic growth layer. First, a little how dendrites look on radar. Figure 1-36 shows a crudely drawn dendrite. However, when dendrites fall, they do not fall oriented in this fashion. As they meander and float to the surface, the dendrites fall in a flattened orientation such that the horizontal plane is much bigger than the vertical, resulting in increased positive ZDR.

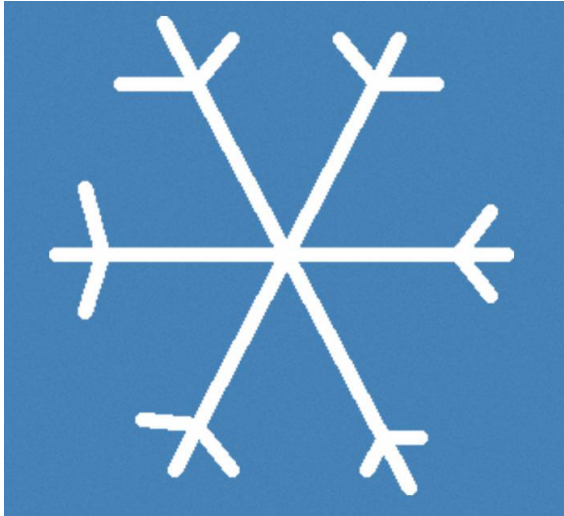


Figure 1-36. Example of the shape of a dendrite. When dendrites fall, they are nearly horizontally-orientated, increasing positive ZDR.

Figure 1-37 shows reflectivity at 9.9° for an all snow event. Overlay temperature contours or use cursor readout to find areas of potential dendritic growth (-12°C to -16°C). Look for CC between 0.95 and 1 to determine if there is strong enough signal for the dual-pol products to be trustworthy. Specifically for dendritic growth, use a broader temperature range to account for uncertainties in overlaid temperature.

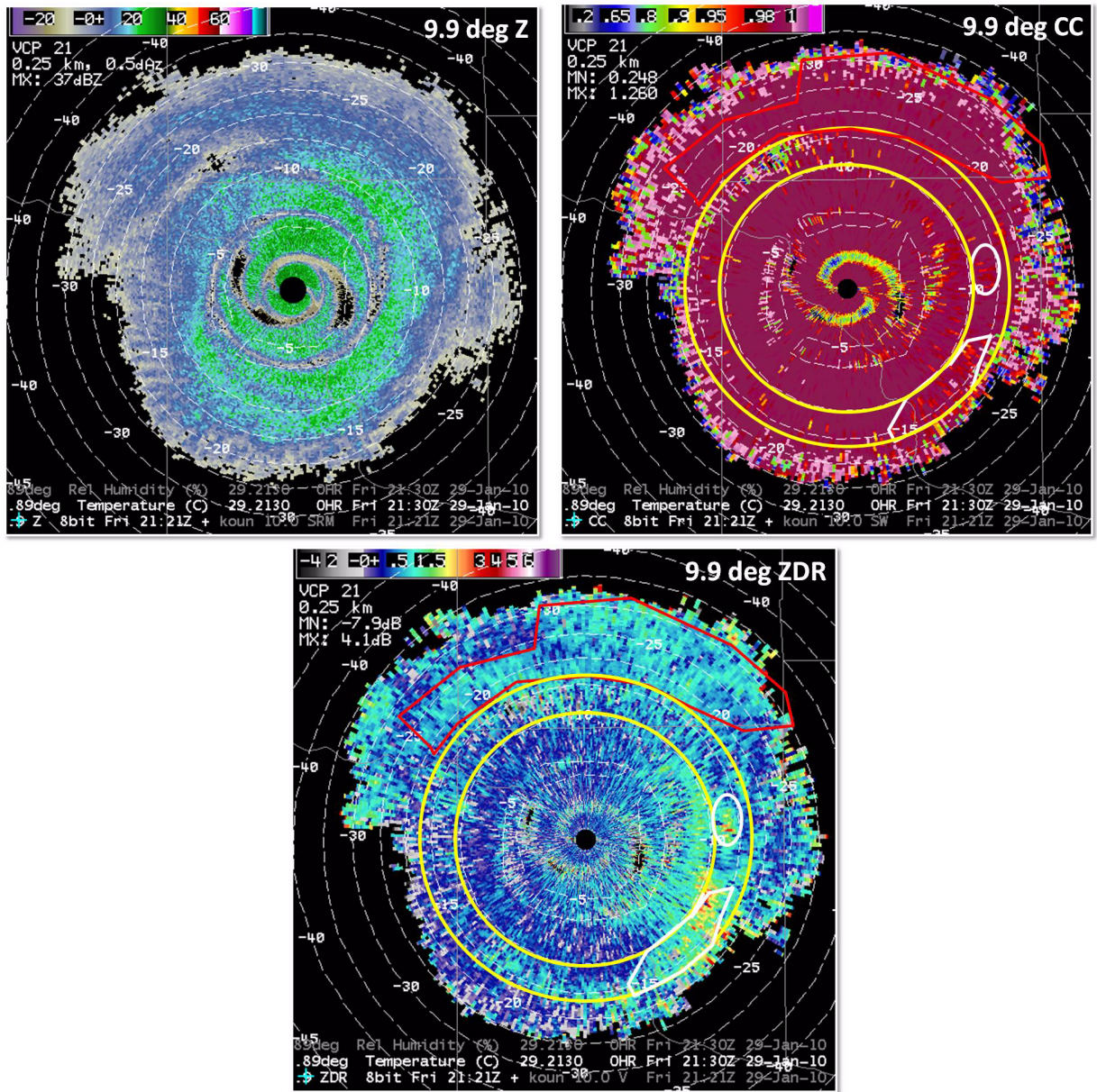


Figure 1-37. 9.9 degree scan of reflectivity (top left), correlation coefficient (top right), and differential reflectivity (bottom) showing the dendrite growth zone.

In Figure 1-37, focus on the area between the yellow rings, roughly from -10° to -18°C . Dendritic growth seems to have slightly lower CC, from 0.97 to 1.0. Notice there are definitely areas in between the rings with slightly lower CC, such as the areas outlined in white. CC doesn't confirm the signature, ZDR is needed for that. ZDR will be signifi-

cantly higher in dendritic growth layers, anywhere from 0.5 to 2.0 dB or higher. Notice the highest ZDR values fall right in the expected temperature range and a bit closer to the ground, particularly east of the radar. This could be mistaken for a melting layer given the high ZDR, but CC and common sense confirms that it is not. Notice the other pristine crystals also with higher ZDR in a broad range of heights north of the radar, outlined in red. If the temperatures are accurate, those may be columns. This was a fluffy snow, with roughly an 18:1 snow to liquid water ratio.

Consider these limitations when analyzing dual-pol radar data during a winter weather event:

- Below beam effects
- Many times the melting layer is not well-defined
- Diagnostic tool only - not a substitute for detailed and thorough environmental assessment

Below beam effects are nothing new to radar analysis in winter weather. Much of the time the environment below the beam dictates the eventual p-type at the surface. The human forecaster will certainly not become obsolete with dual-pol given the important environmental context the human brings to the table.

Many times a melting layer is not well defined. In those cases you'll need to look at each precipitation core individually to see what kind of "stuff" the radar is sampling.

Finally, the dual-pol radar is a diagnostic tool, and cannot be a substitute for a detailed and thorough

Limitations of Dual-Pol Winter Weather Signatures

Below Beam Effects

Melting Layer Not Always Well-Defined

Diagnostic Tool Only

environmental assessment. Again, the human forecaster adds great value here.

Lesson 8: Hail Detection

Hail varies greatly in size, from as little as a quarter of an inch up to 8 inches in diameter. Unlike rain, the shape of hail is not necessarily related to its size. Hail can be irregularly shaped, have large protuberances, and in some cases be oblate with one particular dimension much larger than the other. Hail also has the tendency to tumble, so it tends to appear effectively spherical to the radar. These characteristics are different from pure liquid drops, giving hail a unique signature in dual-pol data.

Hail usually has very high reflectivity (> 55 dBZ), but there have been examples of gigantic, very dry hail in low quantities with reflectivity around 40 dBZ. Differential Reflectivity (ZDR) will most likely exhibit a relative minima between -0.5 dB and 1.5 dB, due to the tumbling motion of the hail as it falls. However, ZDR can be substantially more positive in cases where the hail is mostly melted or mixed with rain.

For the aforementioned reasons, Correlation Coefficient (CC) is usually the most consistent indicator of hail. Even when hail is mixed with rain and there is not a clear signal in ZDR, CC will usually be fairly low, below 0.96 to as low as about 0.70. Specific Differential Phase (KDP) is fairly low (< 0.5 deg/km) in regions of pure hail, but will be high in the presence of mostly melted hail or when hail is mixed with a high concentration of liquid drops.

Overall, a classic hail signature in dual-pol appears as high Z, low ZDR, lower CC. It clearly contains a very high amount of liquid water given the extreme values of KDP. See Figure 8-1 on

Physical Characteristics of Hail

Characteristics of Hail in Dual-Pol Base Products

page 1-143 for an example of a hail core (white oval) as seen in each of these products.

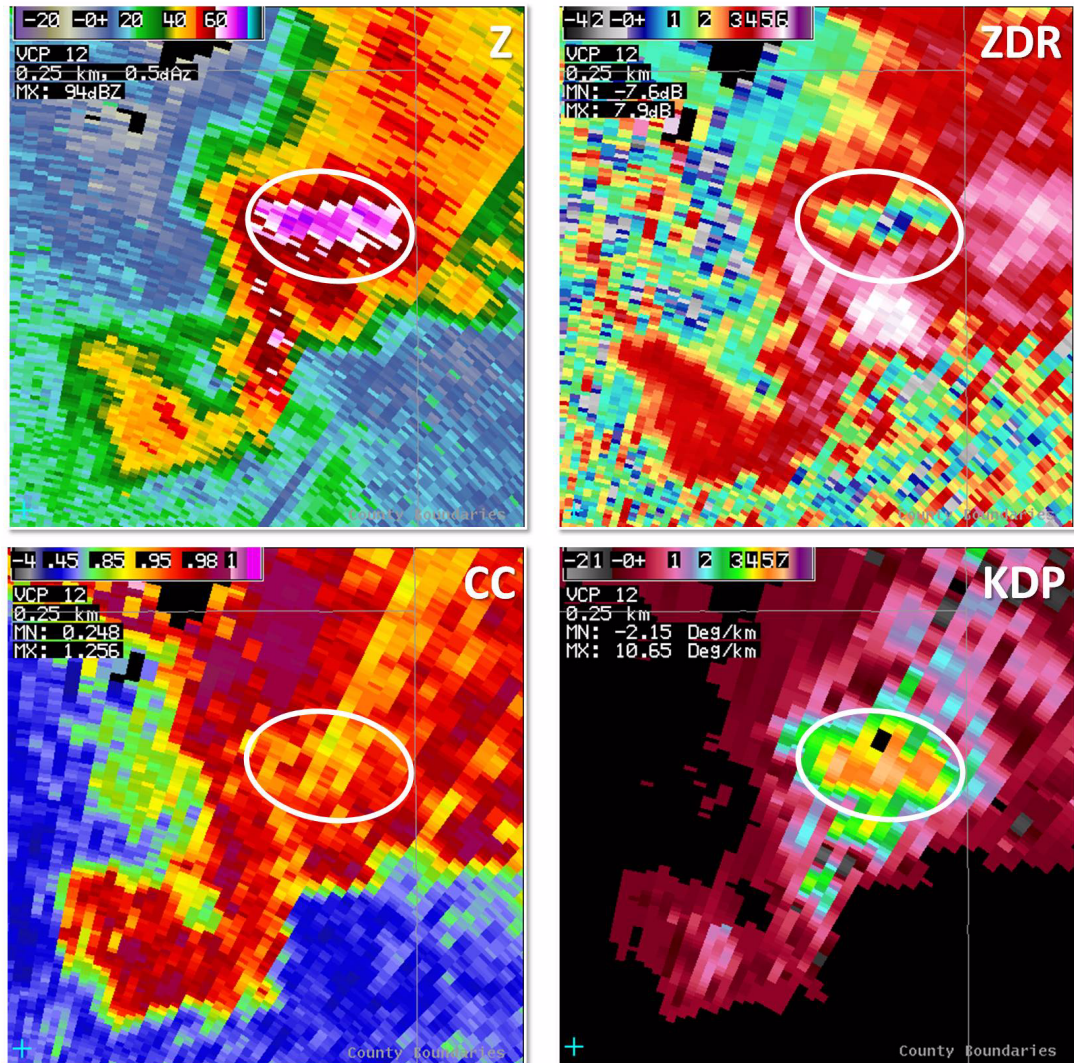


Figure 8-1. Reflectivity (top left), differential reflectivity (top right), correlation coefficient (bottom left), and specific differential phase (bottom right). The white oval marks the location of the hail core

Detecting Hail with PCR All-Tilts

When using PCR All-Tilts to examine a hail core, it's best to start with the lowest tilt to look for indications of hail possibly reaching the surface. Before using dual-pol products, start with reflectivity to get an idea about storm structure and height of the 55 and 60 dBZ levels. Toggle with SRM to get a feel for any rotation and divergent/convergent signatures, all of which help point to a hail threat. Try to use environmental sampling, in par-

ticular the temperature readout. Once done with that, step back down to 0.5 deg and toggle between Z and CC to distinguish precipitation from non-precipitation echoes. Where there is precipitation, find the highest reflectivity areas and look for CC less than 0.96. Then toggle to ZDR and look for local minima. If ZDR is low enough, less than 1.5 dB, hail is likely the dominant signal. Finally, you can toggle to KDP to see if any rain is mixed in with the hail. Values greater than 0.5 deg/km indicate a good amount of liquid coincident with the hail. Figure 8-2 shows a hail signature (white ovals) as seen in each of these products.

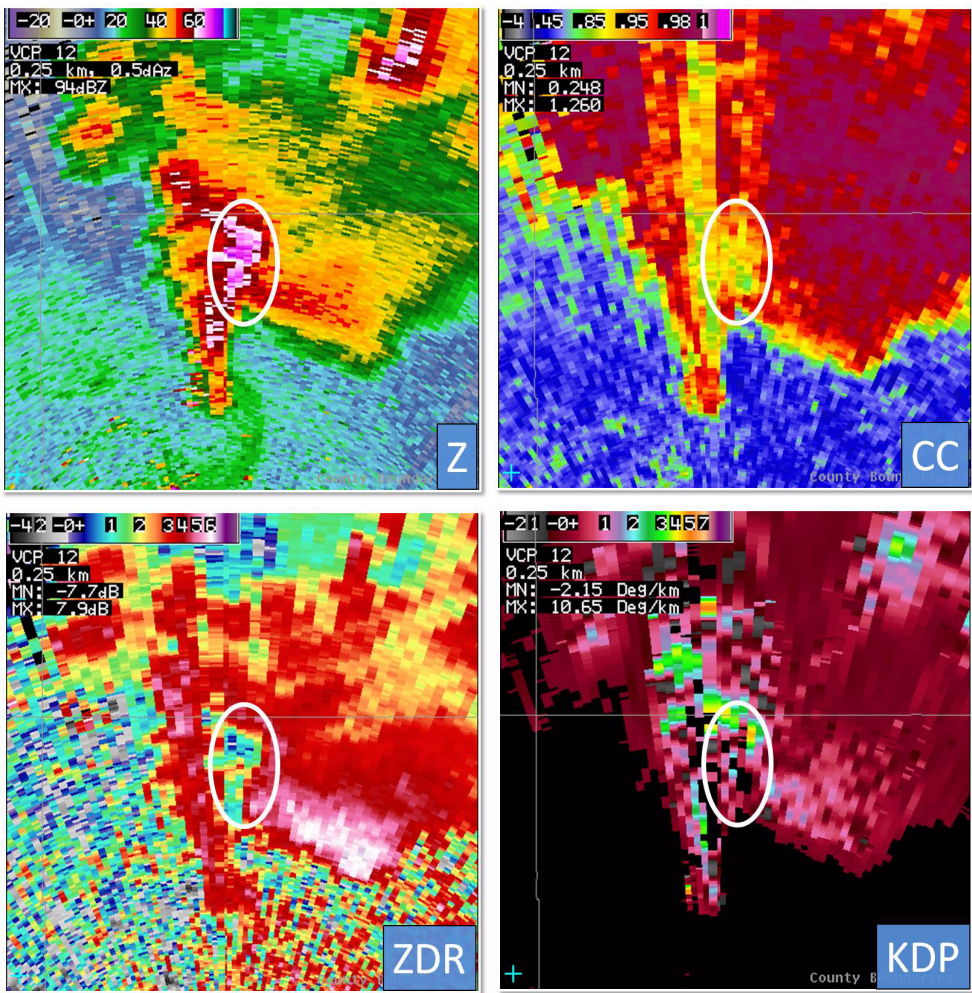


Figure 8-2. Supercell thunderstorm with hail core (white oval) as viewed in 0.5 degree reflectivity (top left), correlation coefficient (top right), differential reflectivity (bottom left), and specific differential phase (bottom right)

It's important to look aloft, too. Looking at the same storm as in Figure 8-2 at 2.4 degrees, high reflectivity is still present (see Fig. 8-3). In light of this height continuity with the hail core at 0.5 deg, examine 2.4 degree ZDR to see what has changed at this height. Since this is right at the environmental melting layer, ZDR has dropped outside of the hail core to just over 0 dB, making it difficult to see the locally suppressed values of ZDR caused by the hail. Some slightly lower CC is still present marking the location of the hail core.

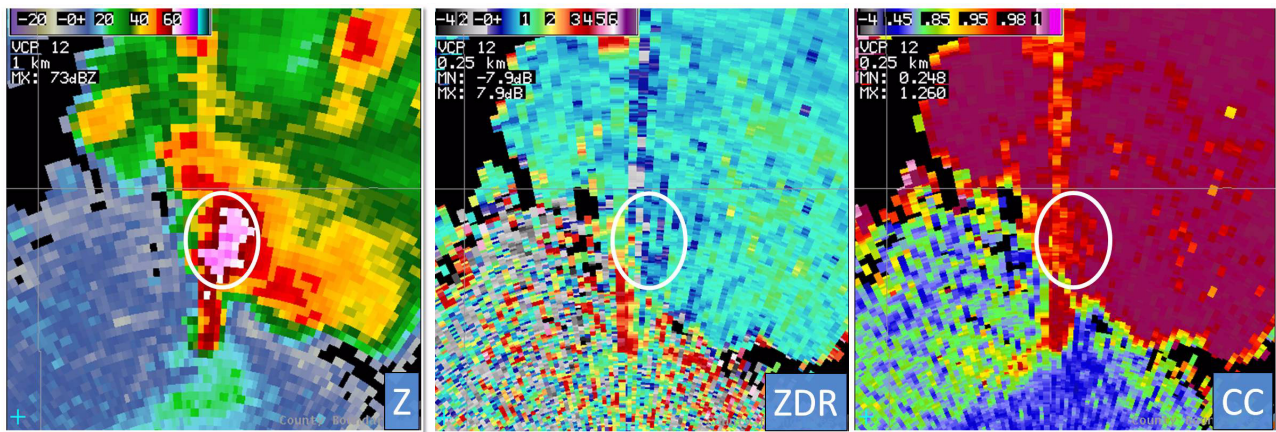


Figure 8-3. Reflectivity (left), differential reflectivity (middle), and correlation coefficient (right) 2.4 degree scan of hail core (white oval) shown in Figure 8-2.

Higher aloft in this case (Figure 8-4), there is still high reflectivity marking the location of the hail core, but ZDR is low everywhere. CC has become high everywhere due to the lack of mixed-phase hydrometeors at this elevation. Hail detection aloft where no liquid is present at any height quickly becomes difficult. This is true for hail of any size unless you have a rare case of dry giant hail really high in a storm, which would reduce CC because of Mie scattering effects.

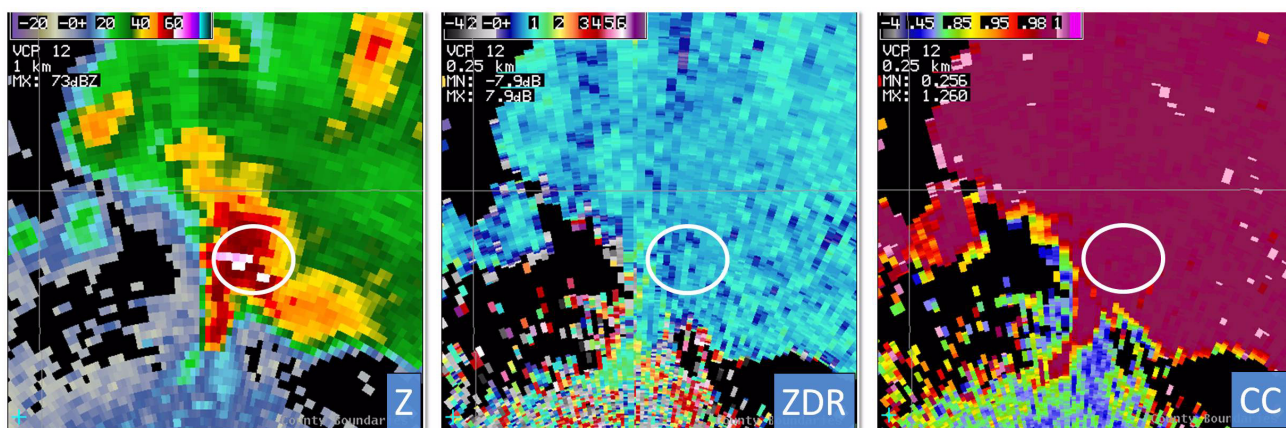


Figure 8-4. 4.0 degree scan of hail core (white oval) shown in Figure 8-2 and Figure 8-3. Reflectivity (left), differential reflectivity (middle), and correlation coefficient (right).

FSI can be used for hail detection with dual-pol. In the FSI cross sections seen in Figure 8-5 on page 1-147, there are actually two hail shafts, marked by the white ovals. As expected, both hail shafts have high reflectivity, although the one on the left, associated with a newer updraft, is deeper with higher values. Taking a look at ZDR (top right panel), both hail shafts are associated with fairly low positive to slightly negative values just above the melting layer, with the lower values extending higher aloft for the newer hail shaft on the left. Note also the depression in the transition to higher, positive values near the surface in each hail shaft below the melting layer. The signal in CC (bottom left) is not as easy to pick out as in the reflectivity or ZDR in this case, but notice the values of CC

FSI Characteristics of a Hail Shaft

are generally low in both hail shafts. KDP (bottom right) is generally very high in both hail shafts reflecting increased liquid water content associated with mostly melted hail and/or a rain/hail mixture.

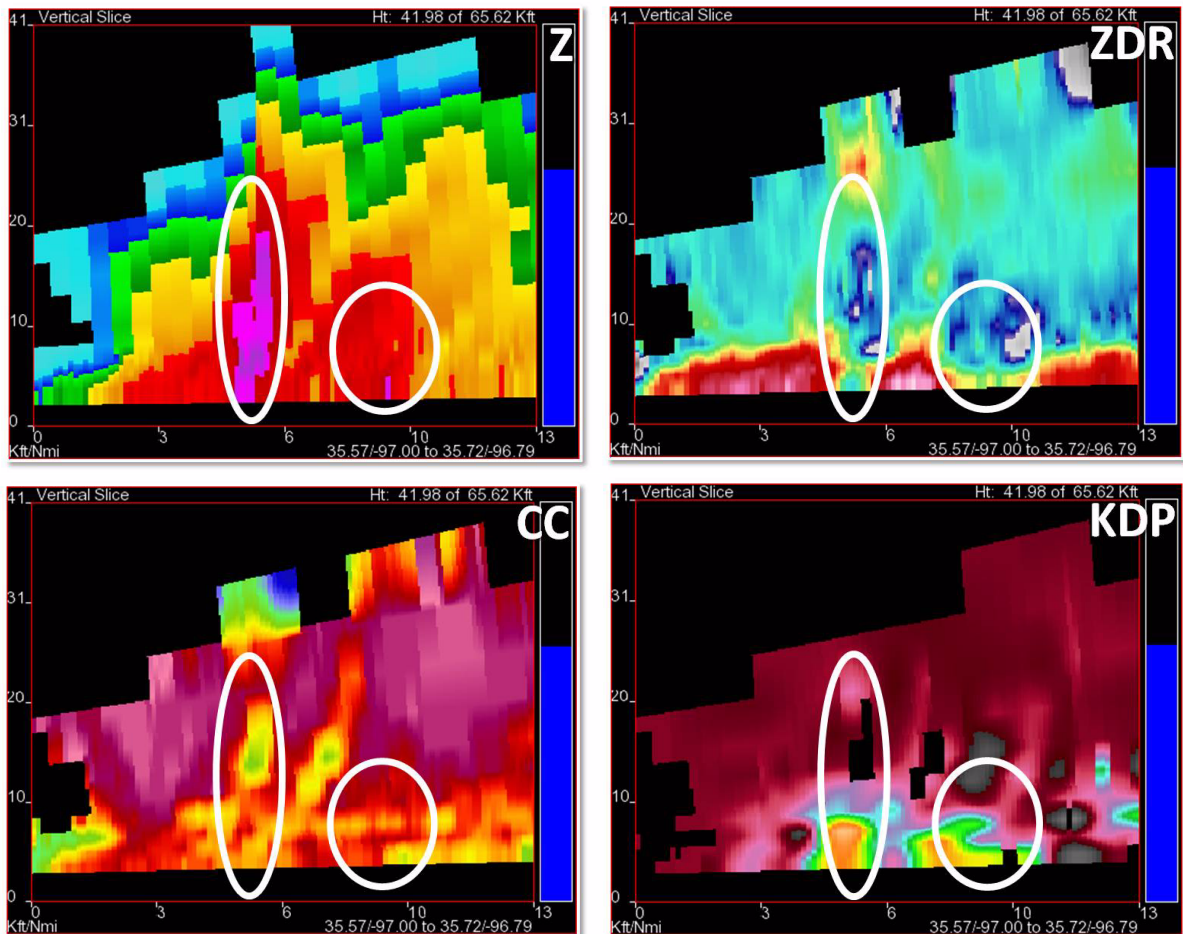


Figure 8-5. Dual-Pol FSI cross section depicting two hail shafts (white ovals). Reflectivity (top left), correlation coefficient (top right), differential reflectivity (bottom left), and specific differential phase (bottom right).

One important signature when it comes to hail detection is the three-body scatter spike, or TBSS.

Three-Body Scatter Spike (TBSS)

In the reflectivity image shown in Figure 8-6, the TBSS is seen as a radially-aligned extension of low Z down-range of the high reflectivity core.

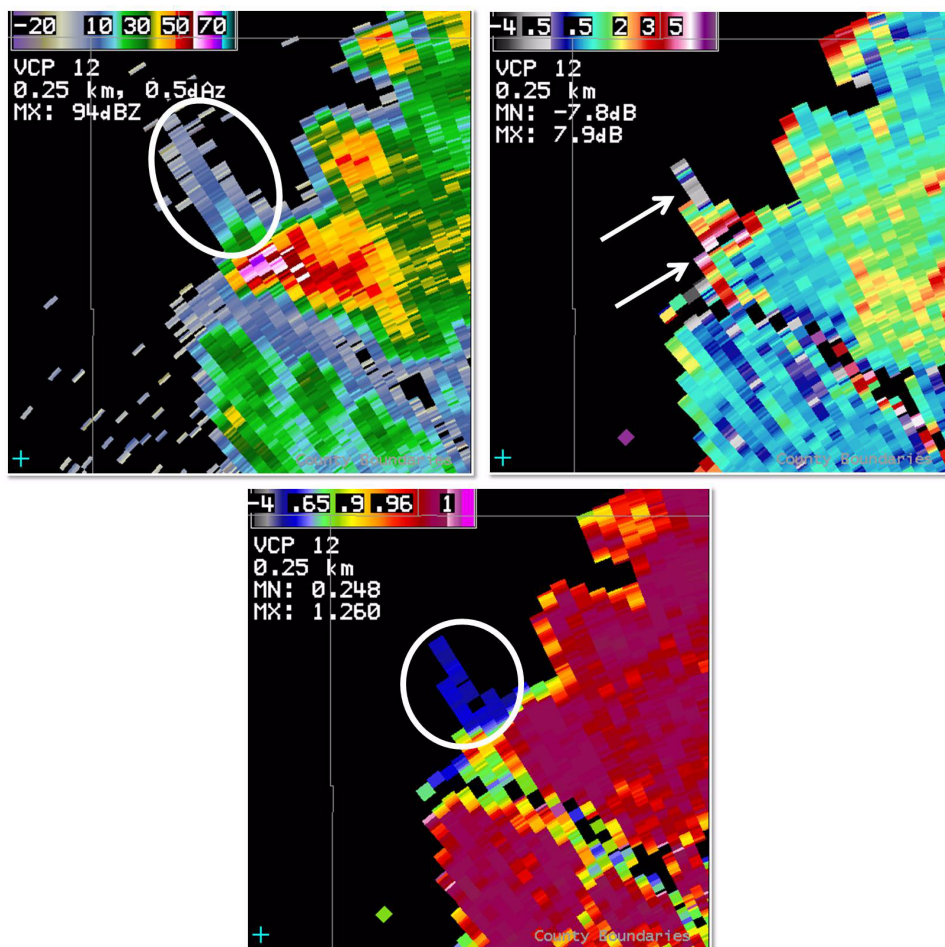


Figure 8-6. Three-body scatter spike (TBSS) as seen in reflectivity (white oval, top left), differential reflectivity (arrows, top right) and correlation coefficient (white circle, bottom).

In ZDR, the TBSS appears as an area of high positive values just down-radial of the hail core, transitioning into lower positive or even negative values farther down-radial. In CC, the TBSS shows up very clearly as a spike of extremely low values, (less than 0.5) on the down-range side of a hail core. CC is especially useful in cases when the TBSS is small or hidden by surrounding weak

echo. Always be on the lookout for those dark blue CC values oriented down radial from a high reflectivity core. They will be very smooth in nature. Conversely, with non-uniform beam filling (NBF), CC will be noisy. Be diligent in your differentiation between NBF and TBSS: They will both have lower CC down radial of enhanced reflectivity cores. The difference is TBSS will have smooth, much lower CC values that don't extend all the way down the radial.

TBSS Cross Section In a cross section of ZDR, the area of high, positive values located immediately behind the hail core is usually somewhat wedge-shaped, as indicated by the arrow on the right in the ZDR image (Figure 8-7). Farther down-range, the arrow on the left points out a transition to negative values of ZDR. In CC (Fig. 8-7, right), the TBSS is marked by very low values (white oval).

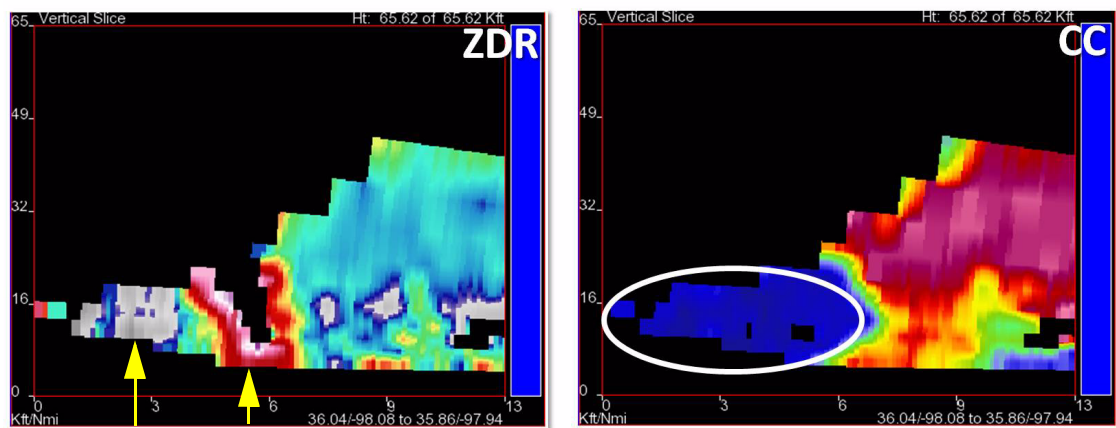


Figure 8-7. Three-body scatter spike (TBSS) signature in differential reflectivity (left) and correlation coefficient (right) cross sections. The two arrows in the ZDR image mark the high, positive values (right arrow) and negative values further down range. The white oval in the CC image indicates the location of the TBSS.

When giant hail (larger than two inches in diameter) is present the hail signature in the dual-pol variables can be very pronounced. Figure 8-8 shows an example of a storm that produced hail up to the size of softballs only a few minutes before this scan. Notice that reflectivity (left) is very high, in this case greater than 70 dBZ, though that is not always the case. Very dry, gigantic hail in low quantities, which tends to fall very near the updraft, can have reflectivity around 40 dBZ. ZDR (middle) is very close to 0 dB in most of the core coincident with the very low CC (right). In some cases with extremely large hail, ZDR may become negative due to Mie scattering. With hail this large, CC is normally lower than 0.85, as in this case. Remember to always keep the dual-pol products in context with reflectivity. Giant hail nearly always falls near the updraft and along the reflectivity gradient.

Special Case: Giant Hail Detection

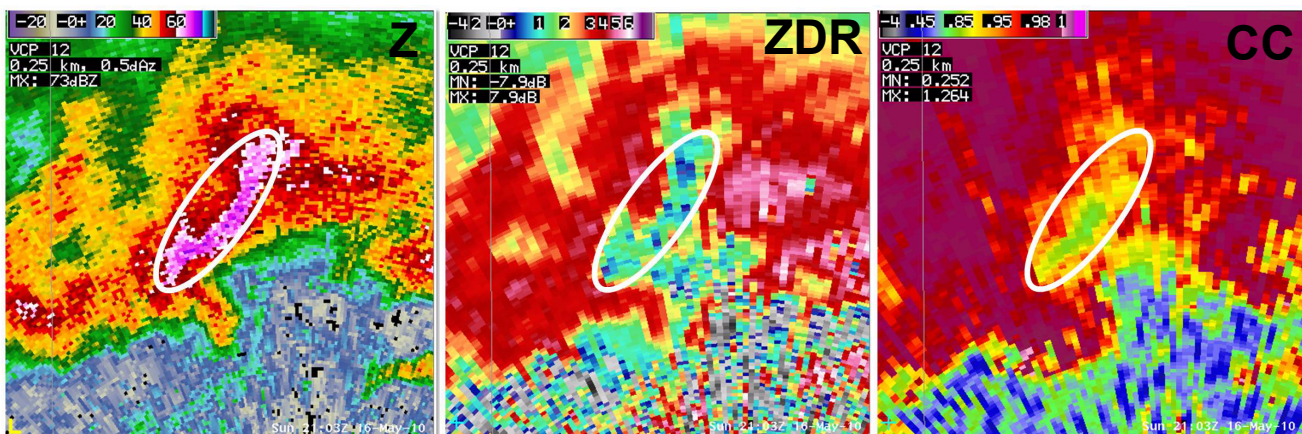


Figure 8-8. Reflectivity (Z, left), differential reflectivity (ZDR, middle), and correlation coefficient (CC, right) output for a storm that had a history of producing up to softball-sized hail. The hail core is noted by a white oval in each image.

Dual-Pol also has the ability to detect hail that has significantly melted, to the point that it's not likely to be severe. This signature is important because hail signatures can be found in just about any convective storm near and just above the freezing level. Therefore, seeing a hail signature doesn't

Melting or Mostly Melted Hail Signature

mean the hail will reach the ground. This section will cover the signature for hail that is probably not severe and often will not reach the ground as hail at all. This signature should be examined at several tilts to verify that hail is indeed melting. Other than very dry hail in low concentration, hail exists with reflectivity greater than 60 dBZ. Don't worry about looking for melting hail at reflectivity less than 60 dBZ as there is too much ambiguity in the signature.

How Hail Melts Let's first discuss how hail melts and what it should look like on radar. For this example, say there is a sphere of solid ice with a diameter of 0.75 inches, falling outside of the updraft below the 0°C level (see Fig. 8-9). Melting begins on the surface of the hailstone. Assume the hail is mostly dry initially.

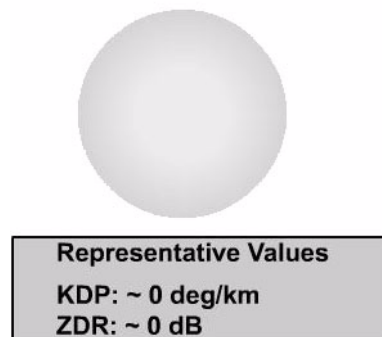
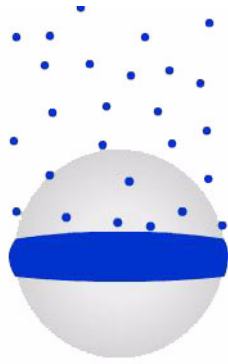


Figure 8-9. Completely frozen hail returns ~0 deg/km in KDP and ~0 dB in ZDR

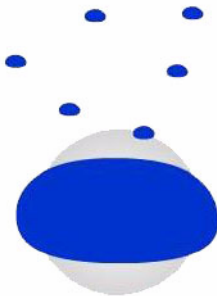
As the surface melts, the meltwater is advected into a torus (shown as a blue band around equator of the hailstone in Figure 8-10) due to drag as it falls. Continuous shedding of small drops occurs from the torus of water. Shed drops fall much slower. The hail is reduced to 0.70 inches in diameter.



Representative Values
 KDP: + 0.5 deg/km
 ZDR: + 0 - 0.5 dB

Figure 8-10. As the surface layer melts, small drops are shed from a torus of water that forms around the equator of the hail stone.

The hail continues to melt and the torus moves upstream as the size of the ice particle decreases. Intermittent shedding of large drops occurs from the unstable torus. The hail is now 0.60 inches in diameter (see Fig. 8-11).



Representative Values
 KDP: 2.0 deg/km
 ZDR: + 2 dB

Figure 8-11. As the diameter of the ice core decreases, KDP and ZDR return higher positive values.

The torus loses its distinction, and a water cap forms around the top (lee side) of the ice core. There is intermittent shedding of a few larger drops and the ice core is now 0.4 inches in diameter. The blue stippled area in Figure 8-12 represents the ice core contained “within” water.



Representative Values KDP +2 deg/km ZDR > +3 dB
--

Figure 8-12. As melting continues and the hail becomes more of a liquid than a solid, positive values of ZDR and KDP increase.

Soon the meltwater forms a stable raindrop shape around the ice core (see Fig. 8-13). There is no longer any drop shedding. The horizontal axis of the ice and water coating is approximately 0.2 to 0.4 inches (~5-9mm).



Representative Values KDP at Max Here: + 3 deg/km ZDR at Max Here: > +4 dB

Figure 8-13. Melted hail becomes less spherical as it continues to melt, further increasing KDP and ZDR.

Eccentric melting of the ice core occurs until the ice is completely melted. All that is left is a large, cold rain drop 3-5 mm in diameter (see Fig. 8-14).



Representative Values
KDP: + 2 deg/km
ZDR: > +3 dB

Figure 8-14. When the hail has melted completely rain is all that reaches the ground.

The example in Figure 8-15 on page 1-155 starts at 9.9 deg near the radar. The hail core inside the oval is at 16 kft, right where melting should begin on this hot summer day. A TBSS is also seen in reflectivity. Melting hail will be mixed with rain so correlation coefficient should be between 0.90 and 0.98, but these are not hard thresholds by any means. For this example, values are around 0.95 inside the circle.

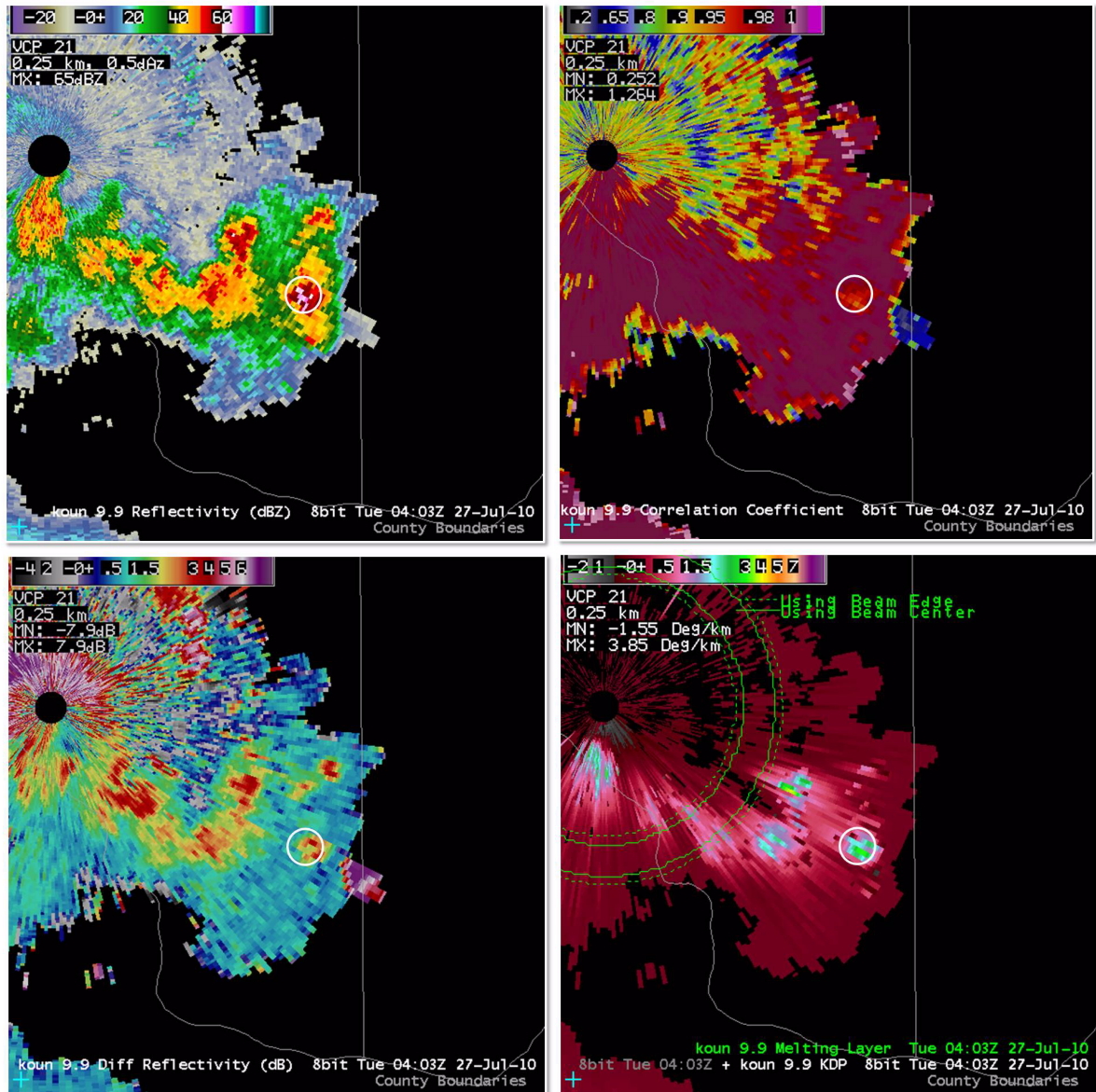


Figure 8-15. Reflectivity (top left), correlation coefficient (top right), differential reflectivity (bottom left), and specific differential phase (bottom right) from a 9.9 degree scan of a near-range storm containing melting hail (white oval).

The most important variable to examine for melting hail is ZDR. Given reflectivity greater than 60 dBZ, we know for sure hail is sampled. With ZDR greater than about 2 dB, it's safe to say that horizontally-oriented "things" are dominating the signal. The only meteorological particle that can exist with high ZDR and very high reflectivity is hail

completely coated in water, and only small, sub-severe hail can be completely coated in water such that it flattens out like a rain drop. ZDR values in the oval are between 2 and 3 dB, indicating that the hail is heavily coated with water.

To help verify the presence of very high amounts of liquid water, KDP should be greater than 1 deg/km, and in reality it is often extreme, well over 3 deg/km. In this example, there are several gates right around 3 deg/km. Altogether, these ranges of values indicate hail that is nearly melted and very unlikely to reach the ground severe. Something to keep in mind is the context of where the radar is sampling the melting hail: If the signature is very near the ground already (i.e. close to the radar), complete melting into rain is a little less likely than if the signature is thousands of feet off the ground.

Strengths of using dual-pol for hail detection include:

- Dual-pol hail detection is more robust than using Z alone.
 - Examining ZDR and CC validates where hail is located
- Detection of significant hail is possible
 - Be careful not to rely solely on the giant hail signature.
- Detection of hail that is mostly melted and not likely to reach the ground.
- TBSSs show up much easier, even with precipitation down-radial of the hail core

Strengths of Dual-Pol Hail Detection

Limitations of Dual-Pol Hail Detection

Limitations of using dual-pol for hail detection include:

- No explicit size estimation
 - Neither human nor algorithm
 - Ability to differentiate between severe and non-severe hail not yet possible
- If hail is detected, it's sometimes impossible to tell if it's reaching the ground

Lesson 9: Tornado Debris Detection

As warning forecasters we need to be very careful about how we use the tornadic debris signature (TDS) in warning operations, as well as how we discuss it with our partners outside the National Weather Service. The most important thing to know about the tornadic debris signature is that it **does not** improve initial lead time for tornado warnings. Equally as important is that this signature also **does not** replace traditional reflectivity and storm-relative velocity base data analysis for tornadic threat assessment. Finally, TDS **will not** be identified with the majority of tornadoes since very specific conditions have to be met for the signature to be sampled by a radar. We'll look at those conditions in depth later on in this lesson.

The TDS **will** give confirmation of a damaging tornado. When properly identified, this signature is as good as a spotter report of a tornado. The rest of this lesson will focus on the characteristics of the TDS, the methodology on how to identify it, and finally how to best incorporate this signature in your warning operations.

The size of tornadic debris can vary widely, but it is generally larger than normal meteorological scatterers. These irregularly-shaped, diverse objects tumble in extreme winds, causing a random orientation. Things like leaves and insulation can be lofted vertically quite a ways, making it possible for the radar to sample the debris.

Tornadic Debris Signature (TDS)

Physical Characteristics of Tornadic Debris

Dual-Pol Characteristics of Tornadic Debris

The presence of tornadic debris can result in a local reflectivity maximum, as seen in Figure 9-1. The great advantage to the TDS is that even when reflectivity does not look like a debris ball, the dual-pol products will help verify the presence of debris.

Given the physical characteristics of tornado debris, it's probably not surprising that the most important discriminator is correlation coefficient. There are no hard thresholds with CC, but look for a local minimum in CC. It will typically be less than 0.80 due to both the random orientation and the irregular shape of the debris. The random orientation of tornado debris means that the ZDR will be reduced to near 0 dB. In the ZDR image in Figure 9-1 (bottom left), the gray areas actually represent negative ZDR values. Finally, the most important, must-have signature is in Storm Relative Velocity (SRM). The dual-pol products should be co-

located or very nearly co-located with a rotational signature.

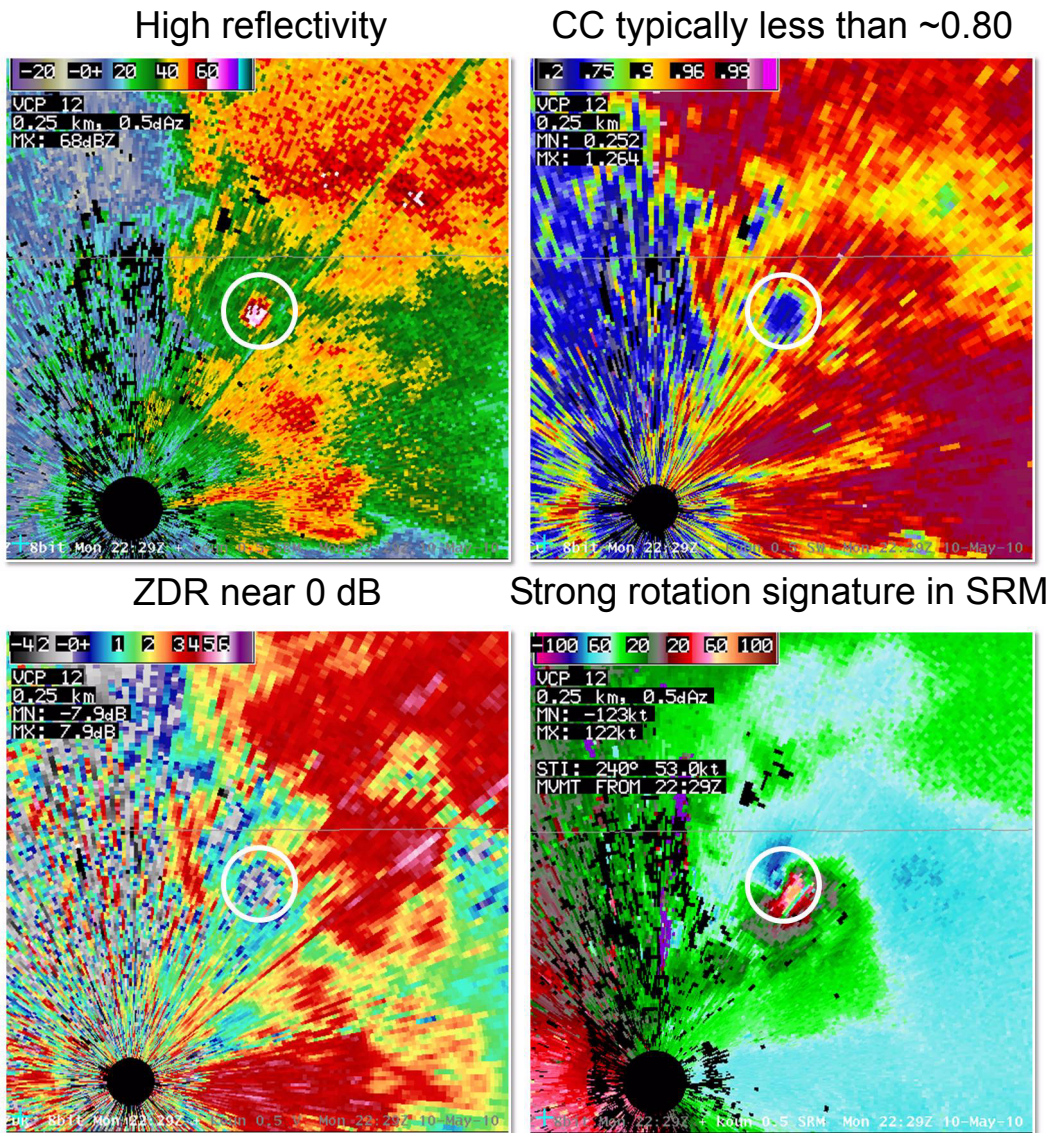


Figure 9-1. Reflectivity (top left), correlation coefficient (top right), differential reflectivity (bottom left), and SRM (bottom right) of a tornadic debris signature (TDS) (white circle).

When should you check for a debris signature? As with TDS and all the other dual-pol signatures, start with a reflectivity and SRM analysis first (see Fig. 9-2). For the tornadic debris signature, issuing a radar-based tornado warning using Z/SRM first is strongly recommended. The TDS signature implies that a tornado is present and doing damage, so if you identify one prior to issuing a warning, it's too late to get any lead time. Issue the

When to Check for Tornadic Debris Signature

tornado warning first based on the merits of a spotter report, the near storm environment, reflectivity, and SRM. Once the tornado warning is out, look for debris since what you are really interested in is confirmation that a tornado is occurring.

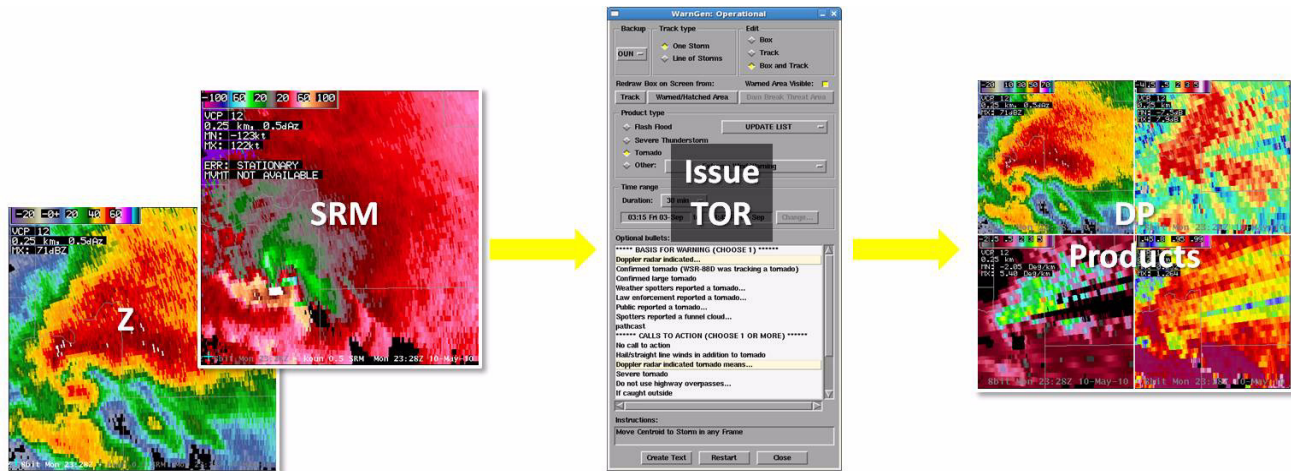


Figure 9-2. Use reflectivity and storm-relative motion products to issue tornado warnings, then look for the TDS to confirm.

There may be cases where the velocity signature looks decent but you are holding off on issuing a tornado warning. In those cases, you can quickly look for debris without having a tornado warning out, but should you identify debris, your subsequent tornado warning would have negative lead time, so it's a gamble. There is so much uncertainty and the learning curve for identifying the TDS is pretty steep, so focus on getting the warning out in a timely fashion using reflectivity and SRM.

How to Check for Tornadoic Debris Signatures

Now let's examine how to check for the tornadoic debris signature:

1. Examine Z/SRM All Tilts
2. Issue tornado warning
3. 3-product toggle (Z-SRM-CC) at 0.5 deg.

- A TDS, if present, will be located within a few gates of the strongest rotation in SRM and have strong reflectivity values
- MUST see $CC < 0.85$ and/or local minimum

4. Toggle to ZDR and look for a local minimum

Once the TOR is out, move onto a 3 product toggle between reflectivity, storm relative velocity, and correlation coefficient at the lowest tilt. Debris will reside closest to the ground, and because time is of the essence, the only tilt you need to use is 0.5 deg. Do not look for a reduction in correlation coefficient unless you are searching the area on top of or within a few gates in all directions of a strong rotational velocity signature. Keep an eye on reflectivity, because if reflectivity values are too weak (< 20 dBZ), correlation coefficient will not be trustworthy. A relative minimum in correlation coefficient should correspond with a strong velocity signature. If the tornado is lofting very small debris mixed with rain CC will be around 0.90 to 0.95. Larger, complex debris sampled by the radar will have correlation coefficient below 0.8.

Keep toggling between Z, SRM, and CC to verify that you are seeing debris. When you are pretty sure you have identified a TDS, toggle over to ZDR. ZDR should show a local minimum collocated with the local minimum in CC. Typically ZDR will be around 0 dB. Use ZDR as a consistency check since SRM and CC within strong enough reflectivity will give the best results with regards to tornadic debris signatures. Figure 9-3

shows three separate tornadic debris signatures in SRM, CC, Z and ZDR.

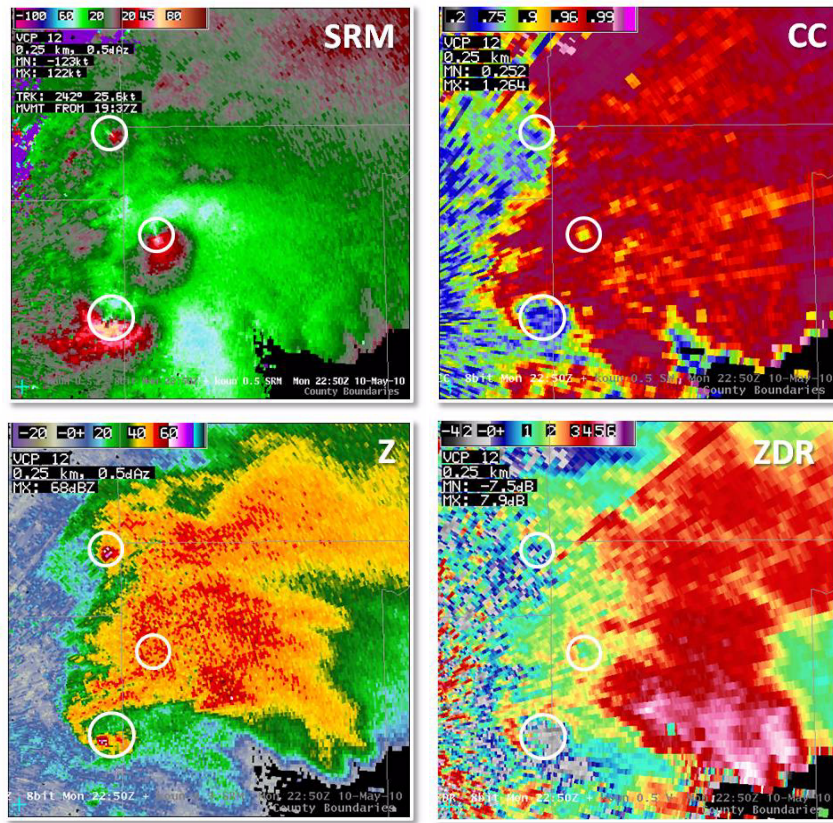


Figure 9-3. Storm-relative motion (top left), correlation coefficient (top right), reflectivity (bottom left) and differential reflectivity (bottom right) showing three TDSs (white circles) at once.

Strengths of Dual-Pol Tornadic Debris Detection

A TDS is confirmation that a tornado is both occurring and doing damage. Get the word out immediately in an SVS that a tornado is confirmed, and then use all other methods of communication you'd normally use after receiving confirmation of a tornado. This signature, when identified properly, is the equivalent of video confirmation or a highly reliable spotter report. Put simply, the TDS by itself can be used to verify a tornado warning, at least until a damage survey team can get out there to check it out.

There are several important limitations to the TDS. These are especially important to avoid misuse and misinterpretation of the signature.

1. Not a predictor of a tornado - no lead time
2. Tornado must be at close range
3. Tornado must hit something to produce a signature
4. Debris signature might be upstream of the strongest couplet

The appearance of the tornadic debris signature will not give you any lead time on a tornado. The tornado is already present and doing damage by the time this signature shows up in the radar data.

Since most of the debris cloud will be shallow and occur on a relatively small scale, the tornado usually has to be at close range to produce this signature. EF-1 tornadoes have been detected at ranges as far as 40 nm, and EF-3/4 tornadoes out to 60 nm. It may be possible to see debris outside of 60 nm, but it would be very unlikely given beam-width and beam height off the ground (barring any non-standard propagation of the radar beam).

The tornado must loft debris when the radar is scanning it to produce a signature. At best the volume scan update time is 4.5 minutes (VCP 12), so the tornado needs to have debris in the air for the 0.5 deg sweep or else you are out of luck. "Something" doesn't have to be huge chunks of debris like a flying cow or Grandma's entire house. Small debris like leaves, twigs, corn stalks, sunflowers, wheat etc., are all excellent scatterers that are fairly easily lofted by even an EF-0 or EF-1 tornado, the trick is being lucky enough for the radar to sample it.

Limitations of Dual-Pol Tornadic Debris Detection

No Lead Time

Tornado Must Be at Close Range

Tornado Must Hit Something to Produce a Signature

Debris Signature Might Be Upstream of the Strongest Couplet

Another limitation associated with the TDS is that sometimes the debris signature will be offset from the rotational couplet. This limitation arises from the fact that the 0.5 deg elevation angle has two separate scans: a surveillance scan, which builds reflectivity and the dual-pol products, and a Doppler scan which builds the velocity products. The surveillance scan is done first, and thus dual-pol products are produced before the matching velocity image. The time between the dual-pol products and the velocity products runs between 14 and 20 seconds depending on VCP. Also, the velocity image is super-res, while the dual-pol products are 1 deg azimuth, which could also cause a bit of displacement. For most cases, the displacement will be 1-2 gates. Keep this in mind so you are not surprised to find debris slightly offset from the rotational couplet.

i

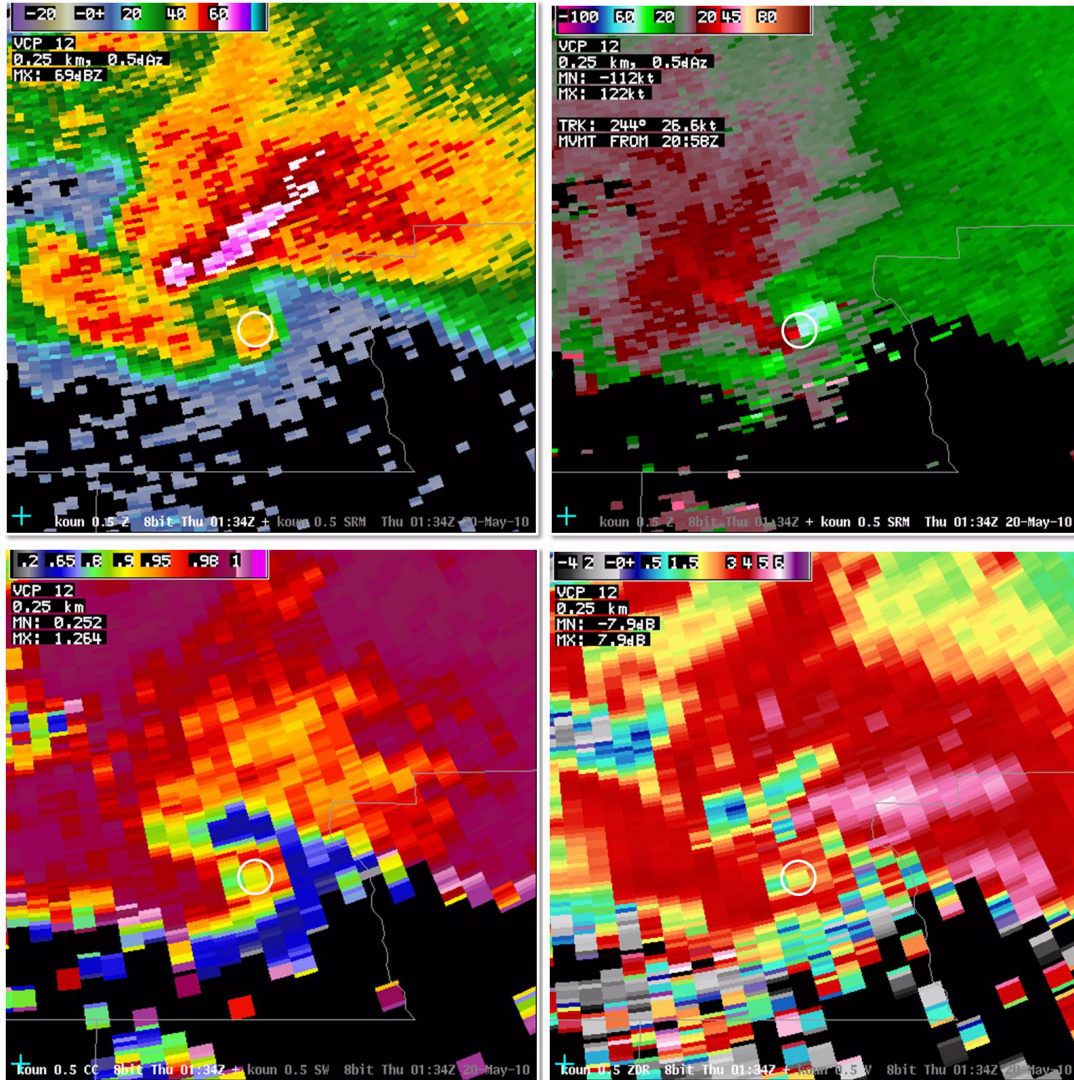


Figure 9-4. Tornadoic debris signature (TDS) as shown in reflectivity (top left), storm-relative motion (top right), correlation coefficient (bottom left), and differential reflectivity (bottom right). Notice the TDS in ZDR and CC upstream of the couplet in SRM

For fast moving storms, like the one in Figure 9-4 that moved around 27 knots towards the ENE, the debris signature shows up upstream of the velocity couplet by a couple of gates. Reflectivity isn't too impressive. An EF-1 tornado is occurring at about 35 nm from the radar at this time. In SRM (top right), there is a very nice rotational signature. The entire rotational signature has reflectivity over 30 dBZ so there is no need to worry about data qual-

ity issues with the dual-pol products. Looking at correlation coefficient, notice that the strongest minimum is 1 radial away from the center of rotation, and upstream of where the circulation is headed. The local minimum ZDR is 1 radial upstream of the rotational signature and co-located with the minimum in CC. This limitation is why you should allow yourself several gates around the rotational signature during your search for the TDS.

Lesson 10: ZDR Columns

The ZDR column is defined as an area of positive ZDR extending above the environmental melting level, as shown in Figure 10-1. Warmer colors represent higher positive values of ZDR and the gray represents values less than 1 dB.

Definition of a ZDR Column

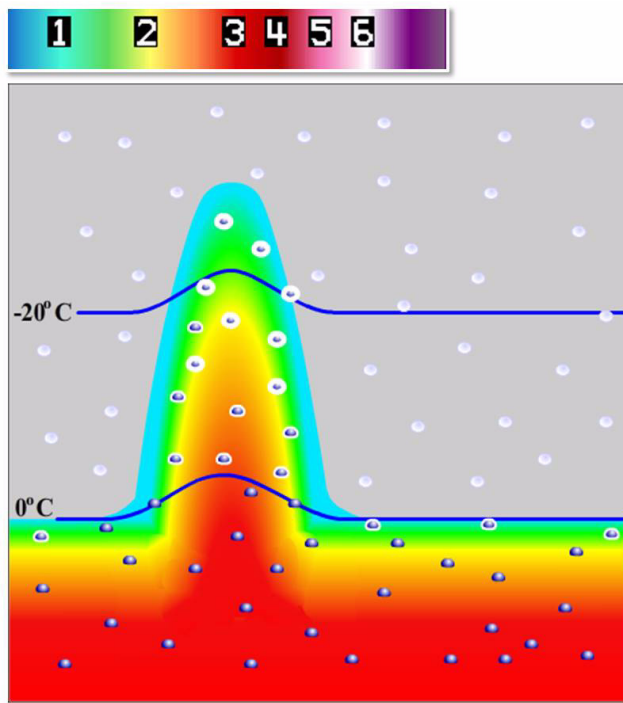


Figure 10-1. Example of a column of positive ZDR extending above the environmental melting level.

The ZDR column signature is associated with updraft. Significantly positive ZDR above the environmental 0°C level implies that liquid drops or partially frozen liquid drops are present. The only way to get liquid well above 0°C is in an updraft. There is no hard ZDR threshold to use, but generally look for values of 1-1.5 dB to mark the extent of the ZDR column. ZDR columns can extend well above the environmental -20°C in the strongest convective storms. This signature implies that an updraft is strong enough to loft liquid far into below-freezing temperatures, leading to the production and growth of hail.

ZDR columns are typically noted along the flanks of updrafts for sheared convective storms that have cloud bases significantly below the environmental 0°C level. With supercells, or other convective storms with very strong updrafts, the ZDR column will reside where vertical velocities are weak enough to allow growth and/or collision and coalescence of rain drops. There also must be a warm cloud layer deep enough to be able to produce liquid drops in the first place. Thus, cloud bases above the 0°C level will rarely have ZDR columns unless they can locally modify the near storm environment. In weakly sheared convective storms (i.e., pulse storms), the ZDR column is often co-located with the updraft.

An example of a ZDR column in FSI is shown in Figure 10-2 outlined by the black line. The approximate environmental melting level is marked with a thick white line. First, note how the positive ZDR values above the 0°C level are connected with the positive ZDR values below the 0°C level. To detect a ZDR column, the enhanced ZDR values must have vertical correlation above and below the environmental 0°C level. Outside of the ZDR column on the right side of the cross section, note the sharp transition at around 9-10 kft from mostly higher positive values of ZDR below the melting level to values of 0.5 dB and less above the melting layer, indicating ice had melted into rain.

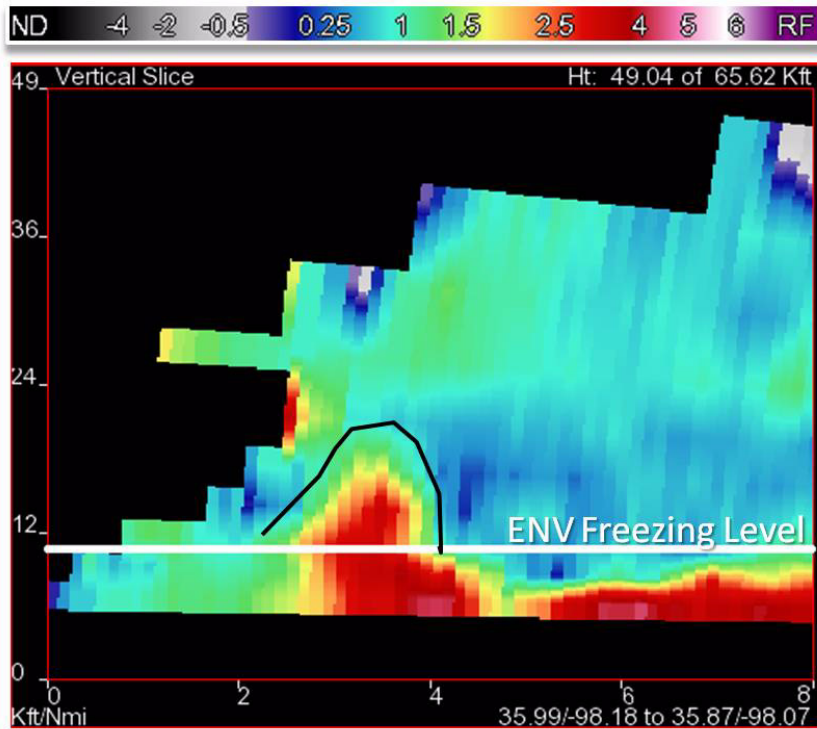


Figure 10-2. Example of ZDR column as seen in FSI.

There are a couple of different ways to look for ZDR columns, both of which require knowledge of the environmental 0°C level. Analyze dual-pol base data using All Tilts Panel Combo Rotate and environmental sampling in AWIPS or CAPPI displays plotted just above the 0°C level in FSI.

1. **Do a storm structure analysis with all D tilts reflectivity and storm relative velocity** to get a feel for the nature of the storm.
2. **Toggle between reflectivity and ZDR**, stepping up in elevation angle until an elevation above the melting layer is reached and most of the ZDR values are less than 1 dB. Focus on areas expected to contain updraft. In Fig. 10-3 on page 1-171, the 0°C level was expected to be around 15 kft MSL, but because the storms are far from the radar and the beam is very wide, the beam is clearly not entirely above it

How to Find ZDR Columns

Detecting ZDR Columns in Panel Combo/Rotate

given the high ZDR values everywhere even at 17 kft MSL.

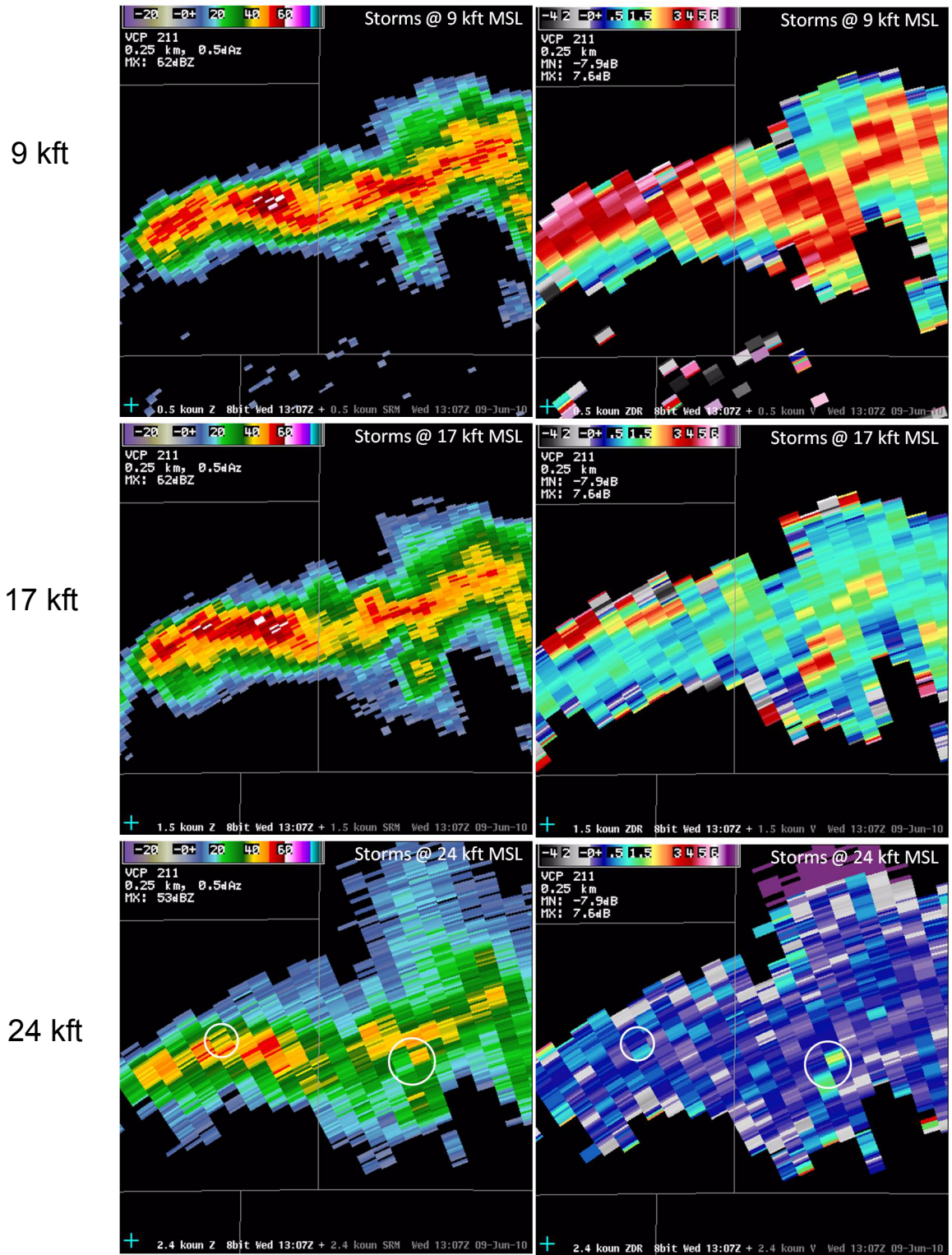


Figure 10-3. Reflectivity (left) and differential reflectivity (ZDR) at 0.5, 1.5, and 2.4 degrees.

3. **Look for pockets of ZDR greater than about 1.5 dB**, checking to see that they have good continuity with values below that height. At 24 kft MSL, which is several thousand feet above the freezing level, the areas in the white ovals have ZDR greater than 1.5 dB.
4. **Ensure that the ZDR column is located in a good reflectivity signal**, roughly 25 dBZ or higher, and also not right along the very edge of the ZDR data. Step down in elevation angle to confirm that enhanced ZDR exists below this feature as well. With both ovals, strong ZDR values exist below, though the western circle isn't as well connected to higher values below. To increase confidence that this is a ZDR column, check correlation coefficient.
5. Near the top of the column, **the co-location of liquid and ice should lead to CC lower than 0.97**. Indeed, CC is right around 0.97 in one of those regions of enhanced ZDR (see Fig. 10-4). The western area however, has CC around 0.99, perhaps indicating that it may not be a ZDR column after all.

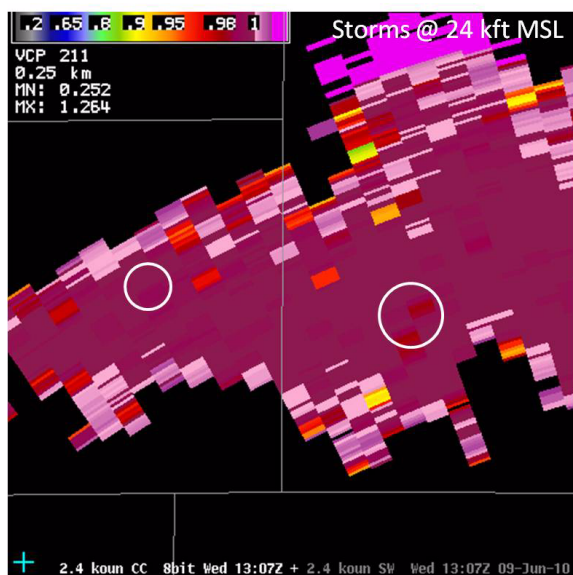


Figure 10-4. Correlation coefficient product output at 2.4° for the event shown in Figure 10-3.

Identifying ZDR Columns Using CAPPI in FSI

Using FSI to identify ZDR columns is also quite useful. When zoomed in to the storm of interest in FSI, take the blue slider bar on the right side of the CAPPI panel and move it to just above the approximate environmental 0°C level. Toggle to ZDR and look for local maxima in ZDR (arrows in Fig. 10-5). Just like looking for a ZDR column using All Tilts, remember to compare ZDR with reflectivity and correlation coefficient to make sure the data is of high quality and the high ZDR is not an artifact. In Figure 10-5, notice that both ZDR columns (marked by the arrows) are in regions of expected updraft. In CC, the reduction in values due to mixed-phase hydrometeors is present, giving more certainty that these are ZDR columns. Finally, be sure to check both the vertical and temporal continuity of any potential ZDR columns. Dragging the blue slider bar is a handy way to gage how far the ZDR column extends vertically.

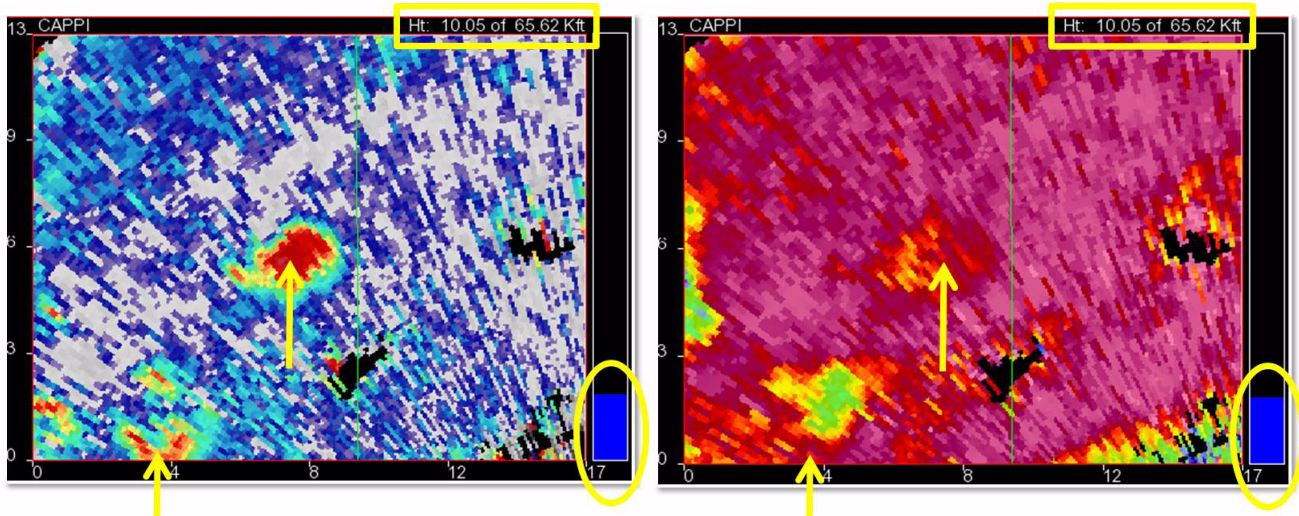


Figure 10-5. ZDR column as seen in differential reflectivity (left) and correlation coefficient (right) using the CAPPI in FSI.

ZDR Column Applications

Aside from an increased situational awareness of updraft strength and location, you may be wondering about ZDR columns applications. There have not been many studies to date that have correlated ZDR column depth and absolute magnitude to

storm severity. However, ZDR columns could be used to compare storms on the same day for relative strength. Looking for ZDR columns prior to supercells splitting has also added some lead time and value in those types of events.

There may be some differences between ZDR columns in storms of different intensities. Since the ZDR column is closely associated with the updraft, watching for consistent differences in the characteristics of the ZDR column between two storms may be helpful for anticipating differences in storm evolution or storm strength.

In Figure 10-6, there really isn't anything special about the storm when viewed in reflectivity. In fact it is over 100 nm from the radar, making it extremely difficult to see anything in the way of structure. Looking at SRM, it looks like there may be some weak rotation associated with this storm, but it still does not stand out all that much.

Relative Updraft Strength

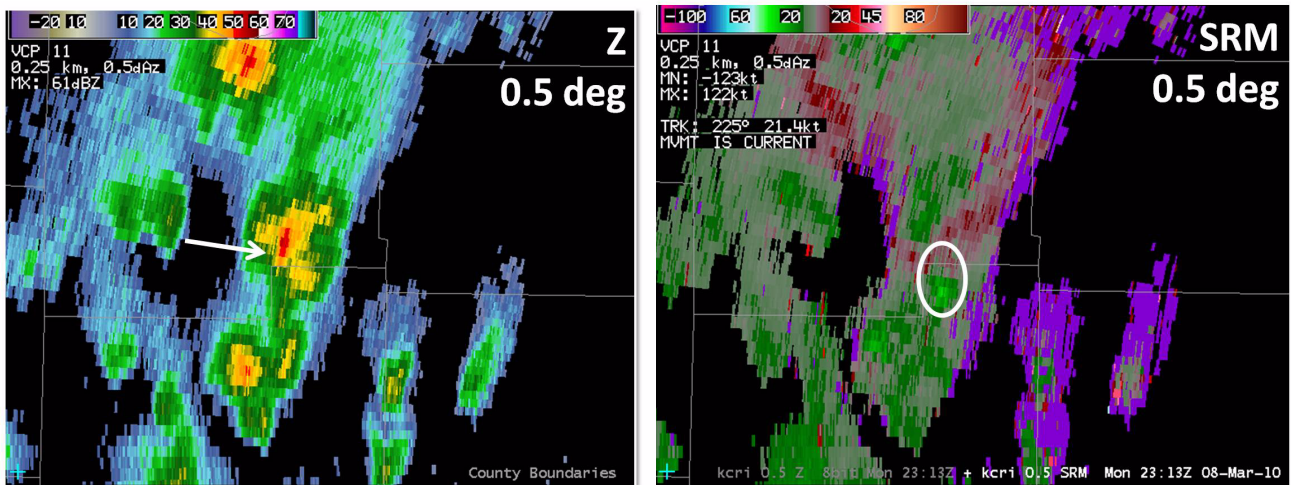


Figure 10-6. Reflectivity (left) and storm-relative motion (right) of a storm about 100nm WNW of the radar.

In ZDR, there is a small area of positive ZDR on the far southwest flank of the storm. At this distance from the radar, the beam is above the environmental melting layer, so any area of

substantially positive ZDR could be a ZDR column. There is a local minimum of CC, indicating mixed-phase hydrometeors, as would be expected with a ZDR column.

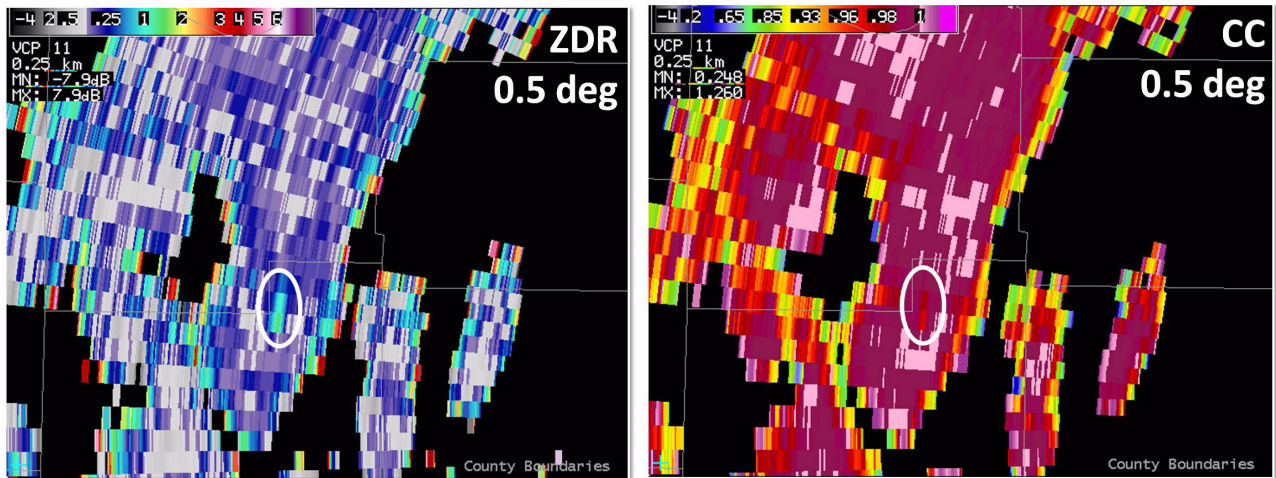


Figure 10-7. Same storm as Figure 10-6 with an area of positive differential reflectivity (left) and a local minimum of correlation coefficient (right).

At this distance it is difficult to check height continuity, but moving forward in time a couple of volume scans (see Fig. 10-8) the positive ZDR has actually increased in coverage and magnitude, so there is at least fairly good temporal continuity.

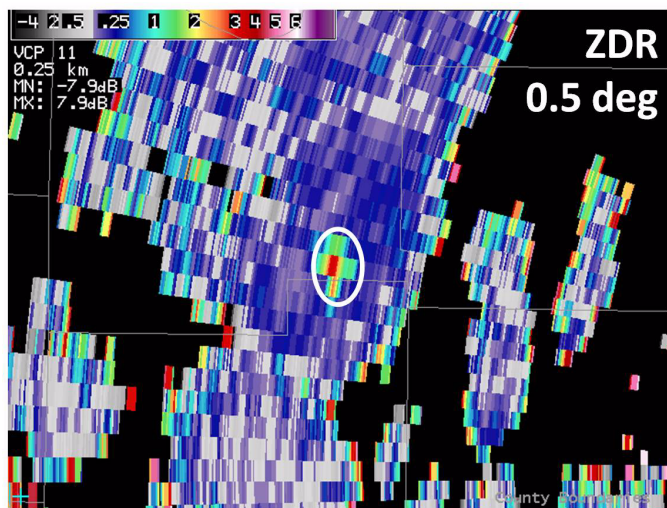


Figure 10-8. Same storm as shown in Figure 10-6 and Figure 10-7, but a couple volume scans later.

The storm in the previous example ended up being the only tornadic storm of the day, but it must be emphasized here that the presence or lack of a ZDR column does not necessarily say anything about the potential for tornadic activity. In this instance, the presence of the ZDR column was merely a clue that there was something different about this storm. Caution is advised as more research is needed on this topic.

Monitoring the ZDR column for clues about storm evolution may be helpful in anticipating storm splitting. Looking at Figure 10-9, the 0.5 degree reflectivity shows a storm with a strong reflectivity core. Looking aloft, there almost appear to be two distinct maxima in reflectivity, but it would be very helpful to see if there really are two distinct regions of updraft.

Storm Splitting

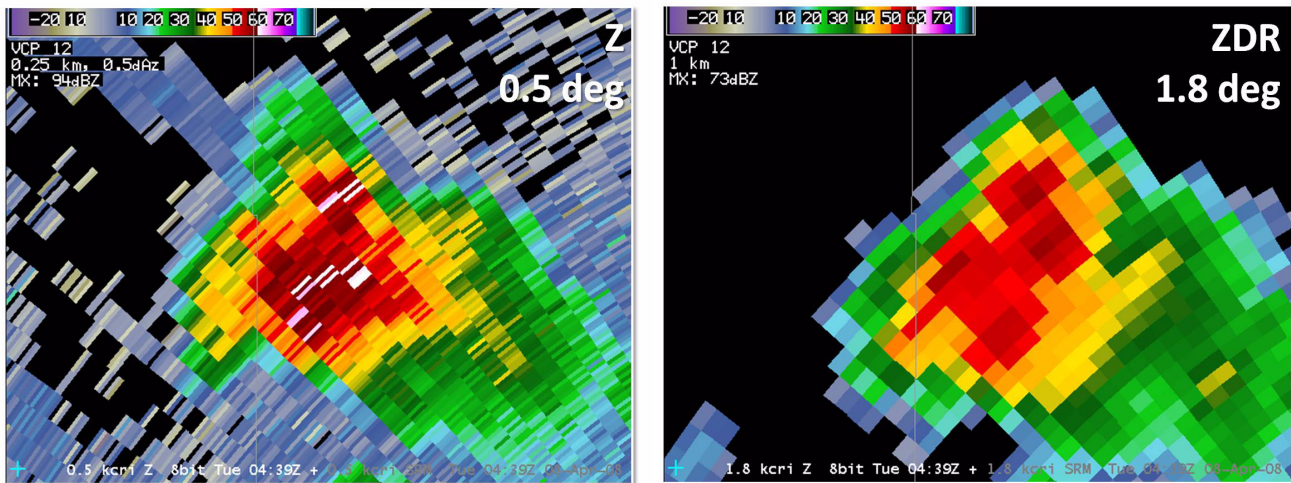


Figure 10-9. Reflectivity (Z) at 0.5 (left) and 1.8 degrees (right).

Taking a look at ZDR in Figure 10-10, this storm actually has two ZDR columns, one on the south-west flank and one on the north.

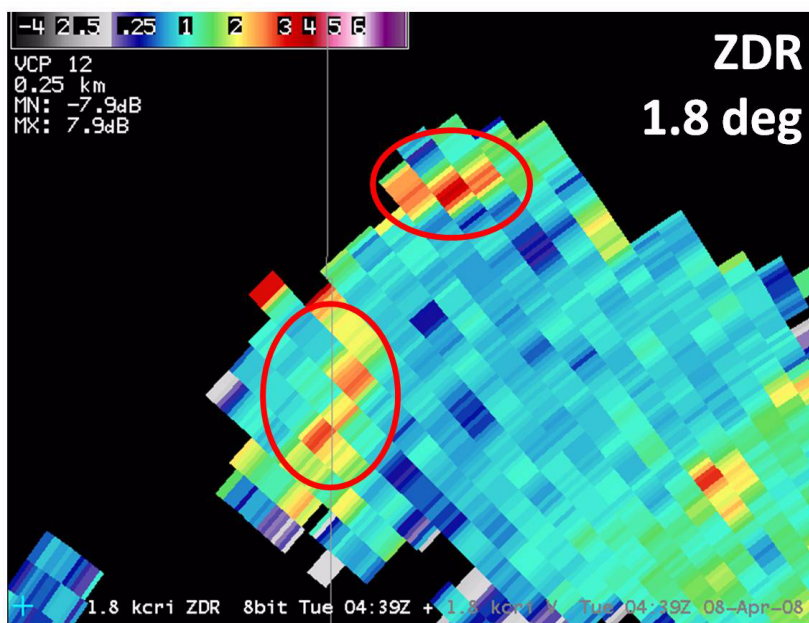


Figure 10-10. 1.8° differential reflectivity output from the storm seen in Figure 9. Notice two distinct ZDR columns (red circles)

In a reflectivity image from about 10 minutes later the storm actually has split, with the northernmost cell now moving off to the north-northeast (see Fig. 10-11). Seeing this signature early in the splitting process could potentially allow a new warning box to be drawn for the splitting storm, or an SVS with the splitting storm's new motion added.

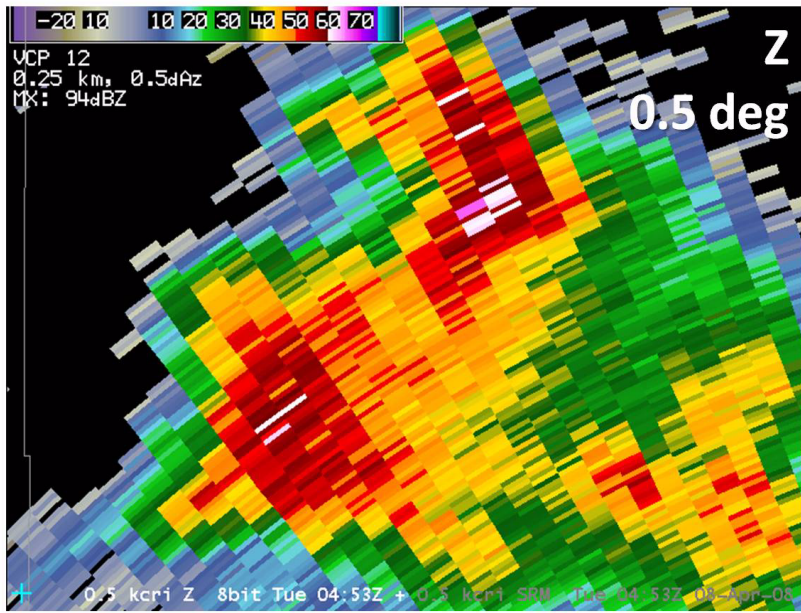


Figure 10-11. 0.5° reflectivity output from the same storm seen in Figures 10-8 through 10-10 about 10 minutes later. Notice how the storm is splitting as indicated by the ZDR columns.

In this case the appearance of two ZDR columns was helpful in anticipating storm splitting, but the presence of multiple ZDR columns does not necessarily mean a split is in progress. For the best understanding of this signature, always keep the location of the ZDR columns in the context of storm structure and the rest of the base products.

There are a few limitations to the ZDR column signature:

- There must be some warm cloud depth to see this signature because there must be liquid or mixed phase hydrometeors present.
- It may be difficult to see the ZDR column or to judge the vertical extent of the column at great distances from the radar due to beam broadening (and increasing height of the beam above the ground).

ZDR Column Limitations

- Searching for a ZDR column on elevation angles greater than 1.5 and less than 6.4 degrees can sometimes cause issues since range folding exists.
- Finally, in general with the ZDR column signature, much more research is needed to define any other potential applications.

Lesson 11: Heavy Rain Detection

As with many of the applications using dual-pol radar, active knowledge of the near-storm environment is crucial. For heavy rain, this is especially true because it keeps a high level of situational awareness of what signatures to expect. If a local or model sounding looks something like the sounding in Figure 11-1, with very thin CAPE, low LCL, a deep warm cloud layer, very high precipitable water, and deep moisture, highly efficient rain production and more of a tropical drop size distribution would be expected.

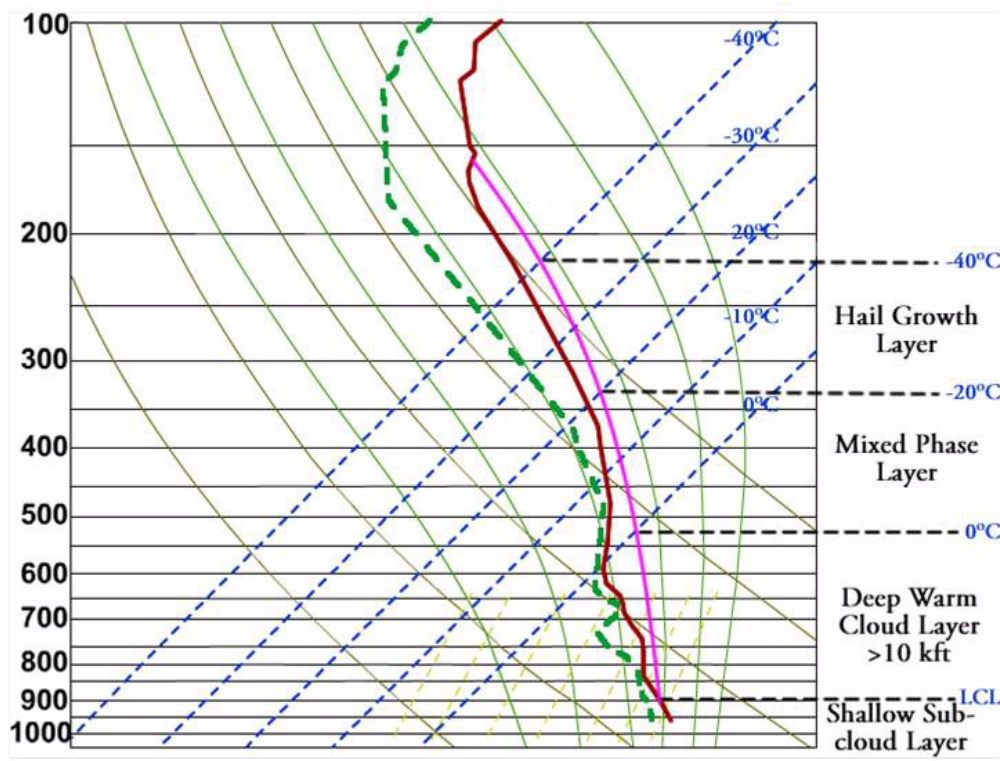


Figure 11-1. Sounding for environment favorable for producing heavy, tropical rains

This lesson will introduce methods to differentiate between tropical (warm) rain, continental rain and rain mixed with hail using the dual-pol radar products. This lesson will show you ways to identify those types of heavy rain as well.

Heavy Rain Detection in a Tropical Environment

Let's start with an examination of heavy rain in a tropical environment where the warm rain processes dominate convection (see Fig. 11-2). The following dual-pol characteristics are certainly not hard thresholds, but merely guidelines for how heavy tropical rainfall might look. All the base data values shown here should overlap in order to say with a high degree of confidence that heavy rain is occurring.

Reflectivity should be fairly high, but not in the realm associated with hail, anywhere from 40 to 55 dBZ. Warm rain processes involve very high numbers of smaller rain drops resulting in differential reflectivity values in the moderate range (between 0.5 and 3 dB). Pure rain will have very high correlation coefficient because it's all one precipitation type, and of roughly the same size. Expect to see 0.98 or 0.99 correlation coefficient values for heavy rain associated with warm rain processes. Finally, KDP should be greater than 1.0 deg/km in order to be heavy rain. Keep in mind that instantaneous precipitation rate can always be examined for an estimation of how strong the rain rates are.

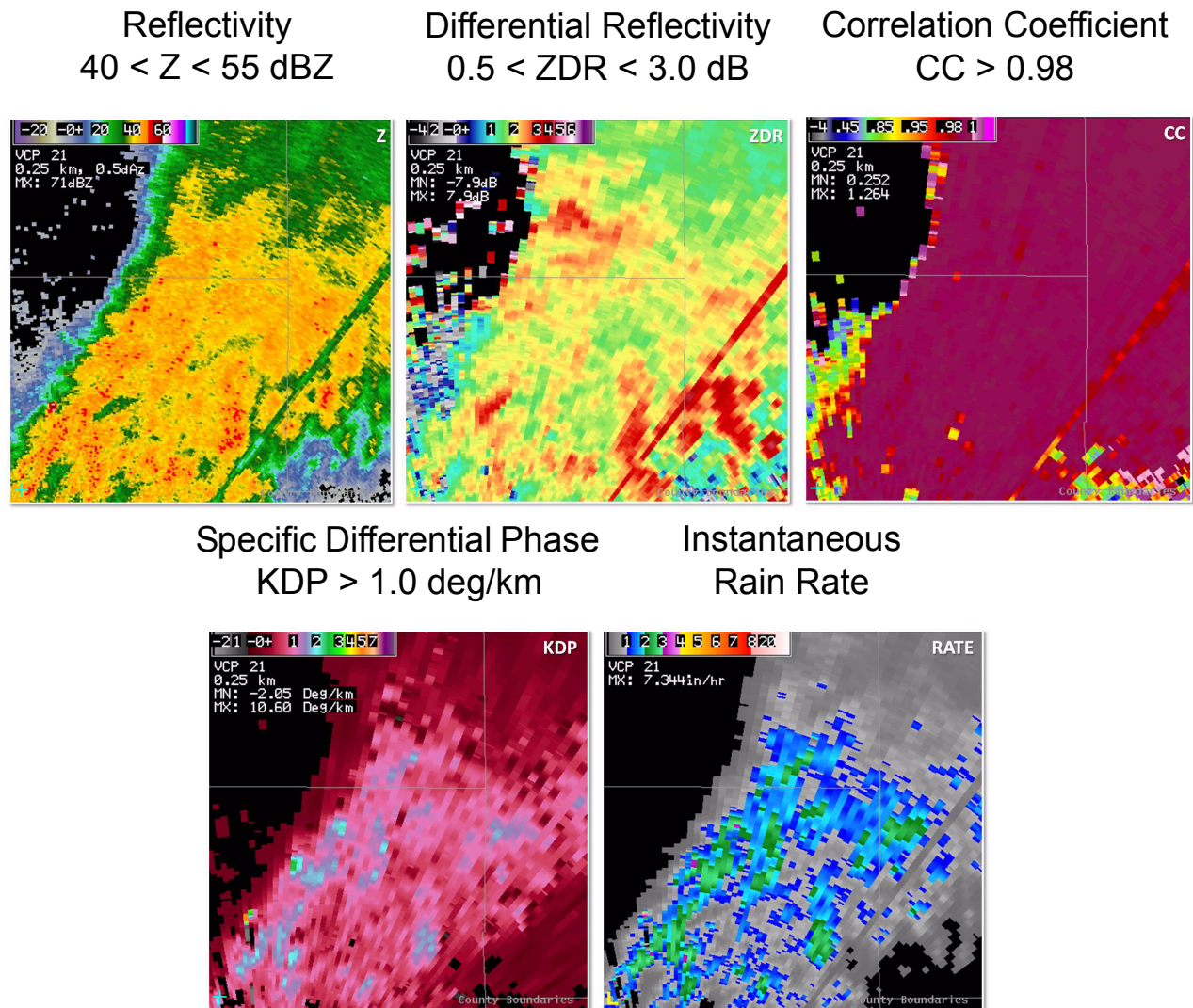


Figure 11-2. A few different dual-pol products during a heavy rain event in a tropical environment

Heavy Rain Detection in a Continental Environment

A continental environment includes a mixture of cold and warm rain processes that lead to the production of heavy rainfall, normally associated with deep, moist, and possibly severe convection.

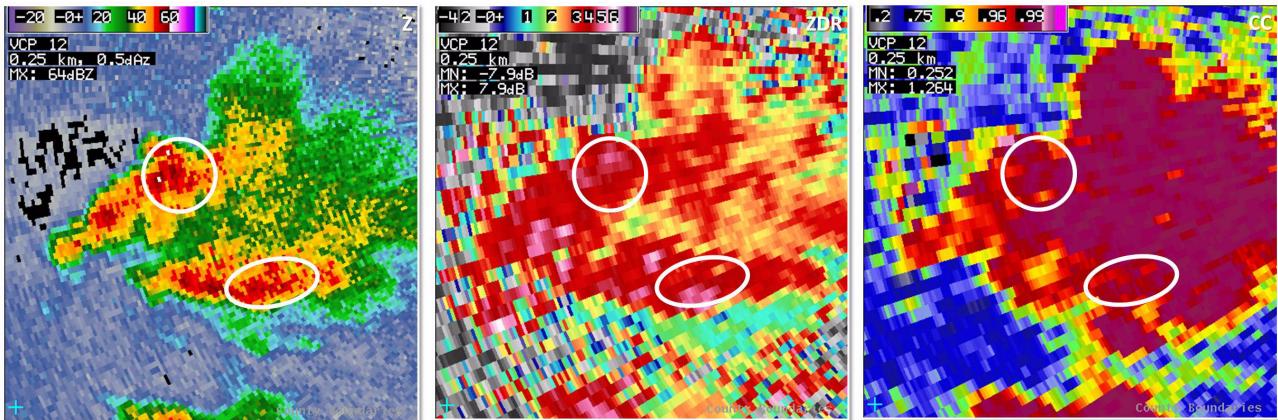
With this type of heavy rain, reflectivity values should be higher (45-60 dBZ) than the tropical case because the drops are larger. We'll focus on the two white ovals that contain 50-60 dBZ echoes in Figure 11-3. Like reflectivity, ZDR values will also be higher in this case, and this is the primary discriminator between tropical and continental heavy rain. Expected values will be between 2 and 5 dB. In this example, values are roughly 4 to 5 dB, indicating large drops.

With reflectivity values in the 50 to 60 dBZ range, there could be hail contamination. The best way to rule out hail is to check the CC. If CC is greater than 0.96, the high reflectivity is most likely due to rain. In the white ovals shown in Figure 11-3, only a handful of gates are around 0.95. The vast majority are very high, indicating pure rain. Lastly, check KDP. Since the drops are large it would take a great number of them to result in heavy rain, and KDP is the perfect product for the job. KDP needs to be high (greater than 1.0 deg/km), with higher values indicating heavier rain.

Reflectivity
 $50 < Z < 60$ dBZ

Differential Reflectivity
 $2.0 < ZDR < 5.0$

Correlation Coefficient
 $CC > 0.96$



Specific Differential Phase
 $KDP > 1.0$ deg/km

Instantaneous
Rain Rate

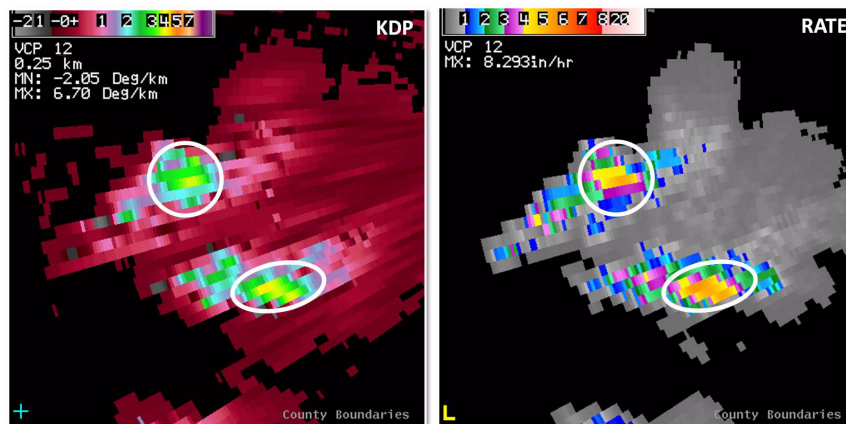


Figure 11-3. A few different dual-pol products during a heavy rain event in a continental environment

One note of caution in the search for heavy rain: be aware of light precipitation masking itself as heavy precipitation. There will be situations where Z will be 30 to 45 dBZ, ZDR greater than 5 dB and CC around 0.98 which might indicate heavy rain. However, if KDP is below 1.0 deg/km, it is not heavy rain; instead it's an area of very large drops in low concentration, leading to minimal rain rates. The figure above verifies that the highest rain rates are inside those two white ovals.

Heavy Rain Mixed with Hail

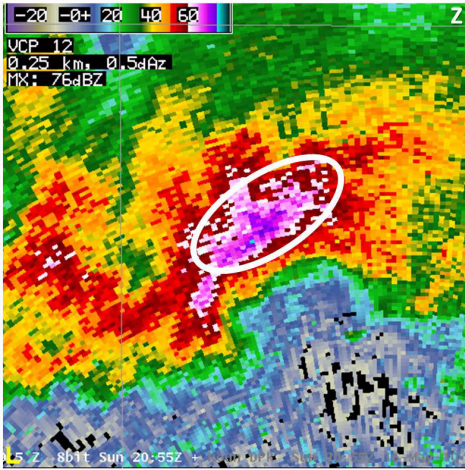
The final type of heavy rain that you can identify with dual-pol is heavy rain mixed with hail, which is normally associated with severe or borderline severe convection just like the previous example.

Heavy rain mixed with hail tends to produce the highest reflectivity values possible with WSR-88Ds, but at a minimum, values of Z for this precipitation type should be greater than 55 dBZ. In the example shown in Figure 11-4, the reflectivity core has very high reflectivity (white oval). ZDR is strongly biased toward the largest hydrometeors, so if the heavy rain contains severe hail, ZDR will be low but positive. If the heavy rain contains hail that is almost melted and completely coated in water, ZDR could be as high as +6 dB. In this example, there is a band of lower ZDR, but also regions of very high ZDR. In general, for heavy rain mixed with hail, don't rely on ZDR.

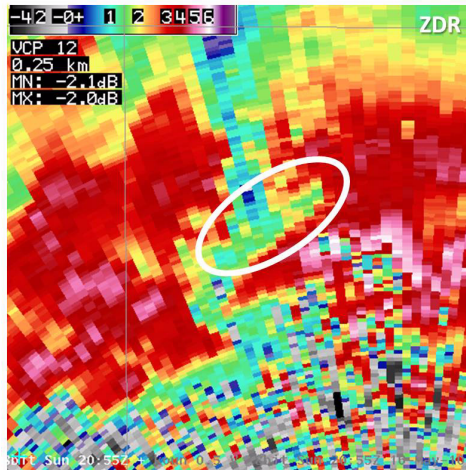
Correlation coefficient values are probably the best discriminator for heavy rain events that contain hail. CC will be much lower with these events than with the other two heavy rain signatures due to the co-location of rain and hail. Expect to see values 0.95 or less. Inside the white oval, most of this region has CC lower than expected for pure rain, indicating that hail is present.

As with the other heavy rain types, examine KDP to get the best picture of where the heaviest rain is. In storms containing heavy rain mixed with hail, KDP will be extreme, perhaps as high as 8 deg/km. In Figure 11-4, KDP is indeed over 8 deg/km, and indeed this storm contained heavy rain and hail. The co-location of very high reflectivity, very high KDP, and CC lower than 0.96 is an excellent indicator of heavy rain mixed with hail.

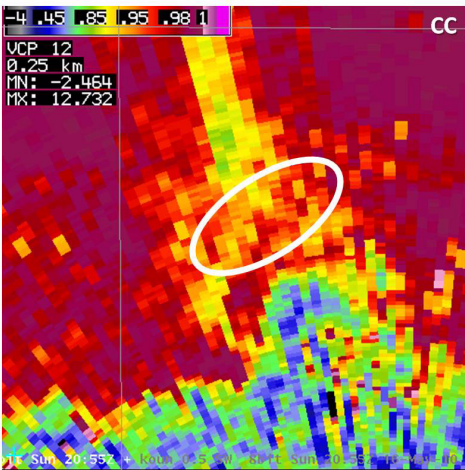
Reflectivity
Z > 55 dBZ



Differential Reflectivity
ZDR = Anything!



Correlation Coefficient
CC < 0.96



Specific Differential Phase
KDP > 1.0 deg/km (extreme)

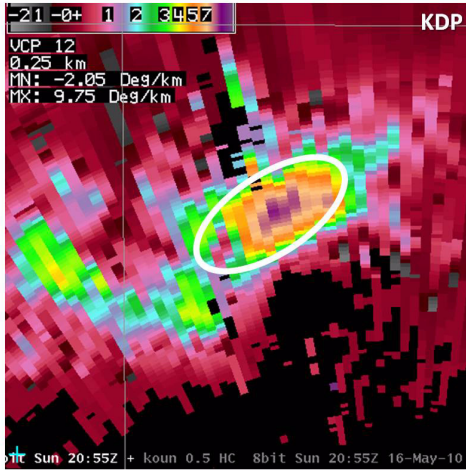


Figure 11-4. Z, ZDR, CC and KDP during an event with a mixture of heavy rain and hail.

A final note: don't be alarmed if this signature results in blacked-out KDP. Recall from the KDP product module that KDP is blacked-out in radar gates that have CC below 0.90.

It is now clear that the most important indicator of heavy rain is KDP. The equation that converts KDP values to rain rate is given in Figure 11-5 in mm per hour, along with a rate table in inches per

KDP and Rainfall Rate

hour. This equation is the one used for dual-pol QPE when the algorithm chooses to use the KDP rate at a particular range bin. This rate table (which also appears in the dual-pol training aid) is useful products to get a quick idea of rain rate in these areas of high KDP.

$$R(KDP) = 44 * |KDP|^{0.822}$$

KDP (deg/km)	Rain Rate (in/hr)
0.2	0.5
0.5	1
1.2	2
2	3
2.8	4
3.6	5
4.5	6

Figure 11-5. Equation and table of values relating KDP to rainfall rates.

Methodology to Detect Heavy Rain Using Panel/Combo Rotate

1. Start with Z
2. Toggle to KDP
3. Go to CC to see if mixed with hail or pure rain
4. Go to ZDR to see median drop size. If less than 3.0 dB in pure rain, be aware of the warm rain processes. If mixed with hail, ignore ZDR.

Any dual-pol radar analysis should start with reflectivity. For heavy rain, look for enhanced reflectivity, then toggle with KDP to determine where the heaviest rain is. Does the location of the high KDP make sense? Next, toggle to CC to see

if there is a rain-hail mix. If CC is lower than 0.96, hail is in there. Finally, examine ZDR to get a feel for median drop size. If hail is not present, ZDR will identify whether there are likely warm rain processes going on.

Using dual-pol to detect heavy rain should increase confidence that a storm or storms are producing heavy rainfall. Hail or no hail, tropical or continental, you can be assured that heavy rain is occurring. For many events across a wide range of CWAs, just knowing the nature of the heavy rain, whether it is tropical or not, is half the battle to anticipating a flash flood. With an awareness and a high degree of confidence in the detection of heavy rain and the nature of the heavy rain, perhaps lead times might increase. Of course, local knowledge of the hydrological antecedent conditions is still crucial and cannot be bypassed even with dual-pol. Given a good handle on hydrologic conditions, use the dual-pol products to zero in on the regions with the heaviest rates and monitor the movement of those rates. Check FFMP early and often to examine accumulations at the basin level and to compare those accumulations to flash flood guidance.

Here is a summary of the strengths of using dual-pol products to detect heavy rain:

- Increases confidence in radar signature of heavy rain
- Can differentiate 3 types of heavy rain:
 - Warm rain (tropical)
 - Cold/warm rain (continental)
 - Rain and hail mix

Using Dual-Pol Products During Flash Flood Warning Operations

Strengths of Using Dual-Pol to Detect Heavy Rain

Limitations of Dual-Pol Heavy Rain Detection

Dual-Pol products can be very helpful during heavy rain events, but keep the following in mind:

- Rates don't always translate into QPE
- KDP blanked out at $CC < 0.90$

There is no guarantee that the radar's precipitation accumulation products will accumulate rain at accurate rates. Even with dual-pol capability, a radar *estimates* precipitation and will suffer from the normal limitations associated with radar-estimated precipitation. Additionally, the dual-pol QPE depends on the hydrometeor classification algorithm, which can suffer from mis-identifications and improper melting level heights, either of which can lead to the application of inappropriate rates.

Additionally, KDP is blanked out in bins where CC is less than 0.90 because CC is far too noisy in those areas. This could occur in severe hail, and it's likely to occur when hail is larger than golfballs. In those cases, you probably won't be able to detect heavy rain. Thankfully, the co-location of baseball hail and heavy rain is rare.

Lesson 12: Non-Precipitation Echoes

One advantage of looking at dual-pol products is the ability to distinguish between meteorological and non-meteorological echo. As shown in the correlation coefficient lesson, most non-precipitation echoes, such as ground clutter or biological scatterers will have CC values less than 0.9. In the example in Figure 12-1, there appears to be widespread, light shower activity all over the place. Looking at the CC product, there are a few areas of high CC, but also places where CC is noisy and much less than 0.90. So the areas inside the white circles in Figure 12-1 really are light showers, but the rest aren't showers after all. What scatterers are responsible for the lower values of CC around the showers? This lesson will lay out a framework for identifying the most common non-precipitation echoes.

Dual-Pol Advantage: Distinguishing Non-meteorological Echo

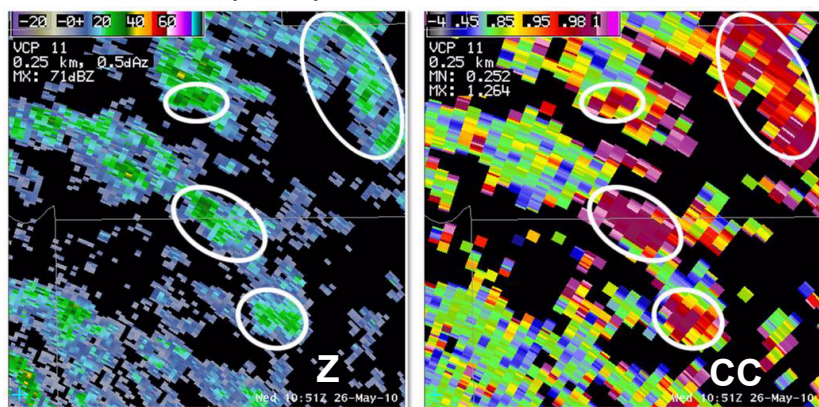


Figure 12-1. Z (left) and CC (right) images showing light showers (which circles) surrounded by non-meteorological scatterers.

As with the other applications of dual-pol products, it is important to always interpret the dual-pol variables in context with reflectivity, velocity, and spectrum width. Also, don't forget the environmental context!

Ground Clutter and Anomalous Propagation

Ground clutter or echoes resulting from anomalous propagation are made up of a variety of objects: trees, buildings, terrain, and pretty much anything else that is ground-based and intercepts a portion of the radar beam. Within a radar beam these objects are irregularly shaped. Since these objects don't move they will tend to have radial velocities right around 0 kts. There are a few exceptions such as cars on a highway or wind farms. Dual-pol characteristics of wind farms will be covered later in the lesson.

Dual-Pol Characteristics of Ground Clutter and AP

In ground clutter or AP (See Fig. 12-2 on page 2-192), reflectivity is usually fairly high and can, in rare cases, even approach 80 dBZ. For the most part though, reflectivity in ground clutter falls within the range of values common in meteorological scatterers, but with a texture that is a bit noisier than is typical for weather echoes. ZDR is also noisy, with a healthy mixture of positive and negative values. CC is usually less than 0.9 and very noisy, although occasionally certain ground targets can send CC above 0.90 in a handful of radar bins. Since CC is typically so low, KDP is not displayed for most areas of ground clutter. For the few places where KDP is displayed, values will usually be 0 deg/km. As mentioned before, ground clutter or AP will be largely stationary in the base velocity product, with a few exceptions.

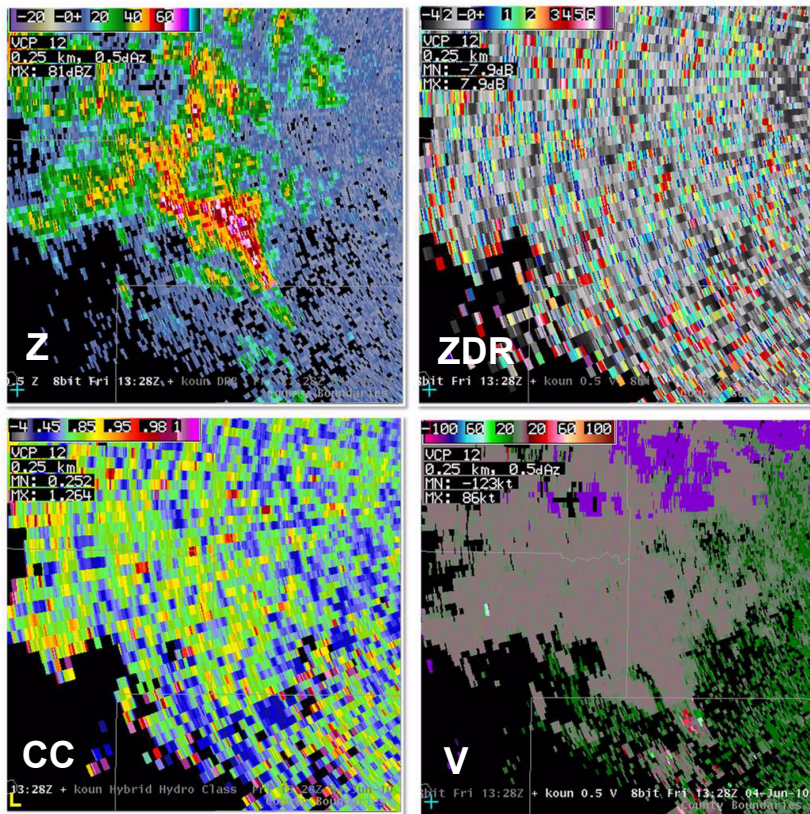


Figure 12-2. AP as seen in Z (top left), ZDR (top right), CC (bottom left) and V (bottom right).

Biological scatterers include birds, insects, bats, and anything else that is alive and flies high enough to be sampled by the radar beam. The shapes of biological scatterers are complex. Additionally, they are often of mixed types and species which complicates identification using the dual-pol radar products. For example, insects and birds may be (and often are!) flying at the same time. Knowledge of your local area is key to beginning to distinguish types of biological scatterers. Without more research, caution is advised when attempting to distinguish between insects and birds. In some cases this will not be possible even with the best local knowledge. Let's take a look at a few examples of how biological scatterers may appear in dual-pol.

Biological Scatterers

Migrating Birds Figure 12-3 is an example of a nighttime bird migration during an event with strong low-level, southerly flow. Considering that it is early March and the surface temperatures are will below freezing, there are probably not many insects mixed in during this event. Notice that, in Figure 12-3, Z is fairly low with even the highest reflectivity values reaching only 20 dBZ.

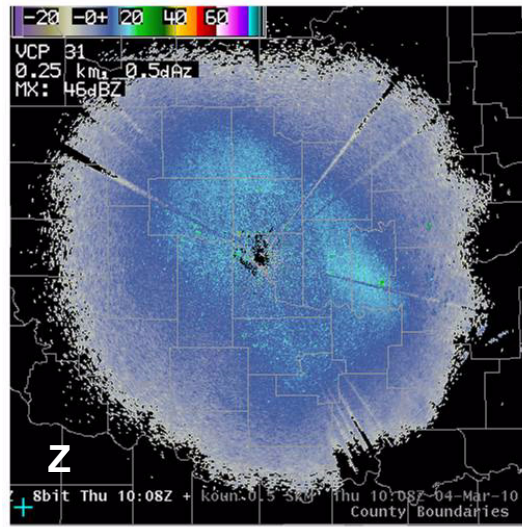


Figure 12-3. Z image of nighttime bird migration.

Taking a look at ZDR in Figure 12-4 on page 2-194, there is a corridor of high, positive values from the south side of the radar through to the north and northwest. These positive values are well-aligned with the low-level flow (white arrow) and it is very likely the viewing angle is such that the birds are being viewed head- or tail-on. Outside the area of positive ZDR, there are 2 lobes of low to negative ZDR on the west-southwest side of the radar and the east through southeast side of the radar (white circles). This is likely the result of a combination of viewing angle and Mie scattering, which you may recall occurs when the target size is significantly larger relative to the wavelength of the transmitted energy from

the radar. Birds always fall into the Mie scattering regime.

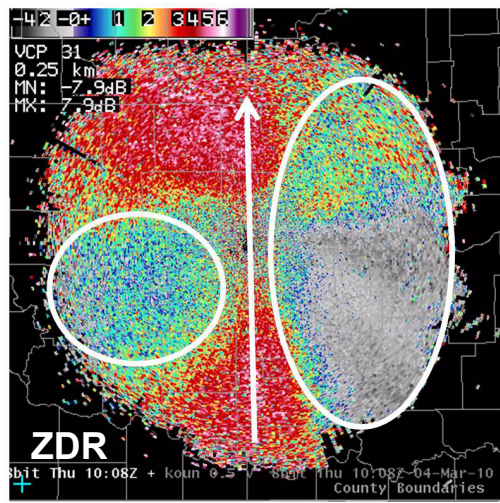


Figure 12-4. ZDR image of the same nighttime bird migration as in Figure 12-3.

Note: due to the complexity of Mie scattering, the pattern of positive and negative ZDR values may be reversed in some cases, as Figure 12-5.

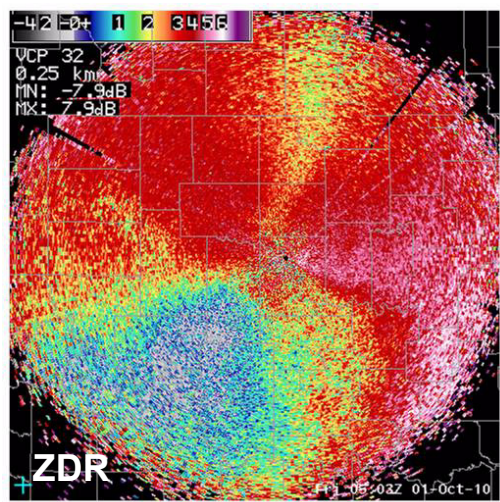


Figure 12-5. ZDR image from the fall showing high positive values of ZDR where migrating birds are detected.

Finally, CC is below 0.90 nearly everywhere, a common characteristic of biological scatterers.

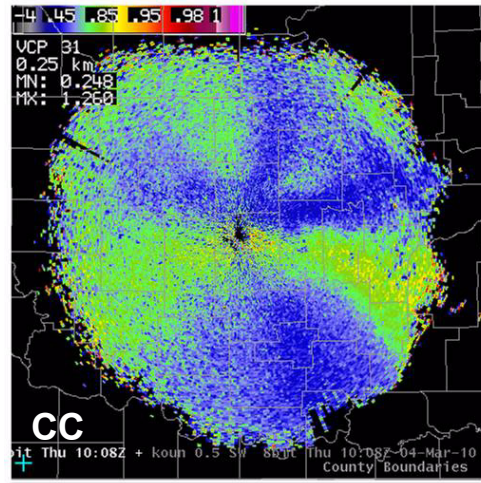


Figure 12-6. CC image of the same nighttime bird migration shown in Figure 12-3 and Figure 12-4.

Local Birds Dispersing

What is the region of strong reflectivity in the white polygon in Figure 12-7? Ground clutter? A strong convective cell on a rather stable January morning? Actually, this is a large number of robins (somewhere around 500,000) dispersing from their roost. Birds dispersing from a local roost often appear as large blobs or rings in reflectivity. Reflectivity varies but occasionally exceeds 30 dBZ (or in extreme cases like this one, 50 dBZ!).

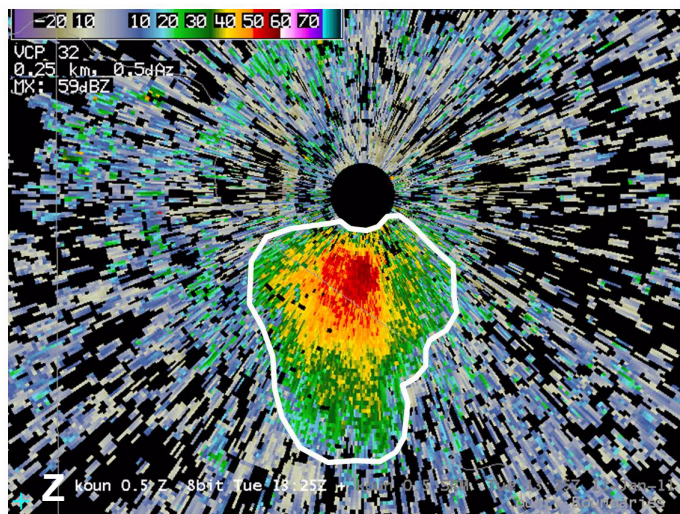


Figure 12-7. Z image showing robins dispersing from their roost.

Toggling to V (see Fig. 12-8), there is strong divergence just south of the radar, another clue that this is not just some kind of bizarre clutter target.

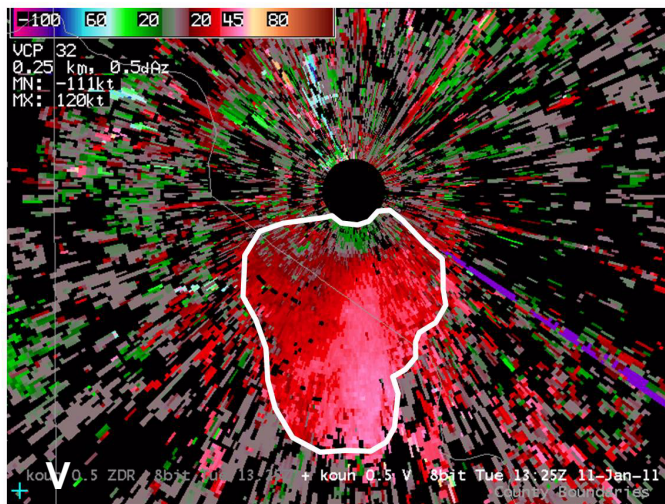


Figure 12-8. V image of the same event shown in Figure 12-7.

In ZDR (see Fig. 12-9), most of the area is positive, but there are also some negative values in there. ZDR is very dependent on size and viewing angle of the birds and therefore may vary greatly.

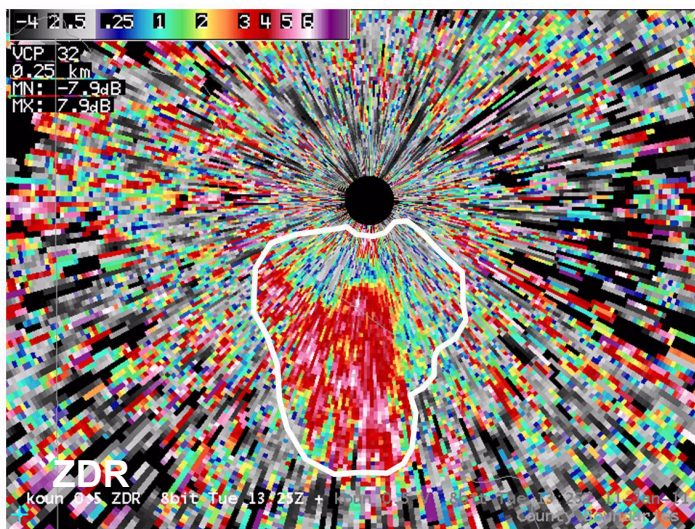


Figure 12-9. ZDR image of the same event shown in Figure 12-7 and Figure 12-8.

The very low CC values shown in Figure 12-10, usually well below 0.90, confirm the presence of biological scatterers. The non-zero velocities indicate this is not clutter and the low CC indicates this is non-meteorological. CC is also not quite as noisy as in the surrounding ground clutter.

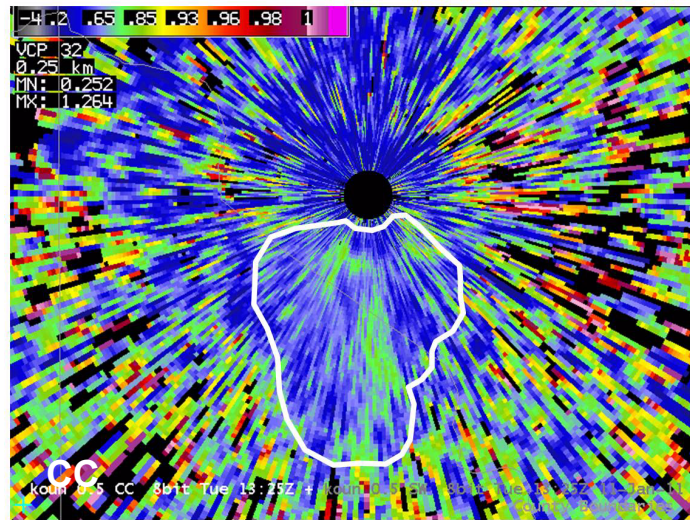


Figure 12-10. CC image of the same even shown in Figure 12-7, Figure 12-8, and Figure 12-9.

Insects Figure 12-11 on page 2-198 shows an example where insects may be the dominant scatterers. Note that this is a best guess based on the time of year (August), the time of day (afternoon), and the presence of a deep, well-mixed layer. In reality there is probably a mixture of birds and insects since insects are a favorite food of many birds.

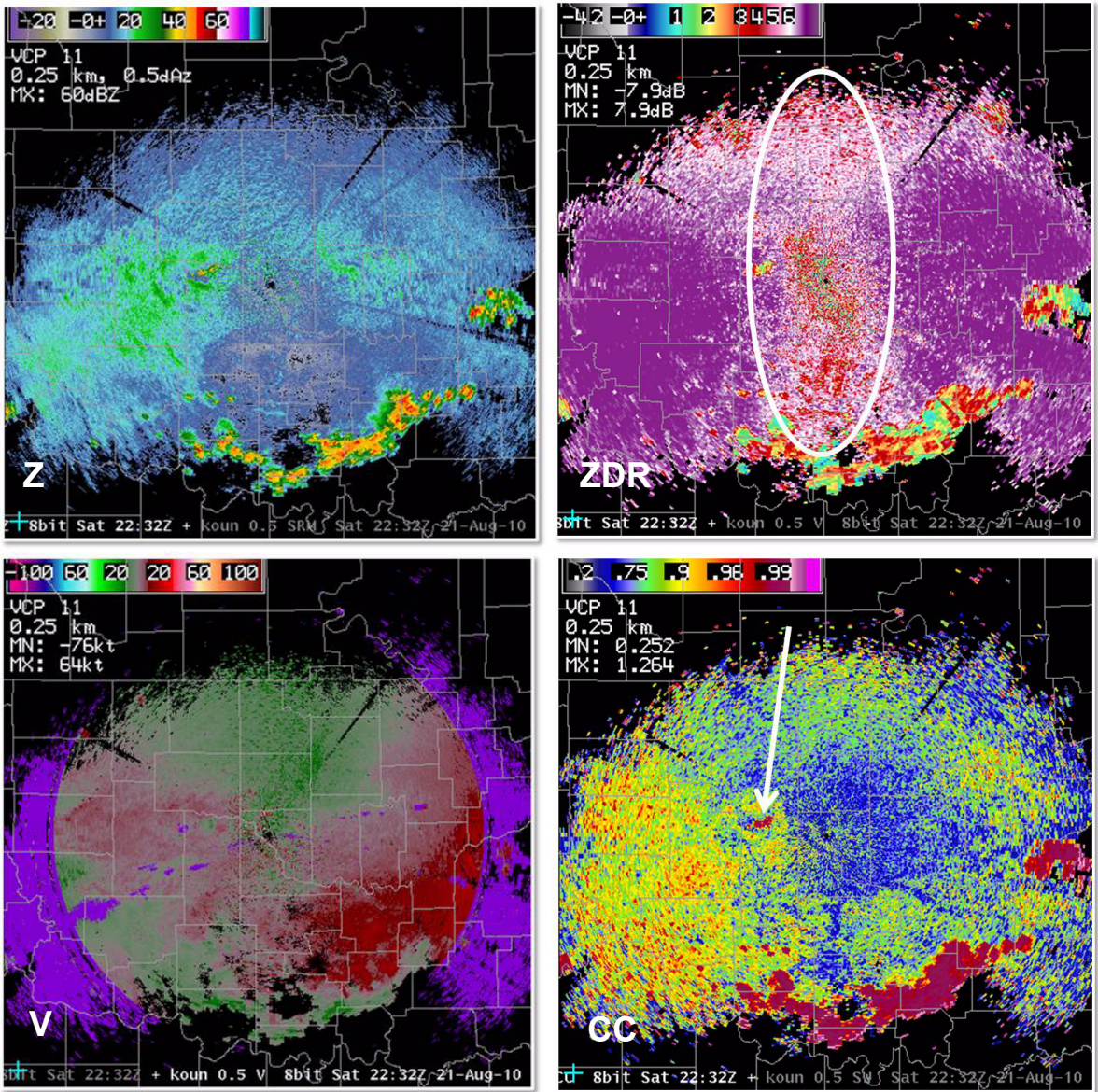


Figure 12-11. Z (top left), ZDR (top right), V (bottom left) and CC (bottom right) showing insects as the dominant scatterers, but with convection also in the area.

Reflectivity is low relative to convective storms, but at times can still be greater than 25 dBZ. ZDR is strongly positive just about everywhere but is slightly lower in the center of the image (see white circle), probably indicating that the insects are preferentially aligned with the mean, low-level wind. Also notice that even with the light winds, the velocity of the insects is non-zero, distinguishing them from ground clutter or AP. Finally, CC is below 0.90 nearly everywhere, except just west of the radar in the region indicated by a white arrow. This is actually a small convective cell embedded in the insect echo, which is easily seen in the CC data.

One caution to consider is that in this case, as is common during the warm season, there may be a mixture of birds and insects. Attributing any one area of echo to either insects or birds must be done with great caution.

Wind Turbines

Wind turbines are very tall and consist of a stationary tower with a set of large rotating blades on top. At any given time, the blades may be rotating or stationary depending on the wind, and each of these conditions may produce different signatures in the dual-pol data.

Figure 12-12 on page 2-200 shows how wind farms appear in the different base products when the blades are in motion. Reflectivity is variable but commonly exceeds 20 dBZ and is dependent on range from radar and refractive conditions. In this example, reflectivity is moderate throughout much of the wind farm seen in the white circle. For comparison, the areas outside of the white circle are areas of clutter not associated with the wind farm. Velocity and spectrum width will both be

rather noisy, with many non-zero values in the velocity product. In contrast, note the near-zero velocities throughout most of the surrounding AP. In spectrum width, the wind turbines also really stand out with much higher values on average than the surrounding AP. ZDR is fairly noisy and looks a lot like ground clutter. CC should be quite low, usually less than 0.80. In this case, it could even be argued that CC is noticeably lower than the surrounding AP.

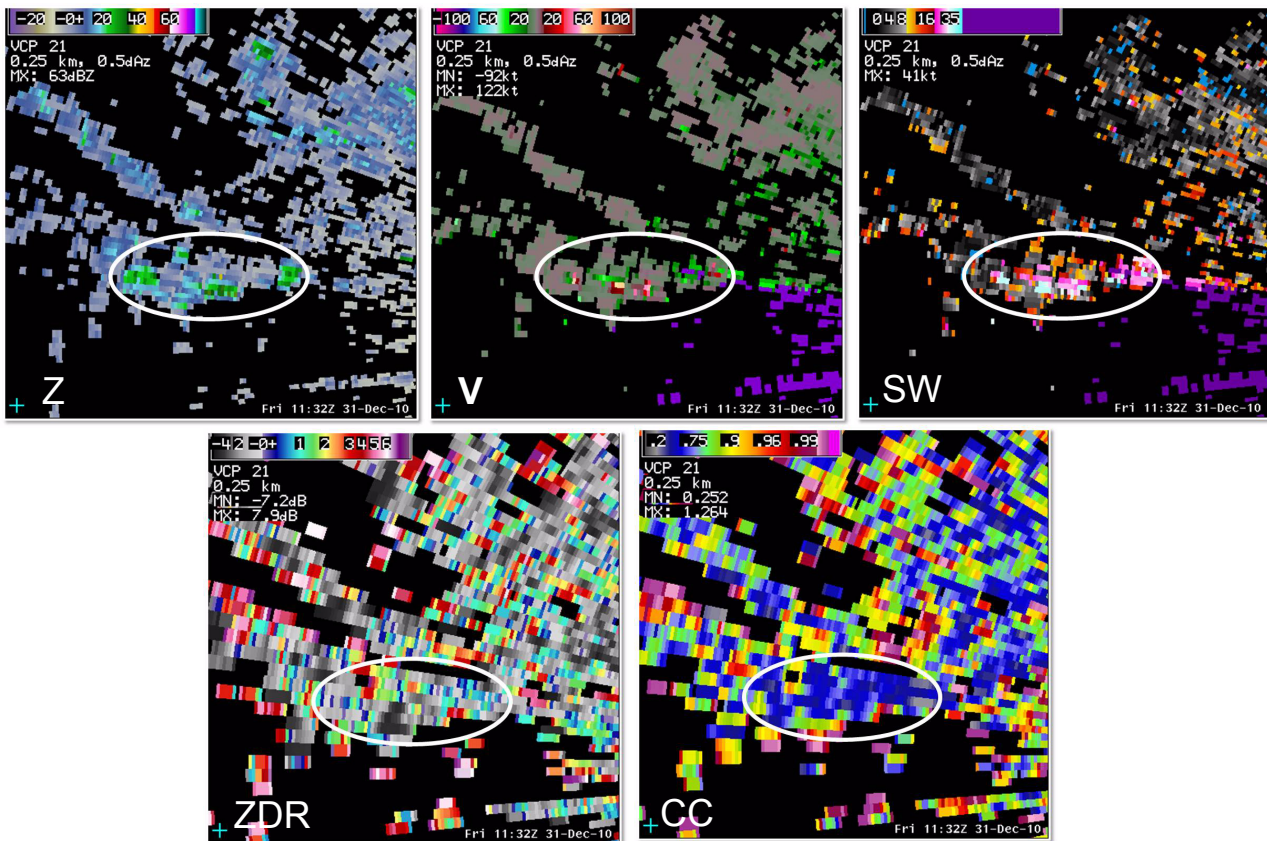


Figure 12-12. Z (top left), V (top right), spectrum width (middle), ZDR (bottom left) and CC (bottom right) images showing how wind farms, with the blades in motion, can affect radar data.

When the wind stops blowing, the blades on the wind farms become stationary. As seen in Figure 12-13 on page 2-202, reflectivity could still be just about anything and ZDR will be fairly noisy, resembling ordinary ground clutter or AP. Even the velocities near 0 kts make this look a lot like AP. The greatest difference is seen here in the CC product, where the wind farms have CC values as high as 0.99. Notice that these are not isolated gates of high CC in a region of noisy, low CC as could be seen in ground clutter or AP. Also, although these blocks of high CC may not appear exactly the same with each volume scan, they can be fairly persistent. Since CC is so high, KDP is calculated. KDP can be fairly noisy, with both strongly positive and strongly negative values. It is unknown how often high CC will occur when the turbines are stationary, but it is one potential scenario to keep in mind since it can cause contamination of dual-pol QPE products assuming you don't have a region of all bins clutter filtering covering the wind farms. Sizable regions of $CC > 0.95$, like those in this example, will force dual-pol QPE to accumulate precipitation, and in areas where KDP and reflectivity are very high, dual-pol QPE will have very high rain rates.

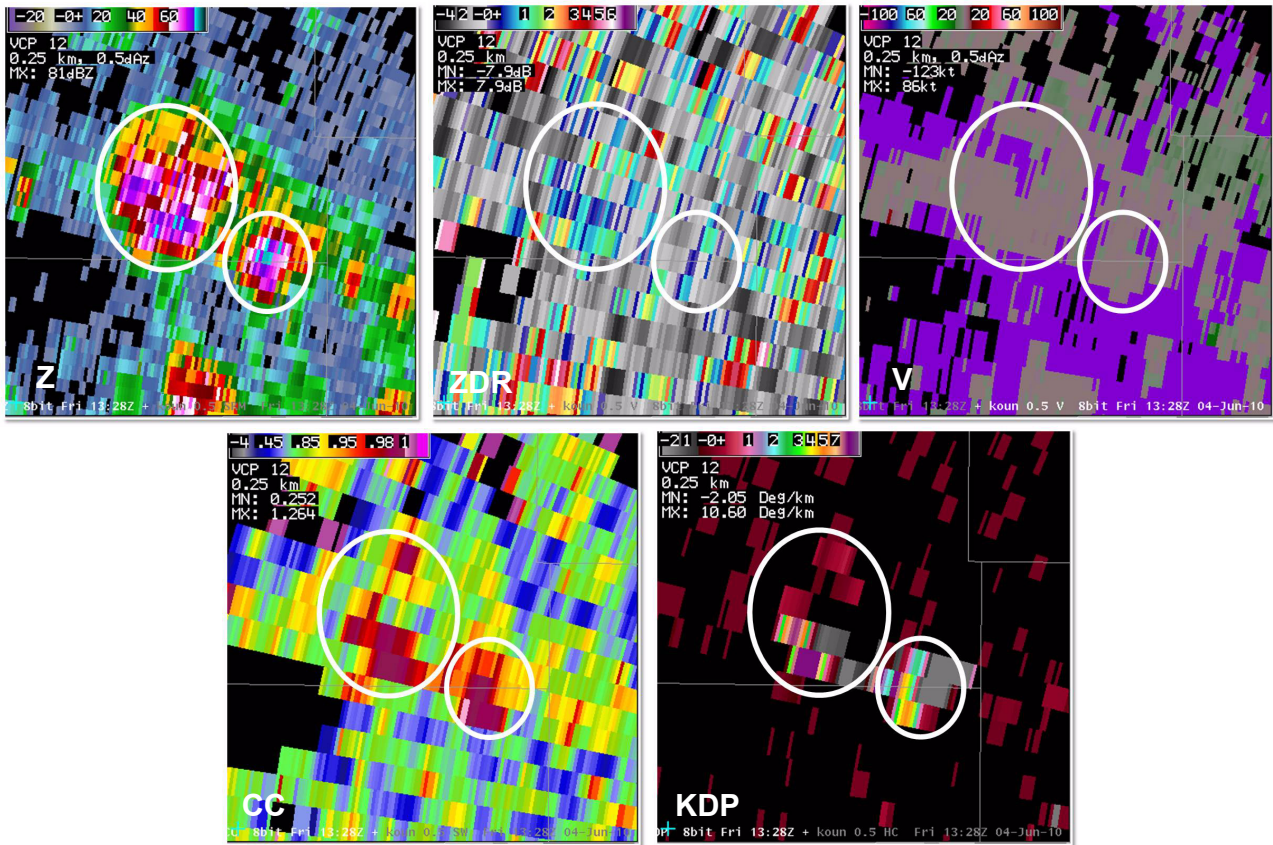


Figure 12-13. Stationary wind turbines as seen in Z (top left), ZDR (top right), V (middle), CC (bottom left), and KDP (bottom right).

Smoke plumes are often made up of more than just microscopic particles. Small bits of ash or embers, as well as plant debris, are often lofted with the smoke, as is certainly the case with significant forest and brush fires. Most of the time, reflectivities in smoke and debris plumes, like the one in Figure 12-14, are fairly low (< 25 dBZ), but can in a few instances be greater. Smoke will commonly have non-zero velocities, but note that the plume itself may appear somewhat stationary with continual regeneration occurring at the site of the fire and advection dispersing the plume downwind. ZDR can be about anything and will be dependent on the shape and orientation of any debris lofted by the fire. CC will usually be very low due to the diverse sizes and shapes of any small

Smoke Plumes

bits of fire debris that have been lofted and should be the most important dual-pol product to monitor in order to verify smoke plumes.

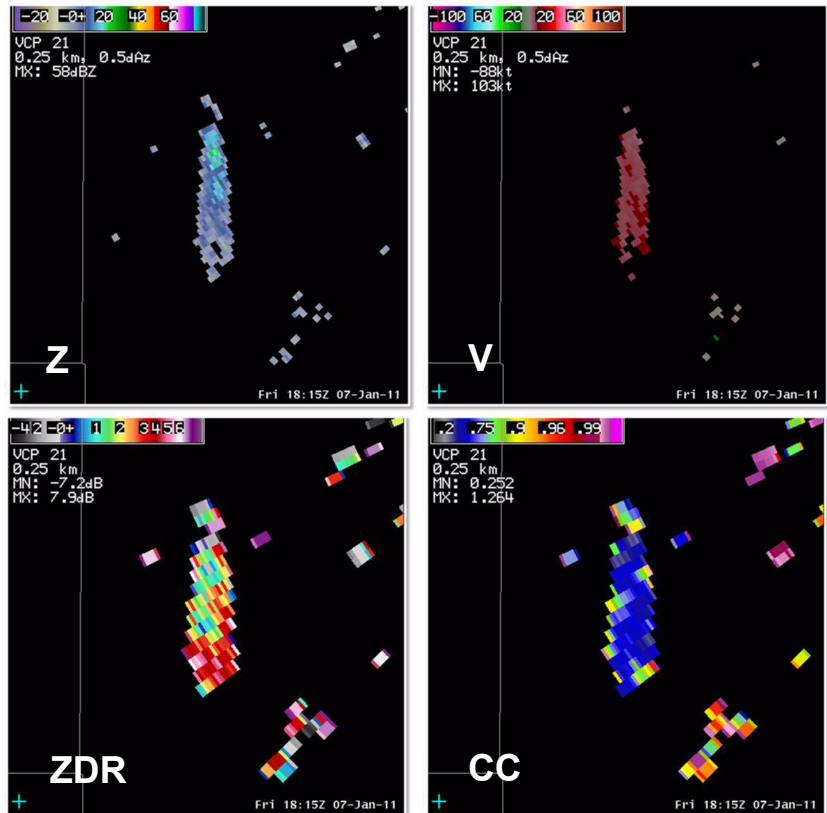


Figure 12-14. Smoke plumes as seen in Z (top left), V (top right), ZDR (bottom left) and CC (bottom right).

Chaff Chaff is released by the U.S. military to mask aircraft, and is usually made of very thin fibers. As these fibers fall they are typically horizontally oriented, but some variation in orientation may occur in turbulent conditions. Chaff, because of its slow terminal fall velocity, will also usually be advected with the mean flow.

Chaff typically has fairly low reflectivity with velocity that is similar to the background flow. It is usually elongated in a band, parallel to the mean winds at that height. Considering these factors, chaff may resemble a band of light precipitation or snow, or as in Figure 12-15 on page 2-204, a boundary of some sort. In the base velocity

product, it looks like the scatterers are moving approximately with the mean flow.

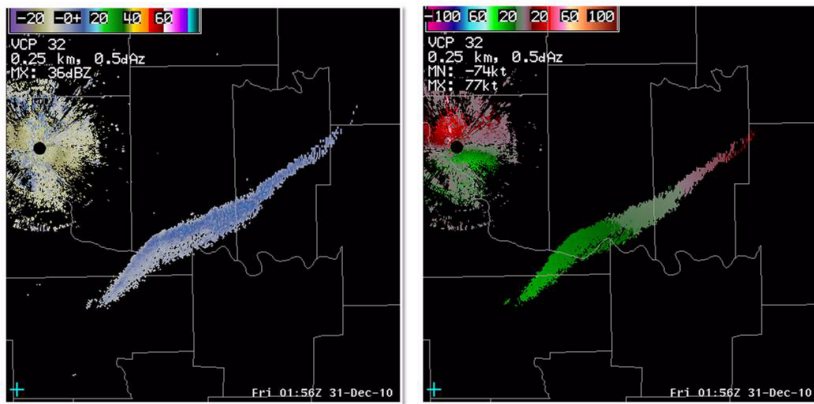


Figure 12-15. Chaff as seen in Z (left) and V (right).

For chaff, ZDR should be positive, sometimes extremely positive. In our example, ZDR is between about 5 and 7.9 dB, the highest value possible in this ZDR product. Chaff should usually produce very low CC of less than 0.6, and as with other non-precip echoes, CC is the most important dual-pol product to monitor. Watch for the relatively smooth and very low values of CC. With such low CC and high ZDR, chaff may look a bit like biological scatterers. Use clues such as behavior and environment to discriminate between these scatterers.

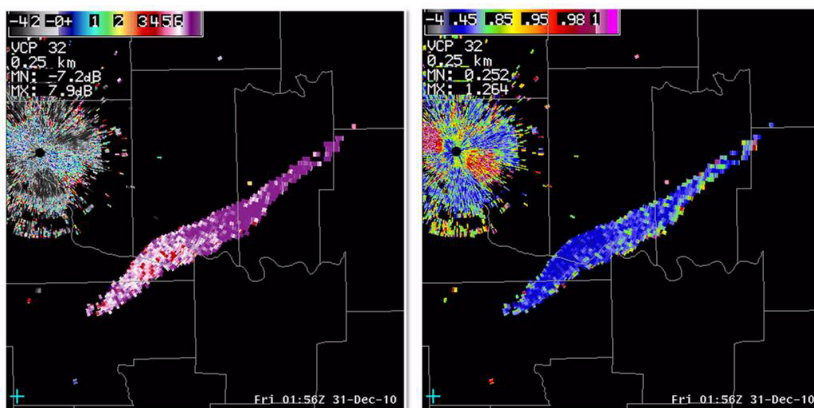


Figure 12-16. Chaff as seen in ZDR (left) and CC (right)

Conclusion As a summary, dual-pol products used alongside traditional reflectivity, velocity, and spectrum width can help distinguish meteorological and non-meteorological echoes. It is also possible to distinguish *types* of non-precipitation echoes. Remember to use all available radar data and environmental information when trying to distinguish types of non-meteorological scatterers. Also, knowing a little bit about what types of non-meteorological scatterers are most likely to occur seasonally or at a particular time of day in your area could help to eliminate some possibilities.